Université de Montréal

Cell wall composition regulates cell shape and growth behaviour in pollen tubes

par
Youssef Chebli

Institut de recherche en biologie végétale. Département de sciences biologiques
Faculté des Arts et des Sciences

Thèse présentée à la Faculté dess Arts et des Sciences
en vue de l'obtention du grade de Ph.D
en Sciences Biologiques
option biologie moléculaire et cellulaire

Août 2012

Université de Montréal

Faculté des études supérieures et postdoctorales

Cette thèse intitulée :

Cell wall composition regulates cell shape and growth behaviour in pollen tubes

Présentée par :

Youssef Chebli

a été évaluée par un jury composé des personnes suivantes :

David Morse, président-rapporteur

Anja Geitmann, directeur de recherche

Tamara Western, membre du jury

Kris Vissenberg, examinateur externe

David Morse, représentant du doyen de la FES

Résumé

L'une des particularités fondamentales caractérisant les cellules végétales des cellules animales est la présence de la paroi cellulaire entourant le protoplaste. La paroi cellulaire joue un rôle primordial dans (1) la protection du protoplaste, (2) est impliquée dans les mécanismes de filtration et (3) est le lieu de maintes réactions biochimiques nécessaires à la régulation du métabolisme et des propriétés mécaniques de la cellule. Les propriétés locales d'élasticité, d'extensibilité, de plasticité et de dureté des composants pariétaux déterminent la géométrie et la forme des cellules lors des processus de différentiation et de morphogenèse. Le but de ma thèse est de comprendre les rôles que jouent les différents composants pariétaux dans le modelage de la géométrie et le contrôle de la croissance des cellules végétales. Pour atteindre cet objectif, le modèle cellulaire sur lequel je me suis basé est le tube pollinique ou gamétophyte mâle. Le tube pollinique est une protubérance cellulaire qui se forme à partir du grain de pollen à la suite de son contact avec le stigmate. Sa fonction est la livraison des cellules spermatiques à l'ovaire pour effectuer la double fécondation. Le tube pollinique est une cellule à croissance apicale, caractérisée par la simple composition de sa paroi et par sa vitesse de croissance qui est la plus rapide du règne végétal. Ces propriétés uniques font du tube pollinique le modèle idéal pour l'étude des effets à courts termes du stress sur la croissance et le métabolisme cellulaire ainsi que sur les propriétés mécaniques de la paroi. La paroi du tube pollinique est composée de trois composantes polysaccharidiques : pectines, cellulose et callose et d'une multitude de protéines. Pour comprendre les effets que jouent ces différents composants dans la régulation de la croissance du tube pollinique, j'ai étudié les effets de mutations, de traitements enzymatiques, de l'hyper-gravité et de la gravité omni-directionnelle sur la paroi du tube pollinique. En utilisant des méthodes de modélisation mathématiques combinées à de la biologie moléculaire et de la microscopie à fluorescence et électronique à haute résolution, j'ai montré que (1) la régulation de la chimie des pectines est primordiale pour le contrôle du taux de croissance et de la forme du tube et que (2) la cellulose détermine le diamètre du tube pollinique en partie sub-apicale. De plus, j'ai examiné le rôle d'un groupe d'enzymes digestives de pectines exprimées durant le développement du tube

pollinique : les pectate lyases. J'ai montré que ces enzymes sont requises lors de l'initiation de la germination du pollen. J'ai notamment directement prouvé que les pectate lyases sont sécrétées par le tube pollinique dans le but de faciliter sa pénétration au travers du style.

Mots-clés : Tube pollinique, paroi cellulaire, pectines, cellulose, pectate lyases, hyper-gravité, prorpiétés mécaniques

Abstract

One of the most important features characterizing plant cells and differentiating them from animal cells is the cell wall that surrounds them. The cell wall plays a critical role in providing protection to the protoplast; it acts as a filtering mechanism and is the location of many biochemical reactions implicated in the regulation of the cell metabolism and the mechanical properties of the cell. The local stiffness, extensibility, plasticity and elasticity of the different cell wall components determine the shape and geometry of the cell during differentiation and morphogenesis. The goal of my thesis is to understand the role played by the different cell wall components in shaping the plant cell and controlling its growth behaviour. To achieve this goal, I studied the pollen tube, or male gametophyte, as a cellular model system. The pollen tube is a cellular protuberance formed by the pollen grain upon its contact with the stigma. Its main purpose is to deliver the sperm cells to the female gametophyte to ensure double fertilization. The pollen tube is a tip-growing cell characterized by its simple cell wall composition and by the fact that it is the fastest growing cell of the plant kingdom. This makes it the ideal model to study the effects of drugs, mutations or stresses on cellular growth behaviour, metabolism and cell wall mechanics. The pollen tube cell wall consists mainly of proteins and three major polysaccharidic components: pectins, cellulose and callose. To understand the role played by these components in regulating pollen tube growth, I investigated the effects of mutations, enzymatic treatments, hyper-gravity and omni-directional gravity on the pollen tube cell wall. Using mathematical modeling combined with molecular biology and high-resolution electron and fluorescent microscopy I was able to show that the regulation of pectin chemistry is required for the regulation of the growth rate and pollen tube shape and that cellulose is crucial for determining the pollen tube diameter in the sup-apical region. Moreover, I investigated the role of the pectate lyases, a group of pectin digesting enzymes expressed during pollen tube development, and I showed that this enzyme activity is required for the initiation of pollen germination. More importantly, I directly showed for the first time that the pollen tube secretes cell wall loosening enzymes to facilitate its penetration through the style.

Keywords : Pollen tube, cell wall, pectins, cellulose, pectate lyase, hyper-gravity, mechanical properties.

Table of content

List of tables

List of figures

List of movies

Abbreviation list

ABP	Actin binding protein
ADF	Actin depolymerizing factor
ATP	Adenosine triphosphate
BK	Brewbaker and Kwack
BP	Band pass
BSA	Bovine serum albumin
CBM3a	Cellulose Binding Module 3a
CCD	Charged coupled device
cDNA	Complementary DNA
CESA	Cellulose synthases
CFP	Cyan fluorescent protein
CGA	1-cyclohexyl-5-(2,3,4,5,6-pentafluorophenoxy)-1λ4,2,4,6-thiatriazin-3-amine
DCB	2,6-dichlorobenzonitrile
DIC	Differential interference contrast
DNA	Deoxyribonucleic acid
EGTA	Ethylene glycol tetraacetic acid
ER	Endoplasmic reticulum
ESTEC-ESA	European Space Research and Technology Centre – European Space Agency
FDA	Fluorescein diacetate
FE	Finite element
FP	Fluorescent protein
FRAP	Fluorescence recovery after photobleaching
FTFLP	Fluorescent tagging of full length protein
g	Earth gravity level
GalA	Galacturonic acid
GAX	Glucoarabinoxylan
GFP	Green fluorescent protein
GTP	Guanosine triphosphate
HG	Homogalcturonan
Ig	Immunoglobulin
LDC	Large diameter centrifuge
LP	Long pass
MW	Microwave
NAD	Nicotinamide adenine dinucleotide
NAD(P)H	Nicotinamide adenine dinucleotide phosphate-oxidase
PB	Phosphate buffer

PBS	Phosphate buffer saline
PCR	Polymerase chain reaction
PG	Polygalacturonase
PL	Pectate lyase
PME	Pectin methylesterases
PMEI	Pectin Methylesterase Inhibitor
$PtdInsP_2$	Phosphatidylinositol 4,5-bisphosphate
RGI	Rhamnogalacturonan I
RGII	Rhamnogalacturonan II
RNA	Ribonucleic acid
ROS	Reactive oxygen species
RPM	Random position machine
Rpm	Revolution per minute
RT	Reverse transcription
RT-PCR	Real time polymerase chain reaction
SDS-PAGE	Sodium dodecyl sulfate polyacrylamide gel electrophoresis
SEM	Scanning electron microscopy
SI	Self incompatibility
SNARE	Soluble N-ethyl-maleimide-sensitive fusion protein attachment protein receptors
TBS	Tris-buffered saline
T-DNA	Transfer DNA
TEM	Trransmission electron microscopy
TIRF	Total internal reflection fluorescence
UDP	Uracil di-phosophate
UTR	Untranslated region
UV	Utlra-violet
VAEM	Variable angle epifluorescence microscopy
XGA	Xylogalacturonans
XTH	Xyloglucan endotransglycosylase/hydrolases
XyG	Xyloglucans
YFP	Yellow fluorescent protein

Nothing shocks me. I'm a scientist

Indiana Jones,

Indiana Jones and the Temple of Doom, 1984

To the best parents one could wish for
who always taught me to pursue
my dreams till the end
and never surrender
in front of any
obstacle…

Acknowledgments

I would first like to thank Prof Anja Geitmann for believing in me. It is an honour and a privilege to have her as a mentor. I am most grateful for all the scientific opportunities, support, guidance, tutoring and help she offered me. I would also like to thank her for her humanity, care, generosity and friendship she continuously shows. I am touched and deeply thankful for everything, Anja.

Without the constant and indefectible support, counsel, blessings and prayers of my parents and my family, none of this would have been possible. Thank you Mom, Dad, Ziz, Naaman, Dalal, Nay, Nad and Léyou for being who you are and for your perpetual encouragements. I would also like to thank all my family in Lebanon, Belgium and Canada for their kindliness, I love you all!

Their encouragements, counsel, help and presence at all times were primordial throughout the evolution of this thesis. I am profoundly grateful to Simon Desharnais, Leila Aouar, Firas Bou Daher, Chloe van Oostende Triplet and Thomas Triplet for everything they did and are still doing!

I would like to thank my friends Monisha Sanyal, Mahsa Naghavi, Minako Kaneda and Samuel Juillot, as well as all my colleagues Marie Glavier, Pascal Arpin, Amir Jafari, Robert Palin, Xudong Sun, Olivier Gossot, Rabah Zerzour, Jérôme Bove, Pierre Fayant and Orlando Girlanda for all the help they provided.

During these years, I had the opportunity to supervise several internship students. Thank you Maxime Grare, Aude Kouma, Lauranne Pujol, Anahid Shojaeifard and Marius Andre for your hard work, commitment and for the excellent times we shared together.

A very special thank to my friend Louise Pelletier for her kindness, her invaluable help in microscopy, her precious advices and for all the care she shows.

I thank all the staff members, professors and students of the Institut de Recherche en Biologie Végétale for all the help and support they provided.

I would like to thank the European Space Agency for giving us the opportunity and providing the technical expertise, the funding and the logistics to study the effect of hypergravity on pollen tube development. I am particularly thankful to Dr. Jack van Loon and to the *Spin Your Thesis!* staff: Dr. Natacha Callens, Tim Setterfield, Carlos Gomez-Calero, Jutta Krause and Alan Dowson.

I wish to thank all the agencies who funded me throughout my Ph.D: The Ann Oaks doctoral scholarship of the Canadian Society of Plant Biologists / La Société canadienne de biologie végétale. The Canadian Space Agency / L'Agence spatiale canadienne. The Marie-Victorin doctoral scholarship of the Institut de Recherche en Biologie Végétale. And various Université de Montréal scholarship programs.

I would like to thank all the members of the jury for critically reading this thesis and providing edifying comments.

Finally I would like to thank God for putting on my way such incredible people and opportunities.

1 Introduction

The first plants probably appeared on Earth around 1 200 million years ago (during the mezoproterozoic era) in form of algal scum, although the first fossil evidence of land plants dates from 470 million years ago (Wellman and Gray 2000), and it is generally thought that plants started to colonize the land between 630 and 510 million years ago (Raven and Edwards 2001; Clarke *et al.* 2011). During evolution, different groups of land plants appeared successively. The first to appear were non-vascular bryophytes (liverworts, worts and mosses), while seedless vascular plants made their appearance along with lycophytes and pterophytes around 425 million years ago. Gymnosperms (vascular seed plants) appeared roughly 325 ± 50 million years ago followed by angiosperms (or flowering vascular seed plants) 200 ± 50 million years ago (Jiao *et al.* 2011).

Plants have contributed to the development of mankind in several ways. More generally, due to their capacity for oxygenic photosynthesis, they have contributed to the richly oxygenated atmosphere that has allowed animal life to develop extensively. Human life, appearing only around 4.5 million years ago, has depended on plants as the foundation for development since the dawn of civilization. Not only are plants essential for food, nutrient supplies and medication, they have also been used as day-to-day tools to tie silex stones together, to set traps for animals and to construct shelters. With time, the importance of plants became more pronounced in fulfilling daily needs, being used for clothing, paper, furniture, housing construction, isolators, and biofuels. Interestingly, most of these applications rely on the composition and structure of the plants in general and in particular, on one major component of the plant cell. This component, called the cell wall, is an outer envelope rich in carbohydrates and polymers that confers to the cell its characteristic mechanical properties.

1.1 The plant cell wall: Role and importance of its mechanical properties

The plant cell wall is a tough outer structure surrounding plant cells. It is characterized by a heterogeneous chemical composition that confers, to each different cell and tissue, specific mechanical properties defined by tensile strength, rigidity, elasticity, and plasticity. These characteristics crucially influence most industrial applications of plant material ranging from the use of wood for construction to the texture of plant-derived food products.

On a cellular level, the plant cell wall provides the cell with protection from pathogen infections, acts as a filtering mechanism and most importantly, plays a structural role (Essau 1977). Because of the cell wall, plant cells are able to build up a high internal pressure called turgor. If the cell wall mechanical properties are not well balanced with the turgor pressure, the cell risks bursting. The cell wall also allows plants to stand upright, as without it, plants would only be a pile of cells collapsed by gravity and without a defined structure. The cell wall thus has a function analogous to the extracellular matrix of animal cells. During plant development, the balance and spatio-temporal regulation of the mechanical properties of the cell wall are therefore vital: while cell growth is ongoing, the cell wall is characterized by higher elastic and malleable properties than the already differentiated cells that have stopped growing and are more rigid.

1.2 Primary and secondary cell walls

The layers of the plant cell walls can be distinguished into two types, a primary cell wall that is formed during cell morphogenesis and that is highly flexible, and a secondary cell wall, which is formed of more complex molecules and appears when the cell has stopped growing. The secondary cell wall is not formed in all cell types but is restricted to cells requiring structural reinforcements such as xylem fibers, tracheids, or sclereids. The secondary cell wall accounts for most of the carbohydrate biomass of the plant and provides additional protection and strength to the whole organism. The secondary wall is deposited between the plasma membrane and the primary cell wall of cells that have stopped

expanding and need mechanical reinforcement. For example, wood consists mostly of secondary cell wall; its mechanical role is to hold the plant up against the gravity.
While the primary cell wall consists mainly of a cellulose-hemicellulose network embedded in a matrix of pectins and proteins and is generally flexible and extensible, the secondary cell wall is more rigid and is mainly formed of cellulose and xylan and contains many glycoproteins and polysaccharides as well as other compounds such as lignin and cutin. Contrary to the primary cell wall which is basically formed of one layer, the secondary cell wall is usually formed of different laminated sheaths where the cellulosic fiber orientation is parallel within an individual layer but can differ between the layers. The importance of the cellulose fiber orientation is detailed in paragraph 1.7. The subsequent deposition of hydrophobic components such as lignin drastically reduces the permeability of the secondary cell wall. Hence, water transport across the secondary cell wall is severely limited and is accomplished through specialized openings in the cell wall called pits. Pits can be found mostly between vascular cells (tracheids and vessel elements) and between parenchyma cells (Essau 1977; Raven *et al.* 1986; Cosgrove 2005; Obel *et al.* 2007).

During morphogenesis, the undifferentiated somatic cell has to undergo several differentiation steps to acquire its final function, size and shape. During this process, the cell undergoes drastic morphological changes. From a relatively simple spherical shape, the cell will develop into a body with more complex geometry such as in jigsaw puzzle-shaped pavement cells, in trichomes, in fibres, in sclereids or in pollen grains. Because the cell wall is the most important architectural element of the plant cell, it plays a central role throughout the morphogenetic processes. The regulation of the local cell wall mechanical properties (reflected by the local chemical composition) is decisive in shaping individual cells, organs and organisms.

1.3 State of the art

The goal of this thesis is to understand the role played by the different cell wall components in shaping the cell and controlling the growth behaviour.

To achieve this goal, I rely on a specific experimental model system, the male gametophyte or pollen tube. The reasons for the use of this system are detailed in the paragraph 1.7.4 (importance of the pollen and the pollen tube) below.

In the following sections of the introduction, I review first what is known about the primary cell wall components in plant cells from a metabolic, regulatory and mechanical point of view. I also review the factors that influence the biological and mechanical regulation of plant cell growth. In a second part, I review what is known about pollen tube growth and finally I expose the goals and objectives of the present thesis. The thesis will be constructed from 8 chapters exploring the roles of the different cell wall components (mainly cellulose and pectins) and the role of several biotic (pectate lyases and pectinase) and abiotic (omni-directional gravity and hyper-gravity) factors in regulating pollen tube shape and growth behaviour. The last part of the thesis consists in a general discussion and elaborates on the perspectives for future research.

1.4 Pectins in the primary cell wall

Pectins are the major component of primary cell walls and of the middle lamella in dicotyledonous plants where they can amount to around 35% of the cell wall dry weight (Smith and Harris 1999). They are rare in non-extensible secondary cell walls. Pectins are polysaccharides rich in galacturonic acid (GalA) with an extremely complex composition as they may contain up to 17 different monosaccharides (Willats *et al.* 2001). Pectins form a highly heterogeneous group. Three different types of polysaccharides can be distinguished depending on the diversity of both their backbones and their side chains: Homogalacturonan (HG), Rhamnogalacturonan I (RGI) and Rhamnogalacturonan II (RGII) (Figs 1.1 and 1.2).

HG and RGII have the same backbone formed by a linear polymer of (1,4)-linked-α-d-GalA. HG do not have any side chains and can be methyl-esterified at *C*-6 or carry acetyl groups at *O-2* and *O-3*. The GalA may be substituted at *C-2* and *C-3* with an apiose thus forming apiogalacturonans found in certain species such as *Lemna minor* and *Spirodela polyrrhiza* (Hart and Kindel 1970; Longland *et al.* 1989). The substitution at *C-3* with a xylose leads to the formation of xylogalacturonans (XGA) that can be found in the seed coats of pea, apple, watermelon fruit and carrot cells (Kikuchi *et al.* 1996; Schols and Voragen 1996; Renard *et al.* 1997; Le Goff *et al.* 2001). In RGII, four heteropolymeric side chains containing more than eleven different sugars can be attached to the main backbone (Vidal *et al.* 2000). The structures of RGII are very well conserved in plants. RGII can also be cross-linked by borate ester links through their apiosyl residues (Ishii *et al.* 1999; Pelloux *et al.* 2007). The backbone structure of RGI differs from HG and RGII as it consists of repeated $[(1\rightarrow2)$-α-l-rhamnose-$(1\rightarrow4)$-α-d-galacturonate$]_n$ disaccharide units, where n can be greater than 100 (McNeil *et al.* 1980; Vincken *et al.* 2003). Galacturonyl residues can be acetylated at their *O-2* or *O-3* positions and rhamnosyl residues can be substituted at *O-4* with neutral sugars (Vincken *et al.* 2003). The diversity of pectins is summarized in figure 1.1.

Pectins are synthesized from nucleotide sugars in the Golgi apparatus. They are polymerized in the cis-Golgi by at least 53 different glycosyl-transferases. Pectins (mainly HG) are then methylesterified in the medial-Golgi by methyl-esterases at the *C-6* carboxyl of GalA. Side chains are then attached to the backbone in the trans-Golgi. Pectins are secreted in a highly esterified form (70 to 80% of all carboxyl groups are esterified) into the apoplast through vesicle exocytosis (Willats *et al.* 2001; Vincken *et al.* 2003).

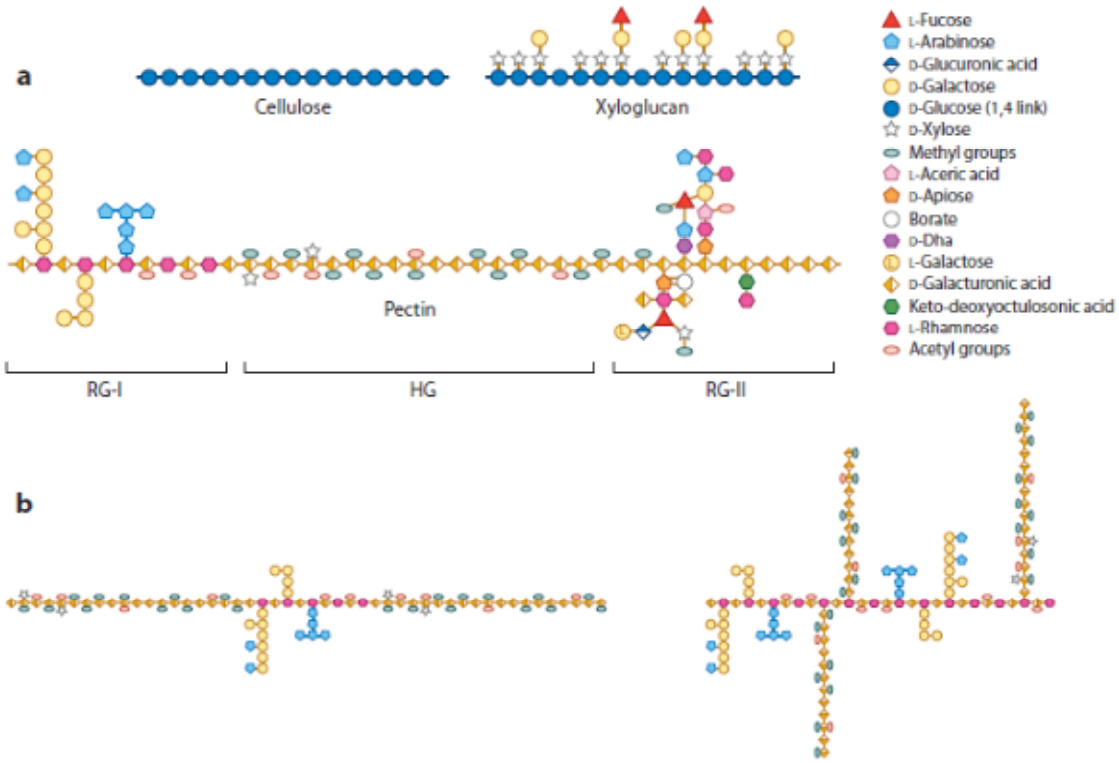

Figure 1.1: Structure of some cell wall components.

(A) Schematic representation of cellulose, xyloglucan, and the pectic rhamnogalacturonan I (RG-I), homogalacturonan (HG), and RG-II. Adapted from (Burton *et al.* 2010) with permission. (B) Alternative models for pectin domain organization. A linear, contiguous arrangement of HG interspersed with RG-I is shown on the left, whereas on the right, HG is drawn as side chains linked to Rha residues of the RG-I scaffold. A combination of both models may also be possible. Adapted from (Round *et al.* 2010) with permission. This figure and legends were taken from (Wolf *et al.* 2012).

Pectins are the major adhesive material between cells; its network serves as a matrix for the deposition, slippage and extension of the cellulose-glucan network and is involved in the regulation of cell wall porosity and modulation of the cell wall pH and ion balance (Cosgrove 1999; Willats *et al.* 2001). Pectins also play the role of signalling molecules during plant defence reaction to pathogen and insect attacks (Collmer and Keen 1986). Because of their stabilizing properties, pectins are wildely used in the food industry as a gelling and thickening agent and many studies have investigated their rheological and gel-

forming properties depending on their pattern of methyl-esterification (Daas *et al.* 2000; Osborne 2004).

The degree of pectin esterification plays an important role in determining the mechanical properties of the cell wall. Pectins are secreted at the cell wall in a highly esterified form and subsequently subjected to the action of different enzymes such as pectin methylesterases (PME), pectate lyases (PL) and polygalacturonases (PG) and different ions such as boron or calcium. PME is known to lead to the de-esterification of pectins *in muro* and render them susceptible either to gelation by divalent ions such as Ca^{2+} or to the action of pectin degrading enzymes such as PL and PG, giving the cell wall different mechanical properties. PMEs, PLs and PGs are known to be implicated in many physiological processes in plant cells such as cell differentiation, cell wall expansion, cellular adhesion and maturation and senescence of fruits (Bosch and Hepler 2005).

1.4.1 Pectin-methyl-esterases and pectins

PMEs catalyze the specific demethylesterification of HG *in muro* at the *C-6* position of GalA, releasing methanol and generating a negatively charged carboxyl group. PMEs have two modes of action; they can either act in a block-wise or in a random fashion. PME isoforms working in a block-wise fashion create long blocks of contiguous free carboxyl groups susceptible to interact with Ca^{2+}, thus forming the 'egg-box' model structure resulting in a stiff gellified three dimensional pectate network (Willats *et al.* 2001). At least 9 contiguous carboxyl residues are required to favour calcium cross-linking (Liners *et al.* 1992). PME isoforms acting randomly lead to a random demethylesterification of the GalA, thus promoting the action of pectinases such as PL and PG, leading to cell wall loosening (Willats *et al.* 2001; Pelloux *et al.* 2007).

Different PME isoforms were identified and isolated in different plant species and tissues. In *Arabidopsis*, 66 ORFs have been annotated as putative full-length enzymes (CAZy, http://www.cazy.org)(Cantarel *et al.* 2009) and transcriptomic studies showed that more than 22 PMEs are expressed in the pollen and leaves (Honys and Twell 2003; Pina *et al.* 2005). In *Arabidopsis*, many studies have focused on the role of different PME isoforms

in the development and differentiation (Pina *et al.* 2005) of organs such as mucilage release from seeds, during pollen and pollen tube development, and in hypocotyl and apical meristem differentiation (Micheli 2001; Jiang *et al.* 2005; Francis *et al.* 2006; Peaucelle *et al.* 2008; Rautengarten *et al.* 2008). In many other plant species PMEs have also been isolated from various organs such as the poplar and mung bean cambium, *Vigna radiata* hypocotyls, the pea root border cells, the yellow cedar seeds, *Solanum tuberosum* stems, carrot roots, *Peunia inflata* pollen, and in the development of a plethora of fruits like apple, kiwi, water melon, fig tomato, strawberries, berries, bananas (Versteeg *et al.* 1978; Kozo *et al.* 1990; Bordenave *et al.* 1996; Louvet *et al.* 2006). The activity of several PME isoforms was found to be temporally and spatially regulated during cell wall formation and maturation in seeds, hypocotyls, root hairs and cambium. Collectively, these findings suggest that during the first developmental stages of the above mentioned tissues, PME isoforms working in a non-blockwise fashion seem to be activated to loosen the cell wall by facilitating the action of PL and PG and thus allowing cell wall expansion. In later stages, during cell wall maturation, other isoforms working in a blockwise manner seem to be activated, leading to stiffening the cell walls via the formation of calcium bridges (Bordenave and Goldberg 1994; Bordenave *et al.* 1996; Ebbelaar *et al.* 1996; Guglielmino *et al.* 1997; Micheli *et al.* 2000; Ren and Kermode 2000; Micheli 2001; Louvet *et al.* 2006; Western 2006; Derbyshire *et al.* 2007; Rautengarten *et al.* 2008; Arsovski *et al.* 2010).

PMEs can be divided into two groups (group I and group II) depending on the absence or presence of a PRO region in the N-terminus of the mature protein. The PRO region shares sequence similarities with a PME inhibitor (PMEI) domain (Camardella *et al.* 2000) and exerts an inhibitory effect on PME activity (Giovane *et al.* 2004; Röckel *et al.* 2008) as shown in tobacco pollen tubes by inhibiting premature deesterification of the pectins in the Golgi apparatus (Bosch and Hepler 2005). In *Arabidopsis,* the PMEs of group I do not have PRO regions; they are characterized by five or six introns and have a molecular weight under 45 kDa, whereas the PME of group II have one to three PMEI-like domains, two to three introns and a molecular weight comprised between 50 and 105 kDa (Micheli 2001; Tian *et al.* 2006). Both groups of PMEs are targeted to the cell wall and the presence or absence of the PRO region does not influence the targeting to the plasma

membrane since the PMEs of group I contain a N-terminus rich in hydrophobic amino acids which could play the role of a membrane target (Camardella *et al.* 2000; Micheli 2001; Al-Qsous *et al.* 2004; Bosch *et al.* 2005; Bosch and Hepler 2005; Tian *et al.* 2006; Pelloux *et al.* 2007).

1.4.2 Pectate lyases (PLs) and pectins

Pectate lyases (also known as pectate trans-eliminases) are known in plants and fungi to hydrolyse the cell wall by transforming non-esterified pectins into unsaturated oligogalacturonades, leading to an increase in the elasticity and/or plasticity of the cell wall. PL activity has been shown for the first time in 1962 in pathogeneous cultures of *Bacillus sp*. (Starr and Moran 1962). The structures and roles of bacterial PLs have been well studied in *Erwinia chrysanthemi* (Wing *et al.* 1990): the bacterial PLs hydrolyse the plant cell walls which leads to the necrosis and death of the infected tissues (Yoder *et al.* 1993; Lietzke *et al.* 1994; Pickersgill *et al.* 1994; Scavetta *et al.* 1999; Herron *et al.* 2000; Herron *et al.* 2003).

In plants, the majority of the studies related to PLs were conducted in the context of fruit maturation. In tomato (Marin-Rodriguez *et al.* 2002), banana (Pua *et al.* 2001) and strawberry (Jimenez-Bermudez *et al.* 2002) PLs play a role during fruit maturation and studies showed that when PL expression was knocked-out, fruit senescence was retarded. Studies conducted on the pollen of tomato (Kulikauskas and McCormick 1997) showed the presence of highly conserved homologous PL coding sequences with *Erwinia*. These sequences were also found to be highly expressed in anthers and pistils of tomato (Kulikauskas and McCormick 1997). PLs are also known to pose a problem of public health as many of them are thought to be implicated in human allergic reactions to pollen (Taniguchi *et al.* 1995; Shreffler 2011; Augustin *et al.* 2012; Suzuki *et al.* 2012).

A number of studies have shown that PL-like genes are highly expressed in pollen grains from tobacco, *Arabidopsis* (Kulikauskas and McCormick 1997), alfalfa (Wu *et al.* 1996) and Japanese cedar (Taniguchi *et al.* 1995), leading to speculation that they might be implicated in the early stages of pollen germination or are employed by the pollen tube to

digest the transmitting tract. Several PLs and PL-like genes have been shown to be expressed in *Nicotiana tabacum* pollen (Wing *et al.* 1990; Kulikauskas and McCormick 1997), and in *Arabidopsis* more than 20 PL-like genes (Pina *et al.* 2005) are expressed in pollen grains. However PLs are known to be synthesized in pollen, it is unknown what role they play. They could potentially be involved in initiating pollen tube growth by softening the aperture wall or could be involved in regulating the cell wall mechanical properties of the elongating tube. Alternatively, they might not act on the pollen itself, but on the apoplast of the pistillar tissues with the purpose of loosening it to facilitate pollen tube invasive growth. These functions are not mutually exclusive. In chapter 6 I show and discuss in more detail the role of PLs during pollen germination and pollen tube growth.

1.4.3 Polygalacturonases and pectins

Other genes coding pectin-degrading enzymes such as pectin-esterases, β-galactosidase and polygalacturonases are expressed during cell differentiation. Their major roles, just like PLs, are to cleave pectins and increase the elasticity of the cell walls. These enzymes are known to be expressed in different organs like leaves, seeds, roots, flowers and in pollen grains as shown by transciptomic studies (Torki *et al.* 2000; Pua *et al.* 2001; Pina *et al.* 2005). They were shown to be required during senescence and abscission of certain organs and fruits (Torki *et al.* 2000). They are also known to be secreted by fungi and bacteria to facilitate their penetration into the plant tissues.

Many of these enzymes are specifically expressed in pollen grains and pollen tubes of *Brassica napus* (Robert *et al.* 1993; Daas *et al.* 2000), maize (Niogret *et al.* 1991) and tobacco (Tebbutt *et al.* 1994), but despite the fact that they are studied in more detail than PLs, their roles in pollen development are still not clear. Just like PLs, their putative role during pollen and pollen tube development could be to facilitate pollen tube elongation by hydrolyzing the middle lamella of the transmitting tissue.

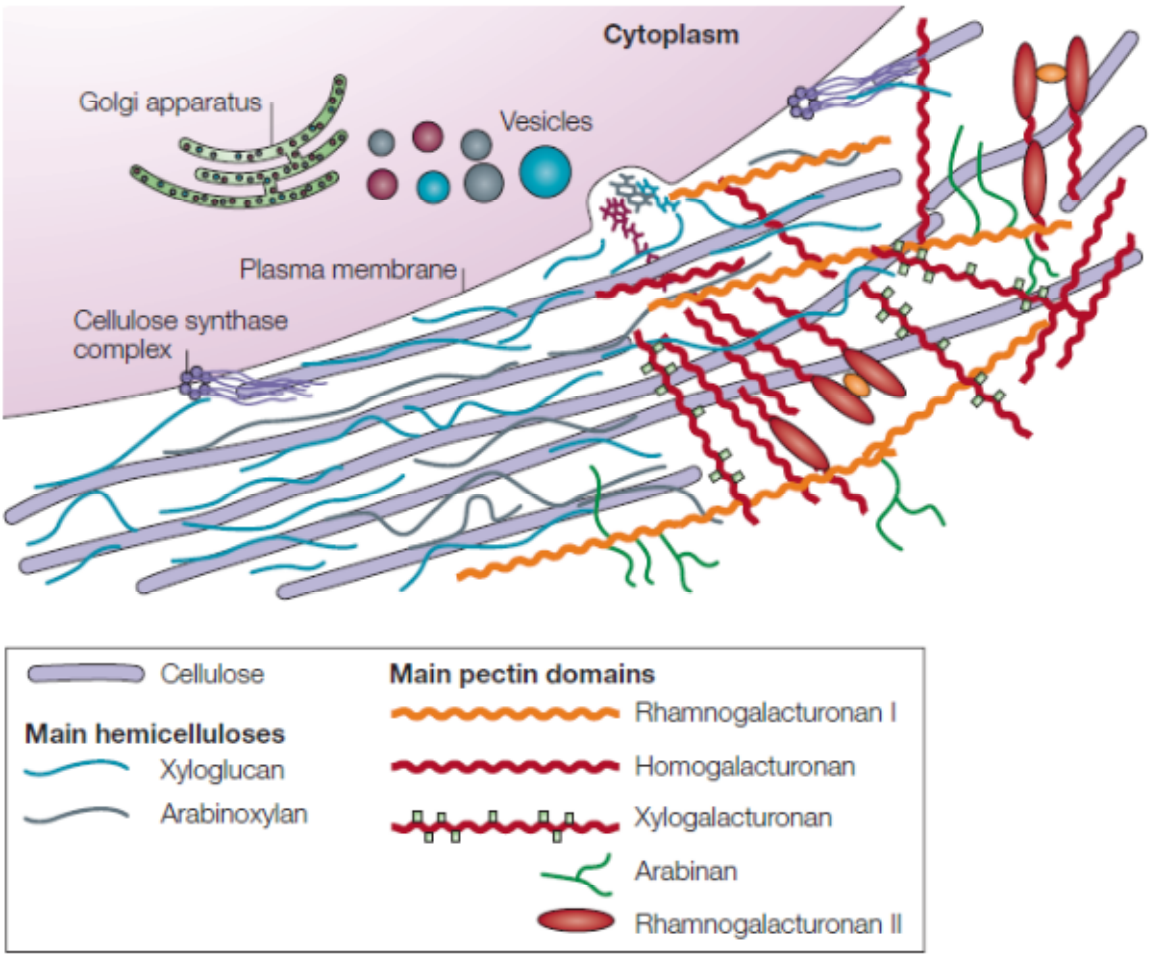

Figure 1.2: Structure of the primary cell wall.

Cellulose microfibrils (purple rods) are synthesized by large hexameric complexes in the plasma membrane, whereas hemicelluloses and pectins, which compose the matrix polysaccharides, are synthesized in the Golgi apparatus and are deposited to the wall surface by vesicles. For clarity, the hemicellulose–cellulose network is shown on the left part of the cell wall without pectins, which are emphasized on the right part of the figure. In most plant species the main hemicellulose is xyloglucan (blue), while hemicelluloses such as arabinoxylans (grey) and mannans (not shown) are found in lesser amounts. The main pectin polysaccharides include rhamnogalacturonan I and homogalacturonan, with smaller amounts of xylogalacturonan, arabinan, arabinogalactan I (not shown) and rhamnogalacturonan II. Pectin domains are believed to be covalently linked together and to bind to xyloglucan by covalent and non-covalent bonds. Neutral pectin polysaccharides (green) are also able to bind to cellulose surfaces. This figure and legend were taken from (Cosgrove 2005).

1.5 Cellulose in the primary cell wall

Cellulose (1,4-β-D-glucan) is the most abundant biopolymer on Earth. It accounts for more than a third of the total dry weight in plants. It is most abundant in secondary cell walls (Fig 1.2), but the primary cell wall contains a significant amount as well. Cellulose microfibrils are formed by parallel chains of 500 to 14 000 β-1,4-glucose linked by hydrogen bonds and by xyloglucans chains (Somerville 2006). Cellulose microfibrils are 3 to 5 nm wide and can reach many micrometers in length (Cosgrove 2005).

1.5.1 Cellulose synthesis

Cellulose is synthesized at the plasma membrane by large enzymatic complexes formed by cellulose synthases (CESA) identified in the late 1990s by molecular and genetic studies (Pear *et al.* 1996; Arioli *et al.* 1998). In angiosperms, cellulose synthases are organized in hexameric arrays called rosettes which were revealed by freeze fracture (Kimura *et al.* 1999). The rosettes are located at the plasma membrane and contain six rosette subunits each of which is formed from six CESA subunits encoded by three different *CESA* genes. The dimerization of different CESAs is thought to be mediated by two adjacent zinc fingers in the N-terminal region of each CESA protein (Kurek *et al.* 2002; Cosgrove 2005). Each species is characterized by a defined number of *CESA* genes (10 for *Arabidopsis*, 12 for maize, 9 for rice, 8 for barley, 7 for aspen ...) with the sequences of the respective orthologues being closer than that of the paralogues (Somerville 2006; Taylor 2008) suggesting that from an evolutionary point of view, the different CESA families were established in the common ancestors of vascular plants. Different sets of genes are required for the synthesis of cellulose in the primary (*AtCESA1*, *AtCESA2*, *AtCESA3*, *AtCESA5*, *AtCESA6*, *AtCESA9*) and secondary walls (*AtCESA4*, *AtCESA7*, *AtCESA8*) (Arioli *et al.* 1998; Fagard *et al.* 2000; Taylor *et al.* 2003; Cosgrove 2005; Taylor 2008). Because of the structure of the rosette, it is thought that cellulose microfibrils are made of 36 glucan chains (Taylor 2008). However, recent studies have shown that because of geometrical and mechanical constraints it is more likely that 18 to 30 glucan chains form the cellulosic microfibrils (Emons *et al.* 2007). Proteomic analysis coupled to computational methods showed that *CESA* are characterized by eight trans-membrane

domains (Nühse *et al.* 2004). The structure of CESA is summarized in figure 1.3. The cellulose synthases are not fixed at one position, but are in constant movement in the plane of the plasma membrane (Paredez *et al.* 2006). This movement seems to be guided by cortical microtubules, but can also occur independently of cytoskeletal guidance. It is thought to be driven in self-generated fashion by the forces created by polymerization and crystallization of the cellulose microfibrils (Emons *et al.* 2007).

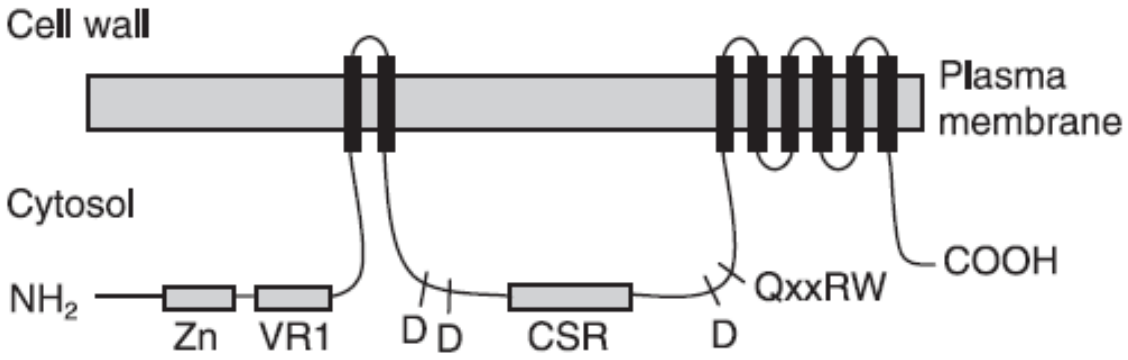

Figure 1.3: Membrane topology of a CesA protein.

Black bars indicate trans-membrane domains. Zn, zinc-binding region; VR1, variable region 1; CSR, class-specific region. Approximate positions of D, D, D, QXXRW processive glycosyl transferase motifs are shown. This figure was taken from (Taylor 2008).

1.5.2 Regulation of cellulose synthesis

Other proteins are known to be important for cellulose synthesis regulation: KORRIGAN, COBRA and KOBITO. *KORRIGAN* encodes for a endo-β-1,4-glucanase and was shown to be required during normal cellulose synthesis in primary and secondary cell walls (Nicol *et al.* 1998; Lane *et al.* 2001). Mutations in *KORRIGAN* result in improper crystallization of cellulose microfibrils and reduced amount of cellulose in the primary and secondary cell walls. This lead to a defect in cytokinesis and cell elongation, dwarfism (Nicol *et al.* 1998), radial swelling of root tips (Lane *et al.* 2001) and collapse of xylem

vessels (Szyjanowicz *et al.* 2004). KORRIGAN is not directly associated with CESA complexes, its roles during cellulose synthesis are not clearly defined and attempts to characterize the subcellular localization of the protein have been inconclusive and inconsistent (various studies proposed association with Golgi, endosomes, primary and secondary cell walls). *COBRA* encodes a glycosyl-phosphatidylinositol (GPI)-anchored protein targeted to the plasma membrane. Knock-out COBRA mutants show a reduction in the amount of synthesized cellulose and a disorganized cellulosic net orientation. This results in deficiency of polarized cell growth of most developing organs in *Arabidopsis* (Roudier *et al.* 2005). *KOBITO* encodes a protein of unknown function but mutants for this gene were characterized by a dwarf phenotype and randomized microfibrils orientation (Pagant *et al.* 2002).

1.6 Hemicelluloses in the primary cell wall

Hemicelluloses are defined as being *"wall polysaccharides that are not solubilized from wall materials with buffers, hot water, or chelating agents but only with more or less strong chaotropic agents such as alkali*'' (Obel et al. 2007). They comprise several families of polysaccharides that have in common a β-1,4-d-pyranosyl backbone but that differ from each other and from cellulose by their respective side chains. Depending on the chemical nature of these side chains, three major families of hemicelluloses can be distinguished, the xyloglucans, the mannans and the xylans. These families can be subdivided in sub-families depending on the nature of all their side chains (Fig 1.2).

1.6.1 Xyloglucans

Xyloglucans (XyG) consist of a backbone of 1,4-linked *β*-d-Glc with several *α*-d-Xyl substituents at *O*6. They are characterized by several side chains made of galactose, fucose, xylose or glucose. The nature of the side chains varies depending on the tissue and on the local physiological requirements. They are the most abundant hemicelluloses present in the cell walls of dicotyledon plants (Obel *et al.* 2007). The XyG backbone is synthesized in the Golgi *cis*-cisternea whereas the addition of the side chains by fucosylation or galactosylation occurs in the *trans*-cisternea and in the transport vesicles (Brummell *et al.*

1990). Once exported to the apoplast by exocytosis, XyG are directly bound to cellulose in the cell wall (Edelmann and Fry 1992) in a non-covalent way (Acebes *et al.* 1993; Hayashi *et al.* 1994a), probably with hydrogen bonds, since their binding to cellulose is pH-dependent (Hayashi *et al.* 1987). Several enzymes such as glucosyl- and xylosyltransferases (Gibeaut and Carpita 1994), XyG-glucan synthase, *α*-Xyl*p*-transferase (AtXT1) (Faik *et al.* 2002), *α*-Fuc*p*-transferase (Faik *et al.* 2000; Vanzin *et al.* 2002; Madson *et al.* 2003), GDP-D-mannose 4,6-dehydratase (Bonin *et al.* 1997), *α*-fucosidase, *β*-galactosidase, *α*-xylosidase, and *β*-glucosidase (Iglesias *et al.* 2006; Obel *et al.* 2007) as well as a multitude of nucleotide sugar interconversion enzymes (Reiter and Vanzin 2001) are implicated in the different stages of XyG synthesis and regulation. In *Arabidopsis*, eight allelic mutants were identified as being implicated in the *de novo* synthesis of xyloglucans and more specifically of l-fucose. These genes were named the *mur* mutants in reference to the wall (*murus* in Latin) (Reiter *et al.* 1993; Reiter *et al.* 1997). The mutant for the *mur1-1* gene which encodes a GDP-D-mannose 4,6-dehydratase isoform (Bonin *et al.* 1997), was found to have a 40% deficiency in l-fucose in root and 1% in aerial parts of the plant when compared to the wild type. This resulted in slightly dwarfed plants with a two-fold reduction in the strength of the elongating inflorescence stems when compared to the wild type (Reiter *et al.* 1993). These phenotypes were later attributed to an l-fucose deficiency affecting not only XyG, but also glycoproteins and pectins (RGI and RGII) (Bonin *et al.* 1997; O'Neill *et al.* 2001). Leaky mutants *mur1-3* and *mur1-7* also show a reduced amount of fucose in leaves (respectively 30% and 10%) but were normal in regard to the wall mechanical strength and growth behavior (Reiter *et al.* 1993; Reiter and Vanzin 2001). In the *mur2* mutant, the absence of fucosyl residues does not have any effect on the plant phenotype or the cell wall mechanical properties, whereas the absence of the α-l-Fucp-β-GalA side chain in the *mur3* mutant leads to a 50% reduction in the etiolated hypocotyls tensile strength and in the swelling of the hypocotyl base (Vanzin *et al.* 2002; Peña *et al.* 2004). All *mur1*,*mur2* and *mur3* mutants can be rescued by the addition of exogenous fucose.

1.6.2 Xylans

Xylans are synthesised in the Golgi apparatus from UDP-xylose (Feingold *et al.* 1959). They are highly complex polysaccharides formed by a backbone of 1,4-linked *β*-d-Xyl with different side chains that can also undergo *O*-acetylation or *O*-methylation or furoylation (Yoshida-Shimokawa *et al.* 2001). The xylan synthase is not yet characterised but it is stipulated to be a part of cellulose synthase like super-family genes (Richmond and Somerville 2000). One of the major xylans is the glucoarabinoxylan (GAX) which has been found to be the major type of hemicelluloses in the monocotyledon Poaceae family (Gruppen *et al.* 1992), in grasses (Ishii 1991a; Ishii 1991b) and in the dicot sycamore (Darvill et al. 1980). GAX structure can be modified *in muro* by xylans degrading enzymes such as xylanase that was found to be located on the maize pollen tube coat (Bih *et al.* 1999; Wu *et al.* 2002). It was hypothesized to play a role in the hydrolysis of the stigma wall to facilitate pollen tube entry. Other xylanases were found in the seed aleurone layer and were postulated to facilitate germination in barley and wheat (Banik *et al.* 1996; Cleemput *et al.* 1997).

1.6.3 Mannans

Just like xylans, a very wide range of mannans exists in plant; the most common are galactomannans, glucomannans and galactoglucomannans. Galactomannans have a backbone of *β*-(1-4)-linked mannopyranose with an *α*-(1-6)-linked galactopyranose attached to the mannose residue and are found in the endosperms of leguminous seeds (Obel *et al.* 2007). The glucomannans have a backbone of *β*-(1-4)-linked mannopyranose and glucopyranose. They have been found in leaves and xylem fibers in *Arabidopsis* (Zablackis *et al.* 1995; Handford *et al.* 2003). Galactomannans play a role as seed storage polysaccharides and in the regulation of water balance during germination of fenugreek and solanaceous seeds (Buckeridge *et al.* 1997; Mo and Bewley 2003). Several mannansynthases have been characterized in guar bean (Dhugga *et al.* 2004) and in *Arabidopsis* (*AtCslA2*, *AtCslA*7 and *AtCslA9*) (Liepman *et al.* 2005). Knock-out plants of *AtCslA*7 did not complete embryogenesis and were arrested in the globular stage. Plants

defective in *AtCslA*7 were characterized by slower growing pollen tubes (Goubet *et al.* 2003). In tomato an endo-mannanase was found to be located at the surface of the pollen and is thought to play a role during pollen development and in the degradation of the cell wall of the transmitting tissue during pollen elongation (Filichkin *et al.* 2004).

1.7 Cell growth and cell wall expansion

During primary plant cell growth, the cell wall constantly yields under the internal turgor pressure until the cell achieves its final shape and function. Tight regulation of this expansion both spatially and temporally are required for the cell to achieve its proper function (Ortega 2004; Geitmann and Steer 2006; Geitmann and Ortega 2009; Geitmann 2010a). In many cases, when growth had been altered due to a default in the regulation of cell wall expansion, the function of the cell was also altered (extensively reviewed in (Cosgrove 2000a; Cosgrove 2000b; Cosgrove 2005; Somerville 2006; Obel *et al.* 2007)).

From a mechanical point of view, expansion primarily takes place at the weakest point of any given structure; therefore shaping the cell would require the cell wall to be more elastic and malleable at the growing sites, and stiffer at the sites that do not grow or grow less. The mechanical properties of the cell depend directly on the chemical composition of the cell wall and on the orientation of its fibrous components. Hence, several biotic and abiotic factors play a role in the regulation of the local cell wall properties.

1.7.1 The orientation of cellulose microfibrils

Although it is a strong simplification, the cell wall can be considered to be a composite material in which fibrous structures (cellulose microfibrils) are embedded in a matrix or gel (pectins, hemicelluloses). The fibrous component has the potential to confer anisotropic mechanical behavior to the material, caused by a preferential direction in the orientation of the individual fibers. As a result, the cell wall material yields more easily in the direction perpendicular to the fibers providing an explanation for the formation of cell shapes deviating from the default sphere. Unlike during isotropic cell growth, where cell expansion takes place on the entire cell surface and evenly in all directions, anisotropic

growth is characterized by an expansion that is typically more pronounced in one direction (Baskin 2005; Geitmann and Ortega 2009). Consistent with this, field emission scanning electron microscopy has shown that in cells growing isotropically, cellulose microfibrils are found to be oriented randomly, whereas in cells elongating anisotropically, the orientation of cellulose is usually transverse to the main axis of growth (Baskin 2005). While this is true for most anisotropically growing cells such as those composing the root and the shoot tissues, it is not the case for the pollen tube, as I show in chapters 3 and 4.

1.7.2 The role of cell wall loosening factors

Several cell wall loosening factors are known to be implicated in the regulation of cell wall mechanics. As detailed above, many proteic and enzymatic factors such as PME, PMEI, PLs, PGs, and ionic factors such as boron and Ca^{2+} control the cell wall mechanical properties of a growing cell by loosening or hardening the pectin matrix. The temporal and spatial regulation of these factors are crucial for shaping the cell geometry. I discuss the role of the regulation of pectin chemistry in determining the mechanical properties and shape of the pollen tube in more detail in chapters 3, 5 and 6.

When the cell is expanding, the wall polymers are stretched under the internal pressure, putting the cell wall under high stress. To prevent the wall from reaching its elastic limit and thus from bursting, the cellulosic network would have to constantly expand through a controlled process of selective loosening and slippage of the load bearing linkages between the cellulose microfibrils. This must be accompanied by a continuous synthesis of cellulose and matrix polymers to prevent the cell wall from becoming too thin, which would lead to a loss of tensile strength. Different molecular players are implicated in cell wall loosing like expansins, yieldins, endo-(1,4)-β-D-glucanase and reactive oxygen species.

1.7.2.1 Expansins

Expansins are a family of non-enzymatic proteins activated in a pH range of 4.5 to 6, which typically corresponds to the cell wall pH of growing cells (Rayle and Cleland 1970; Cosgrove 1989; McQueen-Mason *et al.* 1992). They are implicated in many

developmental processes where cell wall loosening occurs such as fruit softening and ripening, organ abscission, root hair emergence, pollen tube invasion of the style and meristematic cells differentiation (Cosgrove 2000b). Their action is tightly linked to cell wall expansion induced by several hormones such auxin, gibberellin, cytokinin, ethylene and brassinosteroids (Cho and Kende 1997; Downes and Crowell 1998; Cho and Cosgrove 2002; Sun *et al.* 2005). Expansins have been discovered in bacteria and plants. In plants, two families of expansins (EXPA and EXPB) have been identified in mosses, ferns, gymnosperm and angiosperms. In *Arabidopsis thaliana*, 32 expansin genes have been identified (Li *et al.* 2002; Sampedro and Cosgrove 2005).

The precise molecular mechanism by which expansins loosen the cell wall is not yet well understood. During plant cell growth the turgor pressure creates a tensile stress on the cell wall. By loosening the linkages between the cellulosic microfibrils, expansin allows the cell wall to yield. This yielding is accompanied by simultaneous water uptake. It is hypothesized that expansins disrupt the non-covalent links between cell wall polysaccharides, especially the links between hemicellulose and the surface of the cellulosic microfibrils (McQueen-Mason and Cosgrove 1994; McQueen-Mason and Cosgrove 1995; Cosgrove 2005; Yennawar *et al.* 2006).

1.7.2.2 Endo-(1,4)-β-D-glucanase

As stated above, endo-(1,4)-β-D-glucanase (or cellulase) are wall degrading enzymes that are implicated in cellulose synthesis and cell wall loosening. Their role is not yet fully understood, but over-expression of cellulases from poplar in *Arabidopsis*, resulted in enhanced plant growth and suppression caused reduced growth (Ohmiya *et al.* 1995; Ohmiya *et al.* 2000; Tsabary *et al.* 2003). The authors hypothesize that these enzymes loosen the cell wall by releasing the xyloglucans trapped in the cellulose microfibrils.

1.7.2.3 Xyloglucan endotransglycosylase/hydrolases

Xyloglucan endotransglycosylase/hydrolases (XTH) cleave the β-1,4-linked glucose backbone of a XyG polymer and transfer it to the non-reducing end of another XyG by forming a new β-1,4-glucosyl linkage (Nishitani and Tominaga 1992). The roles of XTH

are still debated and not well understood. They were reported to be implicated in various functions such as the integration of new xyloglucans *in muro* (Thompson and Fry 2001), removing xyloglucans that are not tightly fixed to cellulose (Thompson and Fry 1997), hydrolyzing xyloglucans (Farkas *et al.* 1992; Fanutti *et al.* 1993; Bourquin *et al.* 2002; Matsui *et al.* 2005), fruit softening (Redgwell and Fry 1993), cell wall strengthening (Antosiewicz *et al.* 1997) and cell wall loosening (Fry *et al.* 1992). XTH is usually localized in cell walls undergoing expansion or remodelling (Potter 1994; Hyodo *et al.* 2003; Yokoyama *et al.* 2004; Cosgrove 2005) but XTH mutants (knock-out lines or antisense mutants) do not show a clear effect on the mechanical properties of the cell walls, but rather on the formation of tertiary veins in *Arabidopsis thaliana* and in a 20% increase in the xyloglucan chain size in tobacco (Herbers *et al.* 2001; Bourquin *et al.* 2002; Matsui *et al.* 2005).

1.7.2.4 Yieldins

Yieldins were identified in the cell wall of growing hypocotyls of cowpea (Vigna unguiculata L.) (Okamoto-Nakazato et al. 2000a). Their sequences show a close homology to acidic class III endochitinases and concanavalin B (Okamoto-Nakazato et al. 2000b). Although the process leading to yieldins induced cell wall yielding is not well understood, yieldins were shown to be expressed at a higher level in the elongating regions of the hypocotyls compared to their more mature bases (Okamoto-Nakazato et al. 2000b). The authors suggest that yiedins play an important role during cell elongation by controlling the driving force for cell wall extension (Okamoto-Nakazato et al. 2000a; Okamoto-Nakazato et al. 2000b; Okamoto-Nakazato 2002).

1.7.2.5 Reactive oxygen species

Reactive oxygen species (ROS) are by-products of the oxygen metabolism in cells. The most studied are hydroxyl radicals ($^{\bullet}OH$) and hydrogen peroxide (H_2O_2). Their unpaired valence shell electron confers on them the property of being highly reactive molecules. They are known to be implicated in many cellular processes: The response to stress or to physiological processes (root development and gravitropism, stomatal closure, fruit

softening) (Fry *et al.* 2002; Laloi *et al.* 2004), the formation of secondary metabolites (Sachan *et al.* 2010), defense responses, hormone signaling. They can also operate as secondary messengers (Foreman *et al.* 2003; Mori and Schroeder 2004) and act in cell growth regulation and cell wall mechanics (Carol and Dolan 2006; Nick 2010).

ROS were shown to have several effects on the plant cell wall properties. Hydroxyl radicals ($^{\bullet}OH$) are implicated in cell wall hydrolysis and loosening (Müller *et al.* 2009). They stimulate cell enlargement by cleaving cell wall components through the removal of hydrogen atoms from polysaccharides in a non-enzymatic way (Fry 1998). It has been shown that in maize hypocotyls and coleoptyles (Schopfer 2001; Gapper and Dolan 2006) and during cress root and seed germination (Müller *et al.* 2009), $^{\bullet}OH$ increased cell wall extensibility and induced growth. Also, root growth in maize was suppressed by the inhibition of endogenous $^{\bullet}OH$ formation (Liszkay *et al.* 2004). Endogeneous $^{\bullet}OH$ are produced enzymatically by peroxidases (Liszkay *et al.* 2003) and non-enzymatically by copper ions (Fry *et al.* 2002). Because $^{\bullet}OH$ cleavage is not an enzymatic reaction, the amount of released $^{\bullet}OH$ has to be very tightly controlled so that it does not interfere with functional proteins but only with cellulose and hemicellulose.

Hydrogen peroxide (H_2O_2) is implicated in cell wall strengthening (Bunzel 2010). It is formed by the reduction of O_2 by the NAD(P)H oxidase at the plasma membrane. It was shown to lower cell wall extensibility and inhibit growth (Schopfer 1996; Coelho *et al.* 2002; Barceló and Laura 2009). One has to be careful when interpreting the effect of ROS on the cell wall because these molecules are also implicated in plant cell signaling pathways, and the observed effect could be directly or indirectly caused by the presence or absence of ROS. Nevertheless, ROS have been shown to be required for plant cell growth and development. One example is the importance of ROS for pollen germination, where they were detected and visualized in mitochondria of hydrated pollen grains, in the pollen cell wall and at the tip of growing pollen tubes (Boldogh *et al.* 2005; Potocký *et al.* 2007; Smirnova *et al.* 2009; Speranza *et al.* 2012). In low concentrations of ROS, kiwifruit pollen tube germination was inhibited (Speranza *et al.* 2012). The results of these studies

underline the crucial roles of ROS during the initiation of pollen tube germination and elongation.

1.7.3 The role of abiotic factors like gravity

Many abiotic factors are known to influence plant growth and plant cell shape and often this influence is mediated by an effect on cell wall assembly or cell wall mechanical properties. Water, light, nutrient, type of soil, pollution, temperature and humidity are all non-biological factors that are known to have a major effect on plant development and cell shape. All these factors have in common that they are not constant and may vary in space and time. However, one constant factor plants had to adapt to in a specific and permanent manner is the gravity level on Earth. The gravity level has not varied in time and it varies only very slightly in space: 0.5% in latitude and $1/R^2$ (where R is the distance of the object to the center of the Earth) in altitude (Boynton 2001). Plants adapted their metabolism and cell wall composition to this constant factor in a permanent manner. With the advances of space science and the potential of growing plants away from Earth, understanding the behaviour of plants at a macroscopic and microscopic level to a change in the gravity level has become important. In chapter 7, we review the advances made in understanding the role of gravity on the development of plants and on individual plant cells and in chapter 8 we show the effects of hyper-gravity and omni-lateral gravity (or simulated micro-gravity) on the pollen tube cell wall composition and on intracellular trafficking.

1.8 Pollination and importance of pollen

1.8.1 Microsporogenesis in angiosperms

Pollen grains, or male gametophytes, originate from sporocytes that undergo meiosis and mature before being released from the anthers (Twell *et al.* 1998). The initial spore mother cell (microsporocyte) undergoes meiosis resulting in the production of four haploid daughter cells (microspores) into tetrads (Fig 1.4a,b,c). During prophase I, a massive deposition of callose (β-1,3-glucan) occurs between the different microsporocytes and their respective cell walls disintegrate (Fig 1.4a,b). The protoplasts of the

microsporocytes are still connected by 1.5 μm channels traversing the callose layer ensuring their simultaneous development (Fig 1.4b). In the majority of angiosperms, although phragmoplasts begin to form during telophase I, no individual complete walls are formed around the microspores after meiose I. The members of the microspores are then isolated from each other by the formation of a callose wall which is continuous with the callose surrounding the tetrad (Fig 1.4c,d). The different plasmalemma of the microspore are in direct contact with the callose.

After meiosis II, the pollen wall formation begins with the deposition of fibrillar cellulose (primexine) which is fortified by proteins and lipids (probacula) (Fig 1,4d,e). Protosporopollenin is then associated with the probacula giving the structure the property of being resistant to acetolysis. The dissolution of the callose enclosing the tetrads then takes place allowing the expansion of each microspore (Fig 1.4e). The final deposition of sporopollenin seals the shape and size of the pollen grain. At this stage the exine is complete and four layers can be distinguished: the sexine, the bacula, the nexine 1 and nexine 2 (Fig 1.4f). The intine is formed between the sexine and the plasma membrane and is composed of pectins and cellulose (Fig 1.4g,h). In the final stages of pollen maturation the grain is dehydrated and coating substances (from the tapetum), proteins and enzymes (many of them allergenic) are deposited onto the grain (Fig 1.4i). These enzymes are implicated in the incompatibility reactions and cell wall loosening (see below).

Before the pollen is released, the nucleus undergoes an asymmetric mitotic division, giving rise to a vegetative (n) and a generative (n) nucleus (Fig 1.4g). The latter undergoes a second mitosis resulting in the formation of two sperm cells (n). This last mitosis takes place either before anthesis in tricellular species or after the pollen grain germinates in bicellular species (Essau 1977; Brown and Lemmon 1992; Twell *et al.* 1998; McCormick 2004; Takeda and Paszkowski 2006).

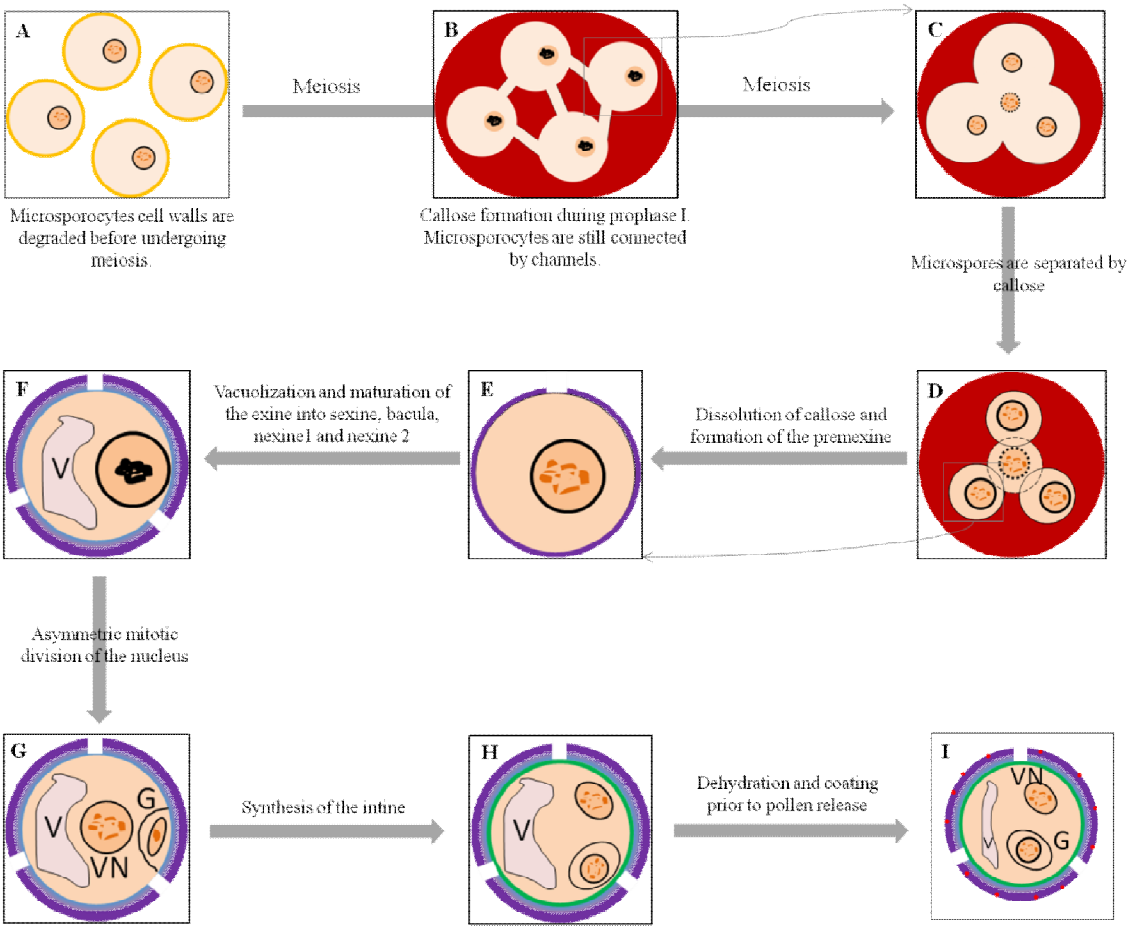

Figure 1.4: Schematic representation of microsporogenesis in dicots.

Before mitosis, cell walls (orange lines) of microsporocytes located in the tapetum (A) are degraded. Callose (red) engulfs the microsporocytes while they are dividing (B) into coenocytic microspores (C) which are then separated from one another by callose (D). The position of the tetrads in (D) is typical of dicots. The individual microspores undergo maturation with the addition of premexine (magenta layer in E) and then the maturation of exine into several layers (blue gradient in F) and vacuolization (F). The nucleus undergoes an asymmetric division (G) resulting in the formation of the vegetative nucleus (VN) and the generative cell (G). At the same time, intine is 22added (green layer in H). Before being released the pollen tube undergoes dehydration (I) and coating with tapetum proteins (red dots in I). C represents a zoom in on one microsporocyte in B. E represents a zoom in of one microspore in D. G - Generative cell, V – Vacuole, VN – Vegetative nucleus. Objects are not to scale.

1.8.2 Pollen tube germination

Once released from the anthers, pollen is carried away by wind, water, insects or birds to fertilize other flowers. To be able to germinate, the pollen grain and the stigma it landed on would have to be compatible in inter-specific (from the same or very close species) and/or intra-specific (self recognition) ways. Inter-specific recognition is common to all plants, and allows the female reproductive tissues to reject pollen grains from a different species. From an evolutionary point of view, the two species would have diverged enough, creating an incongruity between the different reproductive tissues. This incongruity makes the interaction between the pollen (or pollen tube) and the female reproductive tissues impossible (Hülskamp *et al.* 1995). The inter-specific process can also be an active process involving the presence of S-RNase, specially between self-incompatible and self-compatible species, as shown in the Nicotiana genus (Murfett *et al.* 1996). In some angiosperm species, to prevent self-fertilization, intra-specific mechanisms for self-recognition were developed. There are mainly two types of self-incompatibility (SI) mechanisms based on genetic recognition: (1) the sporophytic SI where the pollen SI phenotype is determined by the genotype of the sporophyte parent (diploid genotype of the anther) and (2) the gametophytic SI where the SI phenotype of the pollen is determined by its own gametophytic genotype (haploid) (Goodwillie 1997).

When a pollen grain lands on a compatible stigma, it hydrates by water uptake and produces a protrusion, the pollen tube, which grows through the pistillar tissue. The appropriate pollen-papillar cell adhesion and recognition is crucial for the formation of the pollen tube (Feijó 2010). In species with wet stigmas, the exudates produced by the stigma promote pollen adhesion. Hydration is considered to be a passive process (Swanson *et al.* 2004). In dry stigmas, the process is more complex and implicates a very selective mechanism (Preuss *et al.* 1993). In Brassicaceae the hydration depends on the *S-locus* specific glycoprotein recognition system that is implicated in sporophytic SI (Trick and Flavell 1989; Takayama *et al.* 2000; Takayama and Isogai 2003). In sporophytic SI, if the pollen is incompatible, it does not pass through the stages beyond capture and does not germinate (Heizmann *et al.* 2000). Sporophytic SI, such as in Brassicaceae, is based on the

recognition between a male determinant (SCR or SP11 expressed in the tapetum and the microspore and pollen) and a stigmatic protein kinase (SPR). The auto-phosphorylation of SPR provokes several cascade reactions leading to the inhibition of pollen development (Hiscock and McInnis 2003). In case of pollen compatibility, a mix of wax and fatty acid permanently binds the pollen grain to the stigma, which promotes the hydration process (Hiscock *et al.* 1994) and allows subsequent pollen germination. In gametophytic SI, the pollen is allowed to germinate, but its growth is arrested by several mechanisms. In Solanaceae, Rosaceae and Plantaginaceae, pollen rejection is executed by an *S-RNase* based mechanism (McClure and Franklin-Tong 2006) where pollen tube elongation is arrested when it has reached one third of the style (Franklin-Tong and Franklin 2003). In *Papaver rhoeas*, pollen germination is inhibited within minutes after its contact with the stigma through another mechanism of SI implicating S-glycoproteins. These proteins are responsible for a massive introduction of calcium ions into the pollen tube cytoplasm. This influx of Ca^{2+} disturbs the cytosolic calcium gradient in the pollen tube resulting in growth inhibition (Franklin-Tong and Franklin 2003).

Depending on the species, the pollen tube either has to make its way to the ovary along a hollow style or it needs to invade the transmitting tissue of a solid style. It is assumed that this invasive growth through the apoplast of the transmitting tissue is facilitated by the secretion of cell wall degrading enzymes and/or by inducing programmed cell death. Whether the style is hollow or solid, the pollen tube interacts with the surrounding growth matrix and responds to external cues guiding it to the ovary (Cheung and Wu 2001; Geitmann and Palanivelu 2007). The extracellular matrix of the transmitting tissue is mainly made of sugars, glycoproteins, and contains other elements such as calcium that play a major role in guiding the pollen tube to the ovary but have also been found to be crucial for pollen tube growth *per se* (Cheung and Wu 2001; Geitmann and Palanivelu 2007; Bou Daher and Geitmann 2011). Several guiding, attractant and repellant molecules are secreted by the ovary to guide the pollen tube to an unfertilized embryo sac like chemocyanin in *Lilium*, calcium and EA1 in maize and LURE in *Torenia fournieri* (Higashiyama *et al.* 2003; Higashiyama and Hamamura 2008; Dresselhaus and Márton 2009; Higashiyama 2010). Once the pollen tube reaches the ovary, it enters through the

micropyle and delivers the two sperm cells thus performing what is called the 'double fertilization' that will allow fruit and seed set. The double fertilization consists of the fusion of one sperm cell with the central cell (which will give rise to the endosperm) and the fusion of the second sperm cell with the egg cell (which will give rise to the embryo).

1.8.3 Significance of pollen grains

The pollen and the female gametophyte are the two haploid partners that allow plants to reproduce sexually, thus ensuring the shuffling of genes that allows sexually reproducing species to adapt to changing environments (as opposed to the asexual reproduction). The pollen tube represents the physical connection between the male and female gametophyte that allows the transfer of the immotile sperm cells.

Aside from the significance for plant evolution, pollen has played an important role in many other scientific disciplines such as geology, paleontology, criminology, human health (allergies) and the food industry. The single most important feature of the pollen in most of these contexts is the architectural characteristics of the exine. The exine is formed of an amalgam of stiff polymers conferring to the pollen grain an extremely high resistance to chemical, biological and mechanical degradation (Essau 1977). It is therefore typically the only structure remaining in sediments after millions of years and petrification. Crucially, the geometry of the surface ornamentation is unique in shape and size for each species, hence enabling experts to identify them even based on petrified samples with a precision that is akin to that of human fingerprints. Another use of the shape-based identification is melissopalynology that retraces the plant species used to produce honey with the aim of verifying the authenticity of commercial claims. Its unique shape and resistance to mechanical and chemical stress make the pollen grain indispensable in paleontology, geology and evolutionary studies, in particular to understand when and how different species appeared on Earth and how they evolved and disappeared. Because each species has a specific habitat and because each region in the world is characterized by its plant species, pollen found on clothing can be used to deduce the whereabouts of persons during specific time intervals in criminology or forensic palynobiology (Bryant and Jones 2006; Mildenhall *et al.* 2006). Evidence based on pollen samples has also been used to

prove the presence of mass graves in Bosnia and to convict war crime perpetrators (Wood 2004), as well as to investigate the story behind the death of Ötzi the iceman (Müller *et al.* 2003), or to determine the last meal of a mammoth. It was proposed to add pollen grains to bullets in order for the police to track them more easily (Wolf 2008). Pollen grains (mainly from anemophilous plants) are also a public health concern, as they are known to be implicated in a large number of allergy reactions, due to proteins present on the pollen grain surface or in the cytoplasm (D'Amato *et al.* 2007).

1.8.4 The pollen tube as a model system for plant cell growth

Despite its extremely specialized function, the pollen tube has become an important cellular model system for plant cell and molecular biology. It has been used to investigate the dynamics of cell wall assembly and the spatial and temporal regulation of cell wall mechanical properties. The involvement of the cytoskeleton in plant cell growth has been studied in great detail, and the principles of long-distance and local intracellular transport processes involving vesicle and organelle trafficking have been investigated. Furthermore, the response of tip growing cells to guidance cues poses intriguing avenues for studying intracellular signaling processes from signal perception to cellular response. In my thesis, the following characteristics of the pollen tube were particularly useful:

1- Pollen tubes are single cells easily cultured *in vitro*, which allows high resolution microscopic observation.
2- The pollen tube is the fastest growing plant cell; its high growth rate entails rapid and easily visible cellular responses upon administration of mechanical, chemical or biological triggers.
3- Pollen tubes are characterized by a one-dimensional growth pattern making quantification of the growth process and geometrical parameterization easy.
4- Pollen tubes are characterized by a relatively simple cell wall when compared to other plant cells.
5- Pollen can be stored in the freezer until use and pollen tube germination does not require sterile conditions making experimentation relatively easy.
6- Knock-out and transgenic lines are easily available (specially for *Arabidopsis*).

1.9 Mechanical principles governing pollen tube growth

This manuscript entitled "Mechanical principles governing pollen tube growth" was published in 2007 in *Functional Plant Science and Biotechnology* volume 1, issue 2, pages 232-245.

Youssef Chebli and Anja Geitmann

1.9.1 Abstract

Cellular growth and morphogenesis are central aspects of cellular differentiation. In plant, cell growth is based on the turgor driven expansion of the cell wall and concomitant addition of new cell wall material. In no plant cell does this process occur as rapidly as in the pollen tube, the carrier of the male gametes. This cell is therefore an excellent model system to investigate the processes governing the dynamics of plant cell growth. This review provides a brief overview of the anatomy of the pollen tube focusing on the structural features that are implicated in the growth process – the cell wall and the cytoskeleton as well as spatially focused exocytotic events. The mechanics of the growth process is discussed and various theoretical modeling approaches that explain this process are outlined. In pollen tubes from many plant species the growth process is oscillatory or pulsatory and the ions and signalling molecules that form controlling feedback loops in this growth process are analyzed. A model that explains the oscillatory mechanism based on its mechanical components and that results from converging available data and hypotheses is elaborated.

Keywords: cell mechanics, cellular growth, cell wall, cytoskeleton, feedback mechanism, ions, modeling, oscillation, pollen tube, tip growth, turgor

Abbreviations: **ATP**, adenosine triphosphate; **ABP**, actin binding protein; **ADF**, actin depolymerizing factor; **ER**, endoplasmic reticulum; **GFP**, green fluorescent protein; **GTP**, guanosine triphosphate; **NAD**, nicotinamide adenine dinucleotide; **PME**, pectin methyl-esterase; **PtdInsP$_2$**, phosphatidylinositol 4,5-bisphosphate

1.9.2 Introduction

The pollen tube is formed upon contact of a pollen grain with a receptive stigma. The grain swells through water uptake and forms a cellular protrusion that invades the pistil. The purpose of this process is the transport of the male gametes from their carrier vehicle – the pollen grain – to the ovule where fertilization takes place. Depending on the species, pollen tube growth can occur extremely rapidly with rates up to tens and even hundreds of micrometers per minute. Very conveniently for the researcher, pollen grains are able to form these tubular protrusions *in vitro*, albeit usually not with the impressive growth rates observed *in planta*. However, cellular morphology of the former resembles that of the latter, which is why this single cell is an extraordinary system to investigate processes involved in plant cell growth.

Most types of plant cells grow by expanding large surface areas simultaneously. In the cylindrical cells composing stem tissues, this expansion occurs over the entire cylindrical surface, whereas only the end walls remain almost unaltered in size. Other cell types such as pavement cells in the leaf epidermis grow at more spatially confined sites to generate the typical jigsaw puzzle shape (Mathur 2006). Pollen tubes represent an extreme example of spatially confined growth since cellular expansion is limited to a single very small area at the apex of the growing cell. This mode of growth makes sense from an energetical point of view, because pollen tubes need to invade the transmitting tissue of the receptive flower. If the cylindrical wall of the tube expanded during growth, friction would occur against the surrounding tissue. Confining expansion to the apex minimizes the surface area on which friction occurs. This growth strategy is shared by several other cell types, which incidentally also have an invasive way of life. Among them are root hairs and fungal hyphae, and certain parallels can also be drawn to neuronal growth cones (Palanivelu and Preuss 2000). This illustrates that the tip growth strategy is realized in evolutionary very distant organisms.

Since pollen tubes are easily cultivated *in vitro*, and since even under this suboptimal condition their growth rate is impressive, this cell type has become an important model system for the investigation of the processes that govern plant cell growth.

Numerous labs investigate different aspects of pollen tube growth which have been reviewed in countless articles and books (a collection of articles can be found in (Malhó 2006)). In the present review we will give an overview of the understanding of the mechanics and dynamics of the growth process. We will briefly present the structural features of the pollen tube and how their spatial distribution accounts for the highly anisotropic mechanism of growth. We will discuss the molecular feedback mechanisms that govern growth focusing on a particularity of the dynamics of the growth process – the oscillating change of the growth rate.

1.9.3 Polarity is reflected in the cytoarchitecture

1.9.3.1 Cytoplasm

The anatomy of the pollen tube reflects the extreme polarization of the cellular processes. Starting from the apex, which is also called the growth zone, several distinct regions can be distinguished in the cytoplasm (Fig 1.5). The apical dome is filled densely with secretory vesicles. The only other organelles that can occasionally be observed here are mitochondria and cisternae of the endoplasmic reticulum. The adjacent subapical and distal regions are densely populated by cellular organelles which move in a direction parallel to the longitudinal axis of the cell – towards or from the apex. This movement is rather rapid with rates of several micrometers per second. Most of these organelles turn around once they reach the subapical region (Fig 1.5a). In larger pollen tubes such as lily, this rearward movement occurs mostly in the central area of the cytoplasm, and the flux is therefore characterized as "inverse fountain streaming" (Hepler *et al.* 2001). The shank of the tube contains the male germ unit consisting of the vegetative nucleus and the generative cell or, after its division, the two sperm cells. In longer pollen tubes, the viable part of the cytoplasm is concentrated in the region close to the apex and it is separated from degenerating distal regions and the pollen grain by callosic plugs.

This non-uniform distribution of cellular organelles is indicative of the compartmentalization of cellular functions (Cheung and Wu 2007), in particular with the growth zone being visibly different from the other regions of the cell. The polarity of the

cell is also expressed in the non-uniform distribution of the concentrations of numerous molecules and ions and of the activities of certain enzymes. Among the principal players is calcium, which is highly concentrated in the apex and lower in the shank (Fig 1.5c). Equally important are protons whose uneven distribution results in a pH profile that is characterized by a subapical alkaline band (Holdaway-Clarke and Hepler 2003); Fig 1.5d).

1.9.3.2 Cytoskeleton

The pollen tube cytoskeleton is mainly composed of actin filaments and microtubules. Both are oriented in approximately longitudinal (or slightly helical) direction. Actin is found in the cortical cytoplasm as well as the endoplasm (Geitmann and Emons 2000). The shank of the tube in most species is characterized by the presence of numerous conspicuous actin bundles. On the other hand, the precise configuration of actin in the subapical region and in the apex varies between species as well as with the method of visualization. Important information has been gained from improved chemical or rapid freeze fixation combined with phalloidin staining, but dynamic aspects could only be studied using transformation with GFP (green fluorescent protein; or its derivatives) coupled to actin binding proteins (Kost *et al.* 1998; Chen *et al.* 2002a). GFP coupled directly to actin has not been successful for pollen so far. The consensus of these studies is that angiosperm pollen tubes possess a subapical domain in which actin filament bundles are thinner and denser (also called actin fringe), whereas no significant amounts of filamentous actin are present in the very tip of the tube (Fig 1.5e). The resolution of fluorescence images does not allow the precise characterization of the actin configuration in the fringe, not even when fixation is optimized (Lovy-Wheeler *et al.* 2005). A possible interpretation of the images could be that the front of the fringe corresponds to the advancing polymerization front, whereas the rear end represents the advancing actin bundling front (Fig 1.5e). Alternatively, the fringe could represent a region of high degree of branching and the rear end might be a region of increased depolymerization. These hypotheses are not mutually exclusive. Depending on the degree of bundling either by the pollen tube's own protein machinery or by agents used to fix and stabilize actin, this fringe could thus appear longer or even funnel shaped as has been observed in several species

such as maize, poppy and lily (Gibbon *et al.* 1999; Geitmann *et al.* 2000; Foissner *et al.* 2002). It will be interesting to see whether the corresponding actin binding proteins can be localized specifically to these "front" regions within the fringe that would correspond to high polymerization, depolymerization and/or bundling activities.

Several actin binding proteins (ABPs) act in the pollen cytoplasm to regulate actin polymerization and depolymerization. Villins have been proposed to degrade actin filaments in the apical region where the cytoplasmic Ca^{2+} concentration is higher thus resulting in a tip region that is relatively free of filamentous actin. In the distal region, where the Ca^{2+} concentration is at its basal levels, villin may act as a cross-linker, thus stabilizing the actin network (Kost *et al.* 1998; Yokota *et al.* 1998; Vidali *et al.* 1999; Yokota *et al.* 2000; Vidali *et al.* 2001). Profilin has also been shown to bind G-actin in the apical region, thus preventing actin polymerization (Kovar *et al.* 2000). Villin and profilin have a role in regulating the polymerization of actin filament bundles in root hairs (Baluška *et al.* 2000).

Actin depolymerizing factor (ADF) and cofilin are two ABPs that have the ability to segment and to depolymerize actin filaments. The segmentation activity of the ADF and the depolymerization activity of cofilin are both regulated by pH thus pointing to an important regulatory function of the pH profile (Lovy-Wheeler *et al.* 2006). Other ABPs were described in pollen tubes such as α-actinin, formins (polymerization of actin filaments) and myosins. Several review articles on pollen tube actin and ABPs are available (Vantard and Blanchoin 2002; Staiger and Blanchoin 2006; Yokota and Shimmen 2006).

Microtubules are longitudinally oriented and sometimes adopt a slight helical distribution (Geitmann and Emons 2000). They extend from the pollen grain to the subapical region. In contrast to root hairs, microtubules are absent from the apical domain of angiosperm pollen tubes (Lancelle and Hepler 1992). The role of microtubules in polarized growth may be the control of directionality, because taxol (stabilizing agent) and oryzalin (destabilizing drug) have similar effects on the directionality of tube growth (Hepler *et al.* 2001; Gossot and Geitmann 2007). Reviews that summarize the role of

microtubules in pollen tube tip growth include (Geitmann and Emons 2000; Raudaskoski *et al.* 2001; Cai *et al.* 2005).

1.9.3.3 Cell wall

The pollen tube cell wall is mainly composed of polysaccharides. The main component is pectin which is deposited at the apex by exocytosis. Cellulose and callose are laid down in more distal regions by plasma membrane localized synthases. In the case of *Nicotiana tabacum* cellulose deposits start at 5 to 15 µm from the tip whereas callose is visible starting at a distance of approximately 30 µm from the tip (Ferguson *et al.* 1998). The pattern of callose deposition is very universal, whereas there are considerable species dependent differences for cellulose localization. In *Arabidopsis thaliana* calcofluor label has indicated the presence of microfibrils in the apex (Derksen *et al.* 2002) whereas the apex of other species is devoid of cellulose.

Because of the general absence of a conspicuous "secondary" deposition of cell wall components in the apex, the overall biochemical structure of the cell wall differs considerably between the growing apex and the cylindrical shank of the cell (Fig 1.5g). This difference is even more pronounced due to the gradual change in the configuration of the pectins as they become part of the mature region of the shank. Labeling with monoclonal antibodies JIM5 and JIM7 has revealed that in growing angiosperm pollen tubes pectins have a higher degree of methyl-esterification in the tip than in distal regions (Li *et al.* 1994). For reviews on pollen tube cell wall structure see (Heslop-Harrison 1987; Taylor and Hepler 1997; Geitmann and Steer 2006).

1.9.4 Mechanics of anisotropic growth

In general, the process of plant cell growth is driven by the relationship between turgor pressure, controlled water uptake and mechanical cell wall resistance. The controlled yielding of the existing cell wall under the applied pressure leads to an expansion of the cellular surface while simultaneously new cell wall material is inserted. The combination of these two processes results in a change of cellular shape. The situation is similar in a tip growing cell, with the particularity that the cellular expansion is confined to an extremely

small region of the cellular surface. Similarly to diffuse growth, turgor is believed to be the primary motive force behind tip growth, albeit it might not be the rate-controlling parameter as growth rates cannot directly be correlated with the amount of turgor present in *Lilium longiflorum* Thunb. (Benkert *et al.* 1997).

Given that hydrostatic pressure is a non-vectorial force, the question arises, how it can push a cell to produce a tubular protuberance instead of becoming a ballooning sphere. Green (Green 1969) and others have proposed that tip-localized expansion must be caused by tip-to-base changes in the physical properties of the wall. In other words, the cell wall in the shank of the tube needs to be more resistant to tensile stress than the apical cell wall to assure that the latter yields first thus allowing for tip-confined expansion. However, for geometrical reasons this difference actually has to be bigger than a factor 2. According to the physical laws for thin-walled pressure vessels, tensile wall stress in circumferential direction is twice as high as the tensile stress in longitudinal direction or that in the hemisphere-shaped ends of a cylindrical vessel (Geitmann and Steer 2006; Fig 1.5f). The generation of a tubular structure therefore requires a considerable difference in the yield threshold between the shank and the apex. This difference in the physical properties of the pollen tube cell wall has been demonstrated by micro-indentation for *Papaver rhoeas* (Geitmann and Parre 2004) and other species.

Several cell wall components are likely to be responsible for this mechanical gradient in the pollen tube cell wall due to their non-uniform distribution (Heslop-Harrison 1987; Ferguson *et al.* 1998); Fig 1.5g). Since both callose and cellulose are present predominantly in the shank of the tube they are presumed to play a reinforcing role in this part of the cell. Micro-indentation data as well as enzymatic and pharmacological approaches confirm this (Anderson *et al.* 2002; Parre and Geitmann 2005a). An even more important role is played by pectins and the spatial distribution of the degree of their methyl-esterification. Concerning the physical properties of the cell wall this is an essential feature as de-esterification allows pectins to become gelated in the presence of calcium ions. *In vitro*, this gelation process considerably increases the Young's modulus of this matrix component (Jarvis 1984), thus potentially increasing resistance against tensile stress.

Micro-indentation revealed that this is also true for *in vivo* pollen tube cell walls (Parre and Geitmann 2005b). Furthermore, the enzymatic de-esterification and hardening of the usually rather soft apical wall is able to prevent pollen tube from elongating (Bosch *et al.* 2005; Parre and Geitmann 2005a), thus confirming the crucial role of the physical gradient in the mechanical properties of the cell wall for sustained growth.

1.9.5 Theoretical models for unidirectional growth

The unidirectional growth typical for pollen tubes and other tip growing cells has inspired many attempts to model this process. Most of these were applied to fungal hyphae (Bartnicki-Garcia 2002), but the similarity between the cell types is such that the models could readily be transferred from one to the other. The early theoretical models for tip growth are based on equations that approximate the shape of these cells very closely. However, most of them are limited to geometric exercises that formulate equations from artificial coordinates and reference points (Reinhardt 1892; Da Riva Ricci and Kendrick 1972; Trinci and Saunders 1977; Prosser and Trinci 1979; Koch 1982; Koch 1994; Prosser 1994; Denet 1996). Few tried to take into consideration the geometrical and physical parameters of subcellular structures such as the thickness and chemical composition of the cell wall, the precise location of vesicle fusion or the hydrostatic turgor pressure. The vesicle supply center model for fungal hyphae by Bartnicki-Garcia *et al*. (Bartnicki-Garcia *et al.* 1989) was an attempt to develop a mathematical model based on the intracellular path and secretion of secretory vesicles. The original two-dimensional mathematical formulation was based on the concept that tip growth is produced by wall-building vesicles emanating randomly, and in all directions, from a vesicle supply center which advances moving along a straight path. The subsequent three-dimensional derivation of this model included quantitative measurements of the pattern of expansion of the wall (Bartnicki-Garcia *et al.* 2000; Gierz and Bartnicki-Garcia 2001). Observations of surface expansion are also the basis of models developed by Dumais and co-workers for *Medicago truncatula* root hairs and further versions account for growth fluctuations and changes in morphology (Dumais *et al.* 2004; Dumais *et al.* 2006). This was achieved by rescaling a given wall extensibility profile over time. The same group found interesting parallels between the tip expansion of

lily pollen tubes and rubber balloons swelling under increasing internal pressure (Bernal *et al.* 2007). While model by Dumais *et al.* considers the continuous supply of cell wall material to be provided in bulk form at the very tip of the cell, the vesicle supply center model was further developed by exchanging the theoretical ballistic path of secretory vesicles to the apical membrane for a more realistic diffusive vesicle delivery mechanism (Tindemans *et al.* 2006).

While being able to explain the formation of a cylindrical tube, many of these models nevertheless fail to include parameters important for the functioning of the living cell such as the turgor pressure and the non-uniform biochemical composition of the cell wall. An internal hydrostatic pressure was included in the approach by Goriely and Tabor who modeled the cell wall of a tip growing cell as a stretchable and growing elastic membrane with geometry-dependent elastic properties. They used large-deformation elasticity theory and combined the elastic response with surface re-parameterization to simulate wall rebuilding (Goriely and Tabor 2003a; Goriely and Tabor 2003b).

Few of these models are directly based on geometrical and physiological data obtained specifically from pollen tubes. To allow for experimental validation, future modeling attempts will require precise quantitative data on the pollen tube geometrical features and the mechano-physical properties of its subcellular components. Cytomechanical approaches will therefore certainly gain popularity in this field (Geitmann 2006a; Geitmann 2006b).

1.9.6 Construction of the apical cell wall: exo-/endocytosis

To allow for the construction of the ever elongating tube, new cell wall material as well as membrane bound and secretory proteins need to be transported to the tip in a continuous manner and at a high rate. Exocytosis is therefore a *sine qua non* condition for pollen tube growth. Inhibiting the vesicle supply by adding brefeldin A or monensin arrests pollen tube growth within a few minutes - presumably upon depletion of the apical stock of vesicles (Geitmann *et al.* 1996). The cell wall material deposited at the tip consists largely of pectin polymers which are transported to the apex within vesicles. This transport occurs

via interactions between motor proteins linking the vesicle surface to the cytoskeleton. The actin cytoskeleton is thought to play a major role in this context and myosins have been identified in pollen tubes (Yokota and Shimmen 1994; Shimmen *et al.* 2000). However, dynein- and kinesin-like proteins have also been localized on pollen tube organelles indicating a transport function for microtubules as well (Moscatelli *et al.* 1998; Romagnoli *et al.* 2003; Romagnoli *et al.* 2007). For reviews on motor proteins in pollen see (Cai *et al.* 1996; Cai *et al.* 1997; Cai *et al.* 2005).

While the long-distance transport of vesicles along the cytoskeletal rail system in the tube shank is rather well understood, knowledge about the subsequent steps is scant. Once delivered to the apical region, vesicles seem to accumulate and somehow find their way to the apical membrane where they dock, fuse, and liberate their contents. Vesicle movement in the vesicle-rich growth zone was initially described as Brownian in *Nicotiana tabacum* (de Win *et al.* 1999). However, the situation is probably more complex since TIRF (total internal reflection fluorescence) microscopy has revealed that the movement in *Picea meyeri* pollen tubes is not random and seems to depend on a functional actin cytoskeleton despite the absence of conspicuous F-actin configurations in this area (Wang *et al.* 2006d). The apical actin cytoskeleton, possibly in form of dynamic individual F-actin arrays which are difficult to visualize, is therefore likely to be involved in guiding the vesicles to the designated fusion sites at the membrane.

Vesicle fusion must be spatially and temporally controlled. Spatial control serves to determine the direction of growth (Geitmann and Palanivelu 2007) and temporal control is likely to influence the dynamics of the growth rate. A crucial role in this control mechanism is said to be played by calcium (discussed below) which in turn acts via its activating or de-activating effect on a number of proteins. The signaling pathways targeting secretion are also thought to involve the inositide pathway and phosphorylation cascades (reviewed by (Malhó *et al.* 2000; Malhó *et al.* 2005; Malhó *et al.* 2006; Geitmann and Palanivelu 2007).

Among the proteins that have been proposed to interact directly in vesicle secretion are annexins, SNAREs, and the members of the exocyst complex. Annexins are able to bind to, aggregate, and fuse secretory vesicle membranes in a calcium-dependent manner.

They were immunolocalized in the vesicle-rich zone of *L. longiflorum* pollen tubes (Blackbourn *et al.* 1992) and are thus likely to be involved in the tip growth process. Annexin action is calcium dependent (Trotter *et al.* 1995) thus suggesting that the cytosolic high calcium concentration plays a role in directing vesicle fusion events.

The exocyst, first described in yeast (Novick *et al.* 1995) is composed of eight proteins functioning as a tethering complex guiding secretory vesicles to their specific plasma membrane site prior to the docking and fusion events mediated by SNARE proteins (Cole *et al.* 2005). In yeast, the exocyst was found to be associated with the plasma membrane at the site of cell-surface expansion (Novick *et al.* 1995). While orthologs of all exocyst components have been identified in *Arabidopsis* and rice, their role in tip growth has yet to be elucidated (Cole *et al.* 2005; Cole and Fowler 2006). However, mutants of SEC8, one of the exocyst components, were found to affect pollen tube growth or germination (Cole *et al.* 2005) and further investigations are likely to provide more insight.

SNAREs (soluble N-ethyl-maleimide-sensitive fusion protein attachment protein receptors) are integral membrane proteins. In plants, fusion of the vesicle with the target membrane depends on activated SNARE molecules in the vesicle (v-SNARE) and target (t-SNARE) membranes (Sanderfoot and Raikhel 1999; Nebenführ 2002). While SNAREs were found to be implicated in numerous plant functions (Pratelli *et al.* 2004), they have not been characterized or localized in pollen tubes in the context of exocytosis. Given the intensive secretory activity in these cells, their involvement is likely, however.

Two types of exocytosis have been proposed to occur in pollen tubes: full fusion and transient fusion. Using evanescent wave microscopy, Wang *et al*. (Wang *et al.* 2006d) observed the full fusion type in *Picea* pollen tubes involving the collapse of the vesicles into the membrane as they release their internal components. Transient exocytosis and the resulting rapid endocytosis were proposed to occur in pollen tubes of various angiosperm species (Malhó *et al.* 2005). This exocytosis mechanism is a Ca^{2+}-dependent process coupled to endocytosis which requires GTP hydrolysis and dynamin but not clathrin (Monteiro *et al.* 2005). It is characterized by the formation of a small and short-lived pore which limits the size of particles that can be released or incorporated.

The observation of transient exocytosis points to the initially surprising finding that despite its rapid cell wall production rate and growth sustained by massive exocytosis, the pollen tube actually internalizes material at the tip at the same time. An explanation lies in the fact that an excess of membrane material is transported to the tip of the pollen tubes during exocytosis of cell wall material (Picton and Steer 1983b; Picton and Steer 1985; Steer 1988; Derksen *et al.* 1995). Therefore, endocytosis of membrane is a necessity to maintain the relatively smooth outline of the apical plasma membrane. Next to rapid endocytosis, clathrin-mediated endocytosis is also purported to occur based on the presence of coated pits and vesicles carrying a clathrin-like coat in the tip area of tobacco pollen tubes (Derksen *et al.* 1995). The highest concentration of coated pits was observed in a region 6-15 µm behind the tip in *N. tabacum* pollen tubes (Fig 1.5b). The bulk of endocytosis is therefore purported to occur not at the very apex, but slightly towards the shank. Both, ultrastructural research and, more recently, live cell observations that use fluorescent dyes which are internalized by endocytosis have contributed important information on the dynamics and spatial distribution of these events (reviewed in (Malhó *et al.* 2005)).

1.9.7 Mechanics of Oscillatory growth

In addition to their rapid elongation, pollen tubes exhibit a dynamic feature which makes the investigation of their growth process extremely attractive: their growth rates fluctuate in regular intervals. This allows the investigation of the feedback mechanisms governing growth as signaling steps and physiological processes can be presumed to show temporal variations in intensity. Cross-correlation analysis of the phase shifts between these events and the growth rate should theoretically allow the identification of cause-effect relationships. A compilation of the parameters that have been assessed in this context is provided in Fig 1.6.

While most pollen tubes show a non-continuous growth rate, the frequency and amplitude as well as the shape of the curve representing the growth rate varies considerably between species and depends on experimental conditions. Roughly, one can distinguish between oscillatory growth characterized by a sinusoidal curve and pulsatory growth in

which short growth spurts are separated by extended periods of slow growth. In *L. longiflorum* the oscillations are approximately sinusoidal with a frequency of 15-50 sec (Pierson *et al.* 1996). In *N. tabacum* and *Petunia hybrida*, pollen tubes show slow growth phases lasting few minutes (typically 3 to 8) interrupted by pulse-like elongations lasting few seconds. Pollen tube elongation during these pulses can reach up to 2 μm in *N. tabacum* achieving a peak growth rate up to 0.5 $\mu m.sec^{-1}$ (Geitmann 1997).

The species that is investigated in most detail is *L. longiflorum*. The most prominent oscillations are found in older tubes (>1 mm length). Lily pollen tubes are relatively easy to manipulate and to observe due to their considerable size (16-20 μm diameter vs. 6-10 μm in many other species). In the *in vitro* setup the oscillations in this species have a period of 30-60 sec, and a growth rate oscillating between 0.1 and 0.4 $\mu m.sec^{-1}$ (Messerli *et al.* 2004).

Albeit the unidirectional manner of the pollen tube growth, these growth oscillations represent an ideal system to investigate the temporal relationship between mechanical events governing plant cell growth. The mechanical principle behind this oscillatory behaviour is based on the changing relationship between the turgor pressure and the apical cell wall over short periods of time. The question is, which of the two – turgor or cell wall mechanics – is the mechanical oscillator in this system?

From the mechanical point of view, two models have been proposed: i) fluctuations in the mechanical properties of the cell wall allowing its relaxation under an approximately stable turgor, and ii) surges in hydrostatic pressure driving cell wall expansion. The former is based on the widely accepted understanding of plant cell growth as reviewed by (Schopfer 2006). The latter is based on the "Loss-of-stability" principle proposed by Wei and Lintilhac (Wei *et al.* 2006).

1.9.7.1 Fluctuations in cell wall physical properties

This model is based on the observation that the hydrostatic turgor pressure in growing pollen tubes does not seem to oscillate in *Lilium longiflorum* (Benkert *et al.* 1997). This finding is corroborated by the observation that two growing ends emanating from a single branched cell do not show the same oscillation frequency in *Petunia hybrida*

(Geitmann 1997). If turgor was the determining oscillator, these branched pollen tube ends should oscillate with the same frequency, since the cell can be considered as a single volume in which turgor pressure can be assumed to be identical everywhere. It has therefore been suggested that the tensile strength of the apical cell wall and not the internal pressure varies during the oscillation cycles. This alternation between softening and hardening might for example be caused by the secretion of new cell wall material with high plasticity which allows rapid expansion and subsequently hardens either due to strain hardening or enzymatic activity (Geitmann 1999). It is interesting in this context to note that the thickness of the cell wall changes during an oscillation cycle. The peak of thickness precedes the most rapid phase of the growth pulse (Holdaway-Clarke and Hepler 2003). This phase relationship is intuitively necessary, since it assures the presence of sufficient cell wall material to allow for the subsequent expansion of the cell wall without the resulting thinning that would otherwise lead to rupture. On the other hand it is surprising, as this would mean that albeit being thicker, the tensile stress resistance in the wall would actually have to be lower to allow for rapid expansion to occur. This would require that the newly added material is extremely soft.

Alternatively, the mechanical properties of the apical cell wall material could be controlled by the oscillatory activity of enzymes. The configuration of pectins, the most abundant polymers at the tube tip, is affected by various enzymes. Pectin methyl esterase (PME) acts on the methyl-esterified pectins that are secreted at the growing apex (Bosch *et al.* 2005). The degree of esterification is essential for cell wall mechanics as unesterified pectins are able to bind calcium ions resulting in the gelation of the polymers. This process rigidifies the wall as revealed by micro-indentation (Parre and Geitmann 2005b). It has been proposed that PME activity at the pollen tube tip is subject to a negative feedback mechanism (Holdaway-Clarke *et al.* 1997; Bosch *et al.* 2005). According to this model a local decrease in pH generated by protons released during the deesterification reduces PME activity. This decrease in pH could also activate enzymes such as polygalacturonases and pectate lyases which affect the cell wall. The combined effect of the activation of these two enzymes and PME inactivation would loosen the cell wall and facilitate a growth pulse. The subsequent dilution of negative charges would then cause the pH to rise and thus

reactivate PME and inactivate polygalacturonase and pectate lyase. This would lead to a slowdown of the expansion rate.

To test this hypothesis Messerli and Robinson (Messerli and Robinson 2003) experimentally varied the external pH or buffered the medium. They showed that a decrease in medium pH dampens growth oscillations while not increasing the average growth rate in *L. longiflorum*. The authors interpret the absence of a change in average growth rate as indicative for a turgor controlled growth rather than a cell wall control mechanism. However, we would argue that whereas changes of oscillation frequency and amplitude can be expected upon cell wall softening, the average growth rate over long intervals is likely to be limited by the rate of delivery of cell wall precursor material rather than by the deformability of the wall. Interestingly, buffering the external medium and thus presumably the cell wall pH, resulted in a reduction in growth frequency and an increase in pulse amplitude thus indicating that changes in the cell wall pH are probably not necessary for oscillating growth (Messerli and Robinson 2003). This finding calls the PME-pH model into question even though no proof was provided that the pH buffer in the medium effectively buffers the pH within the cell wall.

An alternative model does not rely on changes in the relative material properties of the apical cell wall, but takes into consideration the total tensile resistance determined by apical cell wall thickness. In this model a growth pulse is proposed to be triggered by a short phase of endocytotic uptake of cell wall material. This leads to a small reduction in cell wall thickness and thus increased deformability which in turn sets off rapid expansion under a turgor that remains relatively constant. This mechanism is suggested by a theoretical mathematical model for pollen tube growth oscillations (Kroeger *et al.* 2008). Internalization of pectic wall material has been observed in other cellular systems (Baluška *et al.* 2002) thus making this hypothesis worth investigating experimentally.

Whether the cell wall or the turgor pressure is the driving factor in the oscillations, the cell wall properties most certainly do influence growth behavior. Agents that change these properties affect the frequency and/or amplitude of the growth rate or are able to induce pulsations in steadily growing pollen tubes. Borate cross-links monomers of

rhamnogalacturonan II, a component of pectin polymers, and thus is known to stiffen the cell wall. It is generally added to the growth medium as pollen tubes require this ion for successful germination and growth. Surprisingly, the partial removal of borate from the growth medium causes growth pulse frequency to decrease in individual pollen tubes of *Petunia hybrida* (Geitmann 1997). The presence of high concentrations of borate in the medium from the beginning of germination on the other hand results in an increased oscillation period that can be explained with the stiffening effect on the cell wall (Holdaway-Clarke *et al.* 2003).

Similarly, in pollen tubes of *N. tabacum* external addition of PME decreases the frequency, whereas addition of auxin (indole-3-acetic acid) results in an increase (Geitmann 1997). Both agents were occasionally observed to trigger the onset of pulsating growth in steadily growing tubes. PME is known to rigidify the cell wall (Parre and Geitmann 2005b), and auxin, through many signaling pathways, indirectly triggers several cell wall loosening agents resulting in the loosening and expansion of the cell walls (detailed in paragraph 1.7.2 and in (Cosgrove 1999; Cosgrove 2000a; Cosgrove 2000b)). Therefore, these findings indicate that during steady growth the tensile stress caused by turgor pressure and elastic tension of the cell wall are basically in an unstable equilibrium permitting continuous expansion. Upon disturbance in one direction or the other the finely tuned feedback processes become amplified and temporally distinguishable thus giving rise to a pronounced oscillatory behavior.

1.9.7.2 Turgor surges

A rhythmic fluctuation of turgor pressure has been suggested to underlie force measurements with a miniature strain gauge on hyphae of the oomycete *Achlya bisexualis* (Johns *et al.* 1999). A similar principle has been proposed for pollen tubes (Derksen 1996; Geitmann 1999). It implies that an increase in cytoplasmic osmolarity leads to a rise of turgor driving rapid expansion. Messerli *et al*. (Messerli *et al.* 2000) then incorporated new metabolic data and suggested that turgor pressure rises preceding a rapid growth phase until it overcomes the yield threshold of the apical cell wall. In this model the wall is thickened preceding rapid growth and the membrane is slack due to bulk exocytosis which had taken

place earlier. The growth surge then stretches both cell wall and membrane. Support for this model is provided by the observation that during experimental changes that correspond to lowering the growth rate amplitude, the slow growth rate is inversely proportional to the preceding peak of growth (Messerli and Robinson 2003). This can be explained if a surge in growth leads to a corresponding drop in turgor that decreases the subsequent growth rate.

Zonia *et al*. (Zonia *et al.* 2006; Zonia and Munnik 2007) attempted to corroborate the claim that turgor surges precede growth surges by measuring the diameter in the apical and subapical region of the cell. They observed that the cellular diameter in *N. tabacum* is at its maximum right before a growth peak. They suggest that the increase in volume in this part of the cell indicates surges of hydrostatic pressure resulting from cycles of vectorial hydrodynamic flow. While their hypothesis has its merits, it is unfortunately based on the erroneous interpretation of cytomechanical data. The authors cite Geitmann and Parre (2004) stating that the mechanical properties of the cell wall do not change over time in growing pollen tubes. A high resolution time course that would have allowed them to draw this conclusion was, however, not assessed in the cited paper. Therefore, Zonia and Munnik cannot conclude their volume changes are due to fluctuations in the turgor pressure, as volume changes could just as easily be achieved by a temporal change in the physical properties and subsequent yielding of the apical cell wall.

Zonia and Munnik make an important point, however, when they mention that the hydrostatic pressure in a single cell is not necessarily identical in all cellular regions. They cite (Charras *et al.* 2005; Langridge and Kay 2006) who observed that over short periods of time local cellular regions can undergo pressure changes that are only gradually equilibrated over the entire cell. This is supposedly possible because of the dense packing of the cellular components which could retain pressure. However, these findings were made on wall-less cells in which the hydrostatic pressure is several orders of magnitudes smaller than in plant cells. At the much higher pressures typical for a growing pollen tube (0.2 to 0.4 MPa, (Benkert *et al.* 1997) it is doubtful whether a local pressure gradient could be established or maintained over a significant period of time. However, if proven it would invalidate the argument of the branched pollen tube mentioned above. More importantly,

they would explain why turgor oscillations were not found in oscillating pollen tubes (Benkert *et al.* 1997) and they would indeed make any attempt to monitor local hydrostatic pressure over time in pollen tubes a huge challenge. Pressure measurements with a turgor pressure probe imply the impalement of the cell with a rather big micropipet, an endeavour that seems impossible to conceive in the growing apex of the tube. An alternative strategy to measure cellular turgor pressure relies on the external deformation of the cell by micro-indentation (Geitmann *et al.* 2004), atomic force microscopy or ball tonometry (Lintilhac *et al.* 2000; Wang *et al.* 2006b). However, while localized measurements at the growing apex are possible with these devices, the experimental results would be influenced by changing cell wall properties rendering conclusions on turgor behavior complex. The ideal solution would therefore be the use of a non-invasive intracellular pressure indicator with spatial resolution, which to our knowledge has not been developed so far.

1.9.7.3 Vesicle fusion

The oscillations in cell wall thickness raise the question of how exocytosis behaves during an oscillation cycle. Is it a continuous process that causes an accumulation of cell wall material at the apex during slow growth, or does the rate of vesicle fusion change over time? The latter is likely, given that the cytosolic calcium concentration undergoes temporal changes (elaborated below) which is known to influence exocytosis rates in other plant and animal cell types (Battey *et al.* 1999; Beutner *et al.* 2001). A first indication that vesicle movement might play a role in the oscillations was provided by the result of pollen tube treatment with brefeldin A and monensin, two drugs interfering with vesicle transport. They cause pulsatory growth in *N. tabacum* to become steady thus abandoning the alterations in growth rate (Geitmann *et al.* 1996). Parton *et al*. (Parton *et al.* 2001) then observed that fluorescence intensity of labeled vesicles close to the pollen tube tip oscillates with the same frequency as the growth rate. Fluorescence intensity at 3 to 5 µm from the apex peaks about 5-10 seconds before the growth rate (corresponding to an average phase shift of approximately -68°) and declines during the fast phase of growth. If one calculates the rate in the change of fluorescence intensity it seems from the graph provided by the authors that peaks in this rate change would pretty much coincide with peaks in growth

rate. This indicates that a high rate of vesicle secretion occurs during fast growth. However, no statistical analysis was done to establish which of the two events starts first - secretion or expansion.

Other data that corroborate the hypothesis that massive vesicle fusion precedes or coincides with an increase in growth rate can be derived from observations of the dynamics of other organelle populations. Lovy-Wheeler *et al*. (2007) observed that the ER localized in the subapical region of growing pollen tubes moves forward in the cortical region preceding the peak of the growth rate by 4 sec (or -51°), followed by a "folding in" that fills the funnel-shaped ER accumulation to form a "platform". This occurs by 3 sec (or -36°) before the growth peak [The discrepancy between the numbers in seconds and degrees arises from different sample sizes and average growth periods]. The authors purport that this ER movement is actin-myosin based and thus active. A different interpretation of the data is possible, however. If one assumes that peaks in growth rate are preceded by massive exocytosis, the number of secretory vesicles and thus the cytoplasmic volume they occupy in the apex should be reduced considerably during such episodes. The resulting deficit in cytoplasmic contents has to be filled and ER lying adjacent to the tip could thus be "sucked" into the tip in a passive manner. In this scenario, the forward movement of the ER simply reflects the secretory activity thus in turn providing information on the temporal relationship between growth rate and exocytotic activity.

Interestingly, Parton *et al*. (2001) also observed a backward movement of vesicles during slow growth in *Lilium longiflorum* and speculated that this corresponds to a cycling of excess material that is not used during slow growth phases. Intriguingly, Parton *et al*. (Parton *et al.* 2003) found later that pollen tubes whose growth had been halted through brefeldin A action still exhibit periodic vesicle cloud movements in the apical cytoplasm. However, being about five times higher these events have a frequency that is significantly different from that of the typical growth rate fluctuations. The authors propose that these movements nevertheless provide the underlying periodicity for growth rate fluctuations and that the reason for the difference in frequency is the lack of a feedback signal in non-growing tubes.

1.9.8 Oscillatory growth - Converging the models

Because of its relatively rapid oscillatory behavior pollen tube growth has become a model system *par excellence* for understanding the feedback mechanisms that govern plant cell growth. From the data summarized above it becomes clear that neither turgor pressure nor cell wall is the exclusive factor that generates oscillations, but that both influence growth behavior. Due to limitations of space, not all experimental data were summarized here, but we will nevertheless try to propose a converged model that is consistent with most of the observations that have been made. More importantly, this model considers the fact that both of the above mentioned models tacitly acknowledge that the "stable" component (cell wall or turgor) does in reality have to undergo some degree of fluctuation. For example, a turgor-driven expansion of the cell will cause the cell wall to thin and/or strain-harden during the process thus altering its physical properties. Alternatively, a growth surge set off by the softening of the cell wall will to some degree alter the hydrostatic pressure in the cell.

We do agree that the cell wall and the turgor pressure are the two mechanical components that determine cellular growth. We suggest that during steady growth, pollen tube expansion is defined by finely tuned feedback mechanisms that react quasi-instantaneously. This situation can be compared with a mechanical system in equilibrium, such as a mass attached to a spring, in which the weight of the mass is in equilibrium with the tension of the spring. The visible result in the pollen tube is a steady expansion rate. Upon disturbance, the system would enter an oscillatory rhythm in which the feedback mechanisms are still at work but are now spatially and temporally resolvable. This corresponds to the mechanical mass being displaced and the spring exerting a restoring force on it. This restoring force, however, does not succeed in stabilizing the mass at its original position, since the mass takes up momentum (kinetic energy) and passes this position. This is the principle of a harmonic oscillator. While the movement of the mass-spring setup will dampen after a while and the oscillations will decay as a result, this can be prevented by a continuous energy transfer from the environment. An example would be the phenomenon of flutter in aerodynamics.

The idea of comparing the pollen tube to a mechanical oscillator is by no means new (for an excellent analysis refer to (Feijó *et al.* 2001). However, in the past many attempts were done to identify the one parameter that drives the oscillations - a signal generator. If we look closer at the mechanical laws of a simple harmonic oscillator, however, a signal generator is not needed. The only elements required are the following:

i) An equilibrium between forces

The tensile force on the cell wall generated by the presence of the turgor pressure, which is counteracted by the elastic tension determined by the deformability of the cell wall.

ii) An initial disturbance

A disturbance of the equilibrium could be achieved by a direct interference with turgor pressure (through changing the osmotic value of the medium) or with cell wall properties (through applying digestive enzymes or cross-linking agents). Alternatively, this effect can be generated indirectly by changing the cytoplasmic calcium concentration, calcium fluxes, proton concentrations etc. all of which result ultimately in a change of turgor or in an alteration of the deformability of the cell wall through addition of cell wall material and/or through its rigidification or softening.

iii) A robust feedback mechanism

This feedback mechanism that is likely to comprise many components (see below) amplifies the initial disturbance into a stable oscillation.

iv) A transfer of energy

This energy is supplied by the pollen tube metabolism. It prevents the two acting forces from balancing out and thus sustains the oscillations. In the case of the pollen tube this energy is supplied in form of cell wall material that is delivered to and liberated at the apex.

A theoretical model that illustrates that these four parameters are sufficient to generate oscillatory behavior has been proposed by (Kroeger *et al.* 2008). We can therefore

abandon the search for a signal generator. Neither the cell wall nor the turgor generates the oscillations, but both contribute to controlling the outcome by influencing frequency and amplitude.

The great advantage of this model consists in the fact that despite its simplicity, it explains most of the experimental data. All the cellular processes that have been studied in the context of oscillatory growth ultimately affect either cell wall, turgor pressure or energy supply. For example the effect of cytoskeletal inhibitors can be explained by the fact that they interfere with vesicle delivery. According to the model (point *iv*) sufficient energy needs to be supplied to sustain oscillations, otherwise they are dampened over time. This is indeed observed in the experimental situation as oscillations are attenuated upon the addition of cytochalasin D, an inhibitor of actin polymerization (Geitmann *et al.* 1996). The model is also consistent with the fact that lily pollen tubes typically start out with steady growth behavior and switch to oscillatory growth at a later stage. It also explains that both cell wall softening and rigidification can induce pulsatory growth in previously steadily growing pollen tubes.

1.9.9 Ion-based parameters influencing - Oscillatory growth

To understand the components of the feedback mechanism influencing the growth oscillations in pollen tubes it is helpful to identify reactions, activities and molecular concentrations that oscillate with the same frequency as the growth rate, but not necessarily in the same phase. Cross-correlation analysis then allows one to identify the temporal relationship between these parameters. The first group of molecules for which the temporal behavior was investigated were ions, such as Ca^{2+}, K^+, H^+ and Cl^- (for reviews see (Feijó *et al.* 2001; Holdaway-Clarke and Hepler 2003; Hepler *et al.* 2006). Two approaches were used – the visualization of temporal changes in the local cytoplasmic ion concentrations using fluorescent dyes and the measurement of ion fluxes using a vibrating probe. The vibrating probe is an electrode filled with ion exchanger liquid that moves back and forth between two positions measuring the difference in electric potential between them (Jaffe and Nuccitelli 1974). From this information the flux of ions in the adjacent region (in this case across the cell wall) can be extrapolated.

1.9.9.1 Calcium ions

The presence of Ca^{2+} in the growth medium is a necessity for successful germination of most pollen species (Brewbaker and Kwack 1963; Picton and Steer 1983a). Cytosolic Ca^{2+} concentration has been measured in various species and using different dyes, such as the ratiometric indicator dyes indo-1 (Rathore *et al.* 1991), and fura-2-dextran (Pierson *et al.* 1994; Pierson *et al.* 1996); for a comparison of methods see (Camacho *et al.* 2000), or the Ca^{2+}-sensitive photoproteins aequorin (Messerli *et al.* 2000) and cameleon (Iwano *et al.* 2004; Watahiki *et al.* 2004). All these studies show that there is a striking tip-focused gradient in cytosolic Ca^{2+} concentration. Depending on species and method used the cytoplasmic region closest to the tip shows a Ca^{2+} concentration between 3 and 10 μM which drops to tens or hundreds of nM within 20 μm from the apex. This gradient is maintained by an influx of Ca^{2+} ions through the apical membrane (Feijó *et al.* 1995a; Feijó *et al.* 1995b; Messerli *et al.* 1999) mediated by Ca^{2+} channels (Dutta and Robinson 2004). While the principal source of Ca^{2+} seems to be extracellular, Ca^{2+} release from internal stores, conceivably from vesicles or ER located in the apical region, is likely to contribute (Kost *et al.* 1999; Hepler *et al.* 2001). The rapid decrease in Ca^{2+} concentration in the subapical region might be due to ion uptake into intracellular stores such as mitochondria, or the binding of Ca^{2+} to secretory vesicles, but no experimental evidence exists so far.

The presence of the Ca^{2+} gradient is closely coupled to growth, since treatment with BAPTA-type buffers (1,2-bis(*O*-aminophenoxy)ethane-*N*,*N*,*N*′,*N*′-tetraacetic acid), which dissipate the gradient, also arrest growth (Rathore *et al.* 1991; Miller *et al.* 1992; Pierson *et al.* 1993). Inversely, growth arrest due to other factors is accompanied by a dissipation of the Ca^{2+} gradient (Franklin-Tong *et al.* 1997). The cytosolic Ca^{2+} is thought to be a key player in the intracellular signal transduction and integration. These signaling pathways have been shown to also be based on phosphoinositides, phospholipases and Rho GTPases (reviewed in (Franklin-Tong 1999; Malhó *et al.* 2000; Malhó *et al.* 2006; Geitmann and Palanivelu 2007). The high cytosolic Ca^{2+} concentration at the very apex has been postulated to provide the spatial information for the localization of exocytosis events. This is confirmed by the observation that the artificial displacement of the highest Ca^{2+}

concentration through local photorelease of caged Ca^{2+} alters the growth direction of the tube (Malhó *et al.* 1994; Malhó *et al.* 1995; Malhó and Trewavas 1996).

It was therefore not surprising that Ca^{2+} also seemed to temporally determine growth rate since its concentration oscillates at the same frequency as the growth oscillations (Holdaway-Clarke *et al.* 1997; Messerli and Robinson 1997). What was surprising, however, was that the peaks in Ca^{2+} concentration do not precede growth peaks, but are delayed by several seconds in pollen tubes of *L. longiflorum* (Messerli *et al.* 2000; Hepler *et al.* 2006). This corresponds to a phase lag of 38° (Messerli *et al.* 2000). The peak in the influx of Ca^{2+} into the apex is even more delayed; values for this phase lag vary between 123° (Messerli *et al.* 1999) and 149° (Holdaway-Clarke *et al.* 1997). This phase relationship indicates that Ca^{2+} is unlikely to be a determining factor in rapid growth events but rather a consequence. However, especially the phase relationship between calcium flux and growth might be skewed by the fact that the cell wall might act as a Ca^{2+} buffer. Anionic sites on newly secreted pectin polymers can bind Ca^{2+} ions and therefore the Ca^{2+} measured with the vibrating probe actually only reflects the Ca^{2+} flux from the external medium into the cell wall. This flux is likely not to correspond to the amount (Holdaway-Clarke and Hepler 2003) nor to the timing of the Ca^{2+} flux across the plasma membrane into the cytosol.

Another possible explanation for the temporal relationship between Ca^{2+} flux and rise of cytosolic Ca^{2+} concentration is the assumption that the main source of the latter lies in intracellular stores. Messerli *et al*. (2000) propose that Ca^{2+} influx through the membrane only raises the cytosolic Ca^{2+} concentration to some critical threshold which then triggers the massive release of Ca^{2+} from internal stores, which is in turn the signal observed in the fluorescence microscope. Evidence for this hypothesis is provided by the biphasic shape of the curve representing the Ca^{2+} surge (Messerli and Robinson 1997).

To understand the role of transmembrane Ca^{2+} flux for oscillating growth, manipulation of external Ca^{2+} concentration as well as pharmacological approaches to inhibit Ca^{2+} specific ion channels were used. The ten-fold increase of external calcium concentration decreased the amplitude of growth oscillations while increasing the basal

growth rate in *L. longiflorum* (Messerli and Robinson 2003). The former can be explained by the cross-linking and thus stiffening effect of Ca^{2+} on the cell wall pectins, whereas the latter might be related to an increase in exocytosis rate due to an increase in cytoplasmic Ca^{2+} concentration. Increased calcium concentrations in the medium also increased the oscillation period (Holdaway-Clarke *et al.* 2003). However, drawing conclusions from the data is not straightforward, since externally applied Ca^{2+} can have at least two effects: modifying the physical properties of the cell wall and changing the intracellular calcium concentration leading to an effect on exocytosis. To eliminate the effect of Ca^{2+} on the cell wall from the equation, inhibitors of calcium channels have been applied to assess the effect of a reduction in Ca^{2+} influx on growth. In particular La^{3+} and Gd^{3+} successfully reduced pulsation frequencies in *N. tabacum* (Geitmann and Cresti 1998) indicating that the influx rate of calcium affects the oscillatory behavior. A recently developed theoretical model for the role of Ca^{2+} in oscillatory growth fits most of these experimental data very well (Kroeger *et al.* 2008).

1.9.9.2 Protons

The medium pH is a very critical condition for *in vitro* pollen tube growth. In lily pollen tubes, the optimum pH for growth is situated between 5 and 6. When the extracellular pH reaches 7, it is unable to support lily pollen tube elongation. In *Arabidopsis* on the other hand, the optimal pH is around 7, lower values reduce the germination rate. Like Ca^{2+}, H^+ concentration in the extracellular medium is higher than its concentration inside the pollen tube. This imbalance in concentration and electric potentials will create a strong force that will cause these ions to enter the cell. Holdaway-Clarke and Hepler (2003) suggested that H^+ may enter at the tip of pollen tubes by using the same nonspecific cation channel as Ca^{2+}.

Initially, no intracellular pH gradient was thought to be present in the pollen tube cytoplasm. This was due to limitations in the methods used (Fricker *et al.* 1997). The problems were based on the high mobility of H^+ ions (compared to Ca^{2+}), the predisposition of dyes to bleach rapidly and the fact that the typical indicator dyes, especially at elevated concentrations, dissipate these presumptive gradients (Holdaway-Clarke and Hepler 2003).

Low concentrations of BCECF-dextran indicator were eventually used successfully to visualize a pH gradient in lily pollen tubes. The apex of these cells is characterized by a slightly acidic domain (pH = 6.8), whereas the base of the clear zone is alkaline (pH = 7.5) (Feijó *et al.* 1999). Using a vibrating probe, Feijó *et al*. (Feijó *et al.* 1999) showed also that there is a proton influx at the extreme apex of the *L. longiflorum* pollen tube and an efflux in the region corresponding to the alkaline zone (Fig 1.5d). They also demonstrated that the alkaline band correlates with the position of the turnaround point of the reverse fountain streaming at the base of the clear zone. It is thought that this alkaline zone is governed by a plasma membrane H^+-ATPase (Hepler *et al.* 2006). It had been shown previously that the activity of the H^+-ATPase seems to regulate the growth rate of pollen tubes. Treatment with an ATPase antagonists such as vanadate inhibits tube growth in lily whereas agonists like fusicoccin, increase pollen tube growth rate (Fricker *et al.* 1997). When pollen tube growth is inhibited, the apical acidic band disappears while the alkaline zone extends.

H^+ influx at the tip oscillates with the same phase as the growth oscillations, but the peak lags behind by 67.5° (Messerli and Robinson 1998) or 103° (Messerli *et al.* 1999). Correspondingly, cytosolic pH becomes more acidic in the tip with changes up to a full unit during a growth cycle with the cytoplasmic acidification following a rapid growth peak (Messerli and Robinson 1998; Feijó *et al.* 1999). The authors propose that the rise in cytosolic pH following a growth pulse may lower the affinity of Ca^{2+} binding proteins for Ca^{2+} thus shutting off Ca^{2+}-triggered vesicle fusion. While cross-correlation analysis indicated that acidification follows growth, alkalinization was observed to actually precede growth peaks in *Lilium longiflorum* and *Lilium formosanum* (Lovy-Wheeler *et al.* 2006). The alkaline band coincides spatially with the cortical actin fringe in these species suggesting that the changing pH might affect the actin cytoskeleton, for example via the action of ADF. Lovy-Wheeler *et al.* (2006) propose that the ADF is stimulated by low pH to fragment F-actin in the cortical fringe resulting in the exposure of new plus or barbed ends that in turn enhance new polymerization of actin.

A change in external proton concentration does not affect pollen tube oscillations very dramatically within the range of pH that permits pollen tube (Holdaway-Clarke *et al.*

2003). However, a lower pH in the external medium has the tendency to increase the amplitude of the growth oscillations. In addition to affecting the cytoplasmic pH, protons are also cell wall loosening agents; in pollen tube walls they may act through the enzyme PME, and either reduce demethylation or stimulate hydrolysis of pectin.

1.9.9.3 Potential players: Chloride and potassium ions

Chloride ions have been shown to play a role in pollen tube growth. The inhibition of presumed chloride channels by inositol-3,4,5,6-tetra*kis*phosphate (Cl^- channel blocker used in animal cells) showed that the pollen tube growth rate diminished accompanied by a swelling of the cell (Zonia *et al.* 2002). Because of problems with the specificity of the vibrating probe to Cl^- channels, reliable data on Cl^- oscillations are not available yet (Messerli *et al.* 2004).

The existence of various types of K^+ channels in pollen tube plasma membrane and in pollen grains have been evidenced using patch-clamp techniques in *Brassica*, lily and *Arabidopsis* (Obermeyer and Kolb 1993; Fan *et al.* 1999; Fan *et al.* 2001; Griessner and Obermeyer 2003; Dutta and Robinson 2004). In *Arabidopsis*, a mutation in the K^+ channel reduces ion uptake in pollen tubes and consequently growth (Mouline *et al.* 2002). Messerli *et al*. (Messerli *et al.* 1999) measured tip-restricted K^+ fluxes in lily pollen tubes using the vibrating probe and observed a lag of 100° with respect to the growth rate. The pulses of K^+ and H^+ are very similar suggesting that K^+ is taken up via a K^+/H^+ co-transporter (Messerli *et al.* 1999). The authors propose that the K^+ influx restores either the total ionic concentration and/or osmotic concentration in the cytoplasm after the increase in cell volume resulting from the growth pulse. This would help the cell to rapidly recover turgor pressure for the increased volume of the tube.

1.9.10 Other oscillating parameters

1.9.10.1 NAD(P)H

NAD(P)H are essential coenzymes with a central role in the control of cellular metabolism. Their high energy status and reducing power drive many key biosynthetic

reactions and ATP production. Because NAD(P)H but not $NAD(P)^+$ possesses an endogenous fluorescence, the reduced form can be detected in living cells. Cárdenas *et al*. (Cárdenas *et al.* 2006) showed that the strongest signal for NAD(P)H in lily pollen tubes is observed 20-40 μm behind the apex, where mitochondria accumulate. This shows that $NADP^+$ and ATP are both located in mitochondria. The cytosolic concentration of NAD(P)H is observed to oscillate during oscillatory growth. Peaks of NAD(P)H follow growth peaks by 77° to 116° (7 to 11s) whereas troughs anticipate growth maxima by 5 to 10 sec corresponding to -54° to -107°. This oscillation was suggested to be due to a periodic change of state of NAD(P)H from reduced to oxidized form thus suggesting that growth peaks might be preceded by increases in $NAD(P)^+$ (Cárdenas *et al.* 2006). It is therefore possible that the transformation of NAD(P)H to $NAD(P)^+$ is coupled to ATP synthesis, which is then harvested to power energy-consuming processes located at the pollen tube apex. Among these could be the proton-pumping ATPase responsible for the alkaline band, actin polymerization (given that G-actin bound to ATP is the preferable form of the monomer), and exo- and endocytosis.

1.9.10.2 Small GTPases and actin

Rho-family small GTPases are important signaling switches in all eukaryotes. A single subfamily has been identified in plants (ROPs: rho-like GTPase from plants). These proteins are known to coordinate various pathways regulating cellular activities such as the production, targeting and fusion of secretory vesicles, remodeling of cell wall, Ca^{2+} gradient and other signaling pathways (Hwang and Yang 2006). ROP1 is highly expressed in mature pollen grains and in its active form it forms a tip-high gradient in the extreme of the pollen tube plasma membrane. The tip-localized activity of ROP1 is dynamic as it oscillates with the same frequency as the growth rate (Hwang *et al.* 2005). The maximum of ROP1 accumulation precedes growth rate by 87°, thus supporting a crucial role of this protein in the control of pollen tube growth. It is not well understood how ROP regulates growth, but it is known that it acts on F-actin dynamics mediated by downstream effectors such as RIC3 and RIC4 (Gu *et al.* 2005). This points at the importance of visualizing filamentous actin in growing pollen tubes to characterize its dynamics in relationship to the

different growth phases. Labeling with GFP-talin has provided first indications that the configuration of the actin cytoskeleton varies over time. Fluorescence intensity of the talin marker in the apex precedes growth rate by -70° (Hwang *et al.* 2005). However, given that talin is an ABP whose dynamics do not necessarily reflect the dynamics of the actin filaments, more detailed information is elusive at present. To obtain these data a labeling method for actin needs to be developed that allows the satisfactory visualization of the apical actin population in living pollen tubes without interfering with its functioning. To date, the available methods have not been able to combine both of these requirements (Wilsen *et al.* 2006).

1.9.10.3 Phospholipase C

The inositol signaling pathway relies on the activity of phospholipase C, an enzyme that cleaves phosphatidylinositol 4,5-bisphosphate ($PtdInsP_2$) into two cellular regulators: diacyl glycerol and inositol 1,4,5-trisphosphate. Phospholipase C has been localized to the apical plasma membrane in pollen tubes of *Petunia inflata* (Dowd *et al.* 2006). Pollen tubes from this species do not show sinusoidal oscillations, but rather extended phases of slow growth interrupted by short growth pulses. It was observed that phospholipase C accumulates on the apical plasma membrane during slow growth whereas during a rapid growth phase the enzyme leaves the membrane and accumulates in the cytoplasm. The presence of the enzyme on the plasma membrane during slow growth results in low levels of $PtdInsP_2$, whereas these levels rise during rapid growth. Dowd *et al*. (2006) propose that this increase in $PtdInsP_2$ sustains growth through regulation of membrane dynamics and/or alterations in cytoskeletal structure. However, the precise phase relationship between accumulation of phospholipase C and growth activity was not assessed and causal relationships cannot be drawn directly from these data.

1.9.11 Pollen tube growth *in planta* - Guidance and invasion

While pollen tubes are an excellent model system to be studied *in vitro*, there is a lot of interest in the *in vivo*, or *in planta* situation. The situation of a pollen tube growing *in planta* is very particular, since it represents the invasion of one organism (the sporophyte

that carries the female gametophyte and future fertilization partner) by another (the male gametophyte). The questions that arise concern in particular recognition mechanisms occurring during cross- and auto-incompatibility reactions (reviewed by (Silva and Goring 2001; Takayama and Isogai 2004) and guidance mechanisms allowing the pollen tube to find its way within a compatible pistil (reviewed by (Palanivelu and Preuss 2000; Cheung and Wu 2001; Geitmann and Palanivelu 2007). In the context of this review we will focus on the mechanical aspect of pollen tube growth through the female tissues of the pistil.

During the invasion of the stigmatic and stylar tissues, in particular in species with solid styles, growing pollen tubes have to invade the apoplast of the stylar transmitting tissue. Even though pollen tubes are able to soften these tissues either by inducing programmed cell death or by enzymatically digesting the cell walls (Hiscock *et al.* 1994; Greenberg 1996; Wang *et al.* 1996a; Hiratsuka *et al.* 2002; Suen and Huang 2007), these processes are unlikely to completely liquefy the growth matrix. The advancing apex of the elongating pollen tube, therefore, has to be able to exert sufficient penetration force and to withstand externally applied compressive stress. While most of the growth force is thought to be provided by the hydrostatic turgor pressure in the cell it was observed that the actin cytoskeleton might be involved in generating an invasive force. Treatment with low concentrations of latrunculin B, an inhibitor of actin polymerization, does not inhibit pollen tube growth but reduces the pollen tube's ability to invade a stiffened growth matrix in the case of *Papaver rhoeas* (Gossot and Geitmann 2007). Whether the force generated by the polymerization of filamentous actin actually forms a mechanical contribution to the invasive force is questionable, however, as these forces have been calculated to be very small compared to that generated by the turgor pressure (Money 1997). However, it is interesting that actin polymerization inhibitors at low concentrations also inhibit growth oscillations in pollen tubes (Geitmann *et al.* 1996). It is, therefore, not altogether absurd to speculate that these growth oscillations might facilitate the invasive growth in pollen tubes (Geitmann 1999).

This idea is particularly intriguing if one considers that in many cases the shape of the pollen tube changes upon the initiation of a rapid pulse phase. The rapidly elongating

apex has a smaller diameter that broadens during the subsequent slow phase (Geitmann 1997; Zonia *et al.* 2001). While intuition suggests that a smaller apex penetrates easier into a stiff matrix, the physical background can be found in fracture theory. Based on energy conservation principles (Callister 1994) it can be calculated that the smaller the width of a crack in a material, the bigger is the stress on the material that enables the propagation of the crack. This could explain why a pollen tube during rapid elongation would be more successful in penetrating the surrounding matrix if its apex was smaller.

1.9.12 Conclusions

In no other cell type can the dynamics of plant cell growth be observed in such a dramatic manner as in pollen tubes. Not only do these cells grow extremely rapidly, but also is the growth behavior oscillatory. This temporal separation of events allows for the investigation of feedback mechanisms that determine the growth process. While numerous pieces of the puzzle have been identified, the completion of the picture will require the acquisition of a lot of additional data and, more importantly, their analysis and interpretation. We proposed a simple mechanical model for oscillatory growth that renders the search for a signal generator superfluous. It is based on three mechanical elements: the turgor pressure, the cell wall deformability and a continuous supply of energy. All other parameters that are known and will be found to influence oscillatory growth ultimately act via their effects on one or several of these key elements. This model might help to understand numerous aspects of the pollen tube growth process and is amenable to refinement.

1.9.13 Acknowledgements

Research in the Geitmann lab is supported by grants from the Natural Sciences and Engineering Research Council of Canada (NSERC), the *Fonds Québécois de la Recherche sur la Nature et les Technologies* (FQRNT), the Canadian Foundation for Innovation (CFI) and the Human Frontier Science Program (HFSP). Kind thanks to Global Science Books, Ikenobe , Japan (http://www.globalsciencebooks.info) for permission to use the text that

originally appeared in: Chebli Y, Geitmann A (2007) Mechanical principles governing pollen tube growth.Functional Plant Science and Biotechnology 1: 232-245.

1.9.14 Figures

Figure 1.5 : Schematic representation of the polar arrangement of cellular structures and processes in the apical and subapical regions of a growing pollen tube (legend on next page).

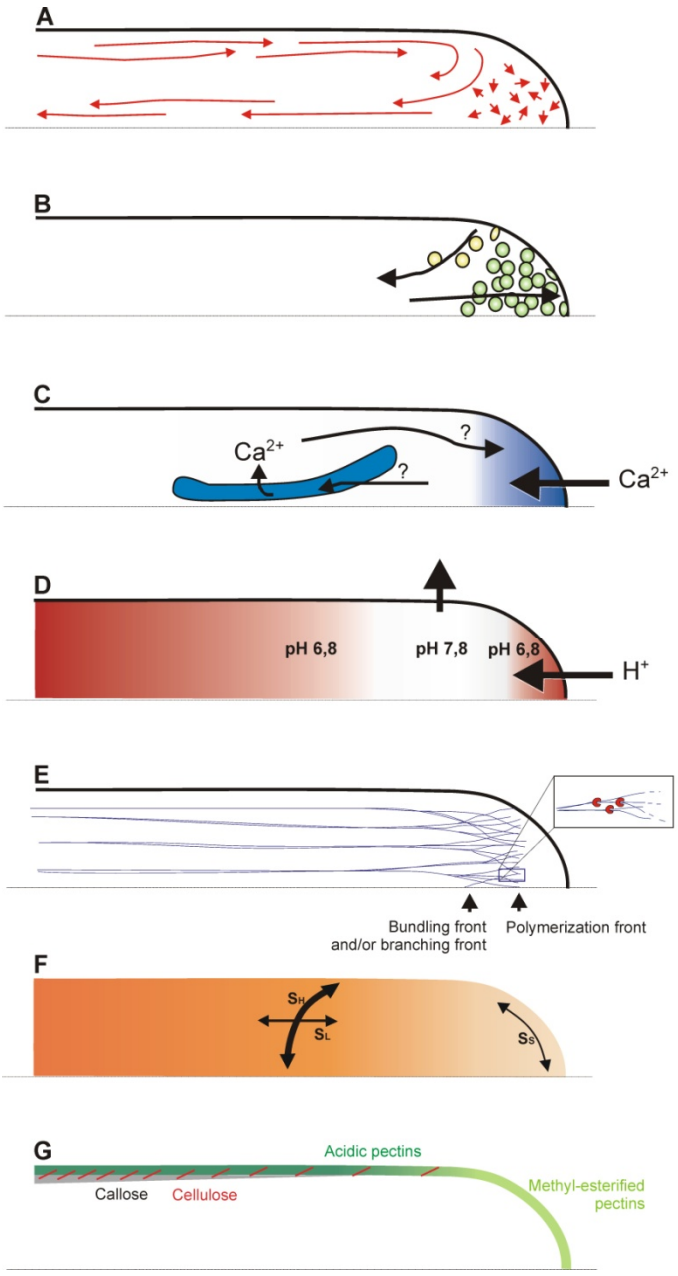

Figure 1.5: Schematic representation of the polar arrangement of cellular structures and processes in the apical and subapical regions of a growing pollen tube.

Because of the radial symmetry of the cell only half of a median section is drawn. Objects are not to scale. (**A**) Cytoplasmic streaming occurs parallel to the long axis. In larger tubes forward movement takes place in the cortex and rearward movement in the center of the tube. Vesicle movements in the apex are more erratic. (**B**) Secretory vesicles (green) accumulate in the apical region were exocytosis takes place. Rapid endocytosis likely takes place in the entire apex, but clathrin-mediated endocytosis (yellow vesicles) occurs predominantly at the base of the apex. (**C**) The cytosolic calcium concentration is high at the very apex and drops drastically towards the shank. Calcium influx occurs through the apical plasma membrane. It is unclear which organelles sequester calcium and to what degree calcium release from organelles contributes to the calcium gradient. (**D**) Proton influx occurs at the tip and efflux in the subapical region. This leads to the formation of an alkaline band that corresponds approximately to the turnaround point of cytoplasmic streaming and to the actin fringe. (**E**) Filamentous actin is arranged predominantly in longitudinal direction. Long cables characterize the shank region, whereas in the subapex actin seems to be branched or less bundled giving rise to a fringe. (**F**) According to the laws of thin-walled pressure vessels the tensile stress in the wall generated by the internal pressure is twice as high in circumferential direction (S_H) compared to longitudinal direction (S_L) or the hemisphere shaped tip (S_S). Shade of orange indicates the degree of cellular stiffness. (**G**) The biochemical composition of the cell wall changes from the apex to the distal region through decreasing methyl-esterification of pectins and addition of callose and cellulose.

Figure 1.6

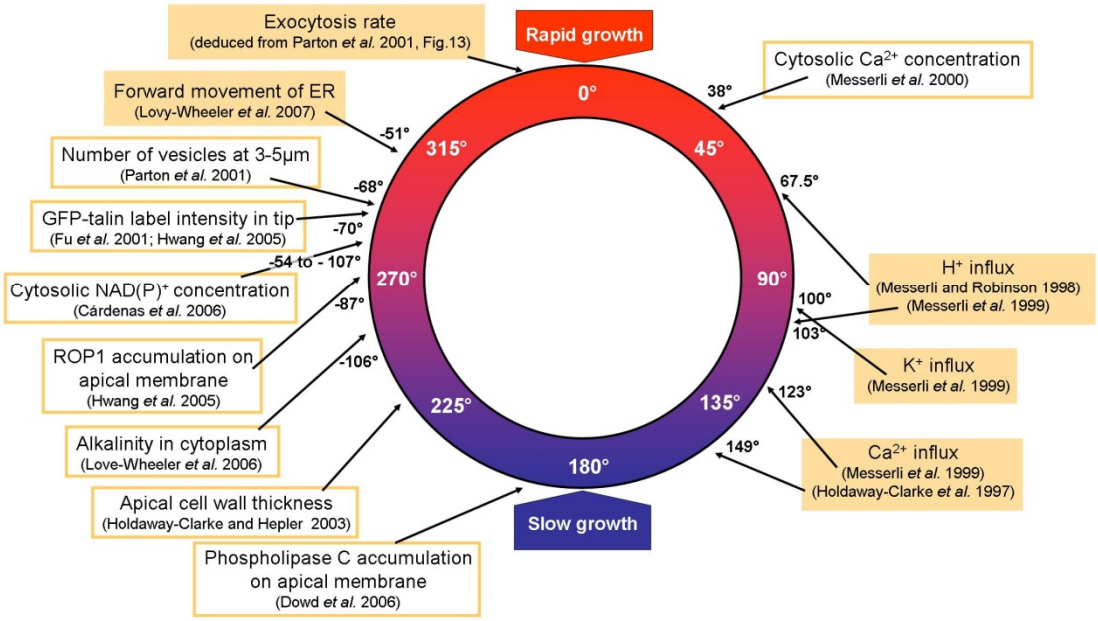

Figure 1.6: Compilation of cellular features and processes that have been observed to undergo changes during oscillatory pollen tube growth.

Note that these data have been acquired on pollen tubes from different plant species. Arrows indicate the phase relationships between peaks in concentration or flux rate of a particular parameter and peaks in growth rate. Phase shifts are indicated as degrees with 360° corresponding to a complete oscillation period. In most cases this phase relationship has been established by cross-correlation analysis - a process that identifies whether a particular process is leading (negative numbers) or lagging (positive numbers) growth. Two classes of parameters can be distinguished: concentrations (orange frame) and movement rates (orange background). The latter are first derivatives of the former. This distinction is important when identifying cause-effect relationships. This becomes evident for example when looking at the label intensity for secretory vesicles, which is highest at -68°. For this particular parameter, however, more important than the *concentration* (the amount of vesicles), is the information that can be derived from the *change* of label intensity, since it corresponds to exocytosis activity, which in turn is a *rate*.

1.10 Goals and objectives

The main goal is to understand the role played by the different cell wall components in shaping the cell and controlling the growth behaviour of pollen tubes.

Several species were used for this study: *Arabidopsis thaliana*, *Lilium longiflorum* and *Camellia japonica. Arabidopsis thaliana* was used for the molecular work because of the easy access to sequence data and all the established molecular biology protocols for the generation of transgenic lines. Moreover, because of the ease of growth and short life cycle of *Arabidopsis*, pollen was always available. Lily and camellia pollen tubes were used because of their ease of and highly reproducible cultivation, their fast growth rate compared to *Arabidopsis* and their much larger diameters, which facilitates microscopical observations.

To be able to achieve our main goal, two prerequisites are required:

1- The optimization of the *in vitro* growth conditions of *Arabidopsis thaliana* pollen tubes.

2- The optimization of microwave assisted protocols for a faster and more efficient sample preparation for optical and electron microscopy.

The pollen tube is an ideal model to study the roles played by the cell wall components during growth because of the simple cell wall composition compared to other cell types and because of the fast rate of growth. My thesis focuses in more detail on the following objectives:

1- Characterizing the *Arabidopsis thaliana* pollen tube cell wall.

   a. The spatial localization of each cell wall component compared to the others.

   b. The roles played by pectins and cellulose during pollen tube elongation.

2- Characterizing the mechanical and biological roles of cellulose and pectins during *Lilium longiflorum* pollen tube elongation.

3- Characterization of the role of pectate lyases during *Arabidopsis thaliana* pollen tube germination.

    a. The role of PLs in pollen grains and initiation of germination

    b. The localization of PLs in pollen grains and growing pollen tubes

    c. The role of PLs during pollen tube elongation

4- Characterizing the role of omnidirectional gravity and hyper-gravity on *Camellia japonica* pollen tubes.

    a. Reviewing the effect of gravity on single plant cells.

    b. The effects of omnidirectional gravity on the pollen tube cell wall composition.

    c. The effects of hyper-gravity on the pollen tube cell wall composition.

    d. The effects of hyper-gravity on the vesicular dynamics and the delivery of cell wall components to the apex of the pollen tube.

2 Optimization of conditions for germination of cold stored *Arabidopsis thaliana* pollen

At the beginning of my PhD, the *Arabidopsis thaliana* pollen tube was rarely used for mechanical, immuno-histochemical, functional and molecular studies. The main reason was the notorious difficulty to obtain reproducible rates of germination and healthy growing pollen tubes *in vitro*. Despite the fact that at that date (early 2007) several studies were published with *Arabidopsis thaliana* pollen germinating *in vitro*, reproducing a high germination rate with the same protocol was a challenge. In our hands, the success of these published protocols was highly variable with rates of germination between 5% and 70%. Because the main studies conducted in the lab at that time by my colleagues and I were based on the use of *Arabidopsis thaliana* pollen tubes (mainly because of the easy availability of mutants), my colleague Firas Bou Daher and I worked on optimizing the best conditions for the *in vitro* germination of *Arabidopsis* pollen. We developed methods for different experimental setups depending on the parameter to be assessed. We were able to show that the growth of *Arabidopsis* pollen requires stringent conditions and we showed that our method was highly reproducible. The present manuscript details our finding and conclusions.

I contributed to this manuscript by performing all the experiments in collaboration with my colleague Firas Bou Daher. While I analyzed all the data related to pollen tubes growing in liquid media, Firas analyzed the data of pollen tubes growing in solid media. I also contributed to the writing of all the sections of the present manuscript.

This manuscript entitled “Optimization of conditions for germination of cold stored *Arabidopsis thaliana* pollen” was published in 2009 in *Plant Cell Reports* volume 28, pages 347-457.

Firas Bou Daher*, Youssef Chebli*, Anja Geitmann

*These authors contributed equally to the work

2.1 Abstract

One of the rare weak points of the model plant *Arabidopsis* is the technical problem associated with the germination of its male gametophyte and the generation of the pollen tube *in vitro*. *Arabidopsis* pollen being tricellular it has a notoriously low i*n vitro* germination compared to species with bicellular pollen. This drawback strongly affects the reproducibility of experiments based on this cellular system. Together with the fact that pollen collection from this species is tedious, these are obstacles for the standard use of *Arabidopsis* pollen for experiments that require high numbers of pollen tubes and for which the percentage of germination under control conditions need to be highly reproducible. The possibility of freeze storing pollen after bulk collection is a potential way to solve these problems but necessitates methods that ensure continued viability and reproducible capacity to germinate. Our objective was the optimization of germination conditions for *Arabidopsis* pollen that had been freeze stored. We optimized the concentrations of various media components conventionally used for *in vitro* pollen germination. We found that in general 4 mM calcium, 1.62 mM boric acid, 1 mM potassium, 1 mM magnesium, 18% sucrose at pH 7 and a temperature of 22.5 °C are required for optimal pollen germination. However, different experimental setups may deviate in their requirements from this general protocol. We suggest how to optimally use these optimized methods for different practical experiments ranging from morphological observations of pollen tubes in optical and electron microscopy to their bulk use for molecular and biochemical analyses or for experimental setups for which a specific medium stiffness is critical.

Key Words

Arabidopsis thaliana - in vitro cell culture - pollen germination - pollen tube

Abbreviations

ATP	adenosine triphosphate
CCD	charged coupled device
EGTA	ethylene glycol tetraacetic acid
FDA	fluorescein diacetate

2.2 Introduction

In the last two decades, *Arabidopsis thaliana* has become an extremely useful organism for studying a wide range of issues in plant biology. This species gained even more importance and became the main tool for plant cellular and molecular biology studies after the publication of "The *Arabidopsis* Genome Initiative" (The Arabidopsis Genome Initiative 2000). It is therefore astonishing that since that date, less than 5% of the PubMed-listed publications on research performed on the male gametophyte of flowering plants have used *Arabidopsis* pollen. Pollen is a widely used cellular system that on one hand is studied to better understand the reproduction process in flowering plants, and that on the other hand exhibits several features that make it an excellent model system to investigate the principles governing plant cell growth in general. The latter is due to the fact that the pollen tube, a cellular protrusion formed from the pollen grain, elongates extremely rapidly with the purpose of delivering the sperm cells to the ovule. Very conveniently for the researcher, pollen germination and the generation of the pollen tube can be achieved *in vitro,* thus offering an excellent opportunity to observe the processes associated with plant cell growth, cell wall synthesis and intracellular transport in a single cell system.

While microscopic observations are often carried out on few individual cells, other experimental approaches require large amounts of material. Myosin extraction from lily pollen tubes (Yokota and Shimmen 1994), RNA isolation for transcriptional profiling and gene expression in pollen grains and pollen tubes (Guyon *et al.* 2000; Becker *et al.* 2003), and vesicle isolation for biochemical and ultrastructural characterization from germinated lily pollen (van der Woude *et al.* 1971) required large amounts of pollen as a starting material. From the need for substantial amounts of *Arabidopsis* pollen material implicated in this type of experiment ensued the necessity to optimize a method for long term storage that would allow pooling pollen from several harvests.

The principal problem associated with large quantity pollen harvest in *Arabidopsis* is the minute size of its flower (1 mm), the resulting low number of pollen grains per flower, as well as the small size of the individual pollen grain. The comparison to other plant species illustrates this point. To obtain the same amount of pollen in weight collected from a single

flower of *Camellia*, pollen from approximately 115 000 plants of *Arabidopsis* needs to be harvested, or, in other words, that of more than one million flowers. To automate bulk pollen collection of *Arabidopsis*, Johnson-Brousseau and McCormick (2004) developed a method using a modified vacuum cleaner equipped with three different meshes that has proven to be very useful. Nevertheless, harvesting the mounts of material necessary for biochemical experiments remains time-consuming.

Not only is pollen harvest from *Arabidopsis* comparably tedious, experimentation on germinating pollen is rendered challenging by the fact that *in vitro* germination is notoriously irreproducible in this species. It is generally agreed upon that existing protocols are highly unsatisfactory as they do not allow the generation of reproducible percentages of germination, even within a single batch of pollen. One reason for this may be that *Arabidopsis* pollen is tricellular which is known to be associated with reduced *in vitro* percentages of germination compared to bicellular species (Brewbaker and Kwack 1963; Taylor and Hepler 1997). Moreover, the 6 stamens of the *Arabidopsis* flower form two distinct groups which mature at different times (Smyth *et al.* 1990), causing a difference in the degree of maturity between the two types of pollen harvested from a single flower (Johnson-Brousseau and McCormick 2004). It was also reported that mature pollen grains undergo autolysis in *Arabidopsis thaliana* after anthesis favoring autopollination (Yamamoto *et al.* 2003). This may be an additional factor responsible for the low germination rate *in vitro*.

The need for significant amounts of material associated with certain experimental strategies could be met easier, if pollen could be stored without the significant loss of viability or germination capacity. The pollen of many plant species can be dried on silica gel and stored at -20°C or -80°C to keep its ability to germinate after several years. Hitherto, this method did not seem to be very successful for *Arabidopsis* pollen. Here we investigated the effect of cold storage on pollen germination and we optimized several parameters of the growth conditions to allow for optimal percentage germination of frozen stored pollen.

Various *Arabidopsis* pollen germination media have been proposed in the literature (Li *et al.* 1999; Fan *et al.* 2001; Boavida and McCormick 2007), their principal ingredients comprise calcium, boric acid, magnesium, potassium and sucrose, components that are

generally found in pollen germination media at varying concentrations. In addition to these elements, the pH of the medium and the growth temperature are two major factors affecting percentage germination and growth (Boavida and McCormick 2007; Chebli and Geitmann 2007).

Here we describe protocols for germination of frozen stored *Arabidopsis thaliana* pollen grains that contain optimized concentrations of these ingredients. In addition, we provide standardized methods for pollen germination and growth in different experimental setups including liquid and solid medium, low and high quantity approaches. These methods are useful for different kinds of studies ranging from morphological observations in electron or optical microscopy (cell wall and cytoskeleton label, live observation of vesicle trafficking, monitoring of ion gradients) to the bulk use for molecular and biochemical analyses.

2.3 Materials and methods

2.3.1 *Arabidopsis thaliana* growth and pollen harvest

Arabidopsis thaliana ecotype Columbia 0 plants were grown in trays in a glasshouse at 22°C day temperature and 20°C night temperature, 50% humidity under 16h daylight and 300 µE m^{-2} s^{-1} light intensity. Approximately 150 seeds (prepared by mixing 50 mg of seeds in 40 mL of 0.1% agar in water to avoid seed clumps) were sown per plate. The mixture was then uniformly dribbled on the soil surface. Plants were irrigated each day and fertilized every second day with Plant-Prod® 20-20-20 fertilizer at 200 ppm. Pollen was collected every day from the time flowers bloomed using a modified vacuum cleaner as described by Johnson-Brousseau and McCormick (Johnson-Brousseau and McCormick 2004). Briefly, using plumbing fittings, three different sized Lab Pak® nylon meshes (80, 35 and 5µm) were fixed in sequence on a plastic pipe which was then related to a 700W Shark® vacuum cleaner. Pollen was collected by passing the modified plastic pipe over the *Arabidopsis* flowers with gentle shaking.

2.3.2 Storage of pollen grains

Pollen was removed from the 35 and the 5 µm nylon meshes and used directly or stored in 1.5 ml microfuge tubes. Unless noted otherwise, pollen was dried on silica gel for 2 hours at room temperature prior to cold storage at either -20°C or at -80°C.

2.3.3 Pollen grain rehydration

Pollen was rehydrated before each experiment. For this purpose after removal from freezer, pollen was placed in a humid chamber for 30 minutes at room temperature. Care was taken not to let the grains get in direct contact with liquid water.

2.3.4 Germination media

For all experiments, unless specified elsewhere, two different versions of the growth medium were used for pollen germination; a liquid version and a solid version containing 0.5% agar (SIGMA A1296). Unless specified otherwise, the germination medium contained 18% sucrose, 0.01% (1.62 mM) boric acid, 1 mM $CaCl_2$, 1 mM $Ca(NO_3)_2$, 1 mM $MgSO_4$, and 1mM KCl with a pH adjusted to 7. For solid medium preparation, agar was added to the mix and heated to dissolve.

For comparison, the following media tested were used with a modified concentration of sucrose (18% instead of the concentration originally published): Brewbaker and Kwack (BK) medium (Brewbaker and Kwack 1963), Lily pollen germination medium (Parre and Geitmann 2005a). The media that were used exactly as published had originally been developed by the following groups: Wu and coworkers (Fan *et al.* 2001), Yang and coworkers (Li *et al.* 1999), and McCormick and coworkers (Boavida and McCormick 2007).

2.3.5 Experimental setups

2.3.5.1 Pollen germination on a drop of liquid medium

200 µL liquid growth medium was placed on a microscope slide forming a dome shaped drop. Hydrated pollen grains were sprinkled on top of the drop using a fine brush. The slides were placed in a humid chamber to avoid dehydration of the medium.

2.3.5.2 Pollen germination in liquid medium in Erlenmeyer flasks

3 mL liquid growth medium were put in a 25 mL Erlenmeyer flask. Hydrated pollen grains were mixed with the medium by vigorous shaking to avoid clump formation. Two or three whole *Arabidopsis* flowers were added to the medium unless specified otherwise. The Erlenmeyer flasks were covered with a Parafilm® layer containing small holes and placed on a shaker at 70 rpm.

2.3.5.3 Pollen germination on solid surface

Hot agar containing medium was poured onto a microscope slide to form a layer with a thickness of about 0.5 mm and left to cool. Hydrated pollen was then sprinkled on the surface using a fine brush. The slides were placed in a humid chamber.

2.3.5.4 Pollen germination in solid medium

Solid medium was prepared as described above and left to cool to 42°C. Hydrated pollen grains were rapidly mixed with the medium by vigorous stirring. The medium was then poured onto a microscope slide to form a layer with a thickness of about 0.5 mm and placed in a humid chamber.

Unless specified otherwise, subsequent incubations were carried out at 22.5°C. Temperature control was ensured by placing the samples in a Sanyo® MIR-153 incubator. Images were taken at 2, 4 and 6 hours after the beginning of incubation.

2.3.6 Viability test

Pollen grain viability was assessed using fluorescein diacetate (FDA) which was dissolved in acetone at 10 $mg.mL^{-1}$ and stored at -20°C. Prior to each experiment, FDA was diluted in

a 10% sucrose solution to a final concentration of 0.2 mg.mL^{-1}. Hydrated pollen was dipped in 250 µL of the FDA solution on a glass slide and kept in the dark for 5 minutes. Observations were made with a Zeiss Imager-Z1® microscope with excitation light at 470 nm and a 515-565 nm band pass emission filter. Only viable pollen grains emit a fluorescence signal under these conditions.

2.3.7 Microscopy

Observations of samples were done either with a Zeiss Imager-Z1 microscope equipped with a Zeiss AxioCam MRm Rev.2 camera and AxioVision Release 4.5 software or with a Nikon Eclipse TE2000-U inverted microscope equipped with a Roper fx cooled CCD (charged coupled device) camera and ImagePro (Media Cybernetics, Carlsbad, CA) software.

2.3.8 Determination of the germination, growth rate and pollen tube length

For each experiment, at least ten images per sample were taken at random positions and the percentage of germination was quantified. Pollen grains were considered germinated when the pollen tube length was greater than the diameter of the pollen grain (Tuinstra and Wedel 2000). To determine pollen tube length, at least fifty tubes were measured for each experiment.

2.4 Results and Discussion

2.4.1 Influence of storage conditions on pollen grain viability

Tests using FDA that fluoresces under UV in living cells (Schnurer and Rosswall 1982) revealed a decrease in pollen viability with duration of cold storage. While 80% viability was observed for fresh pollen or pollen stored at -20°C for 24h only, this percentage decreased to 12% for pollen stored for 10 months with the most significant drop occurring at approximately 6 months (Fig 2.1). Storage temperature (-20°C versus -80°C) did not affect pollen viability differently. At both temperatures viability was around 60% for pollen

grains stored for 2 to 5 months (Fig 2.2). To ensure satisfactory germination of cold stored pollen, we therefore suggest using up frozen stored *Arabidopsis* pollen within a 5 month period.

2.4.2 Effect of storage conditions on germination

In order to be able to pool pollen from different harvests for analyses requiring significant amounts of material, the optimization of storage conditions is pivotal. Generally, drying pollen before freeze storing is advantageous and therefore we tested different times for drying of *Arabidopsis* over silica gel. Drying for 24h reduced the percentage of germination of the pollen before freezing by approximately 20%, whereas pollen dried for 2h had the same percentage of germination as fresh, non-dried pollen. We therefore used the 2h drying period for all subsequent pollen batches.

We then examined the effect of prolonged freeze storage at -20°C on germination. Our data reveal that during the first 5 months of freeze storage the percentage of germination does not decrease significantly compared to fresh pollen. However, after this time the percentage of germination decreased to be below 10% by the time pollen had been in storage for 10 months or longer. These data are consistent with the decrease in pollen viability observed for the same period of time (Fig 2.2).

Contrary to pollen viability, storage temperature strongly affected pollen germination. The percentage of germination of pollen stored at -80°C for four months was 11% while that of pollen of the same age stored at -20°C was 40%. The latter is therefore clearly a preferable temperature for storing *Arabidopsis* pollen - contrary to other species such as lily whose germination activity is conserved very well at the lower temperature. Even though the percentage of germination was lower for pollen stored at -80°C, we observed that this percentage was maintained for periods exceeding one year. This loss of the ability to germinate may in part be due to lysosomal degradation of the cytoplasmic components that is characteristic for *Arabidopsis thaliana* pollen grains (Yamamoto *et al.* 2003).

2.4.3 Optimization of medium composition for the germination of frozen stored pollen in various experimental setups

In different experimental setups pollen is exposed to different conditions, such as availability of oxygen, that might influence its requirement for the individual elements present in the germination medium. We therefore optimized the concentrations for four different experimental setups:

1. **Liquid drop**: pollen is mixed with liquid medium forming a drop of 180 µl placed on a microscope slide.
2. **Bulk germination in liquid** (Erlenmeyer): pollen is mixed with 3 ml liquid medium in an Erlenmeyer flask.
3. **On solid surface**: pollen is sprinkled onto the surface of an agar-stiffened layer of medium.
4. **Within solid medium**: pollen is mixed into an agar-stiffened medium prior to gelation.

We used concentration series for each of the components of the liquid germination medium and assessed the percentage of germination at 2, 4, and 6 hours after incubation for each of the experimental setups. While different pollen batches were used for different experiments (thus resulting in different percentages of germination for the control samples), pollen with identical storage durations were used for all the samples of an individual series of experiments. Table 2.1 summarizes the optimized concentrations. In the following we discuss some of the results in more detail.

2.4.3.1 Calcium

The presence of Ca^{2+} in the growth medium is known to be required for *in vitro* pollen germination and tip growth of most plant species (Brewbaker and Kwack 1963; Picton and Steer 1983a; Li *et al.* 1999; Chebli and Geitmann 2007). It plays a role in cell wall formation and rigidity, directs vesicle trafficking and controls actin dynamics (Chebli and Geitmann 2007) and was also found to affect the period and amplitude of growth rate oscillations (Geitmann and Cresti 1998; Holdaway-Clarke *et al.* 2003). Normal pollen tube growth can only take place in the presence of a calcium concentration that is situated within

a certain range (Brewbaker and Kwack 1963; Picton and Steer 1983b; Holdaway-Clarke *et al.* 2003) that varies between species (Steer and Steer 1989). Within this range, pollen tube tip extension rates are relatively insensitive to small changes in the calcium concentration (Picton and Steer 1983a), whereas outside of this range, growth is severely hampered.

We used different calcium concentrations, 0 mM, 2 mM, 4 mM and 10 mM. These are the total concentrations of calcium in the medium resulting from the equimolar addition of two different sources of calcium: calcium chloride and calcium nitrate. We found that growth in liquid medium (setups 1 and 2) was optimal at 4 mM Ca^{2+} and could not be enhanced further by higher concentrations, whereas growth in solid medium was augmented by 10 mM calcium compared to 4 mM (Fig 2.3). Pollen tubes growing on the surface of solid medium (setup 3) required only 2 mM of calcium for optimal germination that was not enhanced or inhibited by higher concentrations up to 10 mM (Fig 2.4). In all three cases the optimal percentage of germination was approximately 40%. The difference in calcium requirement between the experimental setups might be due to oxygen availability affecting the metabolism of the pollen tube since oxygen is more readily available for pollen growing on the surface of a solid medium than in liquid or in solid medium.

In all three experimental setups we observed the presence of germinated pollen in the control samples devoid of added calcium. Percentages of germination in these "calcium-free" samples were up to 22% on the surface of solid medium. The addition of EGTA (ethylene glycol tetraacetic acid) at a concentration of 0.1 and 0.2 mM to quench any contaminations with calcium did not reduce the percentage of germination (data not shown). Similar observations were made for *Tradescantia virginia* pollen upon Ca^{2+} quenching with EGTA (Picton and Steer 1983a). This may be explained with the presence of a stock of calcium already present in or on the surface of the pollen grains.

Since the two sources of calcium in the medium contained chloride and nitrate ($CaCl_2$ and $Ca(NO_3)_2$), changing the calcium concentration also changed Cl^- and NO_3^- concentrations. To ensure that the observed effects were only related to variations in the calcium concentration and not to the alterations in chloride and/or nitrate contents, we increased the concentrations of these two ions to match those in the 10 mM Ca^{2+} sample using hydrochloric acid and nitric acid. Results showed that there were no significant differences

between the controls (pollen tubes germinating without addition of Cl^- and NO_3^-) and the respective media containing the increased amounts of chloride and nitrate ions (Fig 2.4). From this we conclude that the effect observed under different calcium concentrations was only due to the variations in the concentration of calcium ions.

2.4.3.2 Boron

In the pollen tube, boron is involved in cell wall formation, protein assembly into membranes and cell wall (Blevins and Lukaszewski 1998). Through its effect on H^+-ATPase activity, boron affects pollen germination, tube growth (Feijó *et al.* 1995a; Wang *et al.* 2003) and oscillation behavior (Holdaway-Clarke *et al.* 2003). 100 ppm boric acid was found to be essential for pollen germination (Brewbaker and Kwack 1963). In *Picea meyeri*, boron deficiency decreases pollen germination and affects callose and non-esterified pectin accumulation on the cell wall (Wang *et al.* 2003).

Five different concentrations of boric acid (0 mM, 0.49 mM, 1.17 mM, 1.62 mM and 3.24 mM) were used. Germination of pollen growing on the surface of solid medium (setup 3) was the highest for 1.62 mM of boron whereas higher concentrations were inhibitory (Fig 2.5a). In liquid media (setups 1 and 2) the highest percentage of germination was obtained for concentrations as low as 0.49 mM (Fig 2.5b). Similar results were observed in *Picea meyeri* where 0.01% boric acid (1.62 mM) yielded optimal germination and higher concentrations were detrimental for pollen tube germination (Wang *et al.* 2003). One possible reason for higher boron concentrations required for optimal germination when using a solidified medium is that the boron may be sequestered by the agar molecules (residues of algal cell walls).

2.4.3.3 Potassium

Many pollen species such as lily and *Solanum* require potassium for optimal *in vitro* germination through its possible involvement in the initiation of the osmotic water influx required for pollen germination (Fan *et al.* 2001). The effect of potassium on growth was proposed to be in the maximization of the association of the calcium ions to the cell wall (Brewbaker and Kwack 1963). In *Arabidopsis* a potassium channel has been shown to be

present in pollen protoplast membrane (Fan *et al.* 2001) and its mutation reduces the growth of *Arabidopsis* pollen tubes (Mouline *et al.* 2002). Therefore, we investigated whether or not varying the concentration of potassium in the medium influences pollen germination in *Arabidopsis*.

Different concentrations ranging between 0 mM and 10 mM of potassium chloride were tested. Results showed that in liquid growth medium (setups 1 and 2), potassium concentrations of 1 mM or higher increased the percentage of germination by more than 30% whereas this increase was more than 60% in solid medium (setups 3 and 4). No inhibitory effect was observed for higher concentrations of potassium (Fig 2.6).

2.4.3.4 Sucrose

Since the pollen tube does not perform photosynthesis, a carbon source is required for energy supply and carbohydrate skeleton formation. Therefore, sucrose is generally added to pollen germination media, but the optimal concentration varies greatly between species, for instance optimal *Papaver* pollen growth *in vitro* occurs at 5% sucrose, *Camellia* at 8%, *Lilium* and *Solanum* at 10% (unpublished data). While it was previously observed that sucrose concentrations higher than 15% reduced or prevented *Arabidopsis* pollen germination (Boavida and McCormick 2007), we tested different concentrations of sucrose ranging from 0 to 25%. For our optimized medium, 18% sucrose yielded the highest percentage germination (50%) regardless of the stiffness of the medium (Fig 2.7). This percentage was significantly reduced when sucrose concentration was outside the optimal range of 15 to 20%. In addition to lowering the percentage germination, higher sucrose concentrations reduced pollen tube elongation (Fig 2.8). The requirement for relatively high sucrose concentration for *Arabidopsis* pollen when comparing to other species might be related to the fact that this species has a dry stigma (Elleman *et al.* 1992; Zinkl and Preuss 2000) thus providing an environment with high osmolarity. *Arabidopsis* culture medium with 18% sucrose might provide the environment that is closest to the *in planta* situation.

2.4.3.5 pH

Medium pH is a critical condition for *in vitro* pollen tube growth. For *Lilium*, *Solanum* and *Camellia* pollen tubes, the optimum pH is situated between 5 and 6. Lower or higher pH values drastically reduce the percentage of germination and are unable to sustain pollen tube growth (Chebli and Geitmann 2007).To optimize the pH for *Arabidopsis*, we tested different values: 5, 6, 6.8, 7 and 8. Adjustment of the pH was made immediately prior to each experiment. For solid media, pH was adjusted prior to the addition of agar. In solid medium the optimum pH for pollen germination was 7. When pollen was grown at a slightly different pH (6.8), the percentage of germination was reduced by 40% when quantified after 6 hours of growth (Fig 2.9a).

However, interestingly, we observed that in a solid medium (setup 4) with a slightly acidic pH, pollen grains were able to germinate faster than in a medium with pH 7. After four hours of germination the percentage of germination reached a high value that at this point of time was higher than in medium with pH 7 (Fig 2.9a).

In liquid medium (setup 1) we noticed that the pH variation did not have a dramatic effect on the percentage of germination achieved after 6h. However, the more acidic the medium (pH between 5 and 6.8) the faster the pollen germinated, since percentages of germination were bigger at 2h in these samples (Fig 2.9b). Therefore, in experiments focusing on shorter time periods after germination, a slight acidification of the liquid medium would be advantageous to obtain optimal percentage of germination. On the other hand, total germination as quantified after 6h is higher at pH 7.

In our experiments, we noticed a decrease by 0.4 pH units after 6 hours of growth in liquid medium. This acidification of the medium may affect pollen germination with time. This is consistent with earlier reports that with time, growing pollen tubes tend to acidify the medium eventually resulting in a growth to stop (Tupý and Říhová 1984). An acidification of 0.1 units was also observed in a control liquid sample without any pollen. This decrease in the pH might be due to the metabolism of microorganisms, present in the medium, on the glassware and in higher amounts on the pollen itself. It may also be due to the metabolism of the pollen and pollen tubes where a high degree of ions exchange happens between intra- and extracellular compartments. The use of Tris buffer (5 and 10 mM) reduced the

percentage of germination (not shown), which is why we did not pursue further experimentation with buffers.

2.4.3.6 Temperature

Pollen germination shows a temperature dependent behavior. A controlled temperature was proven to be important for optimal germination and pollen growth in *Arabidopsis thaliana* (Boavida and McCormick 2007). Since various experimental strategies may require incubation temperatures other than room temperature, we tested a temperature range from 4 to 42°C. Best germination for solid medium growing pollen tubes were obtained for temperatures ranging from 22 to 25°C (Fig 2.10). The same was observed for pollen grown in liquid medium in Erlenmeyer flasks, whereas the optimal temperature for pollen in a liquid drops was 30°C (Table 2.1). A similarly surprising optimal germination temperature was observed by Boavida *et al.* (2007) who describe that 28°C increases the germination in the Colombia ecotype.

Approximately 5% of the pollen grains were able to germinate at 4°C in liquid medium and these tubes displayed normal morphology (Fig 2.11) with a mean length of 110µm after 24h of growth. We tested this condition since it would allow image acquisition of living pollen tubes in the environmental scanning electron microscope as image quality decreases with increasing temperature.

2.4.4 Comparison with other media

To demonstrate the difference between our optimized medium and other media that had been developed for pollen germination of various species, we compared them side by side. Using pollen that had been cold-stored for 3 months, our optimized medium yielded significantly higher percentages of germination than the Lily pollen medium (Parre and Geitmann 2005a), the BK medium (Brewbaker and Kwack 1963) and several *Arabidopsis* media (Li *et al.* 1999; Fan *et al.* 2001; Boavida and McCormick 2007) (Fig 2.12a). The tube length of those grains that had succeeded in germinating was significantly longer in our medium than that in the other media (Fig 2.12b). Furthermore, our medium resulted in pollen tubes without apparent morphological disorders, whereas in our hands pollen tubes

grown on the Boavida and McCormick medium (2007) were frequently aberrant with apical swellings. One of the reasons why in our hands our medium was superior to the others might be that it had been optimized for bulk collected, cold stored pollen while the others were optimized for freshly collected pollen and/or for pollen from the most recently opened flowers of the *Arabidopsis* plant.

2.5 Conclusions

Given the importance of *Arabidopsis thaliana* as a model system, the optimization of the conditions for bulk storage and germination of frozen stored pollen should contribute to the increased use of this species in pollen research. Furthermore, we provided optimized conditions for different experimental setups that either use large amounts of pollen or require specific conditions such as low temperatures or medium stiffness. Our optimized *Arabidopsis* pollen growth medium is composed of 18% sucrose, 1 mM potassium chloride, 1.62 mM boric acid, 1 mM magnesium sulphate, 2 mM calcium chloride and 2 mM calcium nitrate, at a pH of 7 with an incubation temperature of 22.5°C. For pollen grown in solid medium, twice the amount of calcium is ideal. For pollen grown in a liquid drop, the optimum growth temperature is 30°C (Table 2.1).

The two main advantages of these methods of *Arabidopsis* pollen germination are the high reproducibility compared to other media described in the literature and the possibility of using large amounts of pollen that has been collected and freeze stored. Therefore, the availability of flowering *Arabidopsis* plants at the time of the experiment is not a limiting factor. Whenever a batch of flowers is mature, all its pollen can be collected and stored for experiments to be carried out at a later time.

The bulk pollen germination makes our methods useful for a variety of experiments requiring large amount of nucleic acid, proteins, or organelles to be extracted from *Arabidopsis* pollen tubes. The wide range of germination conditions make them appropriate for other experiments where low germination temperatures are required (environmental scanning electron microscopy) or different medium stiffness is a limiting factor to the success of the experiments.

2.6 Acknowledgements

Research in the Geitmann lab is supported by grants from the Natural Sciences and Engineering Research Council of Canada (NSERC), the *Fonds Québécois de la Recherche sur la Nature et les Technologies* (FQRNT), and the Human Frontier Science Program (HFSP).

2.7 Table

Table 2.1

	Setup 1	Setup 2	Setup 3	Setup 4
Temperature (oC)	30.0	22.5	22.5	22.5
pH	7.0	7.0	7.0	7.0
Calcium (mM)	4.0	4.0	2.0	4.0
Boron (mM)	0.49	0.49	1.62	1.62
Magnesium (mM)	1.0	1.0	1.0	1.0
Potassium (mM)	1.0	1.0	1.0	1.0
Sucrose (%)	18	18	18	18

Table 2.1: Optimized conditions for *in vitro Arabidopsis* pollen germination in four different experimental setups.

Setup 1: Pollen in liquid drop. Setup 2: Pollen in Erlenmeyer. Setup 3: Pollen on solid surface. Setup 4: Pollen within solid medium.

2.8 Figures

Figure 2.1

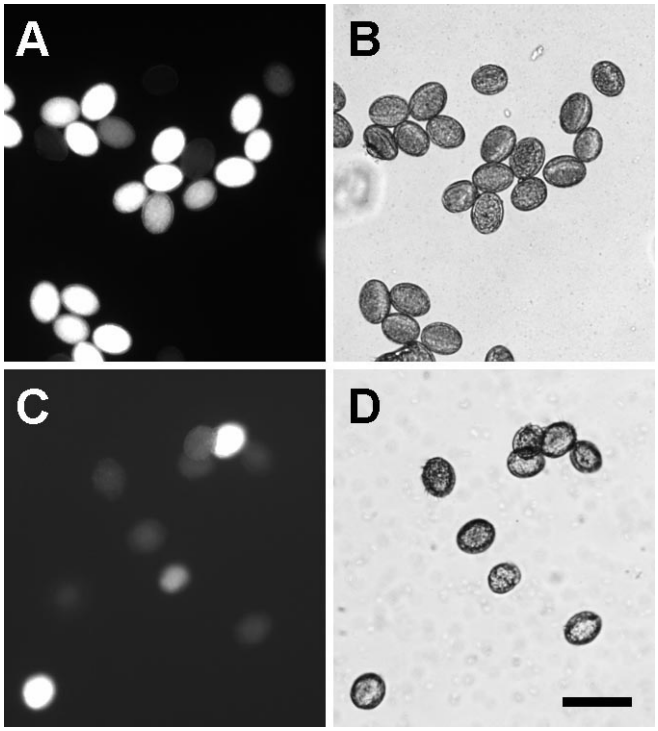

Figure 2.1: *Arabidopsis thaliana* pollen viability test using fluorescein diacetate (FDA).

Viable pollen fluoresces bright white under UV light. Fresh pollen (A,B) and pollen stored for 12 months at -20°C (C,D). Bar = 20 µm.

Figure 2.2

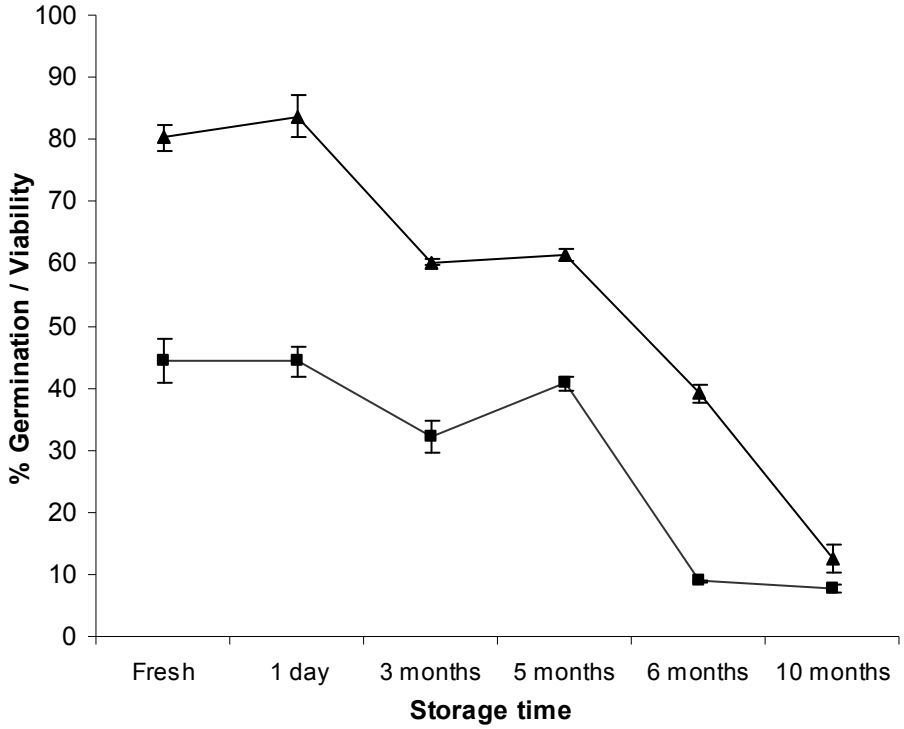

Figure 2.2: Change of *Arabidopsis* pollen viability and germination percentage with duration of cold storage.

Change of *Arabidopsis* pollen viability (▲) and germination percentage (■) with duration of cold storage. Stored pollen was kept at -20°C after 2 hours of dehydration following harvest. Vertical bars represent the standard deviation (n=5).

Figure 2.3

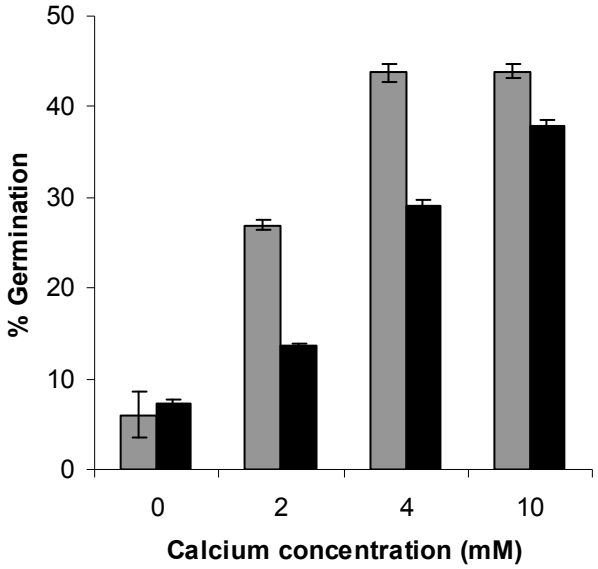

Figure 2.3: Effect of calcium concentration on the percentage of germination of *Arabidopsis thaliana* pollen.

Effect of calcium concentration on the percentage of germination of *Arabidopsis thaliana* pollen grown in liquid drop (grey) and in solid medium (black) after 6 hours of growth. Vertical bars represent the standard deviation (n=5).

Figure 2.4

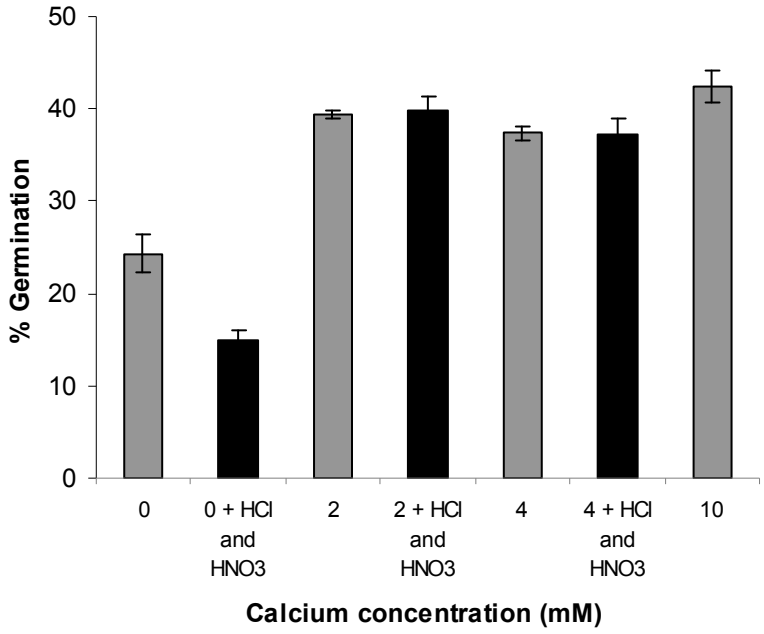

Figure 2.4: Effect of calcium concentration on percentage germination of *Arabidopsis thaliana* pollen.

Effect of calcium concentration on percentage germination of Arabidopsis thaliana pollen grown on solid medium after 6 hours of growth. In a parallel series (black bars), chloride and nitrate levels were adjusted to that of the 10 mM Ca2+ sample. Vertical bars represent the standard deviation (n=5).

Figure 2.5

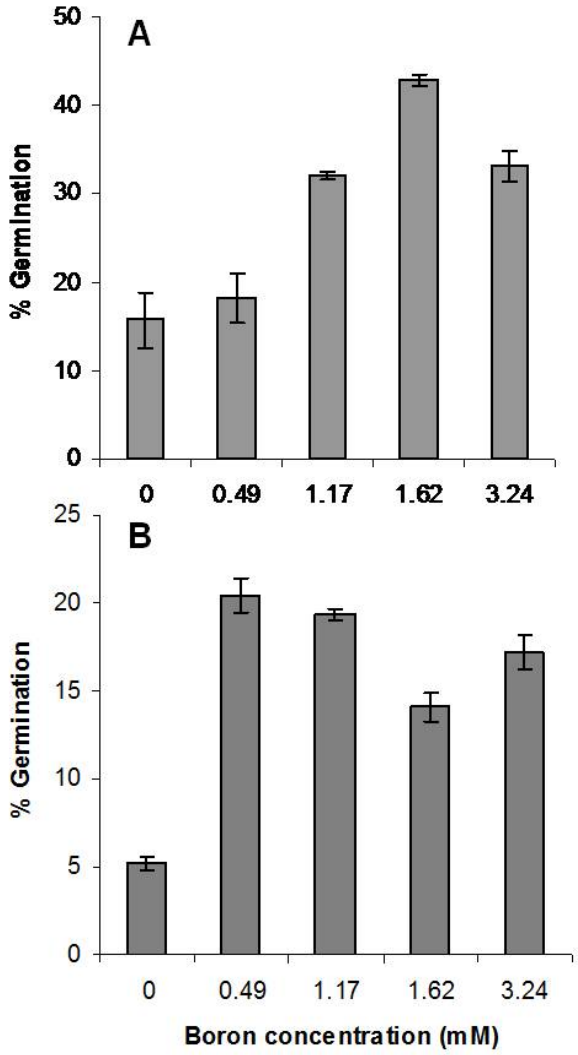

Figure 2.5: Effect of boron concentration on the percentage germination of *Arabidopsis thaliana* pollen.

Effect of boron concentration on the percentage germination of *Arabidopsis thaliana* pollen grown on solid medium (A) and in liquid medium (B) after 6 hours of growth. Vertical bars represent the standard deviation (n=5).

Figure 2.6

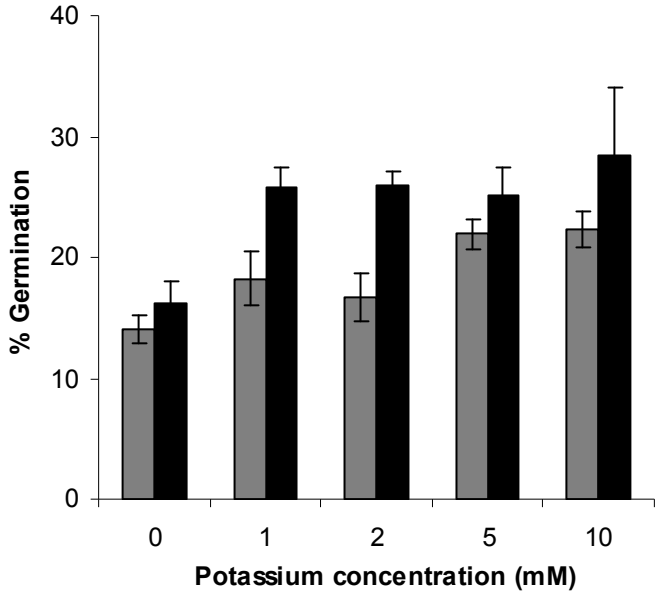

Figure 2.6: Effect of potassium concentration on the percentage germination of *Arabidopsis thaliana* pollen.

Effect of potassium concentration on the percentage germination of *Arabidopsis thaliana* pollen grown in liquid drop (grey) and in solid medium (black) after 6 hours of growth. Vertical bars represent the standard deviation (n=5).

Figure 2.7

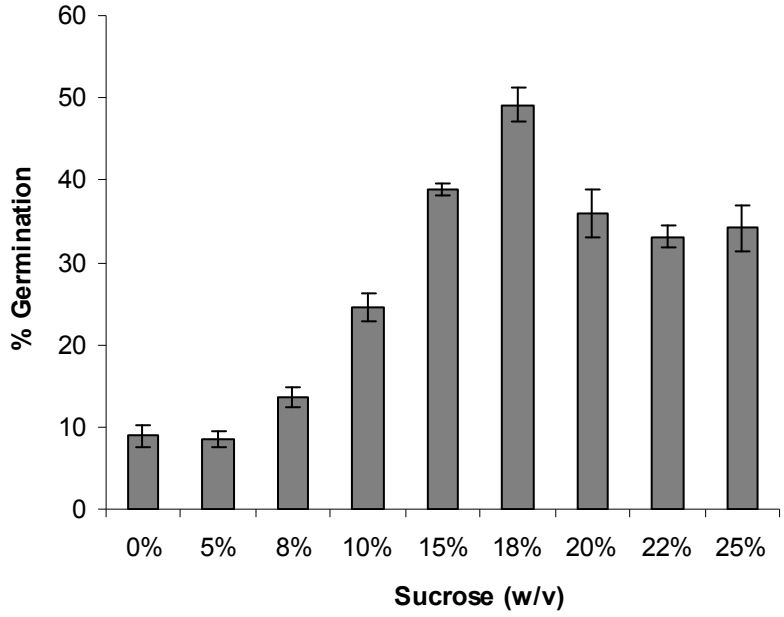

Figure 2.7: Effect of the sucrose concentration on the percentage germination of *Arabidopsis thaliana* pollen.

Effect of the sucrose concentration on the percentage germination of *Arabidopsis thaliana* pollen after 6 hours of growth on solid medium. Vertical bars represent the standard deviation (n=5).

Figure 2.8

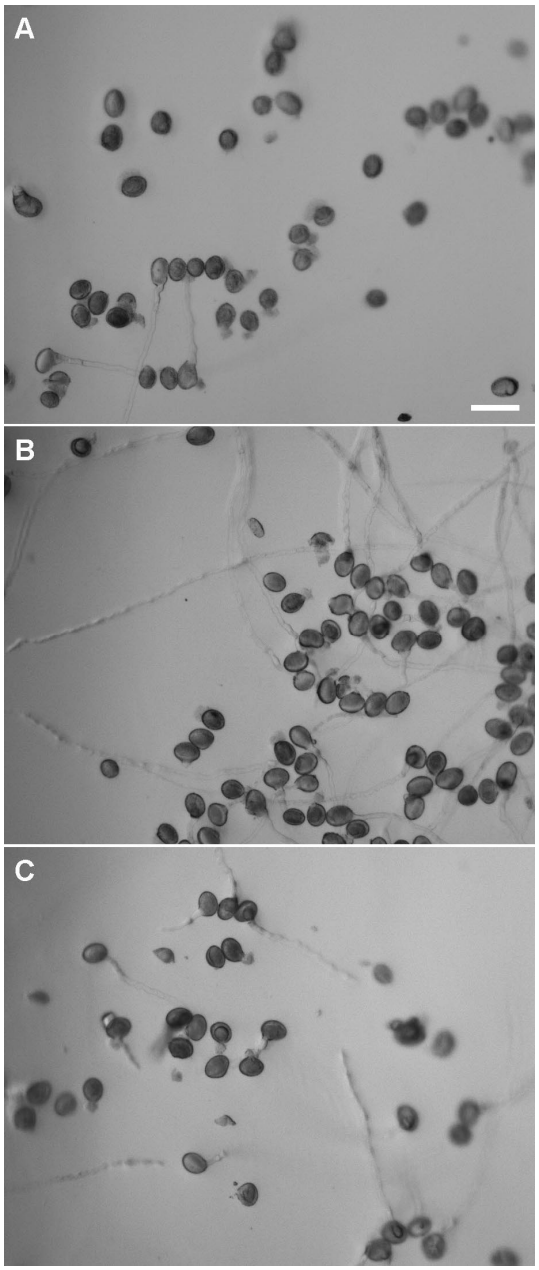

Figure 2.8: *Arabidopsis* pollen germination on agarose medium.

Arabidopsis pollen germination on agarose medium containing 5% (A), 18% (B), and 25% sucrose (C). Bar = 50 µm.

Figure 2.9

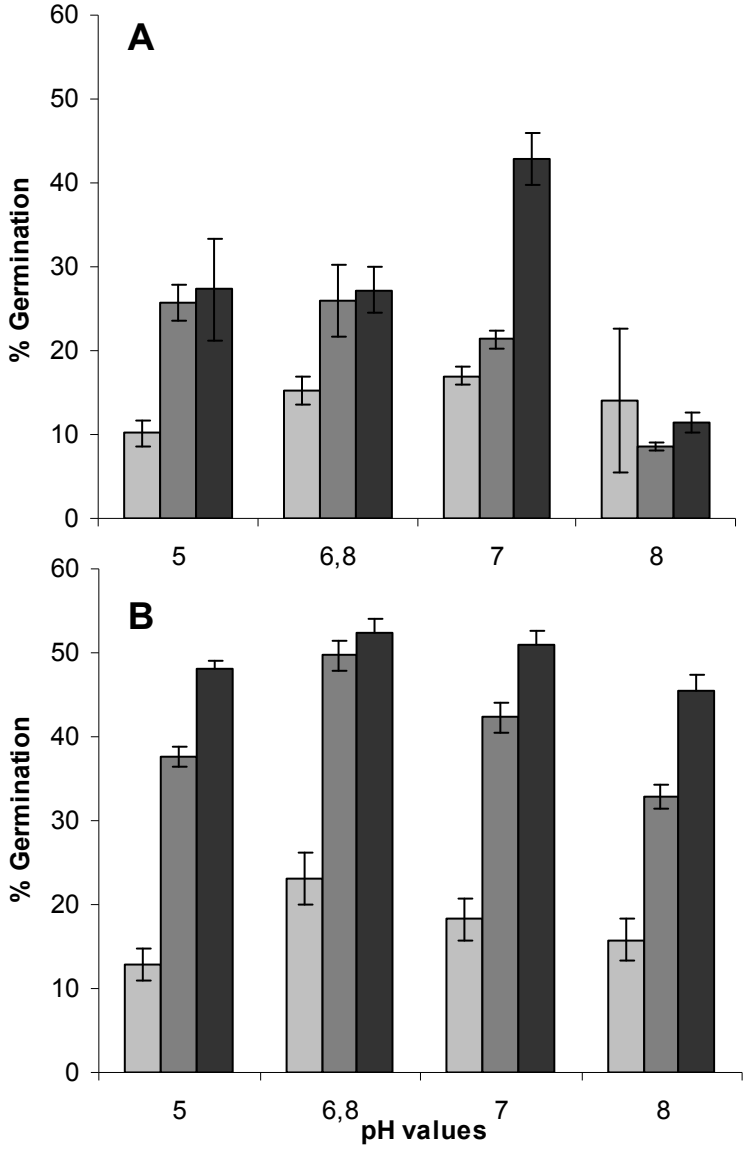

Figure 2.9: Effect of the pH on the percentage germination of *Arabidopsis thaliana* pollen.

Effect of the pH on the percentage germination of *Arabidopsis thaliana* pollen grown on solid surface (A) or in liquid medium (B) after 2 hours (light grey), 4 hours (dark grey) and 6 hours (black) of growth. Vertical bars represent the standard deviation (n=5).

Figure 2.10

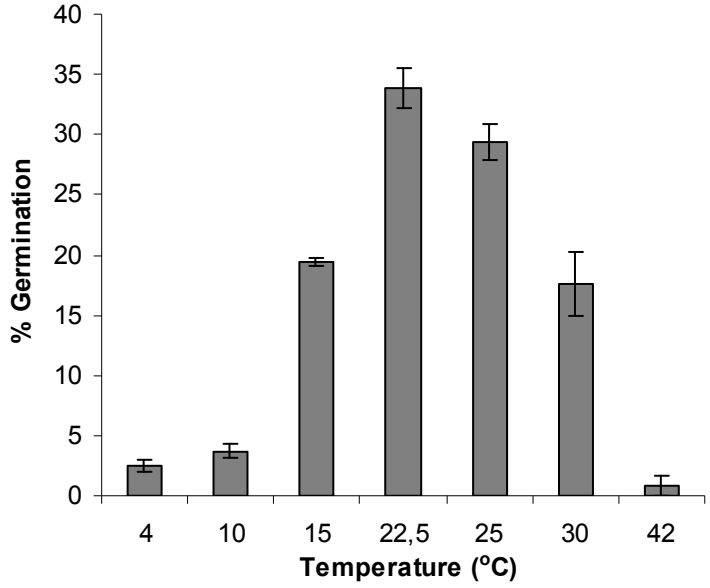

Figure 2.10: Effect of the temperature on the percentage germination of *Arabidopsis thaliana* pollen.

Effect of the temperature on the percentage germination of *Arabidopsis thaliana* pollen grown on solid medium. Vertical bars represent the standard deviation (n=5).

Figure 2.11

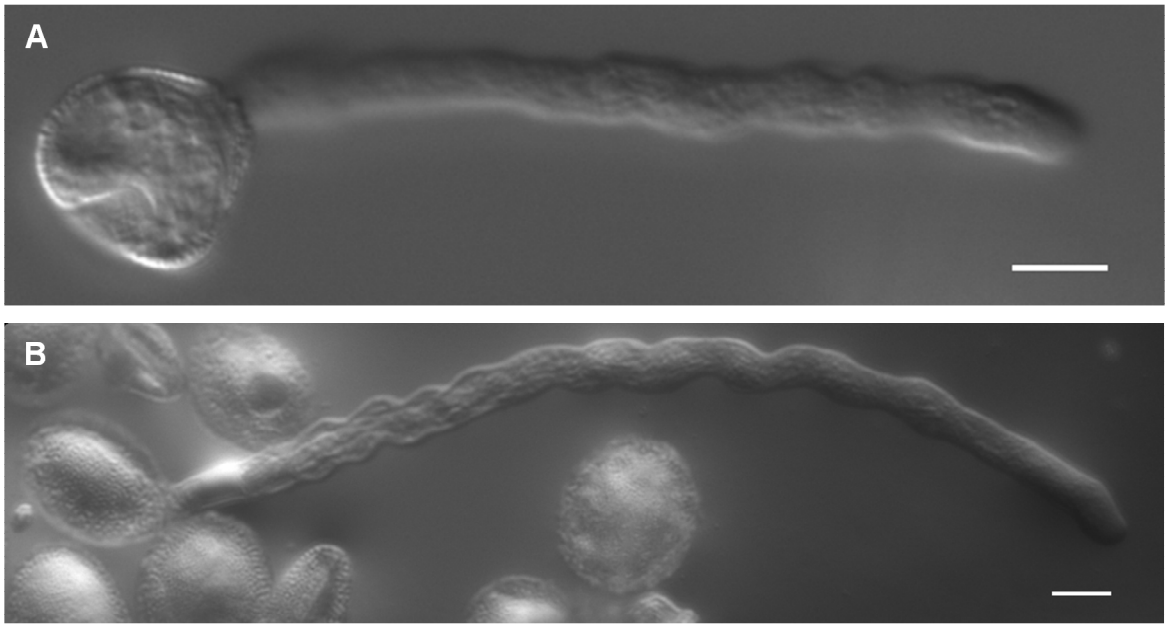

Figure 2.11: Micrographs of *Arabidopsis* pollen tubes.

Micrographs of *Arabidopsis* pollen tubes grown at 4°C for 24 hours (A) in liquid medium and (B) on solid medium. Bars = 10µm

Figure 2.12

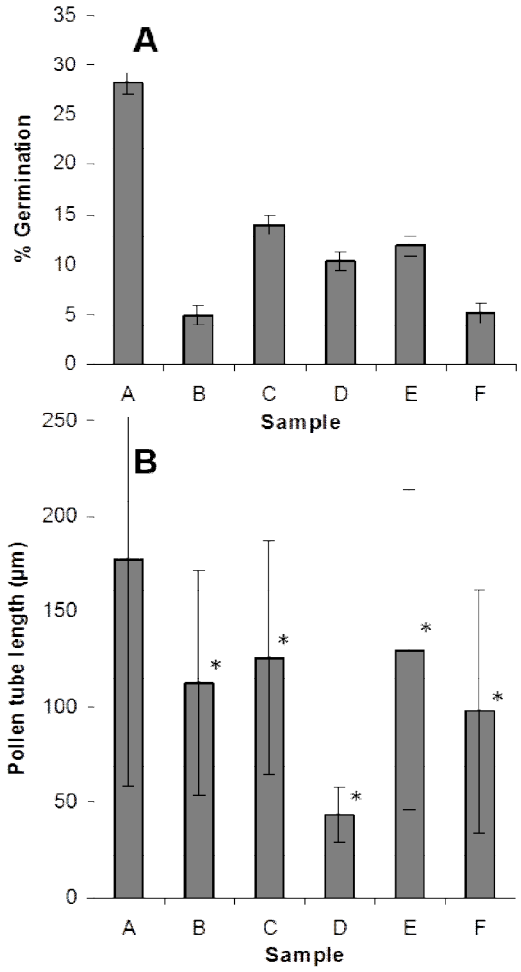

Figure 2.12: Comparaison of *Arabidopsis* pollen percentage of germination and pollen tube length after five hours of growth on different agarose stiffened media.

Arabidopsis pollen percentage of germination (A) and pollen tube length (B) after five hours of growth on agarose stiffened media based on our optimized protocol (sample A), Boavida and McCormick (2007) (sample B), Li *et al.* (1999) (sample C), Fan *et al.* (2001) (sample D), Brewbaker and Kwack (1963) modified with 18% sucrose (sample E), and lily medium (Parre and Geitmann 2005) modified with 18% sucrose (sample F). Bars represent the standard deviation (n=5). * Despite large standard deviations for pollen tube length (B), mean values of samples B through F are significantly different from that of sample A with $p<0.05$ (samples B and E) and $p<0.01$ (samples C, D, F) (two tailed student t-test).

3 Microwave assisted processing of plant cells for optical and electron microscopy

Specimen preparation is one of the most crucial steps in biological microscopy. Any flaw in one of the steps of the protocol can lead to the generation of artifacts, to the destruction of the cellular components or to the degradation of the antigenic properties of the tissue. Because microscopy is one of the principal tools in the Geitmann lab, my colleagues Firas Bou Daher, Leila Aouar, Monisha Sanyal and I developed and optimized a technique for the processing of plant cells for microscopy. This technique is based on the use of microwaves to accelerate diffusion and hence penetration of the different solutions (fixative, dehydrating solution, antibodies, dyes, resin…) into the tissue, as well as the chemical reactions between fixative and specimen. This technique has several advantages, mainly that it is very rapid compared to the bench-top method, allowing the tissues to be in contact with the chemical solutions used for the preparation for shorter periods of time. This enhances the structural and immunological integrity of the tissues. The present manuscript details our findings and the benefits of this technique compared to the bench-top sample processing.

I contributed to this manuscript by preparing the samples for the immunolabelling (Figure 3.2) and transmission and scanning electron microscopy (Figures 3.4 and 3.5b). I also contributed to the preparation of Figures 3.6 and 3.7 and to the writing of all the sections of this manuscript. Firas Bou Daher contributed to the preparation of Figures 3.2, 3.3, 3.6 and 3.7 and to the writing of the manuscript. Monisha Sanyal contributed to the writing of the manuscript and Leila Aouar to Figure 3.5a.

This manuscript entitled “Microwave assisted processing of plant cells for optical and electron microscopy” was published in 2009 in the *Bulletin of the Microscopical Society of Canada* volume 36, issue 3 pages 15-19.

Youssef Chebli, Firas Bou Daher, Monisha Sanyal, Leila Aouar and Anja Geitmann

3.1 Introduction

The technological development of microscope hardware has led to a significant breakthrough by pushing the resolution from the micro to the nano-scale range. During the past century high end electron, optical and atomic force microscopes have been developed for better ultra-structural viewing of the specimen at the atomic level, including 3D visualization. Compared to these impressive hardware developments, progress in specimen processing techniques has been far less dramatic. Despite the increased use of living material in microscopy, numerous applications still require specimens to be fixed and bench time is a major constraint in any kind of sample preparation. The first and one of the most important steps in biological tissue processing for microscopy is fixation. Depending on the specimen, times for chemical fixation may range from half an hour to as much as 24 hours. The entire procedure required for processing biological samples for transmission electron microscopy (TEM) can therefore take between a few days and a week. While this time is necessary to completely fix, dehydrate and embed the specimen, it also allows for unintended processes to occur such as the dissolving of membranes leading to the release of organelle content. This can result in the dilution of the applied solutions and to alterations in their pH value (Russin and Trivett 2001) which in turn may generate structural artifacts. The fixation time is even more critical in case of immunohistochemistry where antigen preservation is crucial for successful labeling. Therefore, efforts to minimize fixation and processing times do not only have the aim to reduce bench time but also or prevent structural impact on the tissue.

In the 1970s, the use of microwave (MW) ovens was first introduced to accelerate sample processing (Mayers 1970; Demaree and Giberson 2001). The first report on MW-assisted aldehyde tissue fixation for the purpose of light microscopy and TEM was made in the 1980s (reviewed by (Giberson 2001). The early MW ovens had no control over power or temperature and the only variable was the exposure time. Currently, MW ovens are available with variable power (wattage), temperature control and MW transparent vacuum systems.

Because of the presence of cell walls, vacuoles, plastids and intracellular air space (Russin and Trivett 2001), plant cells generally require rather prolonged incubation times with fixation and dehydration solutions and thus would profit greatly from an accelerated protocol. In the present study we aimed at the optimization of MW-assisted sample processing for single plant cells for both optical and electron microscopy. We used leaf trichomes and pollen tubes as test specimens. The former are cells differentiated from the leaf epidermis. They stick out from the leaf surface into the air space and are thus not mechanically stabilized by any surrounding tissue. The latter are cellular protuberances formed by germinating pollen grains upon contact with a receptive stigma. Their function is the generation of the two sperm cells and their delivery to the ovary to ensure double fertilization. Pollen tubes are commonly used as a model for the study of anisotropic cell growth and also to understand the structural dynamics and material properties associated with polarized cellular expansion (Geitmann and Steer 2006; Geitmann 2006b). Due to their extremely rapid growth and active intracellular transport processes, high quality fixation of pollen tubes is critical for the preservation of cellular ultrastructure and polarity. We optimized two important variables critical for MW-assisted sample preparation: wattage, correct adjustment of which is responsible for tissue stabilization, and exposure time, which is sample and treatment dependent (Russin and Trivett 2001). During experiments, sample temperature was monitored to control the effect of heating (Demaree and Giberson 2001), and vacuum was used for better infiltration of the cells with the fixation solution (Russin and Trivett 2001). All experiments were carried out in a PELCO cold spot®. The PELCO ColdSpot is a device that captures heat and reflected energy in the cavity of the microwave by circulating and cooling water.

3.2 Optical microscopy

Due to the highly polarized mode of growth, the pollen tube cell wall has a characteristic spatial profile of non-uniformly distributed cell wall polysaccharides. The tip is composed of methyl-esterified pectins that permit, due to their plastic characteristics, pollen tube elongation at this location (Geitmann and Parre 2004; Parre and Geitmann 2005b). On the other hand, the basal part of the tube is composed of non-esterified, stiffer pectins and it is

further characterized by the deposition of cellulose and callose (Chebli and Geitmann 2007). The latter component plays a role in the mechanical resistance of the cell wall against tension and compression stress in the cylindrical part of the cell (Parre and Geitmann 2005a). In longer pollen tubes, callosic plugs compartmentalize the cell allowing the older parts of the cell to degenerate. To sustain the active growth of the pollen tube, cell wall material is constantly added to the growing tip through the fusion of secretory vesicles which are transported to the growing zone via the highly dynamic actin cytoskeleton.

Visualization of both cell wall components and cytoplasmic structures such as the cytoskeleton can be performed combining specific label with fluorescence and confocal microscopy. Due to the extremely fast growth behavior and the polar distribution of cytoplasmic components by selective and directed cytoplasmic streaming, fixation of pollen tubes needs to be rapid for the ultrastructural reality. We tested several staining and immunohistochemical procedures to assess the efficiency and quality of MW-assisted fixation protocols on pollen tubes. Given that we have extensive experience with this cell type and its characteristic labeling profiles we were able to judge the quality of the samples obtained with the MW-assisted protocols comparing them to conventional chemical fixation and rapid freeze fixation.

3.2.1 Methodology

In the optimized protocol all steps were carried out in the microwave operating at 150W under 21 inches of Hg vacuum at a controlled temperature of 26^{o}C ± 2^{o}C.

3.2.1.1 Pectin labeling

Pollen tubes were fixed for 40 seconds in 3% formaldehyde in phosphate buffer saline (PBS) solution. After 3 washes in PBS with 2% bovine serum albumin (BSA), they were incubated for 10 minutes in JIM5 (monoclonal antibody specific for pectins with low degree of methyl-esterification; Fig 3.1a) or JIM7 (monoclonal antibody specific for pectins with high degree of methyl-esterification; Fig 3.1b) followed by 3 washes of 40 seconds each in a 2% BSA solution. Tubes were then incubated for 10 minutes in Alexa 594 anti-rat

secondary antibody (Molecular Probes), washed 3 times and mounted on glass slides for observations.

3.2.1.2 Callose labeling

Pollen tubes were fixed in 3% formaldehyde in PIPES buffer for 40 seconds and washed 3 times in the same buffer. A 10 minute incubation with 0.2% aniline blue in water was used to label callose. Samples were then washed 4 times in PIPES buffer before observation (Fig 3.2).

3.2.1.3 Actin labeling

Pollen tubes were fixed for 40 seconds in a pH9 PIPES buffer containing 3% formaldehyde, 0.5% glutaraldehyde and 0.05% Triton. After 3 washes with the same buffer, pollen tubes were incubated with rhodamine phalloidin for 10 minutes in a pH7 PIPES buffer, washed 5 times and then observed immediately, since actin tends to be unstable even when fixed (Fig 3.3).

3.3 Electron microscopy

3.3.1 Transmission electron microscopy

Sample preparation for TEM is very critical due to the necessity to preserve the cellular ultrastructure. Any inappropriate handling during fixation, dehydration or embedding will be flagrantly expressed in the observed samples as artifacts. MW technology has the potential to strongly reduce sample preparation time while preserving tissue subcellular integrity and antigenicity.

We optimized different conditions for microwave sample processing for pollen tubes. Application of a fixative consisting of 2% formaldehyde and 2.5% glutaraldehyde in phosphate buffer (PB) to pollen tubes growing in a 0.5% agar medium for 40 seconds was sufficient for a very good fixation. Post-fixation was performed using 2% osmium tetroxide solution following 3 washes in PB and 3 additional washes in deionized water. Samples were then washed twice with PB followed by two other washes in water. Dehydration was done using an increasing acetone gradient ranging from 25 to 100% with the last step

repeated thrice. All fixation, washing and dehydration steps were conducted under 150W and 21in of Hg vacuum for 40 seconds each.

For resin infiltration we used SPURR resin in 4 steps with increasing resin concentration up to 100%. These steps were conducted at 300W for 3 minutes each and under 21 in Hg vacuum. Resin polymerization was done in a regular oven at 64^{o}C overnight. This polymerization can also be carried out in a water bath at 60^{o}, 70^{o} and 80^{o}C for 10 minutes each then at 100^{o}C for 45 minutes (Demaree and Giberson 2001). Ultrathin sections were cut with a Leica Ultracut and samples were observed with a JEOL JEM 1005 transmission electron microscope operating at 80 kV (Fig 3.4).

3.3.2 Scanning electron microscopy

Pollen tubes and trichomes were fixed and dehydrated using the same protocol as that for TEM sample preparation. Samples were then dehydrated, critical point dried, gold-palladium coated and observed with a JEOL JSM 35 (Fig 3.5).

3.4 Results and Discussion

Plant cell fixation and processing for microscopical observations are a challenge due to the presence of cell wall, vacuoles as well as high internal turgor pressure. Osmotic changes upon the addition of a chemical fixation solution easily causes cellular collapse or bursting, or, less dramatically but nevertheless critical, spatial rearrangement of cytoplasmic contents (e.g. loss of polar distribution of organelles). The cell wall surrounding the plasma membrane hampers effective penetration of the fixative. Using MW-assisted protocols we succeeded in improving and accelerating sample processing while preserving the cellular integrity. Cytochemical labeling of callose in the pollen tube cell wall reproduced the same characteristic profiles as those described previously using conventional chemical fixation. While antigenicity was shown to be enhanced in some cases (Giberson 2001), in our case, we noticed that it was preserved as revealed by immunolabelling for two different types of pectin. The actin cytoskeleton, a very dynamic and unstable structure, was preserved using MW-assisted fixation and resulted in a spatial configuration similar to that observed after freeze fixation, the gold standard for the quality of fixed plant cell cytoskeleton (Lovy-

Wheeler *et al.* 2005). In electron microscopy, cell structure and subcellular compartments were well preserved when comparing with bench top processed plant cells. This was observed when comparing structural integrity of the subcellular components on pictures taken using both methods.

In addition to this, experimentation time was dramatically reduced using the MW-assisted methods (Figs 3.6 and 3.7). For optical microscopy, sample preparation time reduction varied from 5 fold for cytochemical labeling to 8 fold for actin labeling while time reduction for TEM sample preparation was 26 fold.

3.5 Conclusion

The use of MW-assisted protocols resulted in a dramatic reduction of experimentation time. More importantly, structural integrity and antigenicity were not compromised when comparing to conventional bench-top processing methods for chemically fixed samples. Vacuum MW processing for electron microscopy of pollen tubes gave the same results as compared to the traditional method despite much shorter fixation and incubation times.

On a more practical level, MW technology is affordable, user friendly, it does not require specific installations and older models can be upgraded with a temperature control device. Furthermore, it is very flexible allowing an easy switch mid-protocol to the conventional bench-top method if necessitated by time constraints or logistics.

3.6 Figures

Figure 3.1

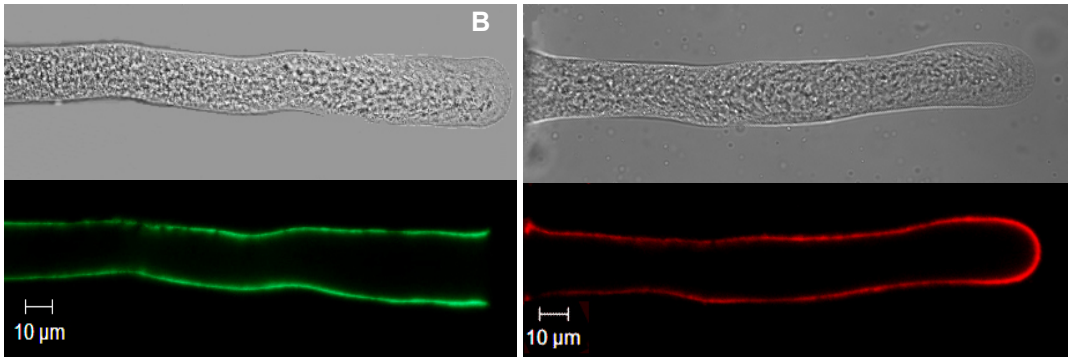

Figure 3.1: Immunofluorescence label of lily pollen tubes.

(A) JIM 5 label of non-esterified pectins reveals the presence of the polymer in the distal region. (B) JIM7 label of esterified pectins is predominantly present at the apex. Pictures represent median pollen tube sections taken with a Zeiss LSM-510 META confocal microsocope.

Figure 3.2

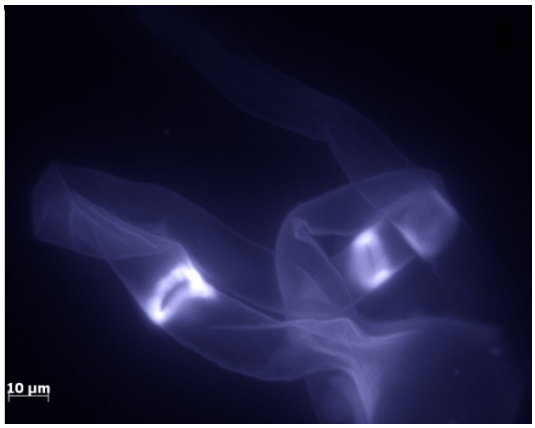

Figure 3.2: Callose rings observed with aniline blue staining in *Camellia* pollen tubes.

These callose rings will develop into callose plugs. Picture represents a Z-stack projection taken with a Zeiss Imager-Z1 microscope equipped with a Zeiss AxioCam MRm Rev 2 camera.

Figure 3.3

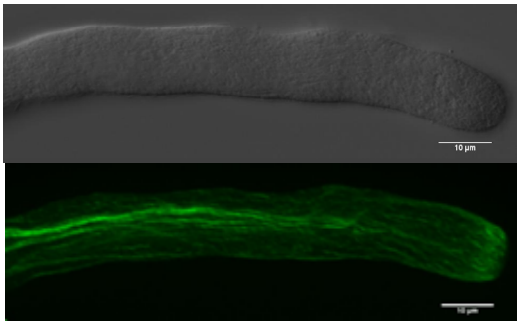

Figure 3.3: *Camellia* pollen tube actin cytoskeleton as visualized by rhodamine-phalloidin label.

Picture represents a Z-stack projection taken with a Zeiss Imager-Z1 microscope equipped with a Zeiss AxioCam MRm Rev 2 camera.

Figure 3.4

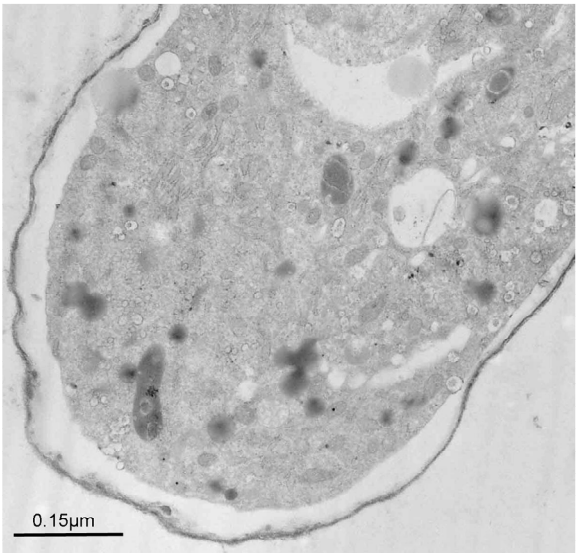

Figure 3.4: Transmission electron micrograph of a cross-section of a *Camellia* pollen tube.

Picture was taken with a JEOL JEM 1005 transmission electron microscope operating at 80 kV.

Figure 3.5

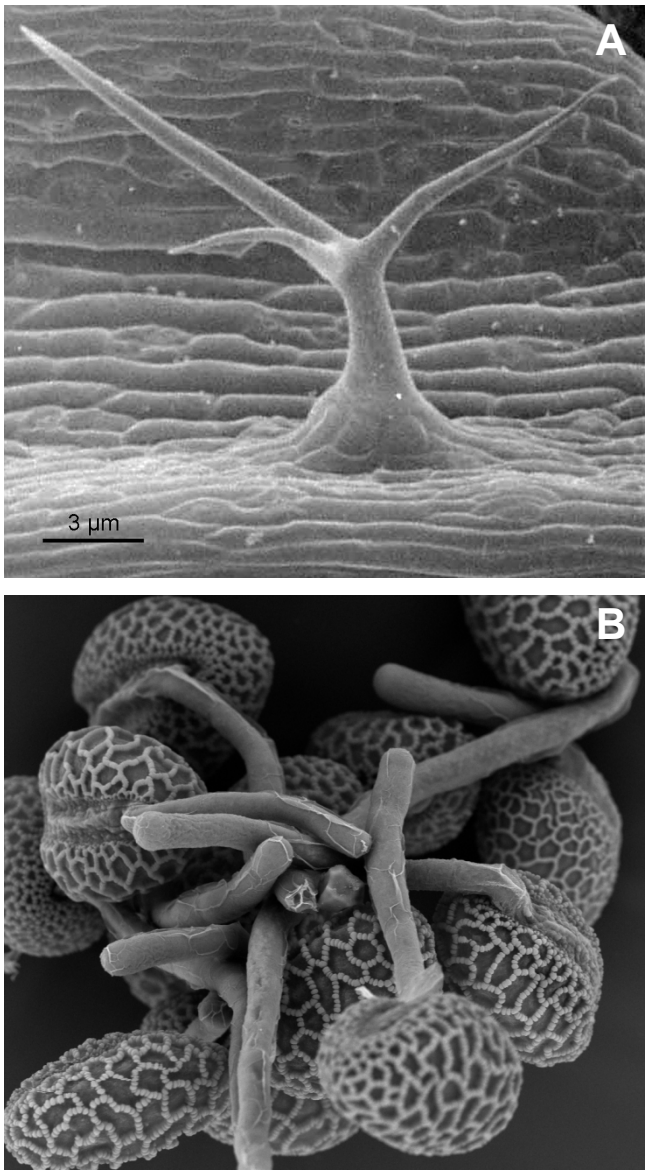

Figure 3.5: Scanning electron micrograph of an *Arabidopsis* leaf trichome and germinated lily pollen grains.

Scanning electron micrograph of an *Arabidopsis* leaf trichome (A) and germinated lily pollen grains (B). Pictures were taken with a JEOL JSM 35 (A) and a Hitachi TEM 1000 (B)

Figure 3.6

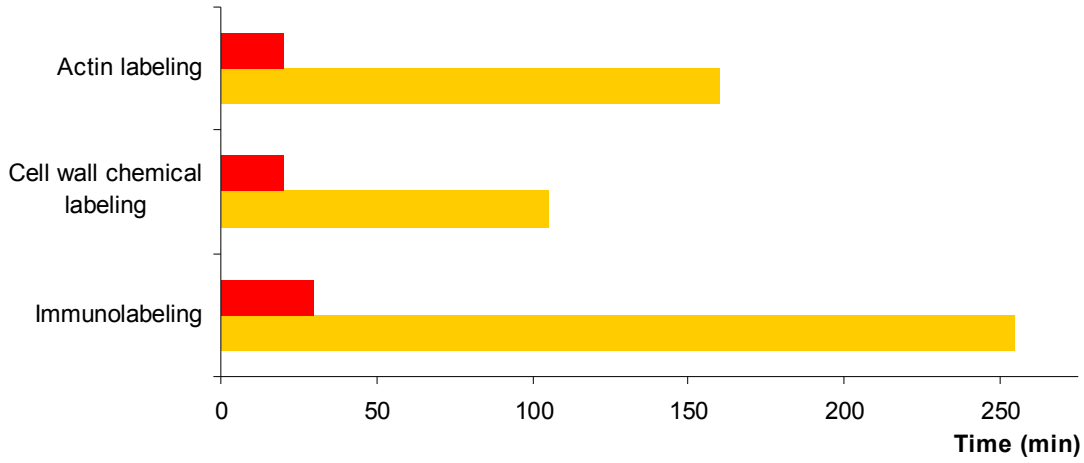

Figure 3.6: Comparison of experimentation time between bench-top (orange) and microwave assisted (red) methods of sample preparation for optical microscopy.

Figure 3.7

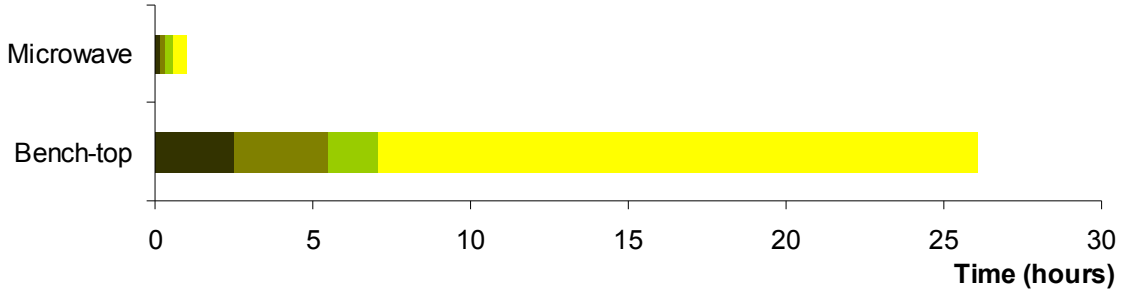

Figure 3.7: Comparison of experimentation time between conventional bench-top and microwave assisted methods of sample preparation for transmission electron microscopy.

Fixation (black), post-fixation (brown), dehydration (green) and resin infiltration (yellow).

4 The cell wall of the *Arabidopsis thaliana* pollen tube - spatial distribution, recycling and network formation of polysaccharides

During pollen tube elongation, the plant cell wall is the most important structure in preserving the integrity of the tube shape, morphology and functional growth. In *Arabidopsis*, more than 200 genes have been so far identified to be involved in the assembly and regulation of the pollen cell wall. Because of the vast collection of *Arabidopsis* mutants, this is the species of choice for studies on the development and metabolism in plants. Therefore, a detailed understanding of the assembly, composition and spatial distribution of cell wall components in the *Arabidopsis* pollen tube is crucial for future studies investigating the effects of external factors, drugs and mutations on the development of pollen tubes. The following paper describes the architecture, the formation and the role of the different cell wall components in the wild type *Arabidopsis* pollen tubes with emphasis on the roles of pectins and cellulose.

I contributed to this article by performing all the experiments except for the micro-indentation (performed by Rabah Zerzour) and the observation of GFP-CES6 (performed by Minako Kaneda). I also contributed to the writing of all the parts of the paper.

This manuscript entitled “The cell wall of the *Arabidopsis thaliana* pollen tube - spatial distribution, recycling and network formation of polysaccharides” was publised in *Plant physiology* 2012, volume 160, pages 1-16.

Youssef Chebli, Minako Kaneda, Rabah Zerzour and Anja Geitmann

4.1 Abstract

The pollen tube is a cellular protuberance formed by the pollen grain, or male gametophyte, in flowering plants. Its principal metabolic activity is the synthesis and assembly of cell wall material which must be precisely coordinated to sustain the characteristic rapid growth rate and to ensure geometrically correct and efficient cellular morphogenesis. Unlike other model species, the cell wall of the *Arabidopsis thaliana* pollen tube has not been described in detail. We used immuno-histochemistry and quantitative image analysis to provide a detailed profile of the spatial distribution of the major cell wall polymers composing the *Arabidopsis* pollen tube cell wall. Comparison with predictions made by a mechanical model for pollen tube growth revealed the importance of pectin de-esterification in determining the cell diameter. Scanning electron microscopy demonstrated that cellulose microfibrils are oriented in near longitudinal orientation in the *Arabidopsis* pollen tube cell wall, consistent with a linear arrangement of cellulose synthase CESA6 in the plasma membrane. Cellulose label was also found inside cytoplasmic vesicles and might originate from an early activation of cellulose synthases prior to their insertion into the plasma membrane or from recycling of short cellulose polymers by endocytosis. A series of strategic enzymatic treatments also suggests that pectins, cellulose and callose are highly cross-linked to each other.

4.2 Introduction

Upon contact with the stigma, the pollen grain swells through water uptake and develops a cellular protrusion, the pollen tube. During its growth *in planta*, the pollen tube invades the transmitting tissue of the pistil and finds its way to the ovary to deliver the male gametes for double fertilization to happen (Heslop-Harrison 1987). Depending on the species, pollen tubes can grow extremely rapidly both *in planta* and in *in vitro* conditions. To fullfil its biological function, the pollen tube has to *(1)* adhere to and invade transmitting tissues (Hill and Lord 1987; Lennon *et al.* 1998), *(2)* provide physical protection to the sperm cells, and *(3)* control its own shape and invasive behaviour (Parre and Geitmann 2005a; Geitmann and Steer 2006). For all of these functions, the pollen tube cell wall plays an important regulatory and structural role. Although the pollen tube does not form a conventional secondary cell wall layer, its wall is assembled in two phases. The 'primary layer' is mainly formed of pectins and other matrix components secreted at the apical end of the cell. The 'secondary layer' is assembled by the deposition of callose in more distal regions of the cell (Heslop-Harrison 1987). Depending on the species, cellulose microfibrils have been found to be associated either with the outer pectic, or with the inner callosic layer. Unlike most other plant cells, cellulose is not very abundant representing only 10% of total neutral polysaccharides in *Nicotiana alata* pollen tubes, whereas callose accounts for more than 80% in this species (Schlüpmann *et al.* 1994).

The biochemical composition of the pollen tube cell wall has been well characterized in many species such as *Lilium longiflorum* (Lancelle and Hepler 1992; Jauh and Lord 1996), *Nicotiana tabacum* (Kroh and Knuiman 1982; Geitmann *et al.* 1995; Ferguson *et al.* 1998; Derksen *et al.* 2011), *Petunia hybrida* (Derksen *et al.* 1999), *Pinus sylvestris* (Derksen *et al.* 1999), and *Solanum chacoense* (Parre and Geitmann 2005b) but for *Arabidopsis thaliana*, the plant model for plant molecular biology studies (Arabidopsis Genome Initiative 2000), there is a striking lack of quantitative information concerning the composition of the pollen tube cell wall as well as the spatial distribution of its components. This is all the more surprising since numerous mutants defective in enzymes involved in cell wall synthesis exhibit a pollen tube phenotype (for example (Jiang *et al.* 2005; Nishikawa *et al.* 2005;

Wang *et al.* 2011)). Two studies have characterized the *Arabidopsis* pollen germinating *in vitro* (Derksen *et al.* 2002) and *in vivo* (Lennon and Lord 2000), but both are qualitative rather than quantitative. A biochemical study by Dardelle and coworkers investigated the cell wall sugar composition in a more quantitative way but does not provide any detailed spatial information (Dardelle *et al.* 2010; Lehner *et al.* 2010). This lack of information is not surprising given that until recently *Arabidopsis* pollen was known to be rather challenging to germinate reproducibly *in vitro* and more difficult to manipulate than the pollen of many other plant species (Bou Daher *et al.* 2009). With the publication of optimized methods for *in vitro* germination (Boavida and McCormick 2007; Bou Daher *et al.* 2009), it has become much more feasible to germinate healthy looking *Arabidopsis* pollen tubes *in vitro* in a highly reproducible way.

The precisely controlled spatial distribution of biochemical components in the pollen tube cell wall is crucial for shape generation and maintenance of this perfectly cylindrical cell (Geitmann and Parre 2004; Aouar *et al.* 2010; Fayant *et al.* 2010; Geitmann 2010a). The pollen tube therefore represents an ideal model system to study the link between intracellular signaling, biochemistry, cell mechanical properties and morphogenesis in plant cells. Because of its typically fast growth rates it responds quickly to any environmental triggers such as pharmacological, hormone or enzymatic treatments. Adding *Arabidopsis* to the group of commonly studied pollen tube species is particularly timely, since one third of the approximately 800 cell wall synthesis genes identified in this species are expressed in or are specific to its pollen (Pina *et al.* 2005). Therefore, the *Arabidopsis* pollen tube has become a valuable system for cell wall studies especially with the increasing availability of cell wall mutant lines (Liepman *et al.* 2010).

Here we describe the biochemical composition of the *Arabidopsis* pollen tube cell wall grown in *in vitro* conditions using immuno-cytochemical labelling coupled with epi-fluorescence and electron microscopic techniques. Rather than relying on imaging alone, we developed a quantitative strategy to assess the precise spatial distribution of cell wall components. This quantitative approach will provide an important tool and baseline dataset for the investigation of mutant phenotypes and for the interpretation of pharmacological studies. Furthermore, we used selective and strategically combined enzymatic digestions to

determine the degree of connectivity between the individual types of cell wall polysaccharide networks.

4.3 Results

4.3.1 Cytoarchitecture of the *Arabidopsis* pollen tube

In our *in vitro* growth conditions, *Arabidopsis* pollen tubes germinated at 2 hours after contact with the growth medium and grew at a rate of 25-50 $\mu m.h^{-1}$ as calculated from pollen tube length at 6 hours after imbibition. *Arabidopsis* pollen tubes had an average diameter of 5 µm with small variations between individual tubes. They were characterized by an apical clear zone extending approximately 2 to 4 µm back from the pole of the cell. For clarity, we will refer to the following cellular regions in this paper: the "tip" or "apex" is characterized by the clear, vesicle filled zone and comprises the first 3 µm extending from the pole of the cell along the longitudinal axis; the "subapical region" is considered to be the region between 3 µm and 10 µm; the "distal region" begins at 10 µm. The "pole" of the tube is the outermost tip of the cell (Fig 4.1a). We use two different measures for the distance. "Longitudinal" indicates the distance from the pole measured on the long axis (symmetry axis) of the cell, "meridional" distance is measured along the periphery of the tube (Fig 4.1a').

4.3.2 High and low esterified pectins show steep, opposite gradients at the same distance from the tube pole

Pectins were labelled with JIM7 and JIM5 antibodies that specifically recognize pectin molecules with high and low degree of methyl-esterification, respectively (Knox *et al.* 1989; Van den Bosch *et al.* 1989). Pectins with high degree of esterification were primarily found at the pollen tube tip, along the first 5 µm meridional length. The amount of highly esterified pectins decreased by two thirds in the first 10 to 12 µm, where it reached a stable value that was maintained along the entire distal region. By contrast, label for low esterified pectin was weak at the tip (around 10% of the maximum label intensity determined in an individual cell) and increased four fold in the first 10 to 12 µm, where it reached a plateau

(Figs 4.1b,b',c,c'). Low esterified pectins showed a somewhat irregularly patterned deposition; this phenomenon has been linked to changes in the growth rate (Li *et al.* 1994; Li *et al.* 1996; Derksen *et al.* 2011). These irregularities are not reflected in the graph (Fig 4.1b'), because the values represent an average of several tubes.

Electron micrographs showed that the cell wall in the distal region of the *Arabidopsis* pollen tube had an average thickness of 0.2 μm (n=10) (Fig 4.2). Pectin label was associated with the outer wall layer that had a fibrillar appearance. No immuno-gold label for pectins was found in the inner, translucent layer. In sections of the distal region, pectins with low degree of esterification seemed more abundant than pectins with high degree of esterification, although direct quantitative comparison was not possible because different antibodies were used (Figs 4.2d,g). Some cytoplasmic vesicles were labelled for highly esterified pectins (Fig 4.2g). For comparison, we also examined the distribution of immunolabel in pollen grains. Here, both types of pectins were found in the intine but label for pectins with a high degree of esterification was predominant (Fig 4.2f). In the grain, a high number of vesicles in the pollen grain cytoplasm were labelled for highly esterified pectins, whereas none were labelled for low esterified pectins (Figs 4.2c,f).

4.3.3 Callose is only detected in the distal part of the tube

To localize callose we performed immuno-fluorescent labeling with an antibody specific for (1→3)-β-glucan. No callose deposition was found in the first 8 μm (meridional) of the pollen tube. Callose deposition began at 10 μm meridional distance from the tip and increased steadily until 40 μm where it reached a plateau (Fig 4.1d'). Occasionally, peaks of fluorescence were observed at intervals of approximately 20 μm, corresponding to a high deposition of callose at the cell wall. Such intense depositions of callose were also typical for cell wall regions about to form a callose plug and for the collar region between emerging pollen tube and pollen grain (Figs 4.1d,d'). Transmission electron micrographs showed that callose was deposited in the inner layer of the pollen tube cell wall. This layer was formed between the pectic fibrillar layer and the plasma membrane and appeared electron transparent (Fig 4.2i), similar to observations made in tobacco pollen tubes

(Derksen *et al.* 2011). In pollen grains, callose label was only found in the intine of the grain (Fig 4.2h).

4.3.4 Crystalline cellulose is more abundant in the apical region of the tube

Calcofluor white is a commonly used stain for cellulose detection in different plant systems. However, although calcofluor white has high affinity for cellulose microfibrils, it is known to stain a variety of other polysaccharides such as callose and chitin (Hughes and McCully 1975; Herth and Schnepf 1980; Wood and Fulcher 1983; Falconer and Seagull 1985). In *in vitro* grown *Arabidopsis* pollen tubes, calcofluor staining revealed a very high amount of microfibrillar polysaccharides at the very tip (first meridional 3 µm) which decreased drastically to half the maximal label intensity in the subsequent 6 µm and reached a plateau in the shank of the tube (Figs 4.1e,e'). Some tubes showed a fluorescent cone in the apical cytoplasm. The shape and location of the cytoplasmic label seemed to correspond to the apical aggregation of vesicles that is typical for growing angiosperm pollen tubes as revealed by label with the styryl dye FM4-64 (Figs 4.4a,b).

For more specific localization, crystalline cellulose was labelled using Cellulose Binding Module 3a (CBM3a) (Blake *et al.* 2006) combined with an anti-polyhistidine antibody and a tertiary antibody coupled to Alexa Fluor 594 (Tormo *et al.* 1996; Moller *et al.* 2007; Alonso-Simón *et al.* 2010). Two populations of tubes could be clearly distinguished; 70.7±1.8% of the tubes showed intense label at the tip (Fig 4.1f) whereas 29.3±1.8% showed no or very low fluorescence intensity at the apex (Fig 4.1g) (n=2857). In tubes with weakly labelled apex, label intensity increased away from the apex to reach a maximum at 20 µm. Remarkably, in all tubes CBM3a label decreased very gradually from this point backwards in the remaining distal region (Figs 4.1f',g').

Transmission electron micrographs showed that crystalline cellulose labelled with CBM3a was deposited in the inner layer of the pollen tube cell wall (Fig 4.2a). The label co-localized with that for callose between the pectic layer and the plasma membrane. Some crystalline cellulose label was also visible in cytoplasmic vesicles both in chemically and rapid freeze fixed samples (Figs 4.2,4.3). To ascertain that this was not background label,

we quantified label density on various cytoplasmic components and the cell wall (Fig 4.2j). No label was visible inside mitochondria, while most of the gold particles where found in vesicles and in the cell wall. CBM3a label was also found to be associated with trans-Golgi network (Fig 4.3a). Occasional label in the cytosol can be explained with the presence of peripherally sectioned vesicles that were not recognizable as such. Similar results were obtained on samples fixed conventionally and by rapid freeze-fixation (Figs 4.2,4.3).

4.3.5 Microfibrils and CESA6 complexes are arranged near parallel to the longitudinal axis of the tube

Microfibril orientation is a crucial parameter that influences the mechanical behavior of the cell wall (Baskin 2005; Geitmann and Ortega 2009; Geitmann 2010b). To be able to determine the principal direction of cellulose microfibril orientation in the *Arabidopsis* pollen tube, we digested the outer pectic layer of the cell wall with pectinase after chemical fixation of the cells (Aouar *et al.* 2010). Scanning electron micrographs of these digested pollen tubes showed that the *Arabidopsis* pollen tube cell wall comprised a fibrous component whose main orientation was nearly parallel to the longitudinal axis of the cell (Fig 4.5b). Given that cellulose microfibrils are the only known fibrous components in the pollen tube wall, this suggests that the net orientation of microfibrils is near parallel with the longitudinal axis of the cell.

To corroborate this further, we observed the spatial arrangement and motion pattern of cellulose synthases (CESAs) in the plasma membrane of *Arabidopsis* pollen tubes. Cellulose synthesis is performed by several CESAs grouped into rosette complexes (Somerville 2006) and in other plant cell types the motion pattern of CESA was found to be correlated with the orientation of cellulose microfibrils (Paradez *et al.* 2006). Variable angle epifluorescence microscopy (VAEM) of *Arabidopsis* pollen tubes expressing *GFP-CESA6* (Desprez *et al.* 2007) revealed that punctate label for GFP-CESA6 was localized uniformly distributed along the pollen tube plasma membrane including the apex (Fig 4.4c). Tangential optical sections of the tube showed that the GFP-CESA6 punctae were frequently aligned in near parallel manner to the longitudinal axis of the tube (Fig 4.5c) and

time-lapse imaging revealed that they move along these lines (Fig 4.5d, Supplemental Movie 4.1).

4.3.6 Fucosylated xyloglucans are uniformly deposited in the cell wall

Cellulose microfibrils alone cannot confer much tensile resistance to the cell wall unless they are cross-linked into a network. Well known cross-linkers of cellulose are xyloglucans, hemicelluloses formed of a backbone of β-1,4-linked D-glucose with α-D-xylose branching (Obel *et al.* 2007). CCRC-M1 antibody was used to label fucosylated epitopes that are found principally in xyloglucans (Freshour *et al.* 2003). Label for these fucosylated epitopes was uniform all along the cell wall of straight growing pollen tubes (Figs 4.1h,h'). Lower label intensity was observed at the tip of the tube compared to the distal region. No label was found at the collar region between the base of the pollen tube and the pollen grain. Contrary to crystalline cellulose, no distinction between two different types of apical distribution patterns could be made. Remarkably, at locations corresponding to changes in pollen tube diameter or growth direction, xyloglucan label was barely detectable (Figs 4.1i,j).

4.3.7 Highly esterified pectins are tightly embedded into the cellulose network

Contrary to our expectations, the fluorescence intensity of label for crystalline cellulose decreased with increasing distance from the apices of most pollen tubes, in particular after the first 10 µm (Fig 4.1f). Since this spatial gradient was mirrored by an increasing degree of de-esterification in cell wall pectins, we hypothesized that crystalline cellulose epitopes in the shank might be partially masked to the antibody by the increasingly gelled pectins. To verify this hypothesis we devised two strategies: *1)* We enzymatically removed the pectic outer layer after fixation in order to expose all putatively masked crystalline cellulose epitopes before labelling with CBM3a. *2)* We treated living pollen tubes with pectin methyl esterase (PME) to de-esterify the apically located pectins and thus facilitate their gelation (Parre and Geitmann 2005b). If the presence of gelled pectin in the shank was the reason for a longitudinal gradient in cellulose label, both treatments should result in

evening out the gradient, but overall label intensity should be higher after treatment *1)* than after treatment *2)*. A combination of both treatments was tested as an additional control. In addition, immunolabel for pectins was carried out in parallel to test the efficiency of the enzyme treatments.

Control samples (not treated with PME nor digested with pectinase) showed significant label at the tip for highly esterified pectins and weak labelling for low esterified pectins whereas in the distal region, labelling was more intense for highly esterified pectins (Figs 4.1b,c, 4.6). Tubes that were treated with PME but not digested with pectinase showed very poor label for highly esterified pectins confirming the efficiency of PME (Figs 4.6, 4.7e,f). Tubes that were digested with pectinase, whether or not exposed to PME, did not show any label for pectins suggesting the pectinase activity was fully efficient even on chemically fixed cells (Figs 4.6, 4.7a,b,i,j).

After treatment with PME only (Figs 4.7e,f,g,h), the crystalline cellulose staining pattern was identical to that of the non-treated tubes (Fig 4.1f), suggesting that the degree of esterification and gelation of the pectins was not responsible for the longitudinal gradient in cellulose label in the distal region. After pectin digestion, more than 80% of the pollen tubes showed less or no label for crystalline cellulose at the apex (Figs 4.6, 4.7c,d). In these cells, crystalline cellulose was only detectable after the first 10 µm. This removal of apical cellulose by pectin-specific digestive action suggests that the cellulose microfibrils in this region do not form an independently stable network. They seem to form links to the highly esterified pectins that are dominant in this region and when these are enzymatically removed, they are washed away as well. Alternatively, the cellulose network may be stably embedded in the solid pectin matrix and not necessarily bound to it. Treatment with PME prior to fixation and pectin digestion was able to restore the crystalline cellulose labelling pattern observed in tubes that were not treated with pectinase (Figs 4.6, 4.7g,k). This implies that *1)* pectin, independently of its degree of esterification, does not mask cellulose epitopes and *2)* that the cellulose network is less embedded or bound to low esterified pectins than to highly esterified pectins. Calcofluor staining confirmed this as the staining pattern was identical to CBM3a labelling. Tubes that were not treated with pectinase displayed high amount of calcofluor staining at the apex and less in the shank, whereas

tubes treated with pectinase showed the same pattern of staining as tubes stained for crystalline cellulose (Figs 4.7h,l).

4.3.8 The cellulose layer is removed when pectin and callose are digested

The enzymatic removal of the pectin matrix clearly resulted in the (partial) removal of the apical population of cellulose microfibrils during specimen preparation, suggesting that microfibrils are either rather short in this region or not well cross-linked, or both. Given these results, we hypothesized that cellulose microfibrils might be physically stabilized by the surrounding pectin matrix. However, at TEM level we had also observed the co-localization of crystalline cellulose with the callose layer. Therefore, we wanted to test the effect of enzymatic removal of callose on cellulose label. We subjected pollen tubes to digestion by lyticase (an enzyme that specifically digests callose) or to a combination of lyticase and pectinase.

When fixed pollen tubes were treated with lyticase alone, the distribution profile of crystalline cellulose was not affected. After combined pectinase and lyticase digestion, no crystalline cellulose was detected in the pollen tube cell wall by immunolabel or calcofluor white stain. The only labelling was visible inside the pollen tube cytoplasm (Fig 4.8), confirming that cellulose microfibrils are interconnected with callose polymers as well as with pectins. Finally, the residual label of small cytoplasmic organelles after enzyme treatment corroborates the presence of cellulose in vesicles.

4.3.9 The mechanical properties of the pollen tube display a longitudinal gradient

Our quantitative assessment of the spatial distribution pattern of cell wall components in the *Arabidopsis* pollen tube indicates a dramatic change in the biochemical composition at the transition region between the hemisphere-shaped apex and the cylindrical shank of the tube. Computational modeling has shown that this transition region must also display a significant change in mechanical properties to ensure stability of the cylindrical shank against tensile stress caused by the turgor pressure (Fayant *et al.* 2010). In order to demonstrate that the observed changes in biochemical composition translate into a change

in mechanical properties, we used micro-indentation to measure the local cellular stiffness of the *Arabidopsis* pollen tube along its longitudinal axis. The spatial profile revealed that the pollen tube apex was significantly softer than the cylindrical region of the cell (Fig 4.9). This is consistent with data from other plant species (Geitmann and Parre 2004; Zerzour *et al.* 2009).

4.4 Discussion

4.4.1 Pectin deposition in *Arabidopsis* pollen tubes takes place at the first 5 µm

The main components of the pollen tube cell wall are pectins which are deposited at the pollen tube tip by exocytosis in high methyl esterified form (Bosch *et al.* 2005). This seems to also be true in *Arabidopsis* pollen tubes since immunolabeling at TEM level showed that cytoplasmic vesicles were only labeled for highly esterified pectins but not for low esterified pectins. The presence of only highly esterified pectins in vesicles of the pollen grain shows that a pool of pectin is already present before pollen germination, allowing pollen to rapidly initiate germination before the cellular machinery required for *de novo* pectin synthesis is fully activated (Geitmann 2010a). During germination, exocytosis events delivering pectin to the elongating cell wall seem to occur only in the first 5 µm (meridional) similar to other species (Li *et al.* 1994; Geitmann *et al.* 1995; Jauh and Lord 1996; Geitmann and Parre 2004; Parre and Geitmann 2005b; Dardelle *et al.* 2010; Fayant *et al.* 2010; Lehner *et al.* 2010).

4.4.2 The spatial distribution of pectin de-esterification determines the pollen tube diameter

The spatial distribution of the different configurations of pectin suggests that de-esterification takes place in the apical region between the first 3 and 10 µm (meridional distance), implying that PME is active in this cell wall region. This spatial profile coincides with that of *Arabidopsis* PME inhibitor (At3g17220) transiently expressed in tobacco pollen tubes which is specifically localized at the pole of the tube and likely endocytosed in

the flanks (Röckel *et al.* 2008) (Fig 4.10b). Mechanical modeling of pollen tube growth has shown that the transition point between curved apex and cylindrical shank coincides exactly with a steep gradient in the Young's modulus of the cell wall necessary to achieve self-similar growth with a strain distribution typical for pollen tubes (Fayant *et al.* 2010). The gelation of pectins into a stiffer material in the transition region stabilizes the cell wall and prevents any further expansion of the cell wall in the sub-apical part of the tube (Fig 4.10b) (Parre and Geitmann 2005b). Micro-indentation confirmed that the cellular stiffness in the shank of the *Arabidopsis* pollen tube is increased compared to the apex.

4.4.3 Callose distribution is consistent with its role in resisting tension stresses

Callose (1,3-β-D-glucan with 1,6-linked branches) is synthesized at the plasma membrane by the callose synthase complex. Callose deposits are visible 30 µm from the tip in *Nicotiana tabacum* (Ferguson *et al.* 1998) and 20 µm in *Lilium orientalis* (Fayant *et al.* 2010). Micro-indentation combined with enzymatic treatments have shown that in the cylindrical distal part of the cell, callose plays a role of reinforcement against compression and tension stresses (Parre and Geitmann 2005a). The spatial profile of our callose label is consistent with previous observations in other species (Ferguson *et al.* 1998; Geitmann and Parre 2004; Parre and Geitmann 2005a; Fayant *et al.* 2010; Derksen *et al.* 2011). Callose deposition in *Arabidopsis* only began after the first 10 µm and reached a plateau in the distal region. Callose plug formation could be seen in older pollen tubes beginning at a distance of 100 µm from the tip. This differs from observations made on *in vitro* (Derksen *et al.* 2002) and *in vivo* (Lennon and Lord 2000) germinating *Arabidopsis* pollen tubes, where callose was found very close to the tip (as close as 5 µm meridional from the pole) and callose plugs were observed to begin to form as close as 40 µm to the tip. These differences in spatial distribution may be the result of a higher *in vitro* growth rate obtained here (30 $\mu m.h^{-1}$ compared to 10.4 $\mu m.h^{-1}$ in (Derksen *et al.* 2002)). Since callose synthase seems to be inserted into the apical plasma membrane (Cai *et al.* 2011), the distance at which the synthesis of callose accumulates to visible amounts may simply result from the ratio between the synthesis rate of the enzymes and the growth rate of the tube. Stress is

likely to increase callose production in pollen tubes, in particular in *Arabidopsis*, since in our hands, *in vitro* culture conditions other than those we optimized (Bou Daher *et al.* 2009) resulted in the presence of callose label at the tube apex (unpublished data). This is consistent with callose synthesis being a known response to mechanical stress and wounding in plant tissues (Jacobs *et al.* 2003; Geitmann and Steer 2006).

4.4.4 Fucosylated xyloglucans are secreted in their final form

Xyloglucans are synthesized and processed in the Golgi apparatus before being exported via secretory vesicles (Edelmann and Fry 1992). Once inserted into the cell wall they are associated to cellulose via hydrogen bonds thus contributing to the formation of a tight network (Hayashi 1989; Acebes *et al.* 1993; Hayashi *et al.* 1994a) . Information about the role and the presence of xyloglucans in pollen tubes is scant. No significant amount of xyloglucan was detected in pollen tubes of *Nicotiana* (Schlüpmann *et al.* 1994), whereas in *Arabidopsis*, fucosylated xyloglucans were found in pollen grains of the *mur1* mutant (Freshour *et al.* 2003). Transmission electron microscopy showed that fucosylated xyloglucans were only associated with the inner layer of the *Arabidopsis* pollen tube wall (Dardelle *et al.* 2010), suggesting that they are cross-linked to cellulose microfibrils.

CCRC-M1 labelling demonstrated that fucosylated xyloglucans were distributed evenly along the *Arabidopsis* pollen tube cell wall. This is consistent with the fact that they are secreted in their final fucosylated form at the apical plasma membrane (Obel *et al.* 2007). In locations where the tubes seem to change direction or diameter, fucosylated xyloglucans were not detected. We speculate that a temporary failure to deliver these linker molecules to the cellular surface may lead to a transient widening of the tube diameter because of a lack of cellulose cross-linking, similar to the phenomenon observed after treatment with cellulase (Aouar *et al.* 2010) and predicted by finite element simulations of the growth process (Fayant *et al.* 2010).

4.4.5 Cellulose synthesis might be initiated in vesicles

Unlike most other plant cell types in which cellulose (1,4-β-D-glucan) typically is the major cell wall component, pollen tubes have a very low amount of cellulose in their cell wall; less than 10% of the *Nicotiana tabacum* (Schlüpmann *et al.* 1994) and approximately 6-7% dry weight of the *Lilium longiflorum* pollen tube cell wall is composed of cellulose (van der Woude *et al.* 1971). In most plant cells, cellulose synthesis is initiated once cellulose synthase complexes have been deposited into the plasma membrane (Somerville 2006). Both our TEM and fluorescence data suggest that crystalline cellulose is present in cytoplasmic vesicles in the *Arabidopsis* pollen grain and tube. It is unclear, whether these vesicles derive from endocytosis and thus represent recycled cellulose, or whether they carry cellulose synthases and newly assembled, short microfibrils. However, their association with the trans-Golgi network and with vesicles located in the apical cytoplasm indicates that at least a portion of these vesicles is destined for exocytosis. This putative cellulose synthesis activity ahead of surface deposition is not unique, since β-glucan synthetase activity has been detected in Golgi vesicle fractions isolated from *Petunia hybrida* pollen tubes (Helsper *et al.* 1977). Furthermore, cellulose residues have been found in the vesicles of pollen tubes from lily (van der Woude *et al.* 1971) and *Petunia hybrida* (Engels 1973; Engels 1974; Engels 1974) and in the alga *Pleurochrysis scherffelii* (Brown 1969). The activation of cellulose synthases prior to their insertion into the plasma membrane may give pollen tubes a head start in assembling the cell wall necessary to sustain rapid elongation.

4.4.6 Spatial distribution and orientation of cellulose microfibrils suggest particular mechanical functions

Whereas the apex of *Nicotiana tabacum* pollen tubes is devoid of cellulose (Ferguson *et al.* 1998), microfibrils were present in the apex of the *Arabidopsis* pollen tube according to both calcofluor and CBM3a label. However, label intensity at the very tip of the tube was variable and two populations of pollen tubes displaying either intense or very weak label at the pole could be distinguished with CBM3a label. The differences in the cellulose pattern within the population may result from the temporal changes in growth behavior of

individual pollen tubes and/or from the abundance of active cellulose synthases at the pollen tube tip (Fig 4.4c). Temporal changes in growth rate are associated with modifications in cell wall thickness at the pole (Li *et al.* 1996; McKenna *et al.* 2009; Derksen *et al.* 2011).

The presence of cellulose in the apex is corroborated by the fact that cellulose synthases are abundant at the apical plasma membrane of the *Arabidopsis* (Fig 4.4c) and tobacco (Cai *et al.* 2011) pollen tubes and it has been proposed that cellulose microfibrils play a role in regulating tube diameter (Aouar *et al.* 2010). Cellulose may confer tensile resistance to the most crucial position on the cellular surface, the transition region between the apical dome and the cylindrical shank (Fayant *et al.* 2010). A direct comparison between the spatial distribution profiles of high and low esterified pectins points at the potential reason for the need of cellulose in the transition region (Fig 4.10b). Although pectin gelation begins before the transition point, the cross-over point between the two pectin configurations in *Arabidopsis* pollen tubes is further distal and complete gelation is only achieved at approximately 10 µm. This is strikingly different from lily pollen tubes in which maximal gelation is reached exactly at the transition point (Fayant *et al.* 2010). Therefore, additional reinforcement by cellulose in this region may be a crucial determinant of tube diameter in *Arabidopsis* pollen tubes.

In the tubular portion of the tube, starting at the transition region, all tubes displayed a gradient with a steady decrease of label intensity for crystalline cellulose with increasing distance from the apex. This longitudinal gradient is in agreement with observations made by others (Derksen *et al.* 2002; Fayant *et al.* 2010). However, the orientation of the gradient - lower abundance of cellulose in more mature portions of the wall - is puzzling. Our control experiments showed that this phenomenon was not a labelling artefact or a result of the masking of epitopes by other cell wall components. This raises the question how the amount of cellulose decreases during cell wall maturation if the maturing wall does not expand? It is possible that cellulose may be reincorporated into the cytoplasm following digestion by endogenous cellulases (Lane *et al.* 2001; Römling *et al.* 2005). A recycling mechanism may allow the fast growing pollen tube to sustain growth over long distances

by ensuring a constant supply of material to its tip region but further research is warranted to provide proof for this hypothesis.

The cellulose in the tubular portion of the tube displays another unexpected property. Scanning electron microscopy and fluorescence based localization and dynamics of CESA6 suggest that microfibrils are produced and oriented almost parallel to the longitudinal axis of the cell. This primarily longitudinal orientation is very different from the circumferential orientation of microfibrils in other plant cell types with cylindrical shape (Baskin 2005; Geitmann and Ortega 2009). However, it is similar to the low pitch of cellulose orientation observed in other pollen tube species (*Petunia:* 45°; (Sassen 1964); *Lilium*: 20-25°; *Solanum*: l5-20°; (Aouar *et al.* 2010). Furthermore, immunohistochemical localization of CESA in tobacco pollen tubes also suggests a low pitched helical arrangement (Cai *et al.* 2011). In the root and shoot cells the circumferential arrangement of cellulose microfibrils is thought to prevent lateral expansion of the cell and forcing cell growth to occur in longitudinal direction. A helical or near longitudinal orientation of the reinforcing fibrous component suggests a different function in pollen tubes. Helical winding would be consistent with a role in stabilizing the tube against buckling and against collapse during curved growth and compression stress in axial direction. Similarly to a helically reinforced catheter, the pollen tube has to invade a mechanically resistant tissue and to ensure that despite its winding journey through the pistil the male germ unit passes unimpeded. The cellulose microfibrils in the cylindrical portion of the tube may thus play an important role in the pollen tube fulfilling its biological function as a catheter-like delivery system for the sperm cells.

4.4.7 The cellulosic network is stabilized by the pectic gel and callose

Treatment with PME prior to pectinase digestion prevented the loss of crystalline cellulose from the tube tip that occurred in tubes only treated with pectinase. This suggests that the degree of pectin esterification plays a role in stabilizing the cellulosic network. When pectins are low-esterified, they tend to gelate in the presence of Ca^{2+}, thus forming a tight gel and losing the ability to bind to the cellulose microfibrils. This can explain why after pectin digestion, label for crystalline cellulose disappeared entirely from the pollen tube

apical region but was only slightly reduced in the distal region. Since pectins are known to bind to cellulose *in vitro* (Zykwinska *et al.* 2005) and *in vivo* (Iwai *et al.* 2001; Oechslin *et al.* 2003; Vignon *et al.* 2004), we hypothesize that the two types of polymers are closely linked in pollen tube wall and that cellulose was washed off together with the highly methyl-esterified pectins following pectin digestion, despite the chemical fixation. Formaldehyde fixation cross-links mostly proteins and the polysaccharidic cell wall moiety may not be stable if one of the components is digested.

The stability of cellulose in the distal region of the tube during pectinase digestion may also be explained by the presence of callose in this portion of the tube. The co-localization of cellulose and callose in the inner, electron translucent cell wall layer is consistent with observations made in *Nicotiana tabacum* (Ferguson *et al.* 1998) and suggests a close connection between the two polymers in this maturing region of the cell wall. This notion is also supported by the finding that double digestion with pectinase and lyticase removed the entire label for crystalline cellulose, leaving only cytoplasmic organelles displaying residual cellulose label. Together, the observations indicate that cellulose is linked to or tightly embedded into both pectins (apex) and callose (shank), and that the cell wall polymers form a tight network.

4.5 Conclusion

During pollen tube growth, cell wall precursors and enzymes are deposited at the tip by exocytosis. During wall maturation, the cell wall components undergo a structural reorganization through different chemical changes and recycling events. Figure 4.10 summarizes our model for the *Arabidopsis* pollen tube cell wall organization and the intracellular transport of the major cell wall precursors. In the cell wall region comprised between 3 and 10 μm (meridional), the pectin de-esterification (through the regulation of the PME activity), the beginning of callose deposition and the regulation of cellulose deposition take place, thus changing drastically the mechanical properties of the cell wall as predicted by FE modelling (Fig. 4.10a). This suggests that in *Arabidopsis* pollen tubes, the regulation of the cell wall chemistry in this transition region is crucial for determining the shape of the pollen tube.

4.6 Material and methods

4.6.1 Plant material

Arabidopsis thaliana ecotype Columbia-0 plants were grown in trays in a greenhouse as described earlier (Bou Daher *et al.* 2009). Pollen was collected every day from the time flowers bloomed using a modified vacuum cleaner as described by (Johnson-Brousseau and McCormick 2004). Pollen grains were then dehydrated over silica gel for 2 hours and stored at -20°C until use.

4.6.2 Pollen culture

Pollen grains were hydrated for 30 min. For fluorescence microscopy and scanning electron microscopy, hydrated pollen was incubated at 22.5 °C for 4 to 5 hours under continuous shaking in a 25 mL Erlenmeyer flask containing 3 mL liquid growth medium containing 0.49 mM H_3BO_3, 2 mM $Ca(NO_3)_2$, $4H_2O$, 2 mM $CaCl_2$, 1 mM KCl, 1mM $MgSO_4$,$7H_2O$, pH 7 and 18% w/v sucrose (Bou Daher *et al.* 2009). For transmission electron microscopy, hydrated pollen was incubated at 22.5°C for 6 hours in a solidified growth medium made of 1.62 mM H_3BO_3, 5 mM, $Ca(NO_3)_2$, $4H_2O$, 5 mM $CaCl_2$, 1 mM KCl, 1mM $MgSO_4$,$7H_2O$, pH 7, 18% w/v sucrose and 0.5% w/v agar (Bou Daher *et al.* 2009). For micro-indentation, pollen was brushed on gelatine coated cover slips, re-hydrated, and covered with drops of liquid growth medium.

4.6.3 CESA6 localization in pollen tubes

Arabidopsis seedlings expressing *pCESA6::GFP-CESA6* were produced from seeds obtained from Herman Höfte (INRA, Versailles, France) (Desprez *et al.* 2007). *Arabidopsis* pollen grains were harvested on a 5 µm filter then hydrated for 30 min at room temperature in a humidity chamber prior to 4 hours germination on *Arabidopsis* medium solidified with 1% agarose (Bou Daher *et al.* 2009). The pollen tubes were covered with a cover slip and sealed with VALAP (1:3 Vaseline®, 1:3 lanolin and 1:3 paraffin wax).

4.6.4 Immunohistochemistry

All steps were carried out in a microwave oven (Pelco BioWave® 34700 equipped with a Pelco Cold Spot®) operating at 150 W under 21 inches of Hg vacuum at a controlled temperature of 30±1°C. For fluorescence labeling, pollen tubes were filtered and subsequently fixed in 3.5% w/v freshly prepared formaldehyde in Pipes buffer (50 mM Pipes, 1 mM EGTA, 5 mM $MgSO_4$, 0.5 mM $CaCl_2$, pH 7) for 40 seconds followed by 3 washes in Pipes buffer. For immuno-labelling pollen tubes were then washed 3 times with phosphate buffer saline (PBS) (135 mM NaCl, 6.5 mM Na_2HPO_4, 2.7 mM KCl, 1.5 mM KH_2PO_4, pH 7.3) with 3.5% w/v bovine serum albumine (BSA). All subsequent washes were done with PBS buffer with 3.5% w/v BSA for 40 seconds. All antibodies were diluted in PBS buffer with 3.5% w/v BSA and incubations were done for 10 min followed by three washes in buffer. Controls were performed by omitting incubation with the primary or the secondary antibody. Pectins with low and high degree of esterification were labeled with JIM5 and JIM7, respectively (diluted 1:50; Paul Knox, University of Leeds, United Kingdom) followed by Alexa Fluor 594 anti-rat IgG (diluted 1:100; Molecular Probes). Callose was labeled with a monoclonal IgG antibody to (1→3)-β-glucan (diluted 1:200; Biosupplies Australia Pty Ltd) followed by Alexa Fluor 594 anti-mouse IgG (diluted 1:100; Molecular Probes). Xyloglucans were labeld with CCRC-M1 antibody directed against fucosylated epitopes (diluted 1:50; Michael Hahn, Athens, Georgia) followed by Alexa Fluor 594 anti-mouse IgG (diluted 1:100; Molecular Probes). Label for crystalline cellulose was performed with Cellulose Binding Module 3a (diluted 1:200; Paul Knox, University of Leeds, United Kingdom) followed by a monoclonal mouse-anti-polyhistidine antibody (diluted 1:12; Sigma) and subsequent incubation with Alexa Fluor 594 anti-mouse IgG (diluted 1:100; Molecular Probes). Cellulose was also stained directly after fixation and washes by incubating for 10 min with 1 $mg.mL^{-1}$ calcofluor white (Fluorescent Brightener 28; Sigma) in double-distilled water.

Following the label procedure and final washes, all samples were mounted on glass slides in a drop of Citifluor (Electron Microscopy Sciences) for microscopical observations. Each experiment was repeated at least 4 times. To label cytoplasmic vesicles, growing pollen

tubes were incubated for 10 min with 6 μg.mL^{-1} FM4-64 (Molecular Probes) prior to observation.

4.6.5 Selective digestion of cell wall components

After 6 hours of contact with the growth medium, 1.28 mg.ml^{-1} pectin methyl esterase (534 units/mg protein, Sigma) was added to the germination medium and pollen tubes were incubated for 45 minutes. Controls were performed by adding enzyme that had been denatured by boiling for 15 minutes. Pollen tubes were then fixed as described above, washed 3 times, and subsequently incubated in PBS buffer containing 5 mg.mL^{-1} pectinase (Sigma) or 1 mg.mL^{-1} lyticase (Sigma) or a mix of the two enzymes for 3 hours with constant shaking. Pollen tubes were then washed 3 times with PBS buffer and 3 times with PBS buffer with 3.5% w/v BSA prior to labelling for fluorescence microscopy as described above.

4.6.6 Fluorescence microscopy

Differential interference contrast (DIC) and fluorescence imaging of immunohistochemical label were done with a Zeiss Imager-Z1 microscope equipped with structured illumination setup (ApoTome Axio Imager), a Zeiss AxioCam MRm Rev.2 camera and AxioVision Release 4.5 software. For calcofluor label, a filter set with excitation BP 450-490 nm, beamsplitter FT 510 nm and emission BP 515/565 nm was used. For Alexa Fluor 594 detection the filter set comprised an excitation filter BP 390/22 nm, beamsplitter FT 420 nm and emission filter BP 460/50 nm. Exposure times were adjusted for each image so that only one or two pixels were saturated prior to insertion of the ApoTome Imager into the light pathway. The ApoTome Imager was then inserted and Z-stacks of 1 μm interval were acquired. Image reconstruction was performed using the AxioVision software by the maximum projection of the stacks. Localization of vesicles was done using a Zeiss LSM 510 META / LSM 5 LIVE / Axiovert 200M system, using the 561 nm laser with an LP 650 emission filter.

Live cell imaging of pollen tubes expressing *GFP-CESA6* was done using a variable-angle epifluorescence microscope (VAEM; lab of Sebastian Bednarek, University of Wisconsin,

Madisson, USA) as described in (Konopka and Bednarek 2008). Briefly, we used a Nikon Eclipse TE2000-U equipped with the Nikon T-FL-TIRF attachment. GFP fluorescence was excited with the 488 nm argon laser and an emission filter 535/30 nm was used. Images were captured with a Photometrics Evolve 512 camera at 4 frames s^{-1}.

4.6.7 Image processing and fluorescence quantification

ImageJ software (Rasband, W.S., ImageJ, U. S. National Institutes of Health, Bethesda, Maryland, USA, http://rsb.info.nih.gov/ij/, 1997-2008) was used for quantification of fluorescence intensity based on maximum projections of Z-stacks. Pixel intensity was measured along the periphery of each pollen tube, beginning from the pole. Values for fluorescence intensity were normalized to the highest value present on an individual tube before averaging over all tubes (n>10 for each sample). Values on the x-axis in the graphs represent the meridional distance from the pole of the cell. Given an average tube diameter of 5 µm and an approximately hemisphere-shaped apex for *Arabidopsis*, a distance of 10 µm on the meridional curvature corresponds to a tube length of 8.6 µm measured along the longitudinal axis.

4.6.8 Sample preparation for transmission electron microscopy

4.6.9 Rapid freeze fixation and freeze substitution

Pollen tubes grown in liquid medium were filtered on 5 µm mesh nylon filters. The filters were plunged into liquid ethane at -173°C in a Leica EM CPC cryo-preparation device. Freeze substitution was performed in anhydrous acetone containing 0.5% (v/v) glutaraldehyde by gradually increasing the temperature to 0°C over a period of 96 hours. Resin infiltration was performed using LR-White hard grade resin (Electron Microscopy Sciences) in 4 steps with increasing resin concentration up to 100%. Resin polymerization was done at 50°C for 48 hours.

4.6.10 Conventional sample preparation for transmission electron microscopy

All fixation, washing and dehydration steps were conducted using a microwave oven (Pelco BioWave® 34700 equipped with a Pelco Cold Spot®) at 150 W and 21 in of Hg vacuum for 40 seconds each. Pollen tubes grown in 0.5% w/v agar medium were fixed in freshly prepared 2% w/v formaldehyde and 2.5% glutaraldehyde in 0.05 M phosphate buffer pH 7.2. Samples were subsequently washed 3 times with phosphate buffer and 3 times with double distilled water. Dehydration was done using an increasing ethanol gradient ranging from 25 to 100% with the last step repeated thrice. Resin infiltration was performed using LR-White hard grade resin (Electron Microscopy Sciences) in 4 steps with increasing resin concentration up to 100%. These steps were conducted three times at 300 W for 2 minutes each, under 21 in of Hg vacuum. Samples were then left in 100% resin over night. Resin polymerization was done at 50°C for 48 hours.

Following both freeze fixation and conventional fixation, ultrathin sections were cut with a Leica Ultracut and collected on 150-mesh formvar coated nickel grids. Samples were observed with a JEOL JEM 100S transmission electron microscope operating at 80 kV.

4.6.11 Immunogold label

Grids with ultrathin sections were floated with the sections facing down on drops of PBS buffer containing 4% w/v BSA for 1 hour. Grids were then incubated for 30 minutes with 1:200 anti-callose, 1:200 CBM3a or 1:100 JIM5 or JIM7. Samples were washed 3 times in PBS-BSA buffer for 10 minutes each. For crystalline cellulose staining, grids were incubated with 1:125 anti-polyhistidine and washed 3 times. Secondary label was carried out with a 1:50 dilution of 10 nm colloidal gold goat anti-mouse or anti-rat IgG (BBInternational). The grids were then washed 3 times with PBS-BSA buffer and with CO_2-free, deionised water. Sections were contrasted with 2% w/v uranyl acetate solution, washed with deionised water and subsequently stained with lead citrate solution (80 mM $Pb(NO_3)_2$, 120 mM $C_6H_5Na_3O_7,2H_2O$, pH 12) and rinsed several minutes with deionised, decarbonated water.

4.6.12 Sample preparation for scanning electron microscopy

Samples for scanning electron microscopy (SEM) were fixed in freshly prepared 2% w/v formaldehyde and 2.5% glutaraldehyde in 0.05 M phosphate buffer pH 7.2. Samples were subsequently washed 3 times with phosphate buffer. Dehydration was done using an increasing ethanol gradient ranging from 30 to 100% with the last step repeated thrice. Samples were then critical point dried, gold-palladium coated and observed with a FEI Quanta 200 3D microscope operating at 20 kV.

4.6.13 Micro-indentation

Pollen was incubated as described and after germination had occurred, cover slips were submerged in the growth medium containing experimental chamber of the micro-indenter. The design and principles of operation of the micro-indenter have been described previously (Petersen *et al.* 1982; Elson *et al.* 1983). The microindentation assemblies used here were mounted on a Nikon TE2000 inverted microscope and used as described earlier (Geitmann and Parre 2004). The motor was programmed to execute a single triangular waveform with a velocity of 4 $\mu m.s^{-1}$ and a total amplitude of 10 μm.

4.7 Figures

Figure 4.1 Organization of the cytoarchitecture and relative spatial distribution of cell wall components in the *Arabidopsis* pollen tube. (legend on next page)

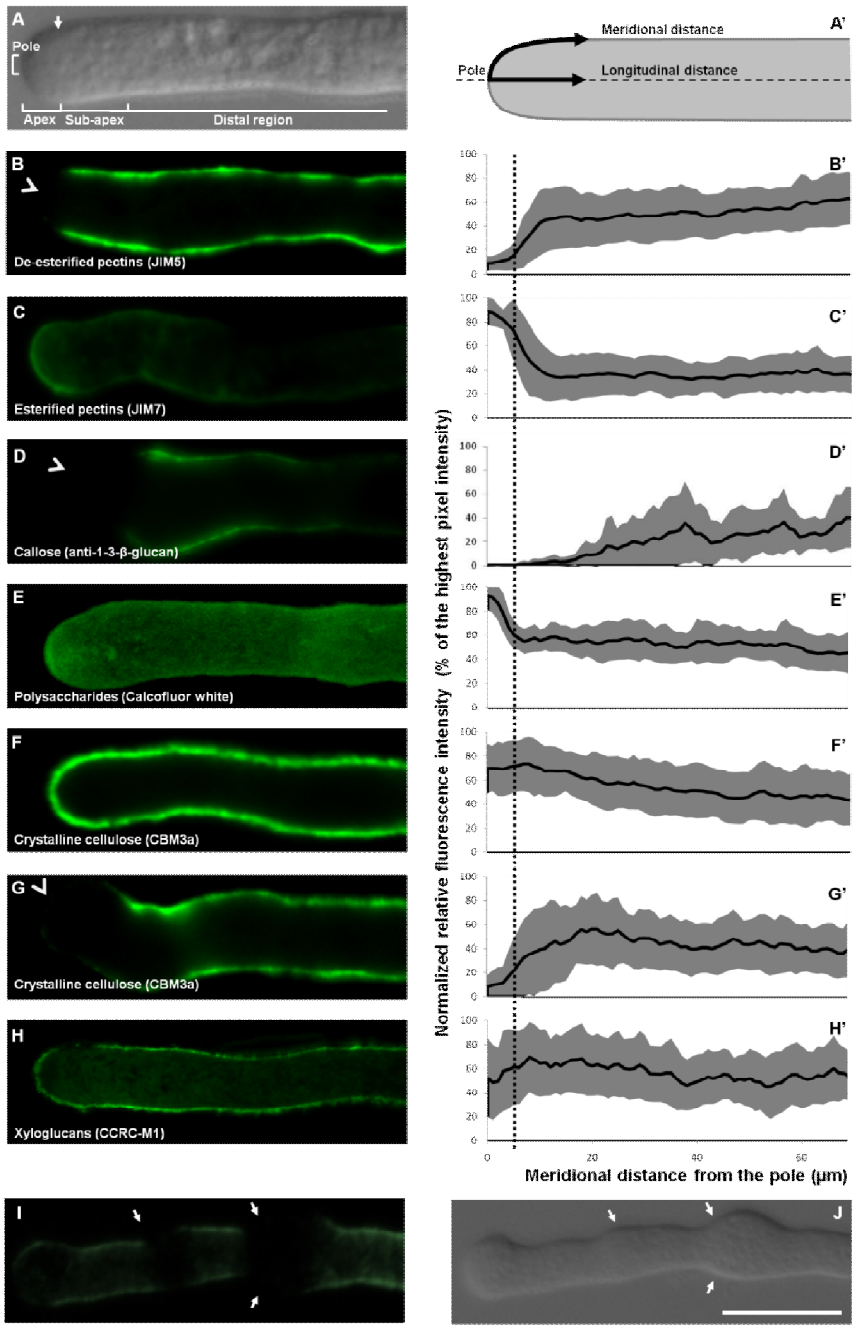

Figure 4.1: Organization of the cytoarchitecture and relative spatial distribution of cell wall components in the *Arabidopsis* pollen tube.

DIC micrograph of a chemically fixed Arabidopsis pollen tube (A) and nomenclature of distance measurements (A'). The first 3 µm (longitudinal distance) correspond to the tip or apex, the subapical region is located between 3 µm and 10 µm and the distal region starts at 10 µm longitudinal distance from the pole. The border between the apex and the subapical region is the transition region (arrow). Fluorescence micrographs (B to I) of median optical sections (left) and corresponding quantification of relative label intensities along the meridional cell surface (right). Specific label was performed using antibodies or histochemical stains for pectins with low (B) and high (C) degree of esterification, callose (D), microfibrillar polysaccharides (E), crystalline cellulose (F,G) and fucosylated xyloglucans (H). Xyloglucan label was absent or barely detectable at locations where the pollen tube diameter changed (I,J) (arrows). In the graphs, the black curve represents the mean relative fluorescence of all analysed tubes, grey areas represent the standard deviation, the dashed line represents the transition region between the hemisphere shaped apex of the pollen tube and the cylindrical shank of the tube. The arrowhead in (D) indicates the pole of the pollen tube. Label for crystalline cellulose revealed the presence of two distinct populations of tubes: approximately 70% of the tubes were intensely labelled at the apex (F,F') whereas 30% labelled only weakly at the tip (G,G'). $n \geq 30$ for each sample. Figures A to J are at the same scale. Bar = 10 µm.

Figure 4.2: Transmission electron micrographs of immunogold label for cell wall polysaccharides.

Arabidopsis pollen grains (A,C,F,H) and pollen tubes (B,D,F,G,I) were conventionally prepared for transmission electron microscopy and labeled for crystalline cellulose (A,B), for pectins with low (C,D,E) and high (F,G) degree of methyl-esterification and for callose (H,I). Black arrows indicate the localization of gold particles. E - exine, I - intine, IW - inner pollen tube wall, OW - outer pollen tube wall. (J) Quantification of label density on ultrathin-sections immuno-gold labelled for crystalline cellulose (n=10 micrographs). Bars = 0.15 µm.

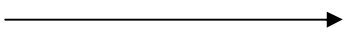

Figure 4.2

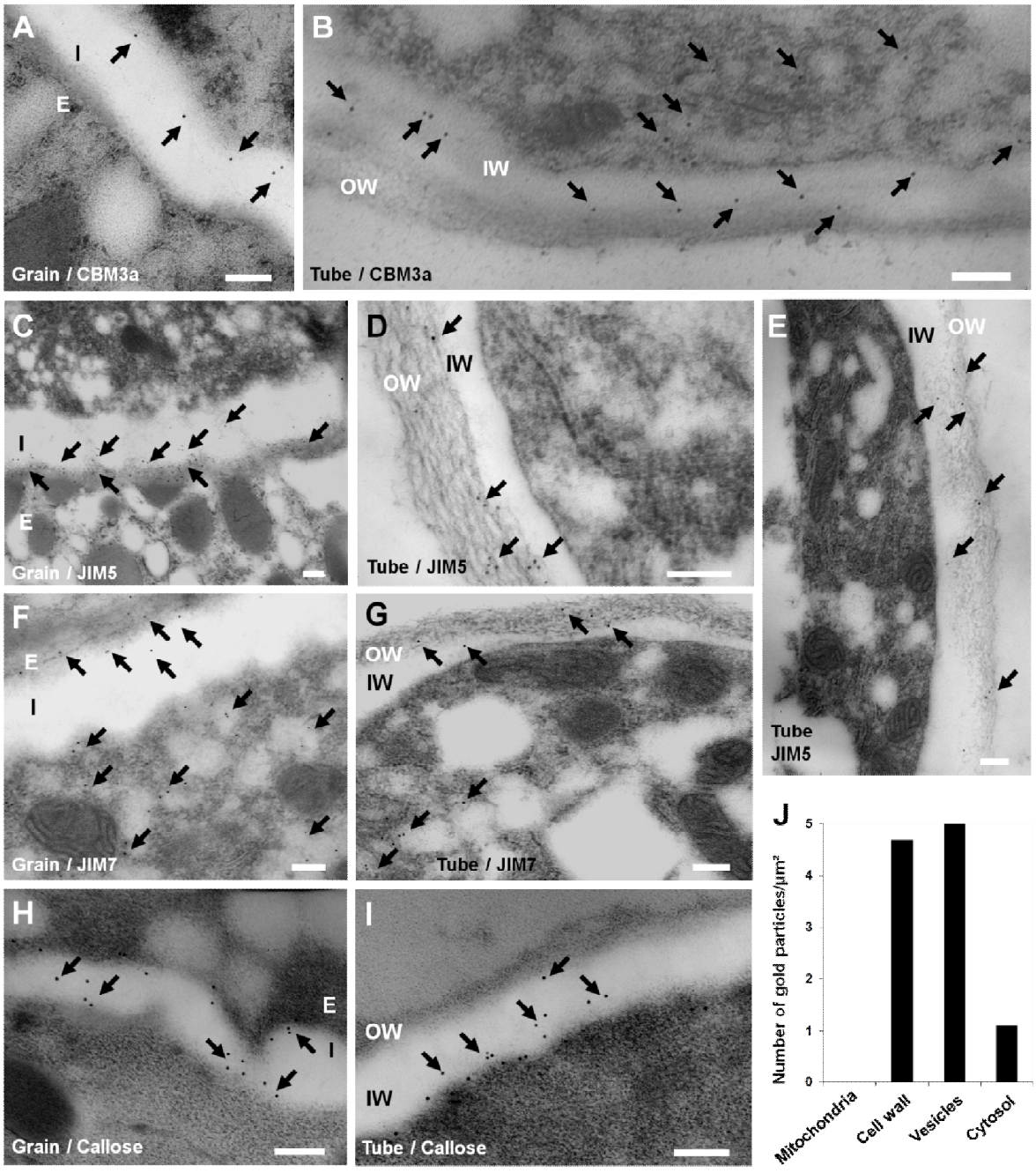
A
I
E
Grain / CBM3a
B
OW
IW
Tube / CBM3a
C
I
E
Grain / JIM5
D
OW
IW
Tube / JIM5
E
IW
OW
Tube
JIM5
F
E
I
Grain / JIM7
G
OW
IW
Tube / JIM7
H
E
I
Grain / Callose
I
OW
IW
Tube / Callose
J
Number of gold particles/µm²
0
1
2
3
4
5
Mitochondria
Cell wall
Vesicles
Cytosol

Figure 4.3

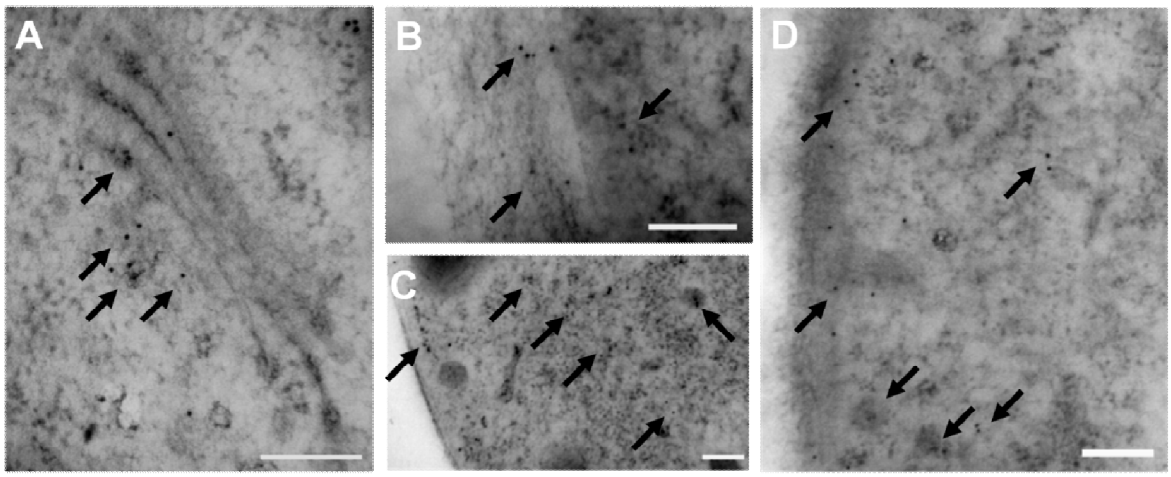

Figure 4.3: Transmission electron micrographs of immunogold label for crystalline cellulose in freeze fixed *Arabidopsis* pollen tubes.

Crystalline cellulose labelled with CBM3a was present in the trans-Golgi network (A), in the cell wall and in cytoplasmic vesicles (B,C,D). Black arrows indicate the localization of gold particles. Bars = 0.15 μm.

Figure 4.4

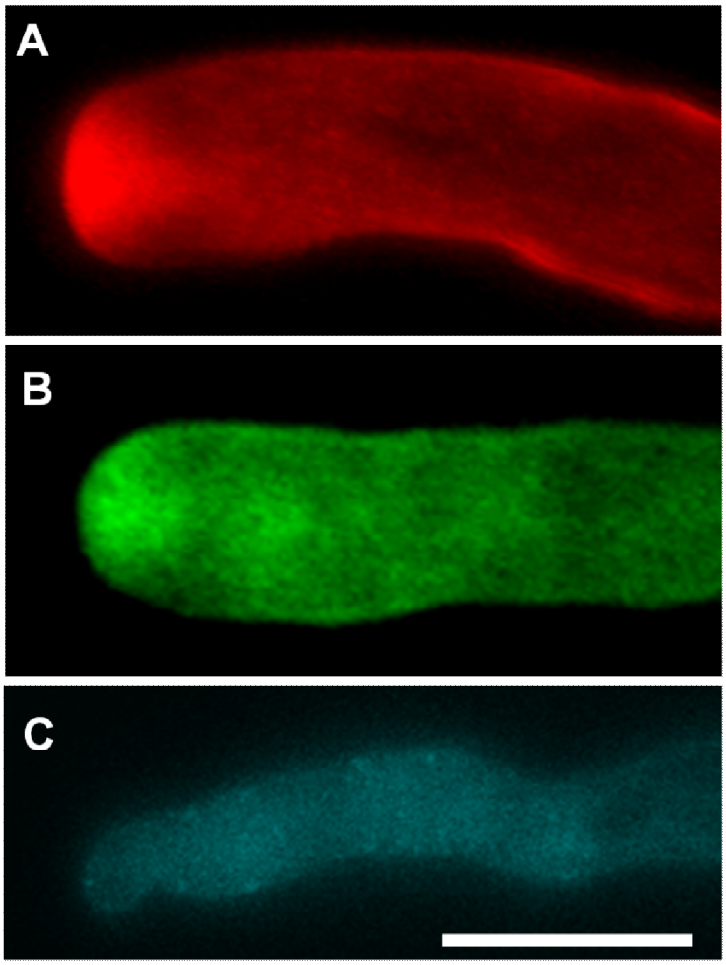

Figure 4.4: Fluorescence micrographs of pollen tubes labeled with the styryl dye FM4-64, CBM3a and VAEM image of a pollen tube expressing *GFP-CESA6*.

Fluorescence micrographs of pollen tubes labeled with the styryl dye FM4-64 (A), CBM3a (B) and VAEM image of a pollen tube expressing *GFP-CESA6* (C). A and B represent maximum projection of z-stacks. Both labelling of vesicles by the styryl dye and label of crystalline cellulose are abundant in the cone shaped apical vesicle aggregation. C is a tangential single optical section and shows localization of GFP-CESA6 in the plasma membrane of both the apical and the distal plasma membrane. Bar = 10 µm.

Figure 4.5

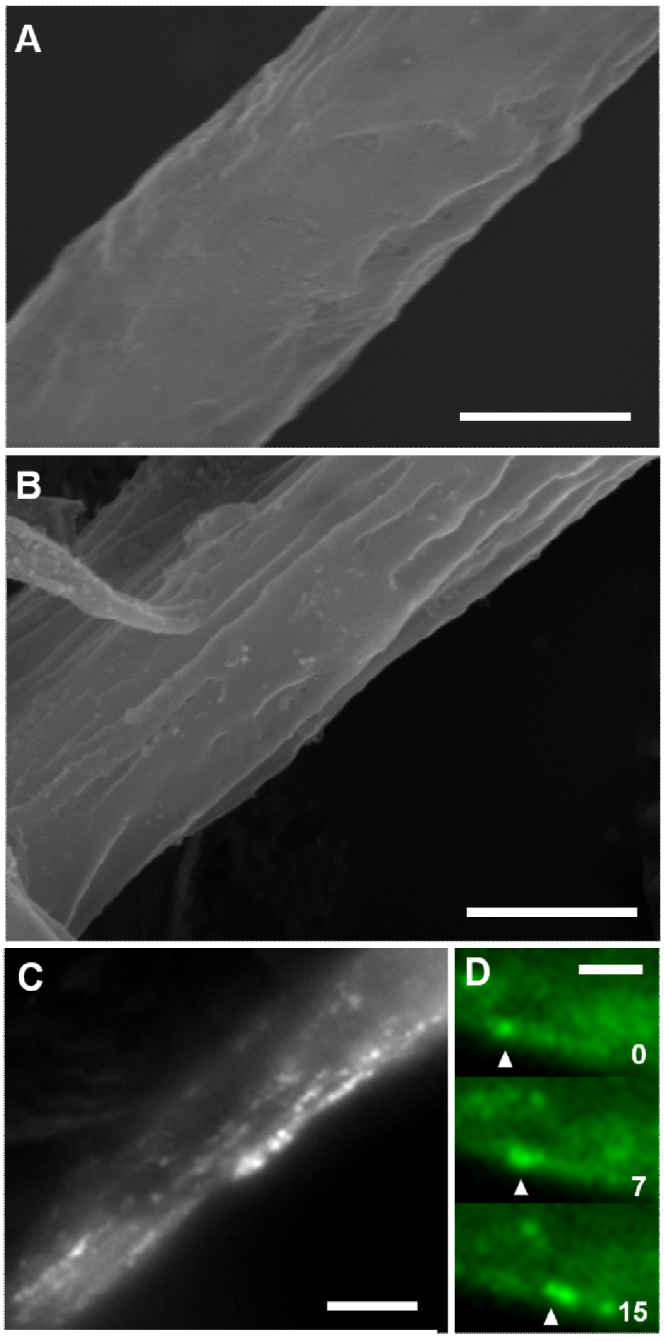

Figure 4.5: Scanning electron micrograph of the surface of *Arabidopsis* pollen tubes and VAEM images of pollen tube expressing *GFP-CESA6*.

Scanning electron micrographs (A,B) of the surface of *Arabidopsis* pollen tubes and VAEM images of pollen tube expressing *GFP-CESA6* (C,D).The control tube (A) displays a smooth surface with shallow undulations representing the outer pectin layer. Tubes digested with pectinase (B) after chemical fixation reveal that the wall contains a fibrous component that detaches in longitudinal direction. A maximum projection of a time lapse series of VAEM micrographs taken over 50 sec (C) shows that GFP-CESA6 punctae move primarily in longitudinal direction. (D) Still images of the same image series. Numbers indicate seconds. Arrowhead indicates one moving GFP-CESA6 complex. Bars = 2 µm (A,B,C), 1µm (D).

Figure 4.6

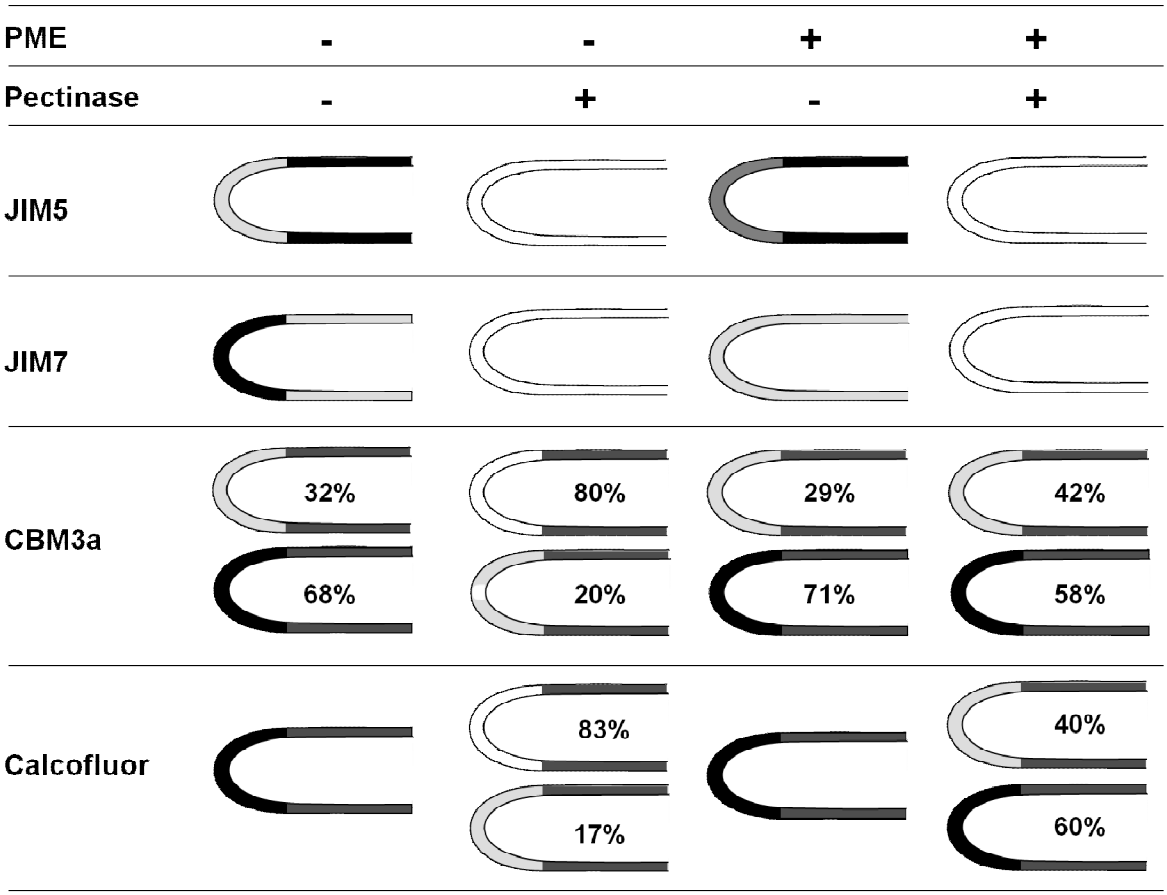

Figure 4.6: Relative fluorescence intensity after enzymatic treatments.

Pollen tubes were subjected to different combinations of enzymatic treatments before (PME) and after chemical fixation (pectinase) and subsequently labeled for pectins and cellulose. The figure summarizes the spatial profiles of relative fluorescence intensities. Black stands for highest label intensity, white for absence of label. Percentage values indicate the size of the two populations if distinct label patterns were observed within individual samples.

Figure 4.7 Distribution of pectins and cellulose after enzymatic treatments (legend on next page)

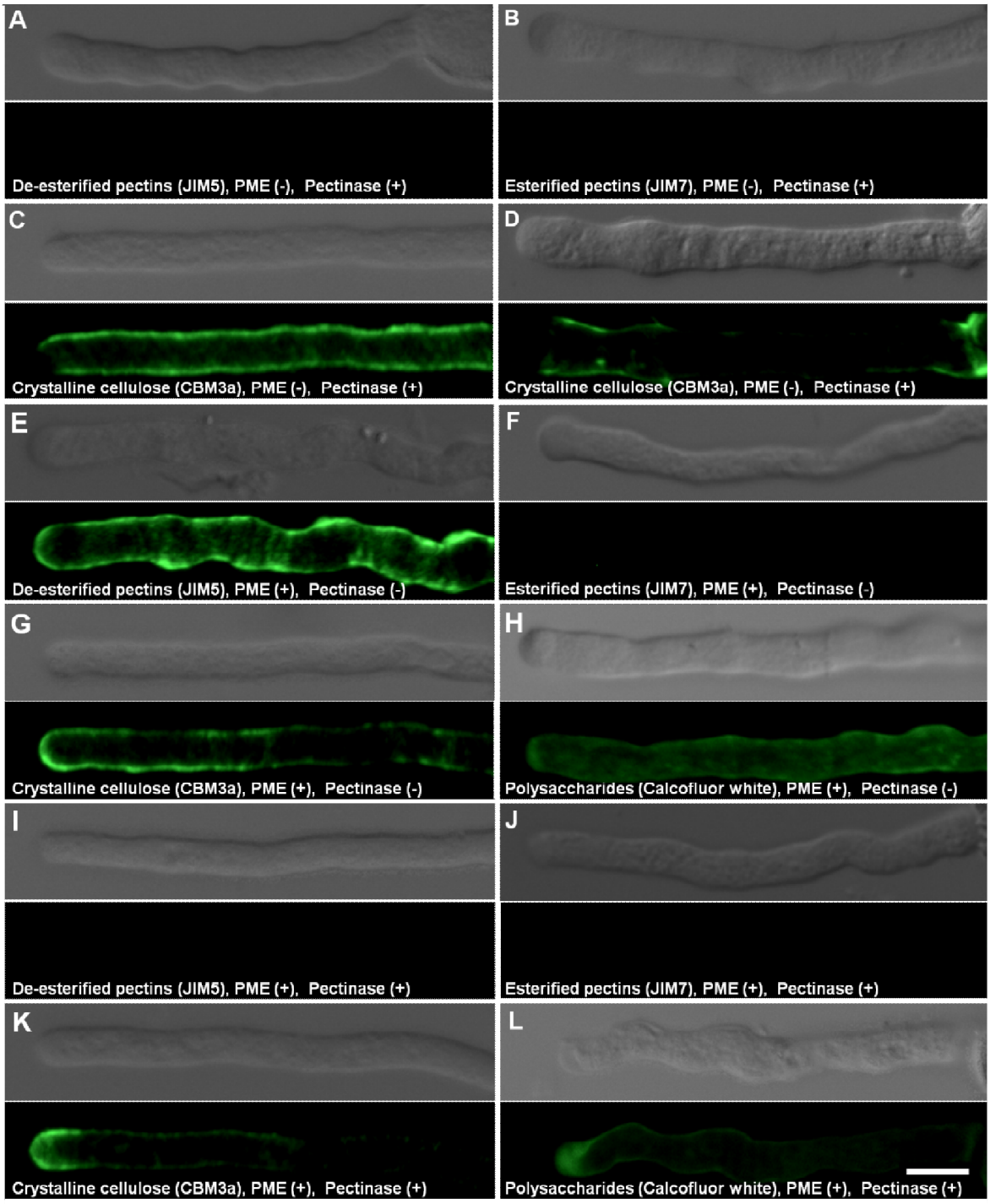

Figure 4.7: Distribution of pectins and cellulose after enzymatic treatments.

As a result of pectinase digestion administered after chemical fixation (A,B,C,D) immunolabel revealed that low (A) and high (B) esterified pectins were digested. Label for crystalline cellulose with CBM3a resulted in two populations of pollen tubes displaying either a small region at the pole devoid of label (C) or an entirely unlabeled apex (D). After treatment of the tubes with PME and subsequent fixation (E,F,G,H), pectins with low degree of esterification (E) were detected along the entire pollen tube length including the apex, whereas label for pectins with high degree of esterification was absent (F). Crystalline cellulose label with CBM3a (G) and microfibril staining with calcofluor white (H) were comparable to the untreated samples. After treatment with PME and pectinase (I,J,K,L), both low (I) and high (J) esterified pectins were digested. Crystalline cellulose label with CBM3a (K) and microfibril staining with calcofluor white (L) were detected in the majority of the tubes. All images were acquired with microscope settings determined to be optimal for the control sample not exposed to enzymatic treatment. Bar = 10 μm.

Figure 4.8

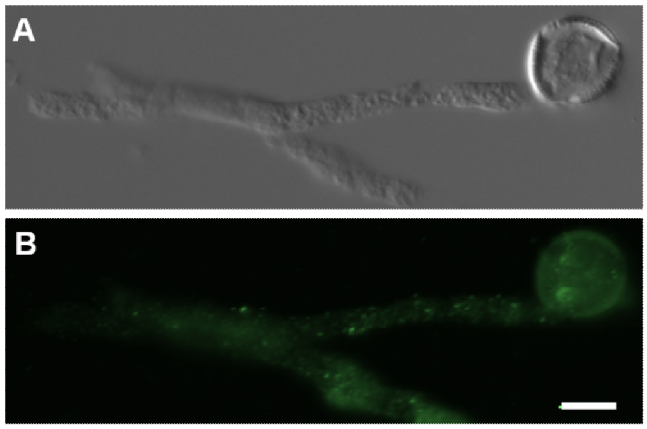

Figure 4.8: Label for crystalline cellulose (CBM3a) in pollen tubes digested with pectinase and lyticase.

(A) DIC image. (B) Crystalline cellulose label was only visible in cytoplasmic compartments. Bar = 10 μm.

Figure 4.9

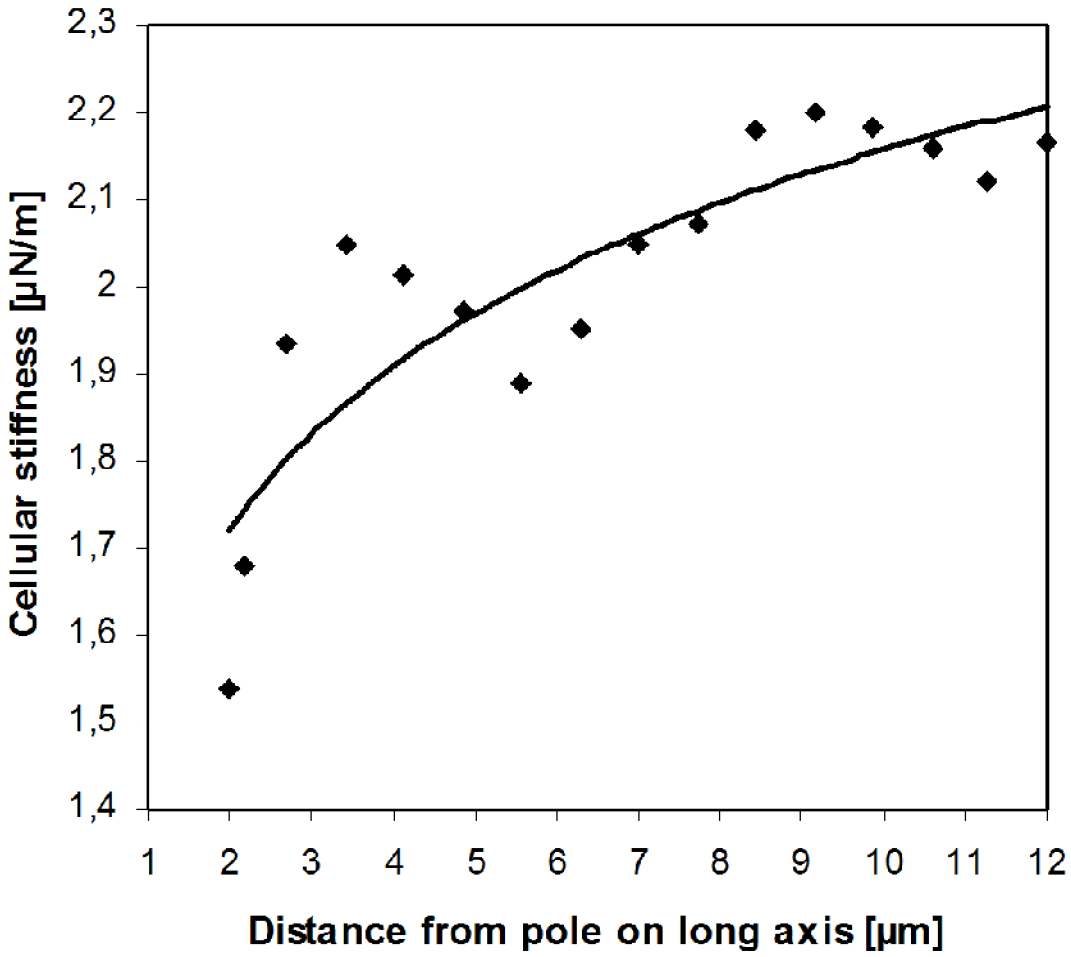

Figure 4.9: Spatial profile of cellular stiffness along the longitudinal axis of the *Arabidopsis* pollen tube.

Stiffness values were acquired with a micro-indenter and are plotted against the distance from the pole measured on the central longitudinal axis.

Figure 4.10 Conceptual model of the assembly and structure of the pollen tube cell wall (legend on next page)

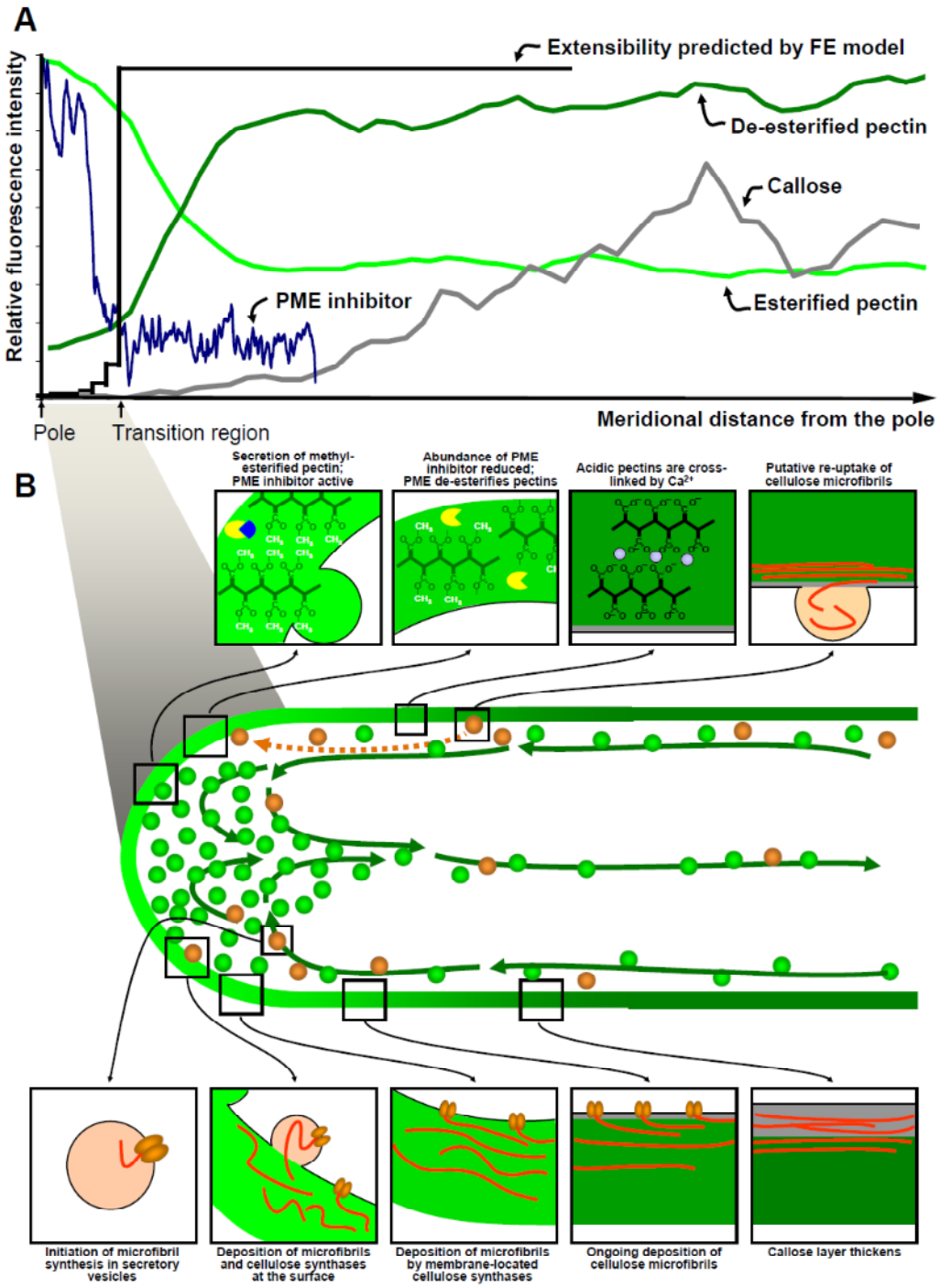

Figure 4.10: Conceptual model of the assembly and structure of the pollen tube cell wall.

Spatial profiles of the relative abundance of cell wall components and cellular stiffness in pollen tubes (A) related to the spatial distribution of assembly and modification processes (B). Highly esterified pectins synthesized in the Golgi apparatus are delivered to the cell wall forming the apical dome (green spheres and arrows). Pectin de-esterification takes place in the shoulders of the apical dome, generating steep, opposite gradients in the abundance of high and low esterified pectins (gradient of green) before reaching a stable level of esterification in the shank (dark green). Curves for pectin and callose are taken from Fig. 1. The gradient in the abundance of PME inhibitor in tobacco pollen tubes (blue curve) quantified from Fig. 4A in (Röckel *et al.* 2008), matches the position of the change in pectin configuration observed in *Arabidopsis* and the increase in Young's modulus (black) predicted by a finite element model for tip growing walled cells (Fayant *et al.* 2010) after normalization for cell size. Crystalline cellulose is found in secretory vesicles (red) and is likely deposited together with cellulose synthases in form of short microfibrils. The abundance of crystalline cellulose in the wall (red lines) decreases slightly towards the distal region of the tube suggesting that they may be recycled by endocytosis (dashed red arrow). Callose (grey) is synthesized at the plasma membrane and is detectable in the distal region only with a steadily increasing abundance. Objects in (B) are not to scale.

4.8 Supplemental data

Supplemental Movie 4.1: VAEM of *Arabidopsis* pollen tube expressing *GFP-CESA6*.

Images were acquired in a focal plane located tangentially at 4 frames.s^{-1} over a period of 50 s and shown here 10x accelerated. The accelerated representation allows to appreciate the movement of the GFP-CESA6 punctae in an orientation near parallel to the longitudinal axis of the tube. Width of the frame equals 21.6 µm.

5 Morphogenesis of complex plant cell shapes - the mechanical role of crystalline cellulose in growing pollen tubes

The shape of the plant cell is regulated by the mechanical properties of its cell wall. In the majority of plant cells, cellulose is the main load bearing component in primary cell walls. In anisotropically growing cells, the orientation of cellulose microfibrils determines the orientation of cell expansion. Pollen tubes are anisotropical growing cells, they only grow at the apical part of the tube by constant addition of plasma membrane and cell wall material precursors. In this paper, we investigate the mechanical role of cellulose during pollen tube growth. With my colleague Leila Aouar, we show that unlike in other cylindrical cells, cellulose does not play a role of the main stress-bearing component against turgor pressure induced tensile stress in the circumferential direction. Rather it seems to play an important role in determining and regulating pollen tube diameter in the sub-apical part of the tube.

I contributed to this paper by preparing and observing the samples to reveal the orientation of the cellulosic microfibrils (Figures 5.1 and 5.2). I also contributed to Figures 5.9 and 5.10 and to the writing of parts of the Material and Methods, Results and Discussion parts of the manuscript.

This manuscript entitled “Morphogenesis of complex plant cell shapes - the mechanical role of crystalline cellulose in growing pollen tubes” was published in 2010 in *Sexual Plant Reproduction* volume 23, issue 1, pages 15-27.

Leila Aouar, Youssef Chebli and Anja Geitmann

5.1 Abstract

Cellulose is the principal component of the load-bearing system in primary plant cell walls. The great resistance to tensile forces of this polysaccharide and its embedding in matrix components make the cell wall a material similar to a fiber composite. In the rapidly growing pollen tube, the amount of cellulose in the cell wall is untypically low. Therefore, we wanted to investigate whether the load-bearing function of cellulose is nevertheless important for the architecture of this cell. Enzymatic digestion with cellulase and inhibition of cellulose crystal formation with CGA 325'615 resulted in the formation of tubes with increased diameter in *Solanum chacoense* and *Lilium orientalis* when present during germination. In pre-germinated tubes, application of both agents resulted in the transient arrest of growth accompanied by the formation of an apical swelling indicating a role in the mechanical stabilization of this cellular region. Once growth resumed in the presence of cellulase, however, the cell wall in the newly formed tube showed increased amounts of pectins, possibly to compensate for the reduced amount of cellulose. Scanning electron microscopy of pollen tubes subjected to digestion of matrix polysaccharides revealed the mechanical anisotropy of the cell wall. In both *Lilium* and *Solanum*, the angle of highest stability revealed by crack formation was significantly below 45°, an indication that in the mature part of the cell cellulose may not the main stress-bearing component against turgor pressure induced tensile stress in circumferential direction.

5.2 Introduction

Plant cell growth and morphogenesis generally entail significant changes in cell shape. To generate a shape other than a sphere, precisely controlled, local expansion and stretching of the cell wall is required, since the driving force - the turgor pressure - is non-vectorial. The requirement for local differences in cell wall mechanical properties becomes particularly evident in cases in which the shape change requires the generation of concave bends such as in star shaped trichomes or astrosclereids. The formation of cellular protuberances necessitates the extreme spatial confinement of growth activity and turgor driven cell wall expansion to a small surface area, whereas the adjacent regions must resist the tensile stress generated by the turgor pressure (Geitmann and Ortega 2009). The cell wall mechanical properties must therefore change significantly within distances on the cell surface as short as few μm. The pollen tube with its characteristic unidirectional mode of growth represents an excellent model system to study the mechanical principles governing monotropic cellular growth (a single, spatially confined site on the cellular surface undergoes expansion) (Holdaway-Clarke *et al.* 2003; Geitmann and Steer 2006; Malhó *et al.* 2006; Wilsen and Hepler 2007; Geitmann and Ortega 2009). Due to its simple cylindrical geometry and its rapid elongation, changes in mechanical parameters are easily quantifiable. The growth rate is correlated with the mechanical properties of the apical cell wall (Zerzour *et al.* 2009) which led to a mechanical model explaining the dynamics of the growth process (Chebli and Geitmann 2007).

To be able to confine turgor driven cell wall expansion to its apex, the pollen tube must exhibit considerable differences in mechano-physical properties of the cell wall between the apex and the shank of the cell (Geitmann and Steer 2006). Quantitative cytomechanical evidence for this mechanical gradient has been provided by micro-indentation (Geitmann and Parre 2004). While much attention has been devoted to the cell wall mechanics of the growing apex, the mechanical properties of the cylindrical shank are of interest as well, since this part of the cell wall needs to resist at least twice as much tensile stress as the apical wall (Geitmann and Steer 2006). Contrary to the apex of the tube which is almost exclusively composed of pectin polymers, the shank is characterized by two or three cell

wall layers containing various cell wall polysaccharides (Heslop-Harrison 1987; Steer and Steer 1989). The outer fibrillar layer is mainly composed of pectins, whereas the inner, secondary layer is callosic and deposited at the plasma membrane surface in the cylindrical shank of the cell (Mascarenhas 1993; Ferguson *et al.* 1998). While distribution and structural roles of pectins and callose in pollen tubes have been investigated in detail (Geitmann and Steer 2006), other cell wall components are poorly characterized in these cells.

Cellulose, a major component in most plant cell walls, is present in uncharacteristically low amounts in pollen tubes (Schlüpmann *et al.* 1994). Depending on the species and method of investigation this polymer has been associated with the outer fibrillar layer or the inner callosic layer (Kroh and Knuiman 1982; Shivanna and Johri 1985; Heslop-Harrison 1987; Ferguson *et al.* 1998). In *Nicotiana tabacum* pollen tubes, visible amounts of cellulose have been detected beginning at 5-15 μm behind the growing tip (Ferguson *et al.* 1998). In plant cells in general, cellulose is deposited in extremely ordered layers in an arrangement that allows the cell to grow and expand by water influx (Lloyd 2006). Since the internal pressure caused by water uptake is a non-vectorial force the orientation of cellulose microfibrils determines the direction of expansion and thus the eventual shape of the growing cell (Green 1962; Emons and Mulder 1998; Kerstens *et al.* 2001; Baskin 2005). The spatial arrangement and orientation of the cellulose microfibrils, therefore, play a central role in plant cytomechanics (Geitmann and Ortega 2009).

In tip growing cells, once the cell wall has become part of the mature, cylindrical region, no expansion of the cell wall in any direction, transverse or longitudinal, is required or desirable. Therefore, the main function of the cell wall in this part of the cell is to provide sufficient tensile resistance to withstand internal turgor pressure. In root hairs, another type of tip growing cell, the geometry of the wall texture is helicoidal where the microfibril orientation changes by a constant angle from one lamella to another (Emons and Mulder 1998) providing inspiration for a theoretical model for the formation of the root hair cell wall (Emons and Mulder 1998; Emons and Mulder 2000). Whether similar principles apply to pollen tubes remains unexplored, since information on the orientation of cellulose microfibrils in this cell type is scarce (O'Kelley and Carr 1954; Sassen 1964; Derksen *et al.*

1999). Since tensile stress in circumferential direction is the biggest stress generated by the turgor in the pollen tube cell wall, we wanted to investigate whether the orientation of cellulose microfibrils indicates a mechanical contribution of this polymer to the mechanical resistance against this stress. We used scanning electron microscopy to study the structure of the cell wall.

We chose pollen of two different angiosperm species, *Solanum chacoense* and *Lilium orientalis*, to allow us to identify common mechanical principles in pollen tubes that *in planta* are exposed to very different mechanical circumstances. The pistils of these two species differ regarding their mechanical resistance to invasion. In lily, a monocot, the style is hollow (Lord 2000) whereas in *Solanum*, a dicot, the style has a solid core of transmitting tissue. Lily pollen tubes, therefore, grow through a presumably soft matrix, whereas *Solanum* pollen tubes need to invade the apoplastic space of the transmitting tissue. From previous studies we know that the composition of the pollen tube cell wall differs between these two species (Parre and Geitmann 2005a) thus offering an excellent opportunity to identify general mechanical principles governing growth.

To manipulate the amount and chemical configuration of cellulose in the cell wall of *in vitro* growing pollen tubes we used two approaches. The herbicide (1-cyclohexyl-5-(2,3,4,5,6-pentafluorophenoxy)-1λ4,2,4,6-thiatriazin-3-amine (CGA 325'615 or CGA) inhibits the synthesis of crystalline cellulose and promotes the accumulation of non-crystalline β-1,4-glucan by causing a disruption of rosette architecture (Kurek *et al.* 2002). The enzyme complex cellulase digests cellulose in two steps, and converts crystalline, amorphous, and synthetic celluloses to glucose.

5.3 Materials and Methods

5.3.1 Plant material

Solanum chacoense plants were grown in the greenhouses of the Montreal Botanical Garden, and *Lilium orientalis* pollen was obtained from a local flower shop. Pollen was dehydrated for 24 h and then stored at -80°C for *Lilium orientalis* and at -20°C for *Solanum chacoense*.

5.3.2 Pollen culture

Pollen was cultured in liquid growth medium containing 100 mg mL^{-1} H_3BO_3, 300 mg $mL^{-1}Ca(NO_3)_2 \cdot H_2O$, 100 mg mL^{-1} KNO_3, 200 mg mL^{-1} $MgSO_4 \cdot 7H_2O$, and 50 mg mL^{-1} sucrose (Brewbaker and Kwack 1963) for *Solanum* pollen and 0.29 mg mL^{-1} MES, 0.01 mg mL^{-1} H_3BO_3, 0.0147 mg mL^{-1} $CaCl_2$, and 50 mg mL^{-1} sucrose for *Lilium* pollen. Approximately 5 mg of pollen was added to 4 ml growth medium placed in 25 ml Erlenmeyer flasks which were incubated at 25°C under continuous slow shaking. Cellulase (Sigma; 6.3 units mg^{-1}; one unit liberates 1.0 µmol of glucose from cellulose in one hour) or CGA 325'615 (generously provided by Syngenta, Basel, Switzerland) were added from stock solutions (Cellulase: 1 and 10% w v^{-1}; CGA: 10mM in DMSO stored at 4°C) either at the beginning of incubation or at various times after germination.

5.3.3 Brightfield observations

Germinated pollen tubes were filtered and subsequently fixed with 3% freshly prepared formaldehyde in Pipes buffer (1 mM EGTA, 0.5 mM $MgCl_2$, 50 mM Pipes) for one hour at room temperature. After fixation pollen was mounted on a microscope slide and observed with differential interference contrast optics in a Nikon TE2000 inverted microscope.

5.3.4 Fluorescence label

For immuno-fluorescence labeling, pollen tubes were filtered and subsequently fixed in 3% freshly prepared formaldehyde and 0.5% glutaraldehyde in Pipes buffer for 30 min. After washing cells were incubated with monoclonal antibodies JIM5 or JIM7 (Paul Knox,

University of Leeds, United Kingdom) diluted 2% in PBS buffer, followed by incubation with goat anti-rat IgG–Alexa Fluor 594 (1% in buffer; Molecular Probes, Eugene, Oregon, USA). JIM5 and JIM7 recognize homogalacturonans with low and high degree of esterification, respectively (VandenBosch *et al.* 1989; Knox *et al.* 1990). Pollen tubes were mounted onto glass slides and observed in a fluorescence microscope using a Texas red filter set. Controls were performed by omitting incubation with the primary or the secondary antibody. Aniline blue and calcofluor white (Fluorescent Brightener 28; Sigma) were used to stain callose and cellulose, respectively, in fixed pollen tubes. After fixation and two washes in buffer, cells were incubated for 15 min with the staining agent (1 mg mL^{-1} aniline blue in 0.15 M K_2HPO_4; 1 mg mL^{-1} calcofluor white in double-distilled H_2O), mounted immediately and observed under UV light excitation.

5.3.5 Fluorescence microscopy

Specimens labeled for cell wall components were observed in a fluorescence microscope (Nikon TE2000) equipped with a Roper FX cooled CCD camera. Images were acquired with ImagePro software (Media Cybernetics). Exposure times of images that had to be compared for fluorescence intensity were identical. Brightness and contrast manipulations of these pictures were only performed uniformly and identically for an entire panel of related images.

5.3.6 Analysis of cell wall anisotropy

Pollen tubes were germinated for 3 h, fixed in a microwave oven (PELCO BioWave 34700 equipped with a cold spot) operating at 150 W twice for 45 sec in Pipes buffer containing 2% formaldehyde and 0.5% glutaraldehyde, and subsequently washed five times with Pipes buffer for 40 sec at 150 W. Pollen tubes were then subjected to enzymatic digestion for 24 h in a 20 $mg.mL^{-1}$ pectinase (pectinase from *Aspergillus niger*, Fluka) solution under constant shaking (110 rpm). Samples were then thoroughly washed with PBS buffer and digestion was repeated for another 24 h followed by washes with PBS buffer. Each sample was subsequently devided in two to be processed for scanning electron microscopy and fluorescence microscopy in parallel.

For electron microscopy, samples were dehydrated through a graded ehtanol series, critical point dried, mounted, and double sputtercoated with gold and palladium. Observations were performed with a FEI Quanta 200 3D microscope operating at 20 kV.

For fluorescence label of cell wall components, samples were incubated 45 min in PBS buffer containing 3.5% bovine serum albumine (BSA) prior to incubation for 30 min with a mixture of 2% JIM5 and 2% JIM7 monoclonal antibodies. After three washes samples were incubated with 1% goat anti-rat IgG–Alexa Fluor 594 (Molecular Probes, Eugene, Oregon, USA) and washed thrice. Subsequently, samples were incubated for 30 min with 1 mg mL^{-1} calcofluor white (Fluorescent Brightener 28; Sigma) in double-distilled water and washed three times. Observations were done with a Zeiss Imager-Z1 microscope equipped with structured illumination microscopy (ApoTome Axio Imager), a Zeiss AxioCam MRm Rev.2 camera and AxioVision Release 4.5 software. For calcofluor label, a filter set with excitation BP450-490 nm, beamsplitter FT 510 nm and emission BP 515-565 nm was used. For Alexa fluor 594 detection the filter set comprised an excitation BP 390/22 nm, beamsplitter FT 420 nm and emission BP 460/50 nm. Exposure times were adjusted to 600 msec for pectin (Alexa fluor 594) observation and 10 msec for cellulose (calcofluor white) observation. ApoTome Imager was then inserted and z-stacks of 1µm interval were acquired. Image reconstruction was performed using the AxioVision software by the projection of the stacks.

5.4 Results

5.4.1 The net orientation of cellulose microfibrils is not transverse

The orientation of microfibrils in plant cell walls is often investigated using field emission scanning electron microscopy. However, the drawback of this approach is that only the innermost or outermost (depending on the angle of view) microfibrils of the cell wall are visible. Furthermore, orientation has to be quantified for each individual microfibril. However, rather than studying individual microfibrils, we were interested in the overall mechanical behavior of the pollen tube cell wall. Hence, the overall orientation of the entire population of anisotropy conveying polymers through the complete thickness of the wall

layer is relevant. To assess this overall behavior we exploited the mechanical principles of composite materials. It is known that cracks and fractures in anisotropic composite materials are oriented parallel to the main fiber orientation (Jones 1999). Identification of the fracture angle is, therefore, an excellent indicator of the direction of material anisotropy in a fiber reinforced composite material.

To induce cracks in the cellulose containing cell wall layer we first removed the pectic outer layer by treating chemically fixed tubes with pectinase. Prior to enzyme treatment, the surface of the pollen tube appeared to be relatively uniformly patterned with small wrinkles in arbitrary orientation (Figs 5.1a, 5.2a). Pectinase digestion exposed a relatively smooth layer that contained cracks, likely induced during critical point drying. The main orientation of these cracks had a pitch of approximately 20-25° (*Lilium*) or 15-20° (*Solanum*) to the longitudinal axis of the cell (Figs 5.1b, 5.2b). Both left- and right-handed pitch orientation was observed.

To confirm that the enzymatic digestion had removed pectin, but not cellulose, we performed fluorescence label for both components on the same batch of cells that had been used for scanning electron microscopy. While both pectin and cellulose are labeled in non-digested tubes (Fig 5.1c,e, 5.2c,e), only cellulose is visible in pectinase digested tubes (Figs 5.1d,f, 5.2d,f).

5.4.2 Cellulase affects pollen tube germination and growth differently in *Lilium* and *Solanum*

In order to germinate, the cell wall at the pollen grain aperture needs to yield to the pressure generated by water uptake into the hydrating cell. The same mechanical principle applies to pollen tube growth during which the apical cell wall needs to yield continuously. While giving way to the hydrostatic pressure, the wall must not undergo failure and rupture. Precise control of the tensile resistance in the cell wall to the internal pressure is therefore essential. If cellulose was involved in the tensile resistance withstanding the force exerted on the aperture cell wall by the turgor, its partial digestion should facilitate germination whereas its complete digestion would be expected to cause bursting. To test this we complemented the germination medium with various concentrations of cellulase and

quantified the germination rate after 2h. At enzyme concentrations up to 0.6%, the germination rate was not significantly altered in either species (not shown) at higher concentrations the grains tended to burst, however.

To assess the effect of cellulase on pollen tube growth we quantified the length of pollen tubes formed in the presence of the enzyme at 2h after incubation. In *Lilium* 0.1% cellulase caused an increase in the length of pollen tubes whereas higher enzyme concentrations resulted in a decrease (Fig 5.3). At 0.5%, 90% of *Lilium* tubes had burst. Growth of *Solanum* pollen tubes was affected differently as no stimulation was observed at the concentrations tested. Pollen tube length was reduced slightly above cellulase concentrations of 0.4% (Fig 5.3a). Bursting started only at 1% or higher concentrations of the enzyme.

5.4.3 Cellulose is implicated in determining the pollen tube diameter

Turgor pressure is a non-vectorial force and, therefore, it acts not only on the cell wall in the growing tip but also on the maturing portions forming the cylindrical shank of the pollen tube. We wanted to test whether cellulose is involved in resisting the tensile stress generated by the turgor pressure in the cylindrical part of the pollen tube. To this end we measured the diameter of pollen tubes grown in the presence of cellulase. For consistency, the diameter was always measured in the region 20-30 μm from the tip. Measurements were taken 2 (*Lilium*) or 4 hours (*Solanum*) after germination. In both species the presence of the enzyme resulted in formation of pollen tubes with increased diameter. In *Lilium*, this effect was visible starting at 0.2% cellulase whereas in *Solanum* only concentrations above 0.5% were effective (Fig 5.3b). Higher concentrations were not assessed since the percentage of burst pollen tubes or grains became significant.

5.4.4 The effects of cellulase addition on pre-germinated pollen tubes

When inhibitors or enzymes were administrated starting prior to germination, the pollen tube had time to adapt to the situation from the time of germination. Therefore, we wanted to assess how tubes germinated under control conditions would react to the addition of cellulase. We used the enzyme concentration that resulted in increased pollen tube length

when applied prior to germination (0.1%) and administered it to pre-germinated *Lilium* pollen tubes at 3h after germination. Pollen tubes were fixed after additional 2h growth in the presence of the enzyme. In 80% of the tubes, the time point of enzyme addition was marked by a local swelling from which a new tubular outgrowth had been formed (Figs 5.4, 5.5). In numerous cases the outgrowth occurred at an angle of approximately 90° to the initial direction of growth (Figs 5.4a, 5.4d, 5.5b). In some cases the outgrowth formed slightly behind the apical swelling (Figs 5.4d, 5.5b). The new outgrowths produced a cylindrical protrusion of the same or slightly smaller diameter than that of the original tube. The diameter of the tube portion grown during pre-germination was not altered by the enzyme treatment with 18.7 ± 0.9 µm compared to the control tubes measuring 18.0 ± 1.4 µm.

For *Solanum chacoense*, no growth stimulating cellulase concentration had been established. We applied 1.5% to pre-germinated tubes, since lower concentrations did not cause any visible effect on most tubes. Addition of 1.5% cellulase or higher concentrations caused *Solanum* pollen tubes to exhibit similar phenomena as *Lilium* pollen tubes treated with 0.1% cellulase. The time points of enzyme addition were marked by local swellings and new outgrowths which frequently originated at angles up to 90° from the original growth direction (Fig 5.6). In addition, we observed numerous cells that were not able to form a new outgrowth but continued growing with a large diameter thus forming a bulbous shape at their apex (Fig 5.6f). In these cells, the length of the tube portions formed during the 2h period following enzyme addition was very limited indicating that growth proceeded extremely slowly or arrested completely.

5.4.5 Cellulase treatment leads to an increased deposition of other cell wall components

The formation of new outgrowths that proceeded to grow with regular cylindrical morphology despite the presence of cellulase led us to hypothesize that the pollen tube must somehow compensate for the lack of cellulose. Therefore, we used fluorescence label to investigate the composition of the cell wall in the parts of the pollen tube formed before and after enzyme addition. Label for cellulose in cellulase treated cells was not visibly altered

or slightly weaker in the older parts of the tube, but significantly lower in the outgrowths formed after addition of the enzyme (Figs 5.5a-c). The weak effect of cellulase application on cellulose label in the older portion of the tube could be due to reduced accessibility of microfibrils to the enzyme because of an abundance of matrix components in this part of the cell.

Label for callose was unaffected by cellulase administration in both the portions grown before and after administration of the enzyme (Figs 5.5d,e). Remarkably, pectin label showed a significant increase in fluorescence intensity in parts grown after the onset of cellulase treatment in both *Lilium* and *Solanum* (Figs 5.4, 5.6f). Pectin label intensity was significantly higher in the outgrowth compared with the corresponding regions on control tubes. Notably, even label for pectins with low degree of esterification that is usually stronger in the distal part of the tube, was significantly elevated in the outgrowth compared to the older part of the same tube (Fig. 5.4e).

5.4.6 Inhibition of cellulose crystal formation affects pollen tube cell wall mechanics

Crystal formation is crucial for the mechanical properties of cellulose. In order to demonstrate that this feature is essential for the mechanics of pollen tube growth, we assessed the effect of the inhibitor of cellulose crystallization CGA. The presence of the drug during pollen germination and tube growth resulted in the formation of tubes with increased diameter (Fig 5.7) but did not affect the average length of the cells (not shown). In *Solanum* pollen tubes this effect was particularly prominent at 100 nM, whereas in *Lilium* the biggest diameter was observed at a drug concentration of 100 µM (Fig 5.7). Whereas at 100 µM all *Solanum chacoense* pollen tubes burst soon after germination, *Lilium orientalis* tubes resisted much higher concentrations of CGA and only burst at 10 mM CGA.

To determine the effect of CGA on pre-germinated pollen tubes, lily pollen germinated under normal conditions for 2h were treated with various concentrations of the inhibitor. At 50 µM, the cells changed their growth direction and showed irregularities in the tube diameter (Fig 5.8a,b). At 100 µM, pollen tube growth was inhibited and apical swelling

occurred. However, the growth arrest was reversible. After rinsing with growth medium lacking the inhibitor, growth was re-established albeit with reduced rates (not shown).

5.5 Discussion

5.5.1 Despite low abundance cellulose plays a role in pollen tube cell wall mechanics

Plant cell walls provide structure to the cell they surround. Depending on the chemical composition they have the ability to resist tensile and compressive stresses thus ensuring structural and mechanical support. By determining not only the shape but also the growth direction of the cell, the wall plays a key role in plant development and survival (McCann and Roberts 1991). Because of their high tensile resistance, cellulose microfibrils play a crucial role in the architecture of the cell wall (Green 1962; Emons and Mulder 1998; Kerstens *et al.* 2001; Baskin 2005; Geitmann and Ortega 2009). In the tip growing pollen tube the abundance of cellulose is untypically low compared to other cells with primary walls (Schlüpmann *et al.* 1994). Nevertheless, interfering with cellulose synthesis affects pollen tube growth. Inhibitors such as 2,6-dichlorobenzonitrile (DCB), an effective and specific inhibitor of cellulose synthesis, cause pollen tubes of *Lilium auratum* and *Petunia hybrida* to rupture or assume a distorted-bulbous shape (Anderson *et al.* 2002). Disrupting cellulose synthesis by isoxaben causes tip swelling and disorganizes cortical microtubules in elongating conifer pollen tubes resulting in a reduction in growth (Lazzaro *et al.* 2003). Our results with cellulase and CGA are consistent with these data. Tubes burst upon addition of high concentrations of these agents, indicating that digesting cellulose or preventing its crystal formation destabilizes the cell wall sufficiently for it to give way to the turgor pressure and rupture.

5.5.2 Pollen tube sensibility to cellulose affecting drugs and enzymes differs between *Lilium* and *Solanum*

Comparison of the data obtained for *Lilium* and *Solanum* pollen tubes reveals that pollen from the two species have very different sensitivities towards cellulase and CGA. While the

germination rate was unaffected by these agents, pollen tube length at 2 hours was increased in lily pollen tubes in the presence of optimal concentrations of cellulase. This might in part be due to a reduction in the time necessary for the germinating tube to pierce the pollen grain aperture resulting from a softening of the cell wall in the intine. The absence of this effect in *Solanum* is consistent with the fact that no visible cellulose depositions are present in the aperture of the *Solanum* pollen grain, whereas cellulose label is intense at the aperture of the lily pollen grain (Parre and Geitmann 2005a).

The cellular diameter of both *Solanum* and *Lilium* pollen tubes was increased by the presence of cellulase in the growth medium. This indicates that cellulose plays a role in resisting against the tensile stress generated in the cell wall by the internal turgor pressure. The effect of the enzyme on *Solanum* pollen tubes was rather small, however, thus indicating that in this species resistance against circumferential tension stress does not rely to a great degree on the presence of cellulose. It was therefore surprising to note that CGA had a much more pronounced effect in *Solanum* than in *Lilium* pollen tubes causing an increase of the tube diameter by approximately 30% at concentrations that were ineffective in *Lilium* pollen tubes. Nevertheless, *Lilium* pollen tubes were not immune against the effect of the inhibitor as their diameter was affected at higher concentrations of the agent. These data confirm that despite its low abundance and differences between species, cellulose in its crystalline form is required to establish a mechanical resistance against circumferential tension stress in the pollen tube cell wall. Differences in sensitivity towards enzyme degradation and inhibitor action between the two species could be explained by different amounts of cellulose within their walls, by different accessibility of microfibrils to the enzyme due to the presence of cell wall matrix components, by different sensitivity of the cellulase rosettes towards the drug, or by the possible structural function of amorphous cellulose that is purported to be formed in the presence of CGA. Further experimental evidence of the relative composition in crystalline and amorphous cellulose in the two species in the presence of the inhibitor is warranted to find the answer to this question.

5.5.3 Growing pollen tubes can compensate for the lack of cellulose with the overproduction of pectin

Pollen tubes were able to resume growth after undergoing a transient arrest upon addition of moderate concentrations of cellulase. To our surprise, even in the continuous presence of the enzyme, the new outgrowth generally had a diameter similar to that of the older part of the cell. Reduced label for cellulose in the newly formed tube confirmed that the enzyme remained active, however. Remarkably, the amount of pectin in the cell walls of the new outgrowths was significantly increased. It is unclear whether this was simply a default consequence of an altered balance between growth rate (slightly reduced) and the rate of pectin deposition (unaltered), or whether the phenomenon resulted from an active change in this balance, i.e. an increase of pectin deposition per cell length. In the latter case the data would indicate that the cell is able to perceive the lack of cellulose and to compensate for it by overproducing another cell wall component with tensile stress resistance capacity. A change in cell wall composition in pollen tubes exposed to mechanically challenging situations had been observed previously (Parre and Geitmann 2005a), even though in that case callose deposition was increased. This astonishing ability of plant cells to regulate their mechanical properties despite the lack of an essential building component has been shown previously in other systems. Primary cell walls of Korrigan, a dwarf mutant of *Arabidopsis* deficient in a membrane-bound endo-1,4-β-glucanase, show an increase in homogalacturonan epitopes and a decrease in cellobiohydrolase I-gold labeling (His *et al.* 2001). Likewise, suspended tomato cells grown on 2,6-dichlorobenzonitrile (DCB) a cellulose synthesis inhibitor, can divide and expand despite the absence of a cellulose-xyloglucan network (Delmer 1987; Delmer *et al.* 1987). Tomato cells that contain markedly reduced levels of cellulose show a significant enrichment in pectic polymers and reduced levels of xyloglucan in their cell wall extractions (Shedletzky *et al.* 1992). This shows that plant cells possess the flexibility to tolerate alterations in cell wall composition (Shedletzky *et al.* 1990) and to compensate for the lack of one component with the overproduction of another. Our data are consistent with this principle. This raises the question how a plant cell perceives the lack of one particular component, or, more generally, the lack of mechanical

stability. While our data do not allow to distinguish, whether pectin synthesis and deposition are upregulated, or whether slower growth allows for more deposition of the polymer per unit cell length, the augmented amount of pectins per surface unit is clearly sufficient in re-establishing the relationship between cell wall and turgor since the stable cellular diameter remains almost unaltered and the newly formed tube is perfectly cylindrical.

5.5.4 Cell wall anisotropy and the mechanics of cellular growth

In cells growing diffusely, the orientation of cellulose microfibrils is known to determine the direction of cell expansion (Baskin *et al.* 1999; Sugimoto *et al.* 2000) since it defines mechanical anisotropy in the cell walls (Burk and Ye 2002; Suslov and Verbelen 2006). Since cellulose microfibrils are highly resistant to tensile stress, cellular expansion takes place in the direction perpendicular to the net orientation of microfibrils, which therefore control cellular morphogenesis (Green 1962). In pollen tubes, cell wall expansion takes place exclusively in the apex (Fig 5.9a). The distal, mature region needs to be stabilized against the tensile stress generated by the turgor pressure but there is no need for a mechanism of controlled yielding in this region. Callose is likely to be responsible in part for this stabilizing function (Parre and Geitmann 2005a), but cellulose might play a role as well.

The most efficient orientation of cellulose microfibrils for reinforcing the cell wall against circumferential tensile stress would be a hoop-shaped orientation perpendicular to the long axis (Fig 5.9b). In *Petunia* pollen tubes, in the subapical region microfibril orientation was indeed described to be preferentially perpendicular to the longitudinal axis. However, the microfibrils in the shank are oriented with a preferential angle of +45° and -45° (Sassen 1964) (Fig 5.9c);. Similar findings were made in pollen tubes of *Pinus* (Derksen *et al.* 1999). Our studies show that the cell wall of *in vitro* grown pollen tubes displays a mechanical anisotropy with a pitch of approximately 15 to 20° for *Solanum* and 20 to 25° for *Lilium* to the long axis (Fig 5.9d). These angles are clearly very different from the theoretically optimal value of 90° and suggests that cellulose does not play an important mechanical role in reinforcing the distal, cylindrical part of the pollen tube against tensile

stress in circumferential direction. The rather longitudinal orientation might suggest, however, that microfibrils confer mechanical resistance to the tensile stress present in longitudinal direction. The pollen tube's way of life illustrates why this might be of importance. Similar to other tip growing cells, the biological purpose of pollen tubes is the invasion of another tissue. The efficiency of the invasion process is maximized by reducing the friction with the surrounding medium. This is achieved by focusing the growth activity to the apical region. Any cell wall expansion of the cylindrical shank in longitudinal direction would result in friction and is thus not desirable. Maybe the low pitch helical arrangement of cellulose microfibrils in the shank is indicative of the importance of prevention of expansion in longitudinal direction.

5.5.5 The pollen tube diameter is determined in the subapical region

The collar region adjacent to the hemisphere-shaped tip is likely to be the mechanically most crucial part of the pollen tube cell wall. Here the tensile stress in maturing cell wall achieves its maximum value due to the shape change from approximately hemispherical to cylindrical, as can be calculated applying the laws of thin pressure vessels and as is observed experimentally (Dumais *et al.* 2004; Geitmann and Steer 2006). A section of cell wall surface that moves from the apex to the cylinder experiences increasing stress in circumferential direction reaching a maximum upon becoming part of the cylinder (Fig 5.10a). At the same time, compared to the rest of the cylinder where increasing cellulose and later callose deposition occurs, this initial cylinder region is likely to be the least stable (Fig 5.10b). A disturbance of cellulose abundance (by cellulase digestion) or structure (by CGA inhibition) therefore changes the resistance to stress in this area (Fig 5.10c) and thus affects cellular diameter. As a consequence, this can lead to the irregular diameter, swelling and/or the formation of an outgrowth observed under the influence of cellulase and CGA (Fig 5.10d). If the pollen tube is grown continuously in the presence of the inhibitor, the tube diameter is consequently changed over its length.

The reason why expansion growth can occur at the growing apex of a pollen tube despite the geometry-induced lower tensile stress in this region is the high degree of cell wall deformability at the tip. A transient arrest of growth induced by a disturbance of the force

equilibrium due to treatment with moderate concentrations of enzyme or inhibitor will probably allow the apical cell wall to rigidify (due to ongoing pectin de-esterification and gelation). As a consequence, a new outgrowth will not form from the pole of the apex, but from the region experiencing the highest tensile stress, the collar region between apex and shank (Fig 5.10d).

It is interesting to note that despite the differences in sensitivity towards cellulase and CGA, pollen tubes of both species, *Lilium*, and *Solanum*, react essentially in a similar manner. They show apical swellings, new outgrowths, and the ability to compensate for the lack of cellulose by depositing higher amounts of pectin. The orientation of the mechanical anisotropy of the cell wall is not even close to hoop configuration, thus confirming that despite considerable evolutionary distance, different growth conditions, and significant differences in cellular morphology, the mechanical principles of pollen tube growth are conserved.

5.6 Conclusions

The orientation of microfibrils in net longitudinal direction is not consistent with a crucial role for mechanical resistance to tensile stress in the cylindrical part of the pollen tube. This corroborates experimental data obtained with the inhibitor DCB (Anderson *et al.* 2002). The situation is different in the subapical region of the pollen tube, however. Here, an increased deposition of pectin is the consequence of an artificial reduction in the amount of cellulose. While this maybe simply a default result, it could also be an active, compensatory mechanism. Prior to the formation of a new outgrowth, the subapical region of the pollen tube is strongly affected by the agents interfering with cellulose mechanics as shown by swellings and irregular growth. As callose is not present in this subapical region, cellulose microfibrils might actually play an important mechanical role here. The transition region between hemisphere shaped apex and cylindrical shank is crucial for pollen tube morphology as the diameter of the tube is determined here and tensile stress in the maturing cell wall reaches its maximal value. Cellulose could thus play an important role by influencing the diameter of the growing cell. This is a crucial function as the diameter of pollen tubes needs to be optimized between the following constraints: *i)* a minimum

diameter must be maintained to allow the male germ unit to pass through the tube and *ii)* the smaller the cellular diameter, the easier it is for the tube to penetrate the transmitting tissue. The latter is based on fracture theory which states that the smaller the width of a crack, the bigger is the stress on the material that enables the propagation of the crack. In addition, a smaller tube will have a smaller surface on which friction with the surrounding surface occurs thus reducing the amount of mechanical work associated with invasive growth. The diameter of the pollen tube, therefore, represents a compromise between these two mechanical requirements and thus presumably requires to be tightly controlled.

To better understand this putative mechanical function of cellulose in the subapical region of growing pollen tubes, it will be essential to precisely quantify the abundance and orientation of microfibrils in this part of the cell, an approach that requires the development of new experimental protocols. It would be important to localize cellulose synthases and to find out whether they are actually actively producing cellulose as close to the tip as is suggested by the presented data. Also, the analysis of mutants affecting cellulose synthase functioning might be promising in this context.

5.7 Acknowledgements

Work in the Geitmann lab is supported by grants from the Natural Sciences and Engineering Research Council of Canada (NSERC), the *Fonds Québécois de la Recherche sur la Nature et les Technologies* (FQRNT), and the Human Frontier Science Program (HFSP). The authors would like to thank Louise Pelletier for technical assistance with the scanning electron microscope and Jens Kroeger for discussions about physico-mechanical considerations. Thanks to Jean Wenger (Syngenta, Basel, Switzerland) for the gift of CGA and to Paul Knox, University of Leeds, Great Britain, for the antibodies JIM5 and JIM7.

5.8 Figures

Figure 5.1

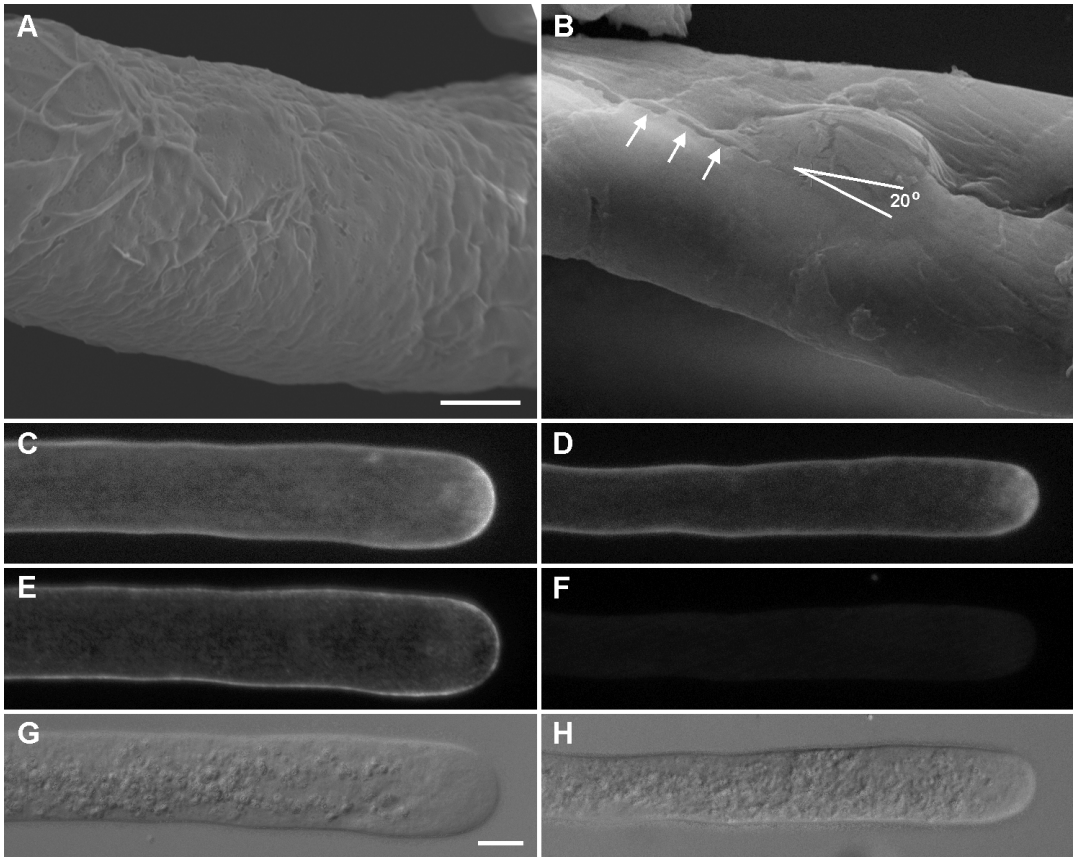

Figure 5.1: Mechanical anisotropy of cell wall mechanics in *Lilium* pollen tubes.

A. Scanning electron micrograph of a control tubes reveals slight waviness of the cell wall surface representing the structure of the outer pectin layer. **B.** Pectinase digestion after chemical fixation reveals a smooth inner layer displaying cracks (arrows) caused by critical drying. Cracks typically have a pitch of 20 to 25° to the longitudinal axis of the cell. Both right- and left-handedness were observed. **C-F.** Fluorescence label for callose (**C,D**) and pectins (**E,F**) of control (**C,E**) and pectinase treated (**E,F**) tubes demonstrating that the enzyme treatment completely removed the pectin moiety of the cell wall while leaving cellulose intact. **G, H.** Brightfield micrographs of the pollen tubes shown in C, E and D, F, respectively. Bars = 5 µm (**A, B**), 10 µm (**C-H**).

Figure 5.2

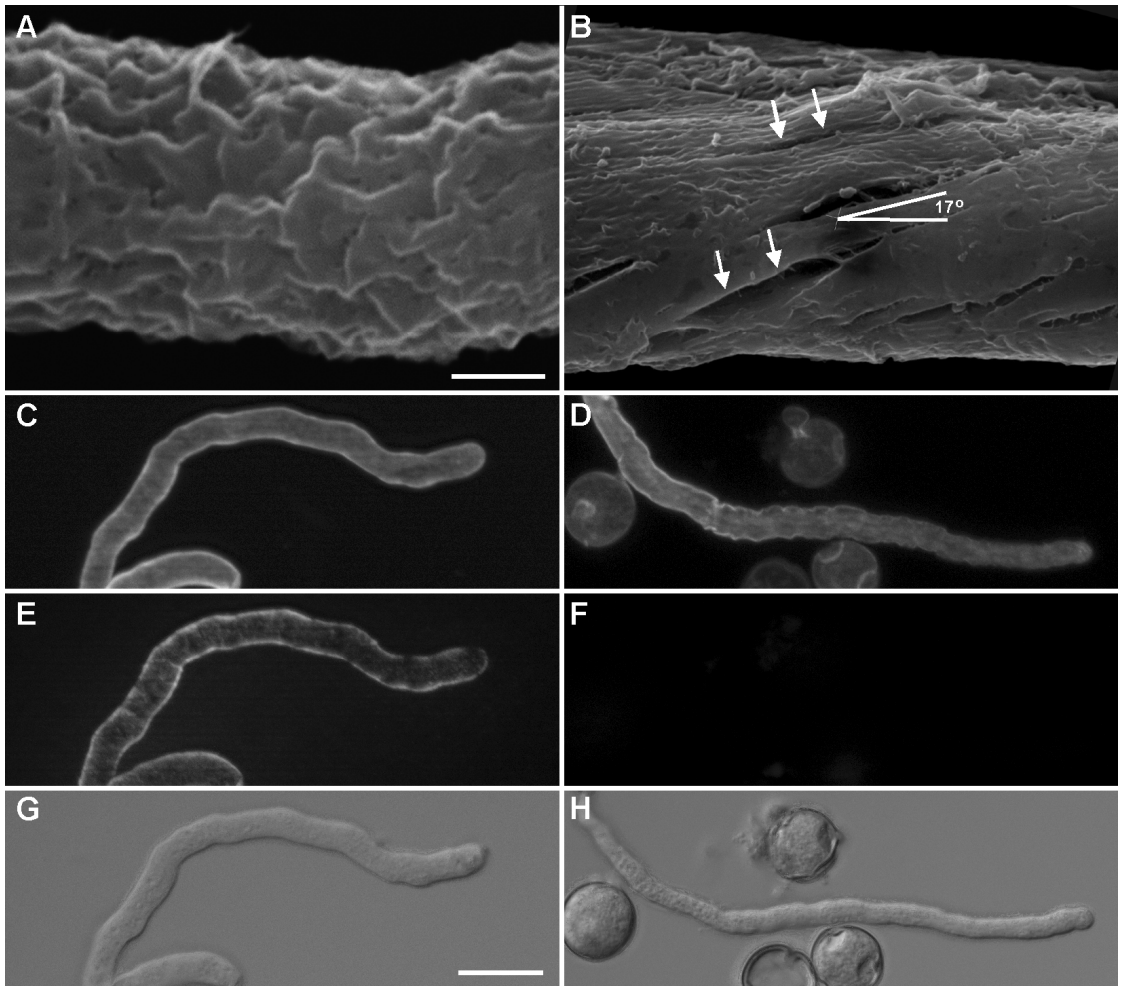

Figure 5.2: Mechanical anisotropy of cell wall mechanics in *Solanum* pollen tubes.

(A) Scanning electron micrograph of a control tubes reveal waviness of the cell wall surface representing the structure of the outer pectin layer. (B) Pectinase digestion after chemical fixation reveals a smooth inner layer displaying cracks (arrows) caused by critical drying. Cracks typically have a pitch of 15 to 20° to the longitudinal axis of the cell. Both right- and left-handedness were observed. (C-F) Fluorescence label for callose (C,D) and pectins (E,F) of control (C,E) and pectinase treated (E,F) tubes demonstrating that the enzyme treatment completely removed the pectin moiety of the cell wall while leaving cellulose in place. G, H. Brightfield micrographs of the pollen tubes shown in C-F. Bars = 3 µm (A, B), 20 µm (C-H).

Figure 5.3

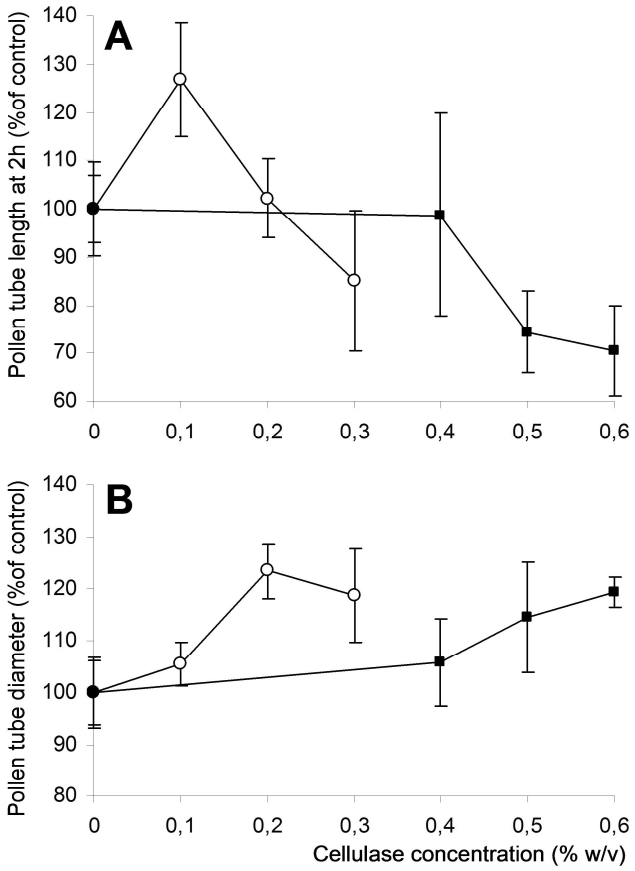

Figure 5.3: Effect of cellulase on pollen tube length and diameter measured 2h after germination for *Lilium* and 4h for *Solanum*.

Effect of cellulase on pollen tube length (A) and diameter (B) measured 2h after germination for *Lilium* (○) and 4h for *Solanum* (■). Data are plotted as percentage of the control values (Control values for pollen tube length: 571.7 µm (*Lilium*), 159.6 µm (*Solanum*); Control values for pollen tube diameter: 17.3 µm (*Lilium*), 6.8 µm (*Solanum*)). Data are from three repeats of the experiment with n = 50, vertical bars are standard deviations.

Figure 5.4

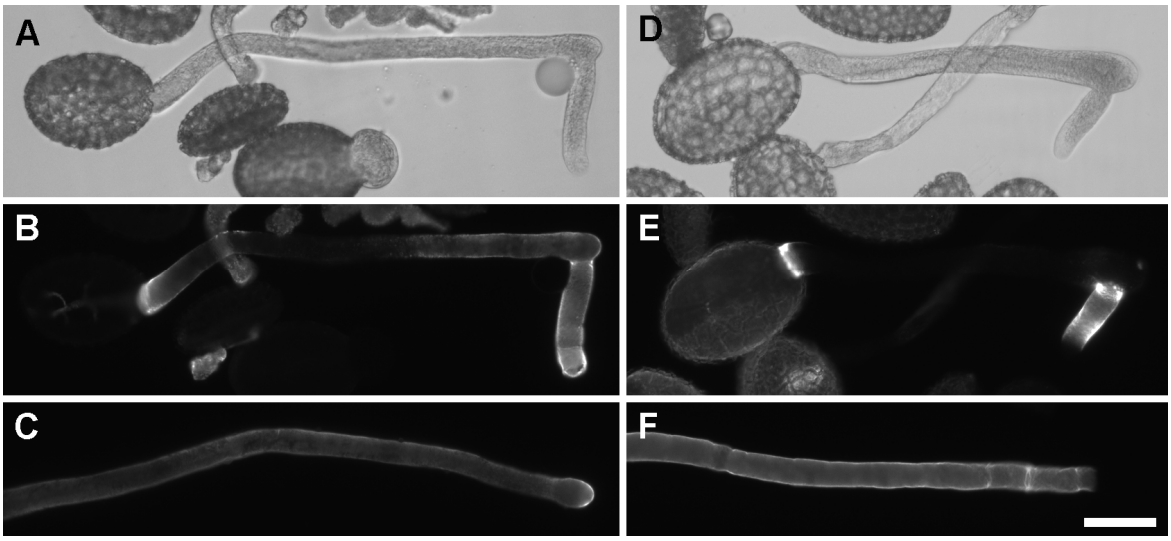

Figure 5.4: Fluorescence label of *Lilium orientalis* pollen tubes for pectins.

(A-C) Label with monoclonal antibody JIM7 for pectins with high degree of methyl-esterification. (D-F) Label with monoclonal antibody JIM5 for pectins with low degree of methyl-esterification. A and D are brightfield images of tubes in B and E, respectively. Pre-germinated pollen tubes were treated with 0.1% cellulase (A,B,D,E) or boiled enzyme (C,F). Upon addition of the functional enzyme the pollen tube transiently arrested growth and a new outgrowth was formed in a different direction. Bar = 50 µm.

Figure 5.5

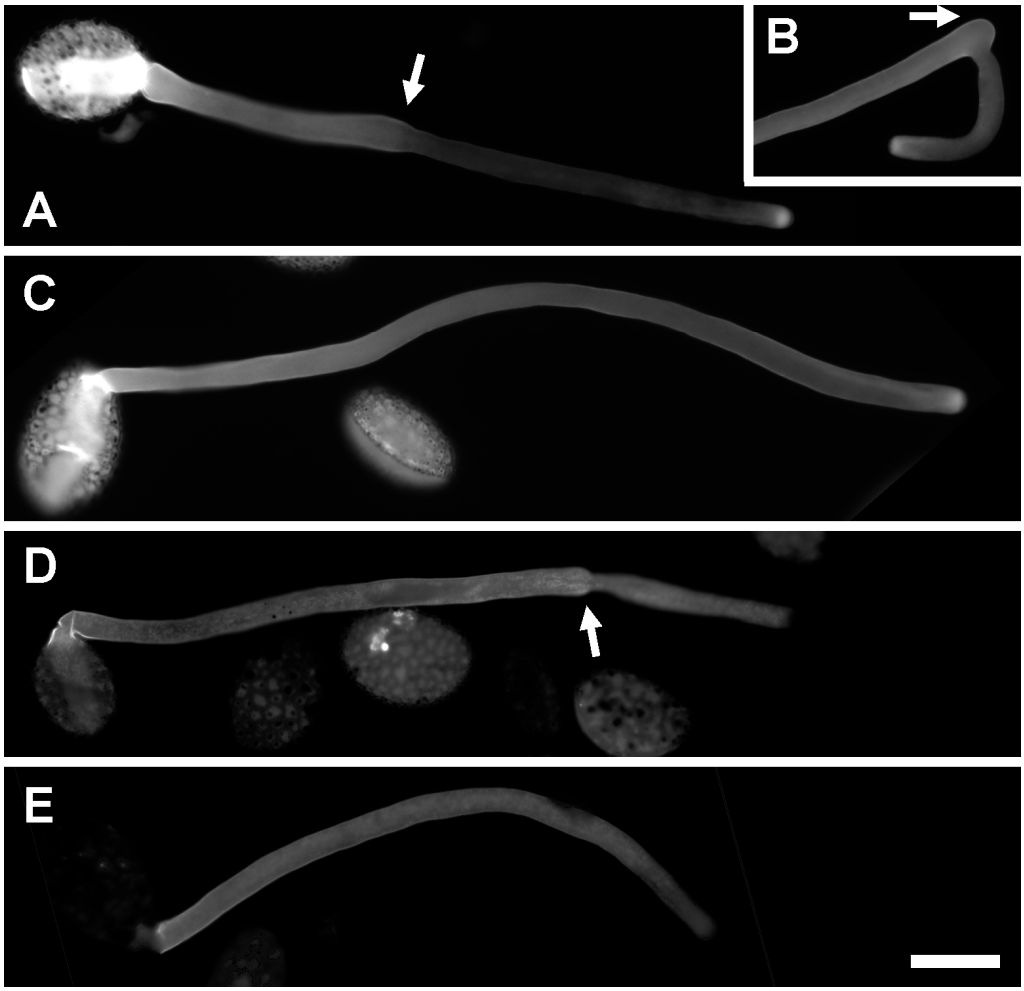

Figure 5.5: Fluorescence label for cellulose and callose in *Lilium orientalis* pollen tubes.

(A-C) Calcofluor white label for cellulose. (D,E) Aniline blue label for callose. Pre-germinated pollen tubes were treated with 0.1% cellulase (A,B,D) or boiled enzyme (C,E). The arrow indicates the length of the pollen tube at the time of application of the active enzyme. Cellulose label decreased significantly in tube portions grown after cellulase application, whereas callose label is not visibly affected. Bar = 50 µm.

Figure 5.6

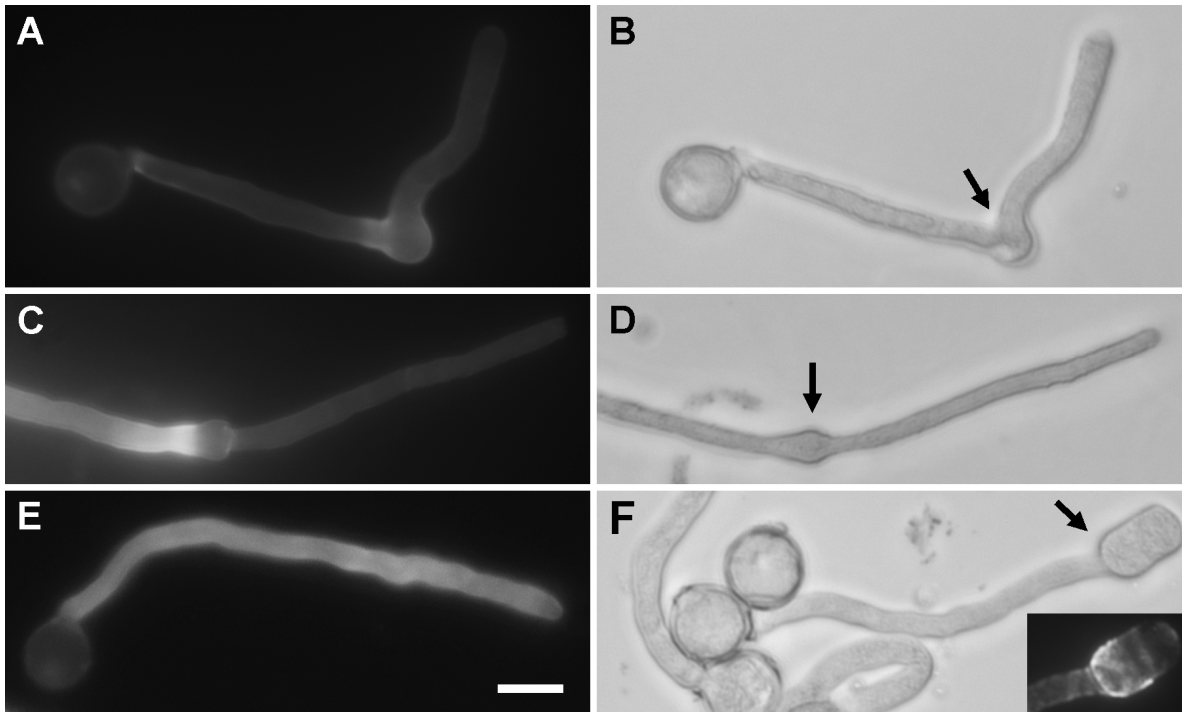

Figure 5.6: Fluorescence label for cellulose in *Solanum chacoense* pollen tubes.

Pre-germinated pollen tubes were treated with 1.5% cellulase (A-D,F). Arrows indicate tube length at time of administration. Fluorescence label with calcofluor white of cellulose (A,C) is very weak in the newly formed portions of the tube compared to the control treated with boiled enzyme (E). (B,D) Brightfield images corresponding to A and C, respectively. F. Example of pollen tube that does not form an outgrowth but continues expanding the swollen apex. Inset shows JIM5 label for pectins with low degree of methyl-esterification indicating the abundance of pectins in the tube portion grown after enzyme administration. Bar = 20 μm.

Figure 5.7

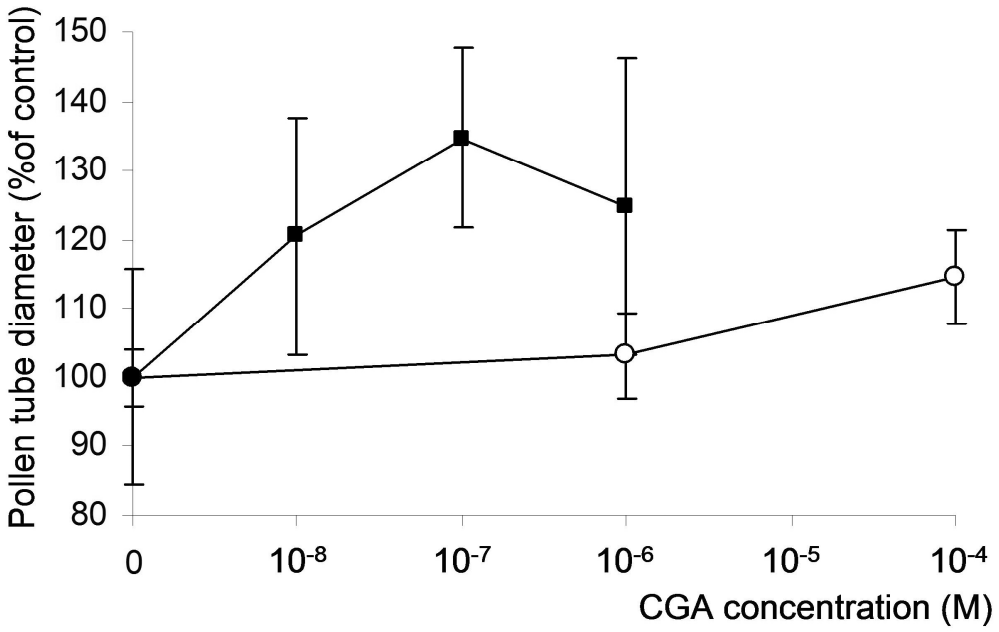

Figure 5.7: Effect of CGA on the diameter of *Solanum chacoense* and *Lilium orientalis* pollen tubes germinated in the presence of this agent.

Data are plotted as percentage of the control values (18.4 µm (*Lilium*), 6.4 µm (*Solanum*)). Data are from three repeats of the experiment with n = 50, vertical bars are standard deviations.

Figure 5.8

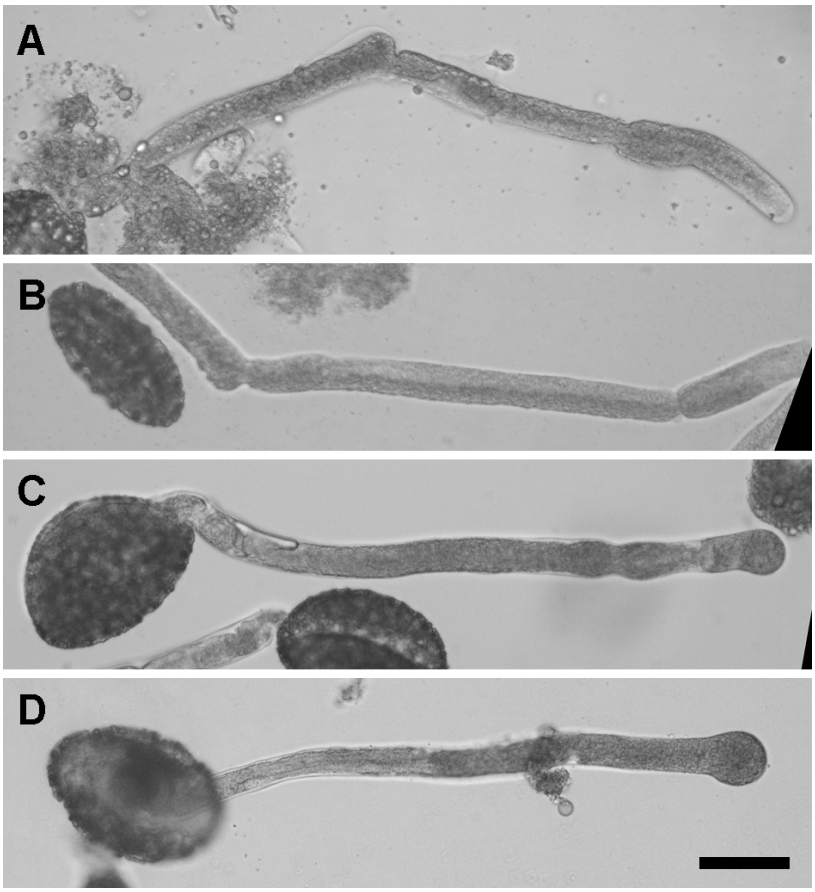

Figure 5.8: Effect of CGA administration on the morphology of pre-germinated *Lilium* tubes.

50 µM CGA (A,B) and 100 µM CGA (C,D) were added to the germination medium at 2h after germination. Observations were made after an additional 1h incubation with the inhibitor. Bar = 50 µm.

Figure 5.9

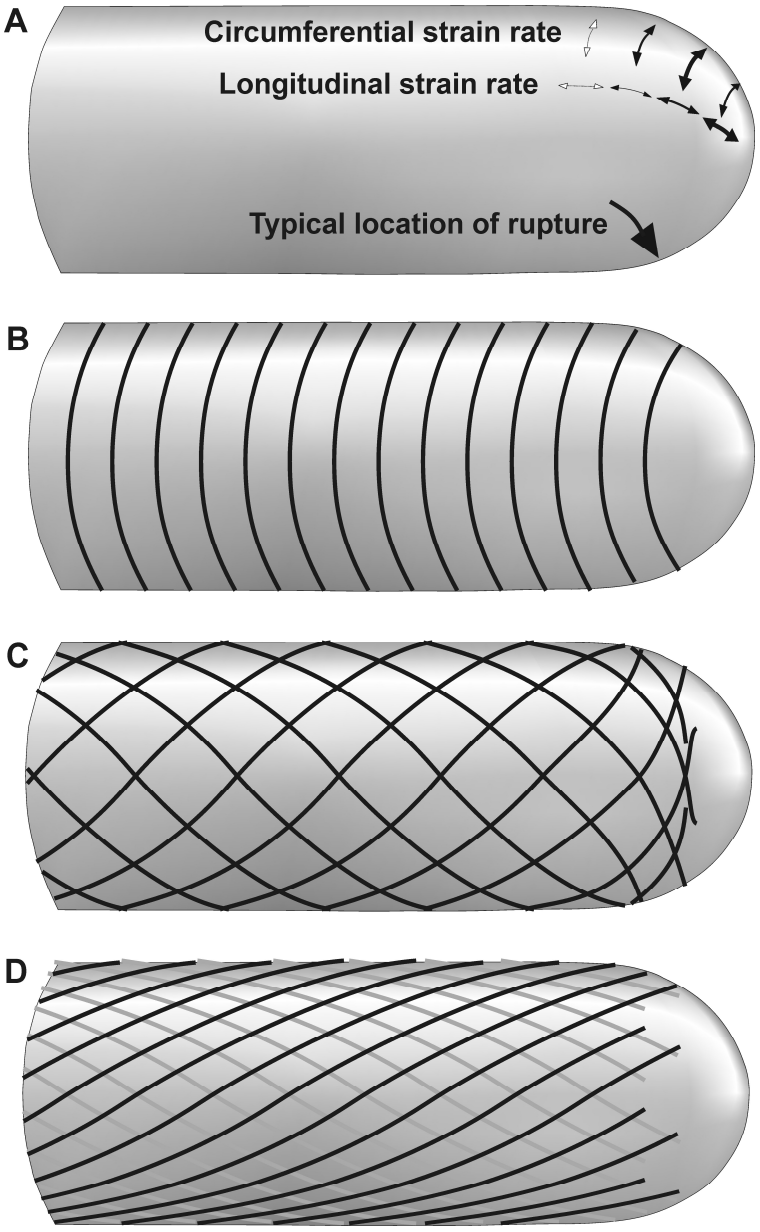

Figure 5.9: Schematic drawing of strain rates and hypothetical configurations of microfibrils in the pollen tube cell wall.

(A) Experimental data on root hairs (Dumais *et al.* 2004) have shown that a surface section while moving from the tip over the hemisphere-shaped curvature to the cylindrical shank initially undergoes both longitudinal and circumferential expansion with an initial stronger component in longitudinal direction followed by bias toward expansion in circumferential direction. Surface expansion in either direction halts upon arrival in the cylindrical part of the shank. (B) Hypothetical ideal orientation of a fiber with reinforcing function in circumferential direction on the surface of a cylinder. (C) Principal microfibril orientation observed in *Petunia* pollen tubes (Sassen 1964). The authors describe that the pitch in the shank is +45° and -45°, whereas in the subapical region the principal direction is rather perpendicular to the long axis. The 45° angle in the shank was also observed in *Pinus* pollen tubes (Derksen *et al.* 1999). (D) Microfibril orientation with a pitch of approximately 25° observed after digestion of the pectin layer in cell wall layer of *Lilium* pollen tubes (this study). Microfibrils in putative inner cell wall layer in grey.

Figure 5.10

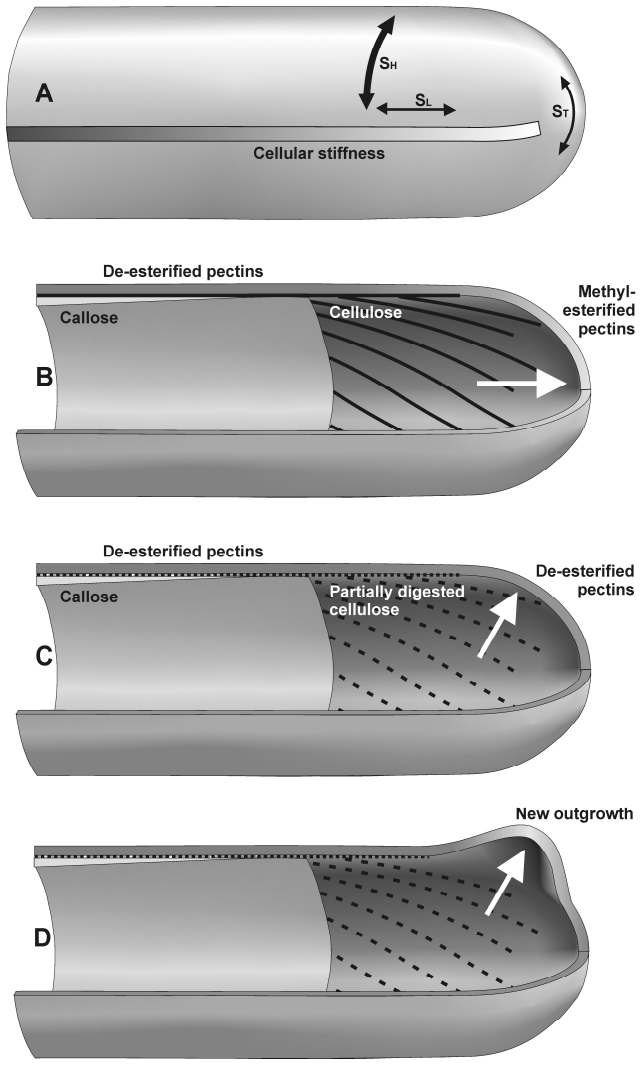

Figure 5.10: Schematic drawing of the mechanical properties and chemical composition characterizing the pollen tube cell wall.

(A) According to the laws of thin walled pressure vessels the tensile stress in longitudinal direction (S_L) is twice as high as the tensile stress in circumferential or hoop direction (S_H) which in turn is equal to the tensile stress at the tip (S_T). (B) The non-uniform distribution of cell wall components and consequently of the mechanical properties in the normally growing pollen tube drives growth to occur in the direction parallel to the length axis of the cell (white arrow). (C) Partial digestion of cellulose due to cellulase causes a transient growth arrest allowing for the apical cell wall pectins to become de-esterified, gelated and thus stiffened through ongoing pectin methyl esterase activity. (D) Through pectin methyl esterase induced hardening of the apical cell wall the relationship between cell wall deformability and tensile stress (due to geometry) favors the formation of an outgrowth in the subapical transition region between hemisphere-shaped apex and the cylindrical shank.

6 Finite element model of polar growth in walled cells

Plant cell growth is determined by the distribution, the local abundance and the chemical properties of the cell wall components. Determining how the cell geometry is shaped from its cell wall properties is crucial to understand the mechanical role played by each component. Using finite element modeling, a numerical technique used in engineering to predict the mechanical behavior of a complex structure, we were able to understand how the pollen tube is mechanically built to (1) maintain its geometry while growing and (2) how it responds to a change in its cell wall mechanical properties. We validated the predictions of the model with new biological data on the distribution of the cell wall components in lily pollen tubes. We also showed that when experimentally altering the distribution of the cell wall components, the pollen tube geometry was altered as expected by the computational model. I contributed to this study by providing all the biological data (Figures 6.1, 6.7 and 6.8).

This manuscript entitled "Finite element model of polar growth in walled cells" was published in 2010 in *Plant cell* volume 22, pages 2579-2593.

Pierre Fayant[1], Orlando Girlanda[1], Youssef Chebli[2], Carl-Éric Aubin[1], Isabelle Villemure[1] and Anja Geitmann[2,*]

[1]École Polytechnique de Montréal, C.P. 6079, Succursale Centre-Ville, Montréal, Québec H3C 3A7, Canada

[2]Institut de recherche en biologie végétale, Université de Montréal, 4101 rue Sherbrooke est, Montréal, Québec, H1X 2B2, Canada

6.1 Abstract

The formation of a cellular protuberance in walled cells requires the local deformation of the wall and its polar expansion. In many cells, protuberance elongation proceeds by tip growth, a growth mechanism shared by pollen tubes, root hairs and fungal hyphae. We established a biomechanical model of the tip growth process in walled cells using the finite element technique. The objective of this study was to identify the requirements for spatial distribution of mechanical properties in the cell wall which would allow the generation of cellular shapes that agree with experimental observation. We based our structural model on the parameterized description of a tip growing cell that allows the manipulation of cell size, shape, cell wall thickness and local mechanical properties. The mechanical load was applied in form of hydrostatic pressure. We used two validation methods to compare different simulations based on the assessment of cellular shape and on the displacement of surface markers during growth. We compared the resulting optimal distribution of cell mechanical properties with the spatial distribution of biochemical cell wall components in pollen tubes and found remarkable agreement between the gradient in Young's modulus and the distribution of de-esterified pectin polymers. This utilization of the finite element method for the modeling of non-uniform growth events in walled cells opens future perspectives for its application to complex cellular morphogenesis in plants.

6.2 Introduction

Cellular growth is a fundamental process during plant development. It shapes cellular morphology, affects cell functioning and ultimately determines the plant phenotype. During expansive plant cell growth, the cell wall needs to be mechanically stretched which leads to its thinning and, vital to cell survival, new material needs to be incorporated into the existing wall to prevent fatal rupture. Growth of plant cells is thus a complex interaction between the internal turgor-generated hydrostatic pressure, which drives this process, and the surrounding cell wall, which controls its temporal and spatial dynamics (Cosgrove 2005; Schopfer 2006; Geitmann and Ortega 2009). Understanding the biomechanical underpinnings of cellular growth processes will help us to focus our attention to those cellular mechanisms and molecular pathways that govern relevant physical players involved in plant development.

Cell morphogenesis in plants comes in a wide spectrum, with diffuse growth at one end of the continuum and the highly polarized phenomenon of tip or polar growth at the other end (Wasteneys and Galway 2003). Combinations of these two processes lead to the generation of complex plant cell geometries such as those of star-shaped astrosclereids and jigsaw puzzle-shaped leaf epidermis cells (Mathur 2004; Smith and Oppenheimer 2005; Mathur 2006; Geitmann and Ortega 2009). Since the hydrostatic pressure driving cell wall stretching is a non-vectorial force, the control of the final cell shape lies in the mechanical properties of the cell wall. The diffuse increase in overall cell size, typical for example for root epidermis cells, is known to be controlled by the arrangement of the cellulose microfibrils (Baskin 2005). Attempts to simulate this diffuse type of expansive growth date back to the first analytical model for cell expansion by Lockhart (Lockhart 1965). The constitutive equations describing growth behavior have been modified and adapted to various experimental situations (Geitmann and Ortega 2009) and efforts to mathematically account for the fiber-reinforced composite behavior of the cell wall are underway (Dyson and Jensen 2010).

The generation of complex cellular geometries, on the other hand, represents a major challenge for analytical modeling. The reasons for the complexity of cells such as those

composing the leaf epidermis are their geometry and their material properties, whose mathematical representation requires numerical modeling approaches. In engineering, the method commonly used to predict the mechanical behavior of complex structures is based on finite element (FE) modeling techniques. For this approach, the structural system is divided into discrete areas, the elements, which are connected by characteristic key points (generally located at their corners), or nodes. The quantities of interest, stresses, strains and displacements, are evaluated at the nodes connecting different elements. The FE technique produces approximate solutions to complex problems and by doing this allows for the calculation of the behavior of structures with complicated geometry and material properties. Finite element modeling has been used recently to model the elastic, temporary deformation of plant tissues and cells under the application of temporary external loads (Bolduc *et al.* 2006; Wang *et al.* 2006c; Hamant *et al.* 2008), but its utility for modeling the mechanics of cellular growth processes remains unexplored. Our objective was to use finite element modeling to represent a spatially confined cellular growth process in plants in order to demonstrate the potential of this approach for plant developmental research.

The experimental system chosen for our modeling approach is tip growth. Tip growth is a widespread mode of cellular morphogenesis found not only in plants (root hairs, pollen tubes), but also in animals (neurons), fungi (hyphae, budding yeasts), alga (rhizoids) and prokaryotes (streptomycetes). The defining feature of this growth process is the spatial confinement of surface expansion to the extremity of the cell. Consequently, all the key processes that control morphogenesis can be observed concomitantly in a small cellular region. The resulting structure is a tubular protrusion capped by a hemisphere or hemispheroid shaped dome.

Among the modes of growth leading to complex geometry, tip growth has the advantage of having a simple radial symmetry. Furthermore, the growth process displays temporal self-similarity, which means that the shape profile of the apical region of the cell stays largely constant in time and simply moves forward along the longitudinal axis of the cell (Goriely and Tabor 2003b). These features permit to easily establish quantitative validation strategies for a theoretical model. Furthermore, tip growth has attracted a number of earlier modeling attempts (Bartnicki-Garcia *et al.* 2000; Bartnicki-Garcia 2002; Goriely and Tabor

2003a; Goriely and Tabor 2003b; Dumais *et al.* 2004; Dumais *et al.* 2006; Goriely and Tabor 2008; Kroeger *et al.* 2008; Campàs and Mahadevan 2009) all of which have their merits and limitations. Most importantly in the present context, all of these models are essentially limited in their application to the simple, radial symmetry of the tip growing cell. Their adaptation to more complex geometries is not or not readily possible. Finite element techniques on the other hand offer this flexibility.

Tip growth is easily affected through mutation, enzymatic or pharmacological action. This interference often results in a swelling (Malhó *et al.* 1995; Kost *et al.* 1999; Parre and Geitmann 2005b; Klahre *et al.* 2006; Klahre and Kost 2006; Aouar *et al.* 2010; Hwang *et al.* 2010) or tapering (Klahre and Kost 2006) of the tubular cell, or in extreme cases, in the arrest of growth or bursting. A phenomenon such as apical swelling is generally claimed to be the result of a "depolarization" of the growth process, but how intracellular events are translated into a change of cellular morphology has not been examined in detail. A crucial question we wanted to address with our theoretical model concerns the nature of the changes to the cell wall mechanical properties that are implied in the generation of phenotypes that differ from the perfectly self-similar elongation pattern typical for the undisturbed cell. Geometrical and biophysical considerations dictate that the cell wall of the growing apex in tip growing cells must have a higher degree of extensibility than its cylindrical portion in order to direct cellular expansion to the apex (Geitmann and Steer 2006). Using a finite element model we wanted to find out how exactly this mechanical gradient must be shaped in order to generate a self-similar growth pattern for a given initial shape and how changes in this gradient affect the shape of the growing tube. To demonstrate the relevance of our theoretical approach, we compared the results of the simulations with the spatial distribution of the biochemical composition of the cell wall and with the growth behavior of pollen tubes, a widely used cellular model for tip growth (Hepler *et al.* 2001; Geitmann and Steer 2006; Chebli and Geitmann 2007).

6.2.1 Construction of the finite element model and validation methods

We used the finite element method (ANSYS 11.0 finite element package, Canonsburg PA) to generate a finite element mesh structure that represents the geometry of a typical tip growing cell and to model the deformation of the cell wall resulting from a hydrostatic pressure load. We constructed a shell based on a parameterized geometrical description that corresponds to the typical shape of the apical region of a pollen tube. We subdivided the structure in several ring-shaped domains along the longitudinal axis in order to be able to assign different mechanical properties to the different regions of the tube. Basic information that is required to develop an FE model includes geometry, mechanical properties, loading parameters and boundary conditions as detailed below. In order to identify the combination of mechanical properties resulting in self-similar growth, we developed a procedure to quantitatively determine the similarity of the simulation results with experimental data on cell shape and growth and hence to validate our model.

6.2.2 Geometry and meshing

Pollen tubes are cylindrical cells capped by an apex shaped like a half prolate spheroid. Using brightfield micrographs, we determined that the shape of pollen tubes is well described by a relationship of $r_L = 1.5 \times r_T$ with r_T being the radius of the tube and thus the short radii of the prolate spheroid and r_L being the long radius of the spheroid (Fig 6.1a). In the present model we used $r_T = 6\mu m$ unless noted otherwise. The structure of the tube was thus defined by the radius of the cylinder (r_T), the long radius of the apical spheroid (r_L) and the thickness t of the shell. For the present model, the thickness of the shell was assumed to be constant at 50 nm unless noted otherwise. The pollen tube shank and its apical region were meshed using user defined thickness and four-node shell type elements with 6 degrees of freedom at each node (SHELL181) (Figs 6.2a,b,c).

In order to assign different mechanical properties to the shell elements depending on their position on the tube surface, the structure was divided along the longitudinal axis into seven domains, six of which were located in the spheroid portion and the seventh being formed by the cylindrical shank (Fig 6.2d). The meridional lengths of domains 1 to 6 were defined by key points, which are anchor points for geometry and meshing. The position of each key

point was defined by the angle θ_i that a connecting line between key point and center of the spheroid formed with the previous domain. These angles could be varied to modulate the shape of the gradient in cell wall mechanical properties. For the sets of simulations analyzed here, the sum of angles 1 through 6 was always adjusted to be 90°.

Domains 2 to 7 were meshed using a mapped mesh consisting of quadrilateral elements arranged in rows. Domain 1 is triangular in shape, however. In order to use the same type of element (4 node shell elements) some of the quadrilateral elements had to be rotated which is done by a free mesh generator (Fig 6.2c). Mesh density was determined through convergence testing. This means that simulations with structures having denser meshes were carried out but no significant difference in the results was observed.

6.2.3 Mechanical Properties

The distribution of the material properties in the cell wall was chosen to correspond to the qualitative information that is available on the distribution of cell wall material in pollen tubes (Parre and Geitmann 2005a; Parre and Geitmann 2005b; Aouar *et al.* 2010). The pole of the cell consists mainly of pectin, an isotropic material. Although cellulose is present, it is randomly oriented (Sassen 1964). We therefore used an isotropic material model to describe the pole region (domain 1). In the shank, cellulose microfibrils display a preferential orientation oblique to the growth axis (O'Kelley and Carr 1954; Aouar *et al.* 2010). It is unknown how exactly microfibrils are oriented in the regions of the apical dome located between pole and shank. Therefore, any potential anisotropy in the plane of the wall, caused by preferential orientation of cellulose microfibrils, was considered by using an orthotropic material model for domains 2 through 6.

In the model, the elastic moduli of shell elements lying within domains 1 (pole) and 7 (shank) are directly user-defined. In domains 2 through 6, the values of the longitudinal elastic moduli are linked by a factor $\mathbf{m_L}$. The transversal value of the elastic modulus is obtained by multiplying the longitudinal elastic modulus by a factor $\mathbf{m_T}$.

The increase of the longitudinal elastic modulus from one domain to the next is represented by the following rule:

$$E_{Li} = m_L \times E_{Li-1}$$

where E_{Li} is the longitudinal Young's modulus in domain i. Modulating parameter $\mathbf{m_L}$ changes the steepness in the mechanical gradient along the longitudinal axis.

The transversal elastic modulus E_{Ti} within each domain I is then calculated by:

$$E_{Ti} = m_T \times E_{Li}$$

The parameter $\mathbf{m_T}$ reflects the degree of anisotropy of the material in the plane of the shell. The elastic modulus in normal direction E_{Zi} was set to always be identical to E_{Ti}.

Given that at the pole, the cell wall consists almost exclusively of pectins, we used 12.5 MPa for the elastic modulus of domain 1 (Chanliaud and Gidley 1999). The longitudinal and the transversal elastic moduli of the shank (domain 7) were chosen to be 4000 MPa to represent its large stiffness compared to the apical region of the tube. Preliminary simulations had shown that lower values would result in an increase in the tube diameter in the shank region. This increase would be incompatible with self-similarity and therefore no further tests were performed with lower values for domain 7. The Poisson's ratio was identical for all domains with 0.3 (Chanliaud *et al.* 2002). This ratio indicates the contraction (elongation) of a stretched (compressed) material in the direction perpendicular to the applied tension (compression).

6.2.4 Boundary conditions

To reduce calculation time, we exploited the radial symmetry of the pollen tube and modeled only a quarter of the cylindrical structure, unless mentioned otherwise (Fig 6.2a). At the axisymmetric borders, radial and longitudinal translations were fixed. Vertical translation was prevented by fixing the base of the shank.

6.2.5 Loading parameters

The turgor pressure within the cell was represented by an internal hydrostatic pressure of 0.2 MPa, unless noted otherwise, based on the values measured in lily pollen tubes (Benkert *et al.* 1997).

6.2.6 Simulation of pollen tube growth

Growth of the cell was simulated by an iterative series of loading cycles. Load was applied and the resulting deformed structure represented the starting geometry for the subsequent loading cycle. To account for the fact that continuous deposition of new cell wall material takes place during tip elongation, the structure was re-meshed after each loading cycle (Figs 6.2b,e). This implied that in order to ensure constant mesh density, nodes were added to accommodate for the increased length of the structure. Cell wall thickness was set back to the original value to mimic the deposition of additional cell wall material by exocytosis. Furthermore, in order to reflect the continuous maturation of the cell wall upon its displacement towards the cylindrical shank, the ring-shaped cell wall regions were redefined after each loading cycle based on the angles that were maintained constant (Fig 6.2e). This implied the redefinition of the keypoints defining the surface domains.

6.2.7 Validation of the model

One of the objectives of the study was to build a model able to represent perfectly self-similar growth. To assess the quality of the different simulation runs, we devised two quantitative validation methods that allowed us to determine how closely the model behaved to the real cell.

6.2.8 Degree of self-similarity

Tip growing cells grow in a self-similar manner when undisturbed. To determine the degree of self-similarity resulting from the FE simulations, the shape of the structure after 100 loading cycles was compared with the initial shape that had been established to fit lily pollen. Comparison was done on the 2D profile of the structure. This difference was quantified by calculating the difference between the initial and the final curves describing the cellular profile using the following algorithm. First, elongation of the cell was calculated from the translation α of the apical pole in y-direction:

$$\alpha = Y_{tip,step100} - Y_{tip,step0}$$

Y-coordinates of the points on the meridian determining the pollen tube profile after the 100th loading cycle was then corrected for tube elongation (in other words, the final and initial shapes were superimposed):

$$Y_{adjusted} = Y_{step100} - \alpha$$

Then, the differences for each point on the curve were calculated by:

$$\Delta X = X_{step100} - X_{step0}$$

$$\Delta Y = Y_{adjusted} - Y_{step0}$$

In parameters described above, "tip" indicates the pole of the cell, "step 0" the original structure, "step 100" the structure after 100 loading cycles. Finally, the deviation of a simulation from the initial shape was calculated by determining the average value for

$$\text{Shape change} = \sqrt{(\Delta X^2 + \Delta Y^2)}$$

for each coordinate of a given profile.

6.2.9 Pattern of surface deformation

Cell wall deformation caused by pressure loading leads to a displacement of material points on the cell wall towards the outside, until the deformed wall becomes part of the non-growing cylindrical shank. The trajectory that a marker on the cellular surface describes during the deformation process reveals the strain pattern on the cellular surface (Rojas *et al.* 2011). A finite element model that describes tip growth in realistic manner will have to produce similar surface strain patterns. To test the simulations their capacity to reproduce experimentally observed surface strain patterns, we fixed keypoints on the finite element structure and followed their displacement over a sequence of load cycles.

This method is not trivial in a finite element approach since during re-meshing all nodes are re-defined. A single node can therefore not be followed over multiple load application and remeshing steps. Therefore, the position of a surface marker was extrapolated using the following approach. A point on the original structure was defined as surface marker and its new position after a single load application was recorded. Following re-meshing, the meridional coordinates of the surface marker in the new mesh were defined by identifying the two nearest nodes. The position of these two nodes was recorded and the subsequent position of this point was maintained between the identified nodes for the next loading

cycle. The position of the surface marker was approximated by assuming it to be in the center between the two neighboring nodes. This process was repeated with each loading cycle. The positions of the surface markers were then plotted to map their respective displacement trajectories.

For each simulation, displacement trajectories for five surface markers located at varying distances from the pole of the cell were performed. The displacement trajectories were then compared to experimental results (Rojas *et al.* 2011) in the same manner as the determination of the degree of self-similarity.

6.3 Results

6.3.1 Identification of crucial parameters

Theoretical considerations suggest (Geitmann and Steer 2006) and micro-mechanical data confirm (Geitmann *et al.* 2004; Zerzour *et al.* 2009) that the cell wall of a tip growing cell has a higher degree of deformability at the apex. However, neither the type of mechanical testing nor the spatial resolution of the micro-indentation approach lends itself to conclude on the precise spatial distribution of extensibility in the apex. Experimental studies (Parre and Geitmann 2005a; Parre and Geitmann 2005b; Aouar *et al.* 2010) corroborate that considerable mechanical support in the cylindrical shank of the cell prevents this region from swelling, but quantitative information is elusive. An objective of our study was to identify the theoretical distribution of material properties within the cell wall of the tip growing cell that is necessary to produce a perfectly self-similar growth pattern. We posed two questions in particular: *a)* How steep does the gradient in cell wall extensibility in meridional direction have to be in order to obtain the initial shape defined by $r_L = 1.5\ r_T$? *b)* Does the cell wall need to possess mechanical anisotropy in its plane? The second question arises from the observation that cellulose microfibrils are present in the apical region of pollen tubes (Sassen 1964) and thus a biochemical basis for putative anisotropy exists.

To simulate extended periods of growth, an internal pressure load was applied repetitively to the finite element structure. The resulting deformation depended on the distribution of material properties in the cell wall, or shell, which were determined by the set of rules

detailed above. To identify crucial parameters leading to self-similar growth for the chosen initial shape, we generated an initial set of 64 parameter combinations by modulating three variables: the angles θ_i defining the spatial distribution of annular domains, and multiplication factors m_T and m_L. The angles were varied such that their sum describing domains 1 through 6 equaled 90° (Fig 6.2d). For m_L we tested the values 1.5, 2, 2.5 and 3, and m_T was tested for the values 0.5, 1, 2, 3 and 4. For all possible combinations of the explored variables, simulations consisting of 50 iterations were performed. To classify the results of this first set of simulations, we assessed the resulting structures for self-similarity by qualitatively comparing their shapes to that of the initial structure. Analyzing all 64 simulations revealed the following tendencies:

6.3.2 Modulation of m_L

Multiplication factor m_L directly influences the steepness of the gradient in cell wall extensibility from the pole towards the shank. When keeping m_T constant, high m_L caused the radius of the elongating tube to progressively decrease after repeated load-cycles, and simultaneously, tube elongation per load cycle was reduced (Fig 6.3). By contrast, at low values for m_L, this tapering was less pronounced or, depending on m_T, resulted in a widening of the tube and an increased tube elongation. The optimal value of m_L that prevented the tube diameter from changing depended on the other two parameters, but was generally 2 or 2.5.

6.3.3 Modulation of m_T

Multiplication factor m_T determines the degree of anisotropy in cell wall extensibility. Increasing the Young's modulus in circumferential direction ($m_T>1$) resulted in a progressive reduction of the tube radius, whereas if the Young's modulus was lower in circumferential than in meridional direction ($m_T<1$), tubes widened (Fig 6.3). Depending on m_L, different values for m_T resulted in a constant tube diameter after repeated load cycles. However for $m_T>1$ the apex became more prolate (pointed), i.e. the ratio between r_L and r_T became higher, whereas for $m_T<1$ the apex became oblate (flatter) (Fig 6.3). Only for $m_T=1$ did we find combinations of the other parameters that resulted in true self-similarity for the

given initial shape. Contrary to m_L, tube elongation per load cycle did only change moderately upon manipulation of m_T.

6.3.4 Size of surface domains

The shape of the gradient in cell wall extensibility in meridional direction can be influenced by changing the size of individual surface domains through manipulation of the distribution of domain angles. The variation of domain angles affected both the degree of self-similarity and elongation rate of the pollen tube depending on m_L and m_T. Generally, large domain angles for either domain 1 or domain 2 caused swelling of the tube. In other words, if an increase in Young's modulus set in too far away from the pole of the tube, a widening of the elongating tube resulted.

Analysis of all 64 simulations allowed us to conclude that no self-similarity could be achieved when the cell wall material was anisotropic ($m_T<1$ or $m_T>1$) (Fig 6.3). Therefore, a second set of 32 simulations was performed in which m_T was kept constant (equal to 1 to maintain an isotropic distribution) while m_L and angle distribution were varied in the same ranges as previously, but using smaller increments (Supplemental 6.1). Qualitative comparison revealed that overall shallow gradients (Fig 6.4a) or a large region of low Young's modulus around the pole (Figs 6.3, 6.4b) caused the expanding tube to swell, whereas steeper gradients (Fig 6.4c) resulted in a reduction of the tube diameter of the elongating tube. Self-similarity was achieved by a number of different gradients or parameter combinations, all of which were characterized by a moderate but steady increase in Young's modulus from domain 1 to 6, and by a significant jump in Young's modulus from domain 6 to domain 7 (Figs 6.4d-f). Within this second set of simulations, the 8 parameter combinations with highest degree of self-similarity were selected based on qualitative comparison (Supplemental Table 6.1) and subjected to further analyses.

6.3.5 Quantitative validation of selected parameter combinations

The 8 simulations selected were analyzed quantitatively for their degree of self-similarity (Figs 6.5a,b) and for their surface strain patterns (Fig 6.5c,d) as explained in the Validation methods. As expected, the 8 simulations displayed only minor differences in self-similarity

(red bars, Fig 6.5e) but they differed significantly in the quality of their surface strain patterns. The two simulations showing the highest degree of self-similarity with a good strain pattern fit were characterized by a steady increase in Young's modulus beginning close to the pole of the cell, and a significant jump of the modulus between domain 6 and 7 (Simulation S12, Fig 6.4e; Simulation S63, Fig 6.4f). The spatial distribution of stress within the tube revealed that the overall stress in the wall of the cylindrical region of the cell is significantly higher that at the pole (Fig 6.5f). The boundaries between surface domains experience small local stress maxima, due to the discrete change in mechanical properties (ringshaped color changes in Fig 6.5f). These do not significantly affect the deformation of the structure, however, as the pattern of the overall strain is nevertheless gradual (Fig. 6.5g). The strain pattern shows highest deformation in the pole region and no deformation in the distal region of the tube. The fact that the strain gradient is oriented in opposite direction to the stress gradient is a consequence of the strong difference in mechanical properties between the two regions.

6.3.6 Effect of geometry and turgor pressure

Once we had established gradients in cell wall mechanical properties leading to self-similar growth, swelling, or tapering, we wanted to assess the effects of cellular geometry and pressure load on the behavior of the model. We generated a new set of simulations based on the mechanical gradients in simulations S12 (self-similar), S51 (swelling) and S14 (tapering) and varied cell size, cell wall thickness and turgor pressure in ranges that were biologically relevant. Within the ranges tested, none of these parameters affected the qualitative nature of the shape change after 50 iterations of the load cycle. Using the mechanical gradient determined for simulation S12, self-similarity was always achieved independently of the thickness of the cell wall (as long the thickness was defined to be identical in all surface domains), the diameter of the tube and the applied turgor pressure (Fig 6.6). The same was true for swelling and tapering behavior (Fig 6.6). The only factor affected was the increase in tube length per load cycle. Higher turgor pressure increased this length, lower pressure reduced it in linear manner.

Cell wall thickness was varied within a range that maintained the wall relatively thin compared to the tube diameter, as is typical for plant cells with primary cell walls. An increase in cell wall thickness reduced tube elongation per load cycle in linear manner (Fig 6.6).

Cell size was altered while maintaining the ratio between the long (r_L) and the short radii (r_T) of the apical prolate spheroid. An increase in tube diameter resulted in a significant increase in tube length per load cycle. Unlike the other two parameters which resulted in a linear response, the increase in tube growth was approximately proportional to r_T^2 (Fig 6.6). The reason for this phenomenon is likely to be that the deformation depends on the total force exerted on the apical cell wall by the pressure which is linearly dependent on the cross-section of the tube which in turn scales with r_T^2. It is important to note that in a quasi-static model such as the present version, the observed changes in tube elongation per load application do not allow any conclusion on the growth rate.

Finally, we used the three parameter combinations generating different shapes to confirm that the finite element structure representing the quarter of the tube (90° structure) behaved identically to the full tube (360° structure). Comparison of the resulting shapes and displacements demonstrated that both structural approaches yielded exactly the same results (Fig 6.6).

6.3.7 Comparison with experimentally determined spatial distribution of cell wall components

We wanted to assess whether the steady mechanical gradient in the apical dome of the pollen tube, and the steep increase in Young's modulus in the transition region between the dome and the shank were reflected in the biochemical composition of the cell wall. It is known that pollen tubes display a non-uniform distribution of cell wall components along the longitudinal axis of the cell (Geitmann and Parre 2004; Parre and Geitmann 2005a; Parre and Geitmann 2005b), but quantitative data are lacking. To quantify the precise spatial distribution of cell wall components in lily pollen tubes, a common model species, we labeled cellulose, callose and pectins in *in vitro* grown tubes and we quantified the relative fluorescence intensity along the perimeter of the cell (Fig 6.7). In accordance with

other pollen tube species, our fluorescence micrographs show that the entire lily tube was surrounded by a layer of pectic polysaccharides. In the apical region these pectins were highly methyl-esterified, whereas they were increasingly de-esterified in the more mature region of the cell wall. The abundance of cellulose did not change significantly over the length of the tube whereas that of callose increased slowly beginning in the subapical region. The quantification of the fluorescence micrographs clearly revealed that the most dramatic changes in cell wall biochemistry occurred between 15 and 20 µm meridional distance from the pole of the cell (Fig 6.7). Given the typical diameter of 18 to 21 µm for lily pollen tubes, this position corresponded exactly to the transition zone between apical dome and cylindrical shank of the cell (marked by a change in background color in the graphs). Importantly, the configuration of pectins changed from a high to a low degree of methyl-esterification at this location which allows their gelling through calcium ions, a process that rigidifies the extracellular matrix. In particular, the distribution of de-esterified pectins (Fig 6.7a) showed remarkable similarity to the curve described by the distribution of mechanical properties established by the FE model (Figs 6.4e,f).

6.3.8 Removal of pectin disturbs cell shape determination

Given the excellent correlation between predictions made by the FE model and spatial distribution of pectin label we wanted to test the role of this cell wall component in determining cell shape. To this end, we exposed pre-germinated lily pollen tubes for 15 minutes to pectinase. As a result pollen tubes developed dramatic swellings in the apical region (Fig 6.8). The virtual absence of fluorescence after immunolabel with JIM5 (Fig 6.8a) and JIM7 (micrographs completely black, not shown) demonstrated the successful digestion and hence removal of a significant portion of the pectin moiety from the pollen tube cell wall.

An FE simulation carried out using identical mechanical properties (Young's modulus 50 MPa) for all surface domains of the tube confirmed that an absence of a mechanical gradient in the cell wall is predicted to lead to a spherical swelling (Fig 6.8e).

6.4 Discussion

6.4.1 Mechanics of growth in walled cells

Growth in walled cells is driven by the internal turgor pressure. However, since turgor is a non-vectorial force, spatial control of the growth process relies on the mechanical properties of the cell wall (Cosgrove 2005; Geitmann and Ortega 2009). As predicted (Geitmann and Steer 2006), micromechanical data revealed a difference in mechanical behavior between the tip of a growing pollen tube and its cylindrical shank (Bolduc *et al.* 2006; Zerzour *et al.* 2009). It had been known from other plant species that this gradient is generated by the absence or scarcity of callose (Parre and Geitmann 2005a) and cellulose (Aouar *et al.* 2010) at the growing apex as well as by the relatively high degree of esterification of the pectin polymers in this region (Parre and Geitmann 2005a; Parre and Geitmann 2005b). The pectic polymers are secreted at the apex of the cell in highly methyl esterified form which renders them essentially liquid and consequently the cell wall is easily deformable in this region. During maturation of the wall, pectin methyl esterase, an enzyme that is secreted together with the cell wall polymers, cleaves off the methyl groups. The resulting negative charge of the pectin molecules attracts calcium ions which cause the polymers to gel and thus to form a matrix of much higher stiffness. Although numerous immuno-fluorescence studies on pollen tube have confirmed the general biochemical differences between non-growing shank and growing apex, no quantitative analysis of the spatial distribution within the apical dome had been published. The quantitative data presented here clearly reveal that the most significant changes in the biochemical composition occur in the transition region between apical dome and tubular shank of the cell. These changes were particularly dramatic in the distribution of pectins with low degree of esterification. The striking similarity of their distribution with the profile of the Young's modulus established using the finite element simulations confirms the importance of the change in pectin conformation for the geometry of the elongating tube. The reduction of the pectin moiety in the pollen tube cell wall through the external application of pectinase and the resulting swelling corroborated further that the presence of the mechanical gradient generated by the changing pectin chemistry is crucial for shape determination in this cell.

6.4.2 Information gained from the finite element approach

Our model has allowed us to draw a number of conclusions that reveal important details about the mechanical principles governing tip growth. The highest degree of self-similarity was achieved when representing the cell wall as having isotropic mechanical properties. This finding does not seem to be consistent with observations in root hairs in which a slight meridional stiffening (corresponding to $m_T<1$) provides the best explanation for tip elongation (Dumais *et al.* 2004). However, unlike the lily pollen tube analyzed here, the shape of a root hair is somewhat oblate with a region of maximal curvature at an annular region around the pole of the cell. Consequently the mechanics of the growth process in this cell type may be slightly different. Furthermore, the increments in m_T tested here were too large to pick up a subtle anisotropy that could putatively provide an even better fit than those simulations we identified in the present set. It remains that the result of our approximate approach is consistent with structural observations. Putative anisotropy would have to derive from a preferential orientation of microfibrils. Cellulose orientation has unfortunately not been determined in the apical dome of lily pollen tubes although our immunolabel shows that cellulose is clearly present in this region. However, in other plant species, microfibrils seem to be short and oriented randomly in the apical region of the pollen tube (O'Kelley and Carr 1954; Sassen 1964; Derksen *et al.* 1999) indicating that they do not generate anisotropy in the cell wall mechanical properties of the tube apex.

More than one parameter combination tested here produced growth patterns with acceptable degree of self-similarity, but not all of them necessarily generated trajectory maps of surface markers that agreed with experimental data. Agreement was obtained for steady mechanical gradients in the apical dome that were followed by sudden increases in Young's modulus in the transition region to the shank. It is, therefore, important to recognize that testing for similarity between the predicted and experimentally observed final shape of a growing structure is not sufficient to identify the correct mechanical profile. Our second validation method, the comparison with surface strain patterns, was therefore crucial to determine the fit of the model with the living cell.

Our model showed that swelling of the tube was achieved when the gradient in Young's modulus along the longitudinal axis was not sufficiently steep, or when the increase in

Young's modulus began too far from the pole. This is consistent with experimental data showing that enzymatic treatments with cellulase, an enzyme that digests cellulose microfibrils, result in a swelling of the tube apex (Aouar *et al.* 2010). The FE simulations suggest that the effect is mediated by a reduction in the Young's modulus in the apical dome. This means that, although they may not confer anisotropy to the pollen tube apex due to their random orientation, the presence of cellulose microfibrils nevertheless seems to contribute to tensile resistance of the cell wall in this region. Similarly, the FE model may help to understand other phenomena that occur upon manipulation of the mechanical properties of the pollen tube cell wall such as those caused by the transient expression of pectin methyl esterase inhibitor, by the overexpression of pectin methyl (Röckel *et al.* 2008) or by exposure to externally applied enzyme (Bosch *et al.* 2005; Parre and Geitmann 2005b). Ongoing controversies about the cellular features controlling growth dynamics in these cells (Zonia *et al.* 2006; Zonia and Munnik 2009; Winship *et al.* 2010) may also gain from this engineering approach to cell biology.

6.4.3 Impact of a mechanical model of tip growth

An accessible mathematical model will draw the attention to the fact that any kind of change in growth behavior is ultimately mediated by affecting cell mechanics. Recognizing this should complement approaches that hitherto focused purely on intracellular processes such as signaling events. Pollen tube swelling (Kost *et al.* 1999; Klahre *et al.* 2006; Klahre and Kost 2006; Hwang *et al.* 2010) or tapering (Klahre and Kost 2006) resulting from manipulations in the signaling machinery of the cell can only be completely understood if the biophysical mechanism that translates biochemical and signaling processes into particular cellular phenotypes are included in the interpretation of experimental data.

A significant advantage of the finite element approach is the fact that the model can easily be adapted to other tip growing cell types. Species-specific differences in the spatial distribution of biochemical components can easily be accommodated rendering the model extremely versatile. Variations in geometry such as tube diameter and shape of the apex can be modified through modulating a single parameter, respectively. Hence, adaptation to the small tubes of *Arabidopsis* (typical diameter of 6 μm) or to the more tapered tip of fungal

hyphae is straightforward. The gradient of mechanical properties and the degree of anisotropy can be altered locally or globally and the model can be equipped with a time-dependent component by using viscoelastic instead of purely elastic properties.

6.4.4 Limitations of the finite element approach

Pollen tube growth is a very rapid process and the deformation of the cell wall involved in the process is extremely large compared with the size of the initial structure. One of the drawbacks of the finite element approach in the context of large deformation was the necessity of operating with cyclic iterations implying that a deformation is achieved through a series of small, discrete steps. During each iterative step the structure was re-created, and, depending on the number of nodes, the shape of the subsequent structure could display small differences compared with the previous structure (e.g. anchor points of the geometry could change). However, given the mesh density we used here, these errors were orders of magnitude smaller than the dimension of the structure.

Another potential shortcoming of our finite element approach was the spatial distribution of material properties in discrete domains. As a result, there were significant and instant changes in the elastic modulus between the successive, ring-shaped cell wall domains. These introduced local stress maxima in the cell wall (Fig 6.5f). However, even after 100 iterations, the resulting structures always had smooth curvatures and the overall strain patterns were gradual (without local maxima). This suggests that these local stresses had negligible effects on the final outcome. Further confirmation of the validity or our model can be derived from comparison with other mathematical approaches. Our profiles for the Young's modulus look remarkably similar to those obtained for spatial distribution of mechanical properties in root hairs that had been generated inferring from a comparison of the strain rates and wall stresses in this cell type (Dumais *et al.* 2004). Therefore, despite the discrete changes in mechanical properties, our approximate approach was sufficient to yield excellent qualitative fit with experimental data.

6.4.5 Potential of the finite element approach for modeling complex geometries

Previous attempts to model tip growth were mostly restricted to geometric interpretations (Da Riva Ricci and Kendrick 1972) or purely mathematical equations (Denet 1996). However, although they may be elegant in their simplicity, their biological relevance is limited due to the low number of parameters. For instance, cell wall thickness or anisotropy are not taken into account in these models. More recent models include the Vesicle Supply Center model for hyphal growth (Bartnicki-Garcia *et al.* 2000), hyphal growth models based on linear elastic (Goriely and Tabor 2003b) and non-linear elastic membrane theory (Goriely and Tabor 2008), a model for root hair elongation based on viscoplasticity theory (Dumais *et al.* 2006), and an approach based on a representation of the cell wall as viscous fluid shell (Campàs and Mahadevan 2009). However, all of these models are limited in their versatility to the simple axisymmetric geometry of the tip growing cell, even though they can explain variations in shape that are based on changes in the tube diameter or the pointedness of the apex.

The most important advantage of the finite element approach consists in its potential to cope with the complexity of cellular geometries and mechanical properties encountered in nature. In most of the mentioned models the thickness of the cell wall is only indirectly considered, whereas in the FE model this variable can be manipulated either globally or - with minor modifications - locally, to accommodate phenomena such as the temporal variation in the thickness of the apical cell wall observed in lily and tobacco pollen tubes (McKenna *et al.* 2009; Zerzour *et al.* 2009). Remarkably, this experimentally observed change in cell wall thickness is associated with temporary growth arrest or periodic temporal changes in the growth rate. Our model has therefore the potential to explain these phenomena at the mechanical level and thus provides a tool to test conceptual models explaining processes such as those displayed during oscillatory growth (Zonia and Munnik 2007). Potential integration with mechanical models operating at the molecular scale offers another intriguing perspective (MacKintosh *et al.* 1995; Wilhelm and Frey 2003). This

would allow us to predict cellular behavior based on the mechanical interaction and behavior of the polymers forming the cell wall (Kha *et al.* 2010).

More importantly, contrary to other models, the FE approach will enable us to model changes in the growth pattern that abandon axisymmetric geometry, such as a change in growth direction. This is a phenomenon that is very typical for fungal hyphae and pollen tubes as these cells are able to follow chemical gradients (Geitmann and Palanivelu 2007). Asymmetric and other complex geometric shapes can be constructed in FE analysis based on 3D data obtained from confocal imaging or other 3D reconstruction techniques. Contrary to earlier models for tip growth, adaptation of the FE model is therefore not limited to tip growth. All the complex cellular shapes that can be observed in plant tissues are likely based on the non-uniform distribution of cell wall components and cell wall dimensions, and, as a consequence, the Young's modulus. Shapes such as those of jigsaw-puzzle shaped epidermis cells could be modeled easily exploiting the discrete approach we used here that is based on the division of the cellular surface into domains with varying mechanical properties. The ability of the FE method to take a complex problem or structure whose solution may be difficult if not impossible to obtain, and decompose it into smaller elements allows us to construct simple approximations of the solution that might provide important information on the mechanics of expansive cellular growth in all cell types with walls.

6.5 Experimental procedures

6.5.1 Plant material and pollen culture

Lilium orientalis pollen was obtained from a local flower shop. Pollen was dehydrated for 24 h and then stored at -80°C until use. Pollen grains were hydrated for 30 min. Hydrated pollen was incubated at 25°C for 2 to 3 h under continuous shaking in a 25 mL Erlenmeyer flask containing 3 mL of growth medium made of 100 $mg.mL^{-1}$ H_3BO_3, 300 $mg.mL^{-1}$, $Ca(NO_3)_2 \cdot H_2O$, 100 $mg.mL^{-1}$ KNO_3, 200 mg mL^{-1} $MgSO_4 \cdot 7H_2O$, and 50 $mg.mL^{-1}$ sucrose.

Pollen tubes exposed to pectinase were grown in regular growth medium for 3 hours 45 minutes before addition of 8 mg/ml pectinase (Fluka).

6.5.2 Fluorescence label

All steps were carried out in the microwave oven operating at 150 W under 21 inches of Hg vacuum at a controlled temperature of 30±1°C. For fluorescence labeling, pollen tubes were filtered and subsequently fixed in 3.5% freshly prepared formaldehyde in Pipes buffer (50 mM Pipes, 1mM EGTA, 0.5 mM $MgCl_2$, pH 6.9) for 40 seconds followed by 3 washes in Pipes buffer. For immuno-labeling pollen tubes were then washed 3 times with PBS buffer (135 mM NaCl, 6.5 mM Na_2HPO_4, 2.7 mM KCl, 1.5 mM KH_2PO_4, pH 7.3) with 3.5% bovine serum albumine (BSA). All subsequent washes were done with PBS buffer with 3.5% BSA for 40 seconds. All antibodies were diluted in PBS buffer with 3.5% BSA. 10 min incubations with the primary antibody were followed by wash steps and 10 minute incubations with 1% IgG-Alexa Fluor 594 anti-rat secondary antibody (Molecular Probes). Controls were performed by omitting incubation with the primary or the secondary antibody. Pectin label was performed with primary antibodies JIM5 (pectin with low degree of esterification) and JIM7 (pectin with high degree of esterification). Label for crystalline cellulose was done with CBM3a (Cellulose Binding Module 3a) followed by monoclonal mouse-anti-polyhistidine antibody (Sigma). These primary antibodies were obtained from Dr. Paul Knox, University of Leeds, United Kingdom. Callose label was done with monoclonal IgG antibody to (1→3)-β-Glucan (Biosupplies Australia Pty Ltd). Cellulose (crystalline and amorphous) was also labeled with 1 mg mL^{-1} calcofluor following fixation. All samples were mounted on glass slides in a drop of citifluor (Electron Microscopy Sciences) for microscopical observation.

6.5.3 Fluorescence microscopy

Observation of samples was done with a Zeiss Imager-Z1 microscope equipped with structured illumination microscopy (ApoTome Axio Imager), a Zeiss AxioCam MRm Rev.2 camera and AxioVision Release 4.5 software. Observations were made using a filter set with excitation BP450-490 nm, beamsplitter FT 510 nm and emission BP 515-565 nm

for calcofluor labeling and a filter set with excitation BP 390/22 nm, beamsplitter FT 420 nm and emission BP 460/50 nm for Alexa fluor 594 detection. Exposure time was adjusted for all images so that only one or two pixels were saturated when not using the ApoTome Imager. ApoTome Imager was then inserted and z-stack images of 1µm interval of pollen tubes were taken and image reconstruction was performed using the AxioVision software by the projection of the stacks.

6.5.4 Image processing and fluorescence quantification

Only z-projections were used for fluorescence quantification. ImageJ (Rasband, W.S., ImageJ, U. S. National Institutes of Health, Bethesda, Maryland, USA, http://rsb.info.nih.gov/ij/, 1997-2008) software was used for fluorescence quantification of cell wall stained components. Pixel intensity was measured along the periphery of each pollen tube, beginning from the pole. Values for fluorescence intensity were normalized to the highest fluorescence value for individual tubes before averaging (n>10 for each sample). Distances on the x-axis of the graphs represent the meridional distance from the pole of the cell.

6.6 Acknowledgements

This project was supported by a grant from the *Fonds de recherche sur la nature et les technologies du Québec* to C.E.A., I.V. and A.G., and by an Ann Oaks scholarship from the Canadian Society of Plant Physiologists to Y.C. We thank Jacques Dumais and Enrique Rojas for making their unpublished data available to us.

6.7 Figures

Figure 6.1

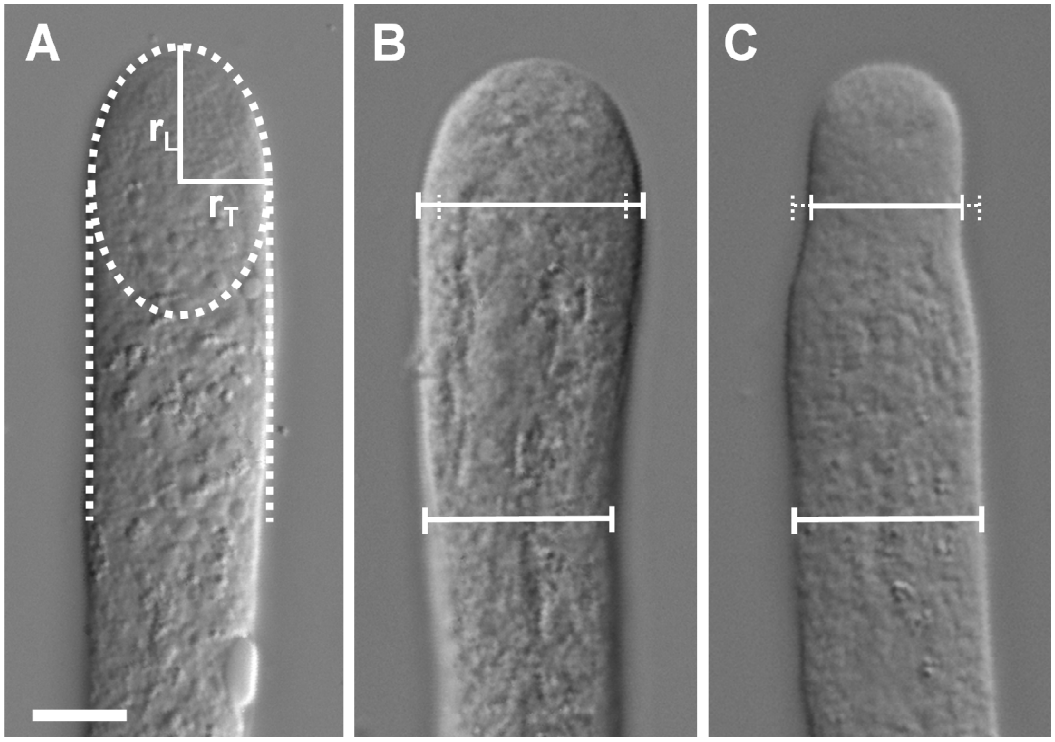

Figure 6.1: Differential interference contrast micrographs of *in vitro* growing lily pollen tubes.

(A) Normally growing tube. The geometry of the tube can be described with a cylinder of radius r_T capped by a half prolate spheroid with short radii r_T and a long radius r_L. (B) Tube showing a swelling apical region. (C) Tube showing a tapering apical region.

Figure 6.2

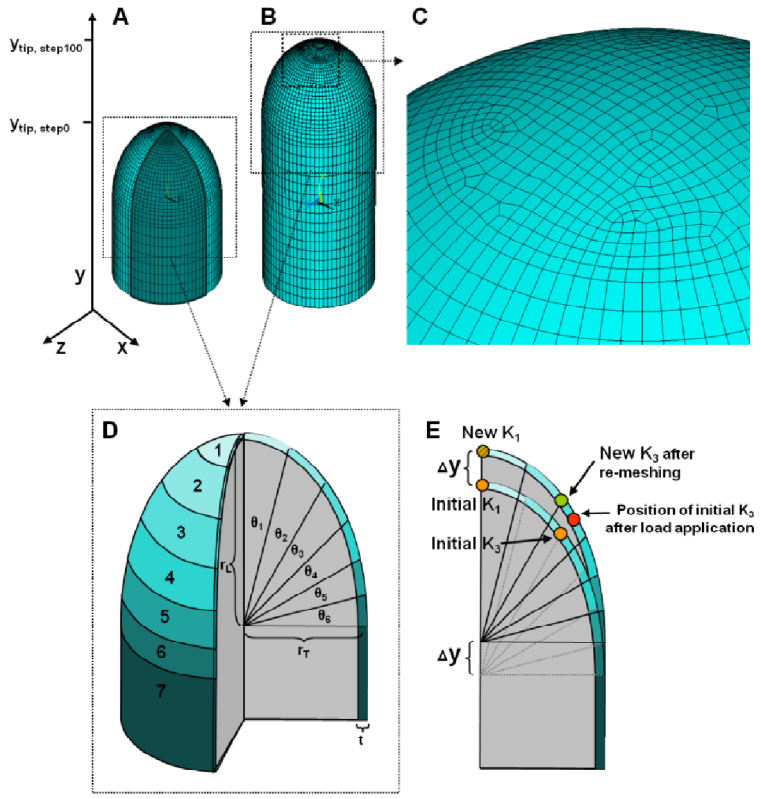

Figure 6.2: Finite element structure of a tip growing cell.

Initial structure (A) and structure after 50 load cycles (B, C) in the case of self-similar elongation. The figures show the full 360° structure and the 90° structure marked in darker color in (A). For most calculations, only the 90° structure is used to exploit radial geometry. The apical region of the cell wall is divided into 6 ring-shaped surface domains defined by the angles θ_1 through θ_6 originating from the center of the prolate spheroid (D). Because of its different geometry, domain 1 is meshed using a different method than domains 2 through 7. This resulted in irregularly arranged shell elements in the pole region (C) The shape of the pollen tube is defined by the short radii r_T and the long radius r_L of the half prolate spheroid and the thickness t of the shell elements representing the cell wall. Deformation resulting from load application causes the displacement of key points defining surface regions. These are re-defined after re-meshing based on the domain angles θ_i (E).

Figure 6.3

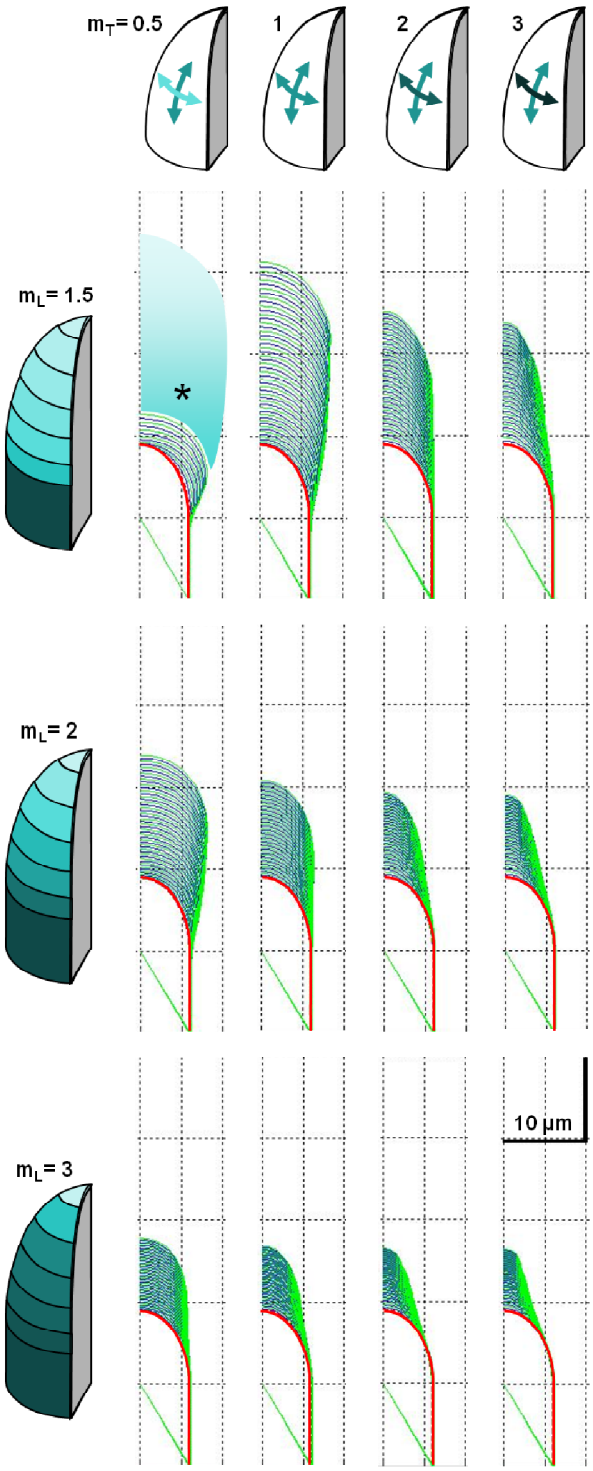

Figure 6.3: Subset of simulations showing the deformation of the cell wall structure after 50 load cycles.

The profile of the original structure is indicated by the red, dashed line. Alternating blue and green lines indicate the results of repeated load cycles. In this subset the domain angles were identical with $\theta_i = 15°$ for i = 1 to 6. Various combinations of multiplication factors m_L and m_T demonstrate that for this particular angle distribution, self-similarity was obtained for $m_L = 2$ and $m_T = 1$. The asterisk indicates an error occurring after the 12^{th} loading cycle due to an instability in the structure.

Figure 6.4

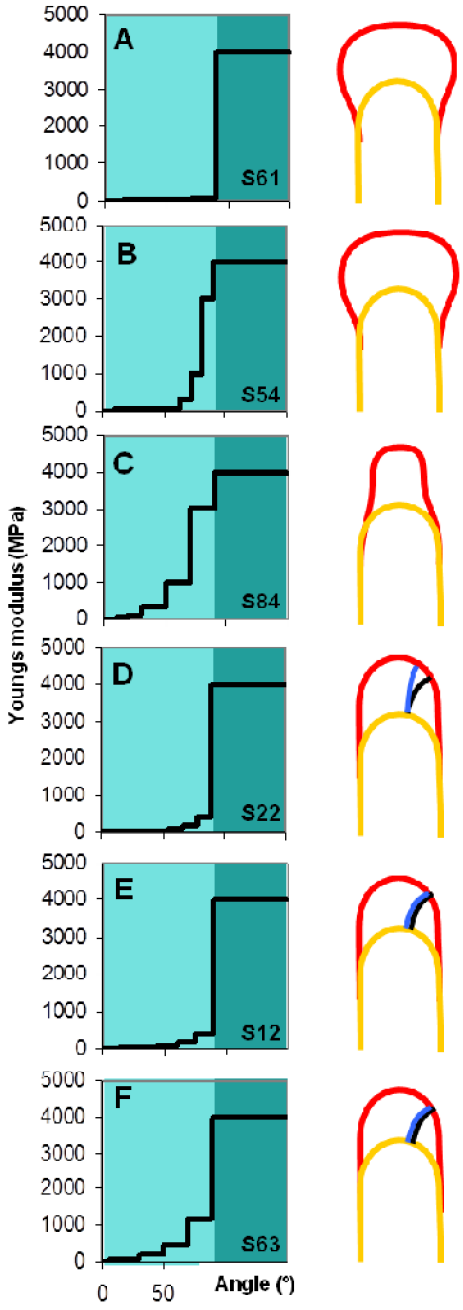

Figure 6.4: Spatial distribution of the Young's modulus in meridional direction of a representative subset of simulations.

For all simulations $m_T = 1$. The apical dome is indicated with light teal, the cylindrical shank with dark teal. Swelling of the apex could be caused by a shallow gradient (A) or by a large polar domain with low Young's modulus and a late onset in the increase of the modulus (B). Tapering was caused by a steeper gradient (C). Self-similar growth could be achieved by various parameter combinations (D-F), but these did not necessarily produce the surface strain patterns observed in growing pollen tubes (D). The simulations producing a good fit with these strain patterns (E, F) showed a steady, moderate increase in the Young's modulus within the apical dome and a sudden jump at the transition region to the shank.

Figure 6.5 Validation of simulations. (figure legend on next page)

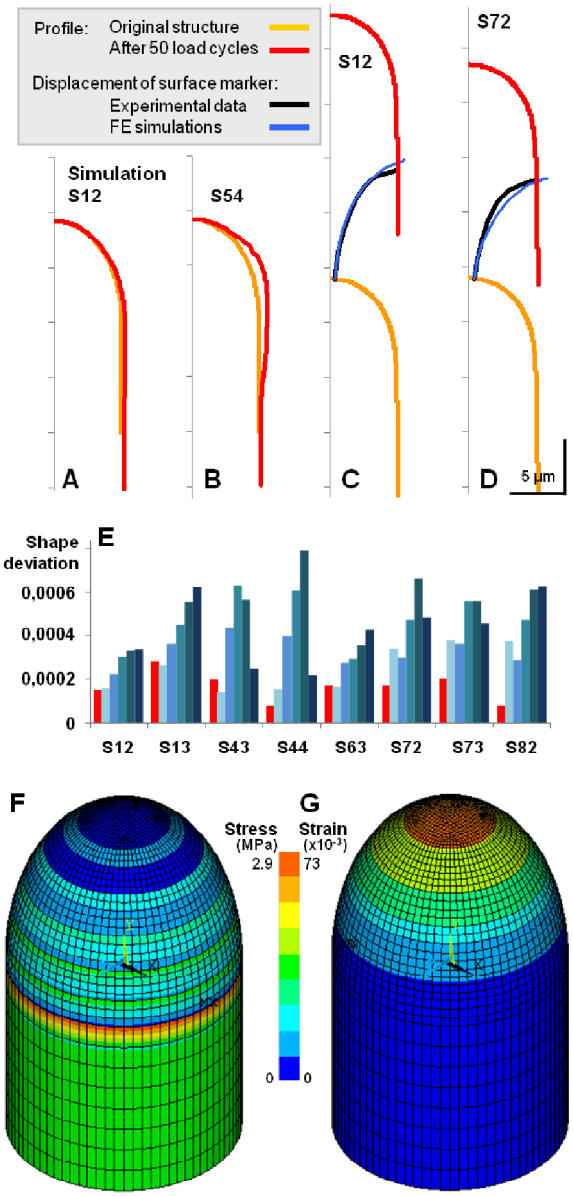

Figure 6.5: Validation of simulations.

Quantitative validation of simulations.(A, B) Self-similarity was assessed quantitatively by comparing the shape profile of a tube after 100 loading cycles (red) with the original structure (orange). Self-similarity was excellent for several simulations (e.g. S12, Fig. 6.5A), but in most others the resulting shape was very different from the original shape (e.g. S54, Fig 6.5B).(C, D) Surface deformation was assessed by comparing the paths of surface markers obtained from the simulation (blue) with experimental data obtained from (Rojas *et al.* 2011) (black). Only very few simulations showed very good agreement between both curves (e.g. S12, Fig 6.5C), whereas others showed varying degrees of deviation from the experimental data (e.g. S72, Fig 6.5D). (E) Quantitative assessment of the quality of 8 simulations previously selected based on qualitative inspection. The red bars indicate the deviation from self-similarity. The blue bars indicate the deviations in the displacement trajectories of 5 surface markers per simulation.(F) Distribution of local stresses upon load application on the surface of the 360° structure using parameter combination S12. Blue color indicates low stress at the pole, green color higher stress in the shank. Ringshaped regions of locally increased stress (green, yellow, orange) are due to discrete steps in Young's modulus between surface domains, inherent to the approximate approach chosen here. (G) Distribution of local strain upon load application on the surface of the 360° structure using parameter combination S12. Blue color indicates low or absent strain in the shank, orange indicates high strain at the pole. Despite the stress artifacts observed in (F), the strain distribution is rather gradual and does not show local maxima.

Figure 6.6

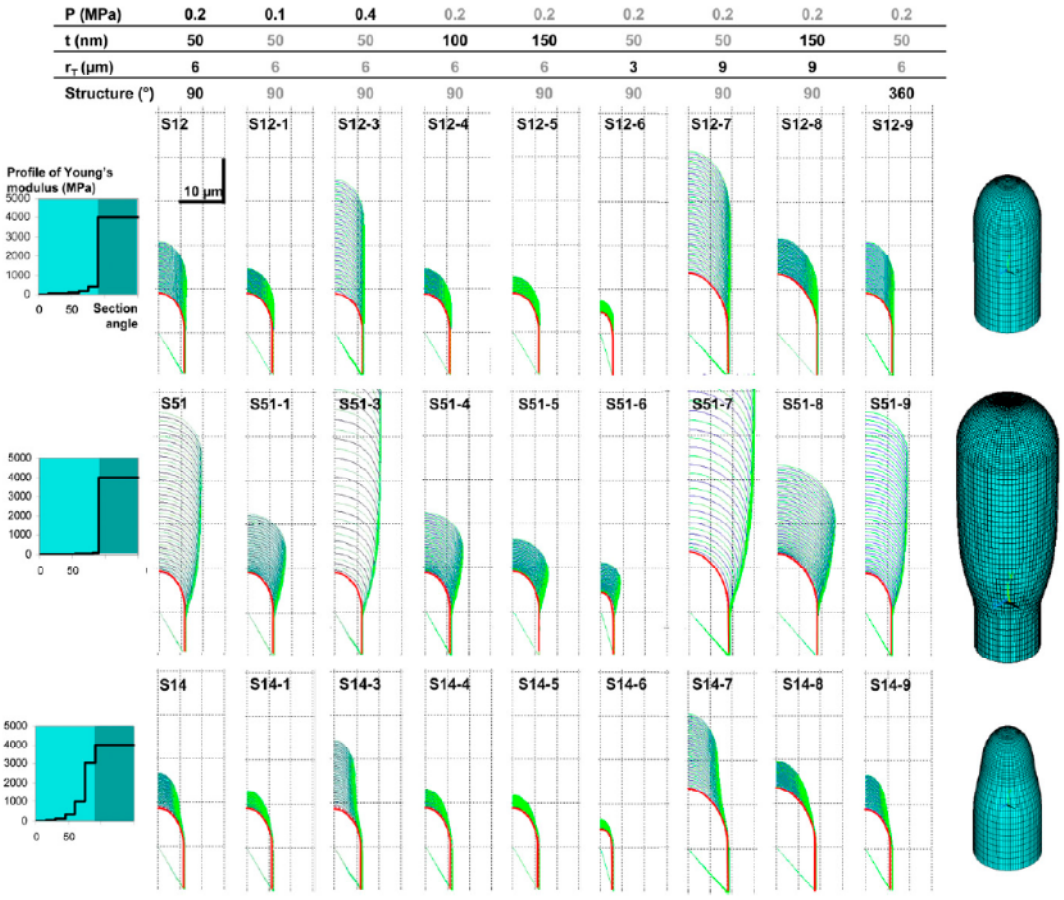

Figure 6.6: Effect of cell wall thickness, turgor pressure, tube radius, and structure on the growth pattern.

Cell wall thickness t, turgor pressure P and tube radius r_T were altered in biologically relevant ranges to test their effect on deformation geometry. The nature of apical deformation (self-similar, swelling, tapering) was not affected by any of the three parameters. The only characteristic altered was the increase in tube length per loading cycle. Simulations performed with a 360° structure demonstrated that it behaved identically to the corresponding 90° structure. All graphs show length profiles. The right column shows 3D representations of the 360° structures. The profile of the original structure is indicated by the red, dashed line. Alternating blue and green lines indicate the results of repeated load cycles. In all simulations $m_T = 1$.

Figure 6.7

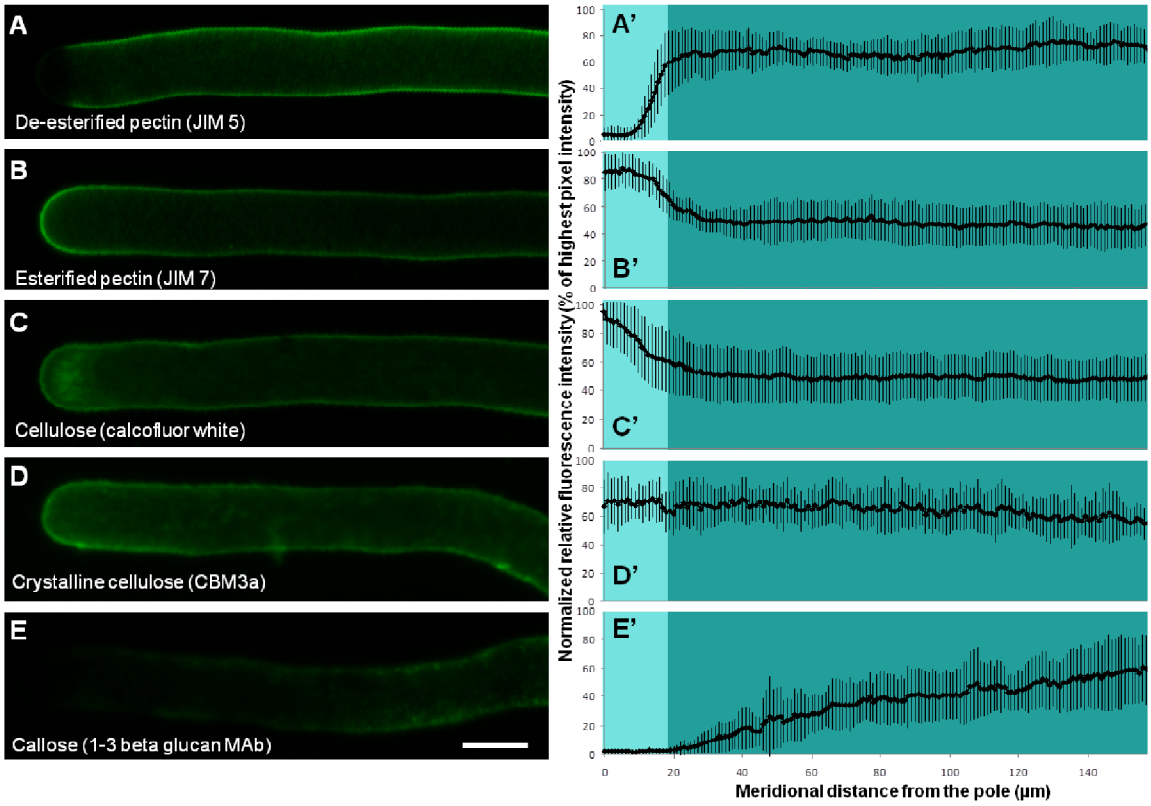

Figure 6.7: Spatial distribution of cell wall components in *in vitro* growing lily pollen tubes.

Cells were treated with specific antibodies and histochemical stains for pectins with low (A) and high (B) degree of esterification, cellulose (C), crystalline cellulose (D) and callose (D). Graphs show relative fluorescence intensity along the perimeter of the cell, normalized for each tube, and averaged over at least 10 tubes. Vertical bars are standard errors. Light teal indicates the apical dome, dark teal the cylindrical shank. Bar = 20 µm.

Figure 6.8

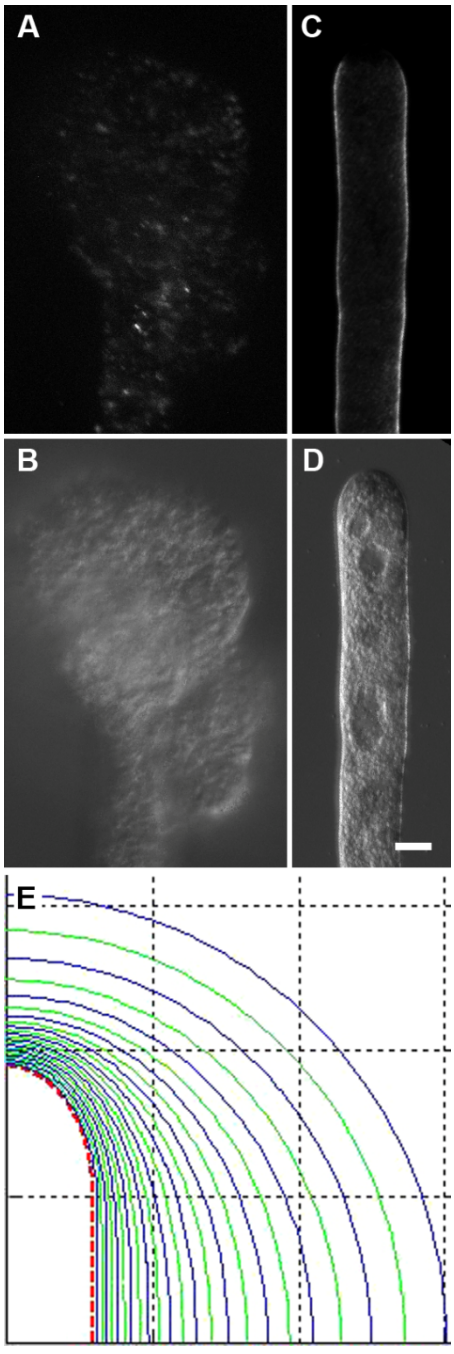

Figure 6.8: Effect of pectin digestion on pollen tube shape.

(A-D) Pre-germinated pollen tubes were treated with pectinase for 15 minutes (A,B). Pollen tubes exposed to the enzyme were swollen at the apex (A), whereas untreated tubes elongated in self-similar manner (C). Immunofluorescence label with JIM5 revealed the near absence of pectins with low degree of methyl esterification in enzyme treated samples (B) compared to the control tubes not treated with the enzyme (D). Note that the images should not be compared quantitatively since in order to reveal residual label in the enzyme treated samples, exposure time had to be at least tripled compared to the control sample. Bar = 10 µm. (E) Finite element simulation using identical Young's modulus for surface domains 1 through 7 resulted in spherical swelling of the structure. The profile of the original structure is indicated by the red, dashed line. Alternating blue and green lines indicate the results of repeated load cycles.

6.8 Supplemental table

Simulation	θ_1	θ_2	θ_3	θ_4	θ_5	θ_6	m_L	Shape of profile	Surface deformation
S11	15	15	15	15	15	15	1,5	+	nd
S12	15	15	15	15	15	15	2	0	0
S13	15	15	15	15	15	15	2,5	-	0
S14	15	15	15	15	15	15	3	–	nd
S21	30	12	12	12	12	12	1,5	++	nd
S22	30	12	12	12	12	12	2	0	–
S23	30	12	12	12	12	12	2,5	0	-
S24	30	12	12	12	12	12	3	-	nd
S31	45	9	9	9	9	9	1,5	++	nd
S32	45	9	9	9	9	9	2	+	nd
S33	45	9	9	9	9	9	2,5	+	–
S34	45	9	9	9	9	9	3	0	-
S41	12	30	12	12	12	12	1,5	++	nd
S42	12	30	12	12	12	12	2	+	nd
S43	12	30	12	12	12	12	2,5	0	-
S44	12	30	12	12	12	12	3	0	-
S61	9	45	9	9	9	9	1,5	+++	nd
S62	9	45	9	9	9	9	2	++	nd
S63	9	45	9	9	9	9	2,5	+	nd
S64	9	45	9	9	9	9	3	+	–
S81	5	10	15	20	20	20	1,5	++	nd
S82	5	10	15	20	20	20	2	+	nd
S83	5	10	15	20	20	20	2,5	0	0
S84	5	10	15	20	20	20	3	-	nd
S71	10	15	15	20	15	15	1,5	++	nd
S72	10	15	15	20	15	15	2	0	-
S73	10	15	15	20	15	15	2,5	0	0
S74	10	15	15	20	15	15	3	-	nd
S81	10	10	10	20	20	20	1,5	+	nd
S82	10	10	10	20	20	20	2	0	-
S83	10	10	10	20	20	20	2,5	-	nd
S84	10	10	10	20	20	20	3	–	nd

Supplemental Table 6.1: Parameter settings used for second set of simulations.

For all simulations the following settings applied: m_T = 1, t = 50 nm, hydrostatic pressure = 0.2 MPa. The shape of the tube after 50 load cycles was assessed qualitatively. "+" indicates swelling, "-" indicates tapering, "0" stands for self-similar. A subset of 13 simulations was assessed qualitatively for the shape of surface deformation patterns. Here "-" stands for insufficient curvature of the deformation trajectory of surface markers when compared to experimental data. Simulations marked in grey were subsequently submitted to quantitative validation for their degrees of self-similarity and surface deformation.

7 Pectate lyases promote pollen germination and lubricate the path of the pollen tube in *Arabidopsis thaliana*

During my thesis I was interested in understanding how the pollen tube is able to invade the transmitting tissue against the impediment of the apoplast. Many studies hypothesized that the transmitting tract secreted self-digesting enzymes and that in some species the transmitting cells undergo apoptosis to facilitate the pollen tube penetration. But the question that interested us was the role of the pollen tube in this process. Is the pollen tube implicated in an active wall loosening (by secreting enzymes) or in a more passive way (by applying enough pressure to penetrate the style) or in a combination of both processes? To answer these questions, we studied the role played by a pectin digesting enzyme, the pectate lyase (PL). As mentioned in the introduction of this thesis, PLs play major roles during plant cell differentiation and maturation. It has always been hypothesized that they might play an important role during pollen and pollen tube development without any clear evidence for their roles. In this chapter, using molecular biology techniques combined with live cell microscopy and protein detection, I investigate the role played by PLs in the early germination and during pollen tube elongation. I show that PLs play a major role in initiating pollen germination and that they are secreted by the pollen tube to digest the transmitting track and facilitate its penetration.

7.1 Abstract

The pollen tube is a cellular cylindrical protuberance formed by the pollen grain upon its contact with the stigma. Its main purpose is to ensure sexual plant reproduction by delivering the sperm cells to the female gametophyte. To be able to accomplish this task, the elongating pollen tube has to emerge from the pollen grain by breaking through its thick wall and it has then to penetrate the pistillar tissue without precociously bursting. Both situations require the loosening of cell wall material - during germination the pollen intine proper has to yield and during pollen tube elongation the apoplast of the transmitting tract needs to be softened to allow for pollen tube passage. Here we investigate the putative role of the pectin digesting enzymes pectate lyases (PLs) in these processes. Using mutant analysis, microscopical observations of fluorescently tagged PLs combined with fluorescence recovery after photo-bleaching (FRAP) experiments and immuno-detection, we show that PLs are required for intine loosening during the first steps of pollen tube germination. During pollen tube elongation, PLs are secreted by the pollen tube into transmitting tract, likely contributing to the digestion and loosening of the pollen tube path. Our data provide direct evidence for the long-standing assumption that pollen tubes secrete enzymes to the extracellular space which are able to interact with the transmitting tissue.

7.2 Introduction

The pollen tube, or male gametophyte, is responsible for delivering the sperm cells to the ovary to perform double fertilization leading to fruit formation and seed set. It is a rapidly growing, cylindrical protuberance that is formed by the pollen grain upon landing on a receptive stigma. In order to perform its task, the pollen tube has to invade the tissues that separate the pollen grain from the female gametophyte: stigma, style, placenta and ovule. Depending on the species, long distances (up to tens of centimeters) have to be covered, especially while traversing the style. To navigate the style, the tube has to proceed either through a tissue-lined canal or by invading the solid transmitting tissue filling the central cavity of the style. Particularly in the case of the solid style, pollen tube growth is therefore challenged mechanically by the impedance presented by the apoplast of the transmitting tissue. In *Arabidopsis*, the transmitting tract is made of cylindrical cells surrounded by a fibrous extracellular matrix (Lennon *et al.* 1998). The pollen tube is thought to employ various methods to facilitate invasive growth by softening the transmitting tissue, for example by inducing programmed cell death and/or secreting digestive enzymes presumed to target the apoplast (Ori *et al.* 1990; Cordeiro *et al.* 1994; Sessa and Fluhr 1995; Ramalho-Santos *et al.* 1997; Vieira *et al.* 2001; Chen *et al.* 2002b). However, although numerous cell wall digesting enzymes are known to be expressed by the pollen tube (Bosch and Hepler 2005), no direct experimental proof has been brought forward that these are actually secreted to the outside and employed to digest the transmitting tract. The reason for this lack of information is the fact that proper pollen tube growth also requires the action of cell wall modifying enzymes, and they might thus be produced in the context of its own morphogenesis.

The pollen tube grows by constant addition of cell wall material at the apical plasma membrane. The adjacent apical cell wall continuously yields under the internal pressure of the tube (Geitmann and Steer 2006). Morphogenesis of the cylindrical tube relies on the spatial and temporal control of the stiffening and maturation processes in the cell wall material (Fayant *et al.* 2010). This maturation is reflected in the distribution of the cell wall components along the longitudinal axis of the tube (Fayant *et al.* 2010; Geitmann 2010a).

Many biochemical pathways involving numerous enzymes were shown to be implicated in regulating pollen tube cell wall expansion and pollen tube growth (Bosch and Hepler 2005; Geitmann and Steer 2006; Chebli and Geitmann 2007; Wolf *et al.* 2012). Among the most crucial biochemical processes during pollen tube morphogenesis is the transformation of pectin during the maturation of the wall material (Chebli and Geitmann 2007). Pectins are secreted in highly methyl-esterified form at the apex, and their de-esterification allows gelation and stiffening by calcium ions. Various pectin modifying enzymes such as pectin-methyl-esterase, polygalaturonase and pectate lyase are known to be implicated in the regulation of the pectin biochemistry in plant cell walls in general and pollen tubes in particular (Bosch and Hepler 2005). These biochemical reactions contribute to the regulation of cell wall mechanics by balancing between the required degrees of stiffness, elasticity and plasticity of the wall, thus ensuring the morphogenesis of a cylindrical cell.

One of the cell wall modifying enzyme families produced by the pollen tube is the pectate lyase family. These hydrolytic enzymes have been shown to be implicated in pectin hydrolysis during cell wall expansion, cell adhesion and differentiation, and during the maturation and senescence of fruits. Pectate lyases are also a major allergens for humans (Radauer *et al.* 2008; Shahali *et al.* 2012; Suzuki *et al.* 2012). In tomato (Marin-Rodriguez *et al.* 2002), banana (Pua *et al.* 2001) and strawberries (Jimenez-Bermudez *et al.* 2002), PL activity enhances fruit maturation and their absence delays senescence. The enzyme acts on the pectic chains by cleaving the α-1,4-polygalacturonic acid chain by a β-elimination mechanism (Herron *et al.* 2000). A number of studies have shown that pectate lyase and pectate lyase like genes are highly expressed in pollen grains from tobacco, alfalfa (Wu *et al.* 1996), Japanese cedar (Taniguchi *et al.* 1995), *Nicotiana tabacum* (Wing *et al.* 1990; Kulikauskas and McCormick 1997) and in *Arabidopsis* (Kulikauskas and McCormick 1997). More than 20 pectate lyase like genes are expressed in pollen grains of *Arabidopsis* (Pina *et al.* 2005) leading to the speculation that they might be implicated in the early stages of pollen germination or in the digestion of the transmitting tract. However, no experimental proof has been provided hitherto to show that the enzyme has the function to act on the surrounding growth matrix, and that it is not simply implicated in the pollen tube morphogenesis by acting on its own wall.

Here we investigate the role of the four most expressed pectate lyase (PL) like genes At1g14420 (PL1), At2g02720 (PL2), At3g01270 (PL3) and At5g15110 (PL5) during *Arabidopsis* pollen tube germination and elongation. Using fluorescence microscopy combined with Western blot analyses we show that PLs are important for the initiation of pollen tube germination and for pollen tube elongation. We also show that PLs are secreted by the pollen tube, suggesting that they are employed to loosen the surrounding transmitting tissue cell wall to facilitate its elongation.

7.3 Material and Methods

7.3.1 Plant material

Arabidopsis thaliana ecotype Columbia-0 plants were grown in trays in a greenhouse at 22°C day temperature and 20°C night temperature, 50% humidity under 16h daylight and 300 µE m^{-2} s^{-1} light intensity. Plants were irrigated every day and fertilized every second day with Plant-Prod® 20-20-20 fertilizer at 200 ppm. Pollen was collected every day during anthesis using a modified vacuum cleaner as described by Johnson-Brousseau and McCormick (Johnson-Brousseau and McCormick 2004). The T-DNA mutants used for At1g14420 and At2g02720, were generated in the context of the GABI-Kat program and provided by Bernd Weisshaar (MPI for Plant Breeding Research; Cologne, Germany) (Rosso et al. 2003). The T-DNA mutants used for At3g01270 and At5g15110 were obtained from the National Arabidopsis Stock Center (NSAC) (Scholl et al. 2000). T-DNA insertion lines and lines expressing fluorescent tagged pectate lyases, constructed as described below, were grown on a MS medium with the appropriate antibiotic (50 µg.mL^{-1} kanamycin, 50 µg.mL^{-1} hygromycin and/or 5.25 µg.mL^{-1} sulfadiazine) before being transferred to the soil. Male sterile *Arabidopsis thaliana* Landsberg erecta was obtained from Ravishankar Palanivelu (University of Arizona).

7.3.2 *In vitro* and semi *in vivo* pollen tube growth

In vitro pollen germination was conducted on solidified *Arabidopsis* pollen tube growth medium (Bou Daher *et al.* 2009) for 3 to 6 hours depending on the experiment. For semi *in vitro* germination, stigmas of male sterile *Arabidopsis* plants were cut and placed on a solidified germination medium. Hydrated pollen grains were placed on the stigma and left to germinate for 3 to 4 hours. Pollen grains were considered germinated when the length of the pollen tube exceeded the diameter of the pollen grain. Pollen tube length was measured after 6 hours of imbibition.

7.3.3 Fluorescent tagging of pectate lyases

For native expression, the constructs included the promoter sequence 5'-UTR (about 1000 bp), the 3'-UTR and the terminator region (about 200 bp). The location of the fluorescent tag relative to the target gene was determined based on computer-assisted predictions of protein folding, cleavage sites and functional domain probabilities. *Arabidopsis* plants expressing *PL1* (At1g14420), *PL2* (At2g02720) and *PL3* (At3g01270) were generated using the fluorescent tagging of full length protein (FTFLP) technique (Tian *et al.* 2004). Briefly, two sets of primers P1-P2 and P3-P4 were designed to amplify each target genes in 5' and 3' fragments, respectively. P1 and P4 flanked the complete sequence and contained attB1 and attB2 recombination sites respectively in addition to gene specific sequences. P2 and P3 contained both gene specific sequences and sequences specific to the fluorescent protein (FP). PL1 was labeled with the cyan variant of the yellow fluorescent protein (CFP) while PL2 and PL3 were labeled with yellow fluorescent protein (YFP). Primer sequences are listed in Supplemental Table 1.

To produce a fluorescently labelled PL whose expression was regulated by the endogenous promoter, individual PCR reactions were carried out to amplify the 5' end of the target gene (flanked with an attB site and a FP specific sequence), the FP (now flanked by target gene specific sequences) and the 3 end of the target gene (now flanked by an FP specific sequence and an attB site). The fluorescent tag was combined to the two target gene PCR fragments using a triple template PCR with a forward primer containing the attB sites. All individual PCR fragments were amplified using Phusion (Finnzymes) DNA polymerase

and triple template PCR was performed using ExTaq (TaKaRa) DNA polymerase. DNA was extracted from gel using QIAquick gel extraction kit (Qiagen). Final PCR fragments were introduced into pDONR Zeo (Invitrogen) entry vector using a BP (Invitrogen) recombination reaction according to the manufacturer's instructions. Positive clones were verified by sequencing. The chimeric gene was introduced in pBIN-GW (Tian *et al.* 2004) and pMDC107 (obtained from the Arabidopsis Biological Resource Center) (Curtis and Grossniklaus 2003) destination vectors using LR recombination reaction (Invitrogen) according to the manufacturer manual. Plasmid extraction from bacteria was done with a QIAprep spin miniprep kit (Qiagen).

To produce PL-FP fusions whose expression was under the control of pLAT52, total RNA from leaves was extracted with Trizol (Invitrogen) according to the manufacturer manual. cDNA was synthesized from 5 µg RNA using the SuperScript® III First-Strand Synthesis SuperMix (Invitrogen), and PL cDNA was amplified from the cDNA using the primer sequences shown in Supplemental Table 1 and the ExTaq (TaKaRa) DNA polymerase. Final PCR fragments were introduced into pENTR TOPO vector (Invitrogen) using a TOPO cloning reaction (Invitrogen) according to the manufacturer manual. Positive clones were verified by sequencing. The chimeric gene was introduced between the 3- end of pLAT52 and the 5'-end of a GFP coding sequence in a modified pMDC107 vector. pLAT52 is a strong, pollen-specific promoter conventionally used for chimeric gene expression in pollen grains instead of the constitutive promoter p35S which is not expressed in pollen grains.

7.3.4 *Agrobacterium* mediated transformation

Wild type and corresponding PL1, PL2 and PL3 knock-out mutants of *Arabidopsis* were transformed using *Agrobacterium* mediated transformation. PL1, PL2 and PL3 knock-out plants were transformed with their respective fluorescent tagged PLs expressed under the native promoter. *Agrobacterium tumefaciens* cells (strain GV3101) were grown overnight in 500 ml of LB-medium supplemented with kanamycin (50 $\mu g.ml^{-1}$), rifampicin (100 $\mu g.ml^{-1}$) and gentamycin (50 $\mu g.ml^{-1}$) until an OD of 1.7. After centrifugation at 4000 g for 15 min, the cells were suspended in 400 mL of a 4% sucrose solution and 0.02% Silwett

77®. Arabidopsis plants were submerged upside-down in the *Agrobacterium* solution for 15 seconds, then gently shaken for 5 seconds, wrapped in plastic foil and kept on their side overnight. The second day, plants were unwrapped and left to grow in the conditions stated above. Seeds were left to dry before collection.

7.3.5 Genotyping

Knock-out lines were verified by a triple primer PCR with a specific T-DNA primer and two specific gene primers (Supplemental Table 1). The presence of fluorescent-tagged PLs in the different *Arabidopsis* lines was verified by confocal laser scanning microscopy as described below and the presence of the gene verified by PCR using a primer specific to the gene and a primer specific to the fluorescent protein. Only homozygous lines were used in this study.

7.3.6 Semi-quantitative RT-PCR

Semi-quantitative RT-PCR was used to determine the expression levels of the PLs in whole flowers of (1) knock-out lines, (2) transgenic lines expressing fluorescent PLs, and (3) hydrated wild type pollen grains. Total RNA was extracted and cDNA was synthesized as described above. Primer sequences are listed in Supplementary Table 1 while Supplemental Table 2 summarizes the different RT-PCR conditions. A total of 7 µL of each reaction mix was loaded on a 1% (w/v) agarose gel stained with ethidium bromide and band intensity on the photographs was quantified using ImageJ software. The endogenous expression levels in the transgenic lines expressing fluorescent PLs were used as a reference value for expression after normalization based on the actin expression profile. In order to amplify only the transgene, the corresponding reverse primer was chosen on the fluorescent protein.

7.3.7 Microscopic observations

In vitro and semi *in vivo* grown pollen tubes were observed with a Zeiss Imager-Z1 microscope equipped with a Zeiss AxioCam MRm Rev.2 camera and AxioVision Release 4.5 software. Pollen tubes expressing fluorescent PLs were observed with a Zeiss LSM 510 META / LSM 5 LIVE / Axiovert 200M system. In *Live* observation mode, GFP and YFP

were excited with the 488 nm argon laser and a LP 505 emission filter. In *Meta* observation mode CFP was excited with a 458 nm laser and a BP 470-500 nm emission filter, while GFP and YFP were excited with a 488 nm laser and emission filters of LP 530 and BP 505-550 respectively were used. For FRAP experiments, the 488 nm line of the argon laser was used at maximal power, output set to 12-16% for image acquisition and 100% for photobleaching, and emission filter LP 505. Quantification of FRAP was performed with the Zeiss LSM 5 Duo software. Quantification of fluorescence intensity was made at the tip of the pollen tube, the bleached region and in an area of the image that was not bleached. Values were corrected to compensate for bleaching caused in the imaging mode by dividing fluorescence intensity in the bleached region of interest by that in an unbleached region.

7.3.8 Detection of PL2-GFP in the growth medium

Wild type pollen grains and pollen grains expressing fluorescent tagged PLs were grown on *Arabidopsis* male sterile stigmas that had been cut and placed on top of a 35 µm filter mesh soaking in growth medium. Pollen tubes were grown until they passed through the cut stigma and proceeded to grow in the liquid medium for 3 hours. The liquid growth medium was then collected and filtered with a 30 kDa Centricon® regenerated cellulose membrane (Millipore) to remove sugar, salts and small molecular weight proteins (under 30 kD). For the detection of PL2-GFP 20 µL of sample was mixed to 20 µL of 4 x loading dye (100 mM Tris-base, 40% glycerol, 5% SDS, 0.005% bromophenol blue, 10% β-mercaptoethanol, pH 6.8), heated at 95°C for 10 min and separated by SDS-PAGE. Separated proteins in the gel were electrophoretically transferred onto a PVDF membrane at 35 V overnight at 4°C. The blotted membrane was rinsed in TBS buffer (140 mM NaCl, 2.7 mM KCl, 19 mM Tris-HCl, pH 7.4) and then blocked with 3.5% skim milk in TBS for 2 hours. The membrane was washed a second time with 3.5% milk. TBS and anti-GFP (Sigma) or anti-actin was added to a final concentration of 1:1000 and 1:20 000, respectively and incubated overnight at 4°C. The membrane was then washed 3 times with TBS containing 0.05% Tween 20 for 10 min. A peroxidase conjugated IgG anti-mouse (BioShop) at a final concentration of 1:20 000 was used as a secondary antibody. The bound antibodies were detected with a chemiluminescent HRP substrate (Millipore)

according to the manufacturer's instructions. Detection was done with an ImageQuant Las4000 biomolecular imager (GE).

7.4 Results

7.4.1 PL expression in pollen grains

The four PL genes investigated here (At1g14420 (PL1), At2g02720 (P2), At3g01270 (PL3) and At5g15110 (PL5)) were selected because of their high expression levels in pollen grains (Pina *et al.* 2005). RT-PCR showed that the four genes are expressed in hydrated pollen grains (Fig 7.1).

7.4.2 Pollen grains from PL knock-out mutants display lower germination rate and shorter pollen tubes

T-DNA insertion lines were used to study the effect of the lack of a given PL on the development of pollen tubes. RT-PCR was used to determine whether the expression of PLs was completely knocked-out in the mutants. The results confirmed that PL1, PL2 and PL5 were not expressed in the respective t-DNA insertion lines, whereas PL3 seemed to be partially expressed, but reduced compared to the WT (Fig 7.2).

To assess how the absence of PL expression influences pollen tube growth, pollen tubes were grown both *in vitro* on a solidified agar medium and in *semi in vivo* conditions. Only pollen grains from homozygous knock-out lines were used. The germination percentage of pollen from the 4 knock-out lines was less than half of that observed in the WT pollen (Fig 7.3). In *in vitro* conditions, WT pollen tubes started to germinate 30 mins after imbibition whereas *pl2* pollen germinated 1 hour after imbibition and *pl1, pl3* and *pl5* pollen germinated 2 hours after imbibition. Pollen grains were considered germinated when the pollen tube length was greater than the diameter of the pollen grain (Tuinstra and Wedel 2000). In both *in vitro* and *semi in vivo* conditions, the pollen tube growth rate was reduced by 47% in the knock-out lines compared to WT pollen tubes as calculated from pollen tube length measured at 4 to 6 hours after imbibition (Fig 7.3). However, after 24 hours of *semi-in vivo* growth, the length of the WT and knock-out pollen tubes was similar. To assert that

the observed phenotypes were due to the lack of PL expression, we complemented the *pl1*, *pl2* and *pl3* knock-out lines with their respective fluorescently tagged PL genes expressed under their respective native promoters. Pollen grains from homozygous complemented lines started to germinate 20 minutes after imbibition and although 18% to 25% lower than the WT, their germination rates were 30% to 40% higher than the corresponding knock-out lines. Pollen tube growth rate after 6 hours of imbibition was not significantly different from the WT, but significantly different from those observed in the corresponding knock-out lines (Fig 7.3).

Attempts were made to obtain double knock-out lines by crossing two different homozygous knock-out lines and then selfing. We crossed knock-out homozygous of *pl1* with *pl5* and *pl2* with *pl3*. Crossing the resulting double heterozygous lines never yielded a double homozygous mutant. Segregation in T2 was WT (8.1%±3%), double heterozygous (33%±3%), homozygous for one gene and heterozygous for the other (48.7%±3%) and WT for one gene and homozygous t-DNA insertion for the other (10.2%±3%) for both crossings.

7.4.3 PLs are located at the collar region of the pollen grain aperture and at the tip of the pollen tube

To determine the subcellular localization and to monitor the intracellular dynamics of PL1, PL2 and PL3, we transformed *Arabidopsis* WT plants with the genes for fluorescently tagged PLs, controlled either by the respective native promoter or by the strong, pollen specific LAT52 promoter (Twell *et al.* 1991). The rationale for using a combination of these two different approaches was to (1) understand the effect of PL over-expression on pollen tube development, (2) to be able to localize the fluorescently tagged PLs in case the native promoter was weak and (3) to compare the subcellular localization in both cases, because the expression of a protein controlled by different promoters is known to affect its localization (Röckel *et al.* 2008).

Confocal laser scanning microscopy of pollen expressing the fluorescently tagged proteins showed that PLs were abundant in the cytoplasm of non hydrated and hydrated pollen grains (Figs 7.4a,e,i). Immediately prior to germination, they were specifically located at

the collar region delineating the site of outgrowth of the future pollen tube within the pollen tube aperture. Under their respective native promoters, the three PLs were located specifically at a narrow region on the apex of older pollen tubes longer than 45 μm (Supplemental Movie 7.1), whereas they could not be detected in the distal region of the same tubes (Fig 7.4, Supplemental Movies 7.1 and 7.2). In younger tubes, PLs could be seen at the very tip and in the distal region close to the aperture but they were largely absent from the sub-apical region.

Remarkably, while prolonged observation in the confocal laser scanning microscope caused tagged PL fluorescence in the shank region to gradually bleach, the label in the continuously elongating apex did not bleach during observation (Supplemental Movie 7.2). This suggests that new, unbleached protein was continuously delivered to the growing apex, consistent with the high exocytosis activity occurring in this region.

To prove that PLs were not localized at the plasma membrane but in the cell wall, growing pollen tubes were treated with a 50% sucrose solution. In plasmolyzed pollen tubes, tagged PLs were not associated with the plasma membrane but were mainly localized in the periplasmic space between the retracted plasma membrane and the apical cell wall (Fig 7.5). Weaker label was also visible at the apical cell wall.

When PL1-CFP and PL3-YFP were expressed under control of the pLAT52, fluorescence was detected at the apical cell wall and also in cytoplasmic organelles, possibly Golgi, endosomes and/or endoplasmic reticulum (Fig 7.4d). As this appeared to be an artifact induced by overexpression, further characterization of these organelles was not pursued. The pattern of subcellular localization of PL2-YFP expressed under pLAT52 was identical to that observed when expressed under its native promoter (Figs 7.4g,h).

To assert that the chimeric genes expressed under their respective native promoters were not significantly overexpressed in the mutants, we assessed transcript levels in the inflorescence using semi-quantitative RT-PCR. The presence of the chimeric genes caused a decrease in the expression of the respective native genes. Expression of *PL1-CFP* was significantly higher than the endogene expression, *PL2-YFP* was statistically at a lower level than the endogene expression and *PL3-YFP* was at the same level as the corresponding endogene (Supplemental Fig 7.1).

7.4.4 PLs are secreted by the pollen tube at the apex

The absence of PLs in the distal region of the pollen tube suggests that the enzymes either exert their function in the apical cell wall of the tube proper or that they are extruded into the surrounding growth matrix to exert their role in the apoplast of the transmitting tissue. If the target of the PLs was the pollen tube cell wall proper, an explanation for the spatially highly confined localization at the apex is warranted, as other enzymes inserted into the pollen tube cell wall, such as pectin methyl esterase, can be found in the entire pollen tube cell wall (Röckel *et al.* 2008). However, a proteic inhibitor of this enzyme, the pectin methyl esterase inhibitor, is located only at the pollen tube apex and the spatial confinement of its localization has been hypothesized to be ensured by removal from the wall through endocytosis in the flanks of the tube (Röckel *et al.* 2008). Such a mechanism could also be envisaged for the highly pole focused localization of PLs. It could then be hypothesized that the enzyme removed from the wall in the subapical region would be recycled immediately to the pole of the cell thus minimizing the amount of new PL to be synthesized and delivered to the apex. To test this hypothesis, we photobleached the secretory vesicles in the shank region that are about to be delivered to the apex. If PLs at the pole were predominantly obtained from the putative PL pool reincorporated at the subapex, this bleaching would not be expected to have a dramatic effect on the fluorescence intensity of the PL label at the pole. The results did not support this hypothesis. When vesicles in the pollen tube shank were bleached, the fluorescence at the pole disappeared almost completely for a period of 1 to 3 seconds. This suggests that the majority of the tip localized PLs is not recycled in the flanks but derives from the shank localized sites of synthesis, likely the Golgi. FRAP analysis showed that the half-time recovery for PL1 and PL2 was between 14 and 15 seconds and that the mobile fraction was 85% and 65%, respectively (Fig 7.6). The findings were further confirmed by the fact that no internalization of fluorescence was visible at the apical plasma membrane.

New PLs are constantly delivered to the apex (as suggested by the absence of bleaching under continuous laser illumination), but not reincorporated by endocytosis (as indicated by the FRAP approach). However, if confocal scanning is used only at intervals (i.e. no bleaching expected), the fluorescence intensity of PLs at the pole or the meridional width of

the PL rich domain do not increase over time. This suggests that the continuously delivered PLs are extruded into the surrounding medium. Consistent with this, the localization of PLs in the periplasmic space after retraction of the plasma membrane shows that PLs are highly soluble. To further corroborate that PLs are truly extruded from the tube, we grew pollen tubes expressing GFP labelled PL2 on top of a cut stigma (semi-*in vitro* setup) and, once they emerged from the cut end of the stigma the pollen tubes were allowed to grow into the surrounding liquid medium. The stigma and pollen tubes were then removed and the remaining medium was used to test for secreted proteins. Salts and sugar were removed from the liquid medium by purification and a Western Blot was performed to detect GFP. The blot showed that GFP labelled PL2 was present in the growth medium, indicating that it was secreted by the pollen tubes (Fig 7.7). Label with anti-actin antibody was used as a negative control to show that the GFP-PLs on the blot were not derived from burst or damaged pollen tubes or pollen grains.

7.5 Discussion

7.5.1 Pectate lyase in required during the initiation of pollen grain germination

The pollen grain wall is made of two layers, the exine formed from sporopollenin, tryphine and wax and the intine composed largely of cellulose and pectins (Rowland and Domergue 2012) (Van Aelst and Van Went 1992). Together these wall layers form a very stiff envelope that protects the pollen grain from environmental stresses. To be able to germinate the pollen tube has to pass through the intine either by softening the different components through digestion or breaking of polymer linkages, or by exerting sufficient force to push it outwards or a combination of both (Geitmann 2010a). A multitude of cell wall hydrolyzing enzymes and agents is produced by plants, fungi and bacteria (Willats *et al.* 2001; Vincken *et al.* 2003; Cosgrove 2005) and among these many are expressed in pollen. Proteomic and genomic data have indicated the expression of xylanase, xyloglucan endotransglycolase/hydrolase, expansins, polygalacturonases, pectin methyl-esterases and pectate lyases in pollen grains of *Arabidopsis* (Pua *et al.* 2001; Pina *et al.* 2005). Some of

these enzymes have been shown and others have been stipulated to play important roles in the first stages of pollen tube initiation by hydrolyzing and loosening the grain wall at the aperture prior to germination (Bosch and Hepler 2005; Dai *et al.* 2007; Suen and Huang 2007; Valdivia *et al.* 2009). Other components such as reactive oxygen species appear during pollen hydration and during the lag phase prior to germination and were also shown to be important for pollen tube emergence (Speranza *et al.* 2012).

PLs in particular, were shown to be expressed in pollen grains (Pua *et al.* 2001; Pina *et al.* 2005). PLs were stipulated to be involved in pollen wall softening but their temporal activation and subcellular localization has remained elusive (Kulikauskas and McCormick 1997; Pua *et al.* 2001; Bosch and Hepler 2005; Pina *et al.* 2005). It was hypothesized that their role during pollen germination was to cleave the pectin matrix of the intine. This would result in locally loosening the intine cover in the aperture, thus allowing the turgor pressure inside the hydrated pollen grain to initiate germination by pushing the cell wall outwards. Vesicles filled with cell wall precursors (mainly pectins) would then fuse at the collar region and elongation of the pollen would begin (Taylor and Hepler 1997).

Here we investigated the potential role of pectate lyases during initiation of pollen tube growth and its elongation. Using RT-PCR and fluorescence localization we showed that PLs are expressed in hydrated pollen grains and that PL1, PL2 and PL3 are abundant and specifically localized at the aperture of the pollen grain prior to germination. Pollen performance of knock-out lines showed that the germination percentage was reduced by up to 60% as the result of the suppression of a single PL. Taken together these results suggest that pectate lyases are implicated in the initiation of pollen germination, likely by locally softening the intine wall, thus providing a specifically localized surface region that is conducive to the formation of a protuberance.

The pollen tubes that were able to emerge from the grains of knock-out lines displayed a reduced growth rate when compared to the wild type pollen tubes. However, this was only true after 6 hours of growth but not after 24 hours, when the length of the WT and knock-out pollen tubes was identical. This suggests that individual PLs may enhance pollen tube performance quantitatively but are not essential for their overall capacity to elongate *in vitro*. Their action seems to be more critical during the first stages of pollen germination

since the percentage of germinated pollen grains was markedly reduced in the knock-out lines. Delayed germination due to a missing PL would also explain why obtaining double homozygous mutants was not possible. According to normal Mendelian segregation, the percentages resulting from the self crossing of a double heterozygous t-DNA insertion line would be 6.25% wild type for both genes, 50% homozygous for one gene and heterozygous for the other, 25% double heterozygous, 12.5% homozygous for one gene and wild type for the other and 6.25% double homozygous. This was not the case in the observed crossings, where no double homozygous were obtained and the number of double heterozygous increased drastically to 33%. One explanation for this would be that the double knock-out pollen grains (25% of the population of pollen grains formed by a heterozygous plant) were disadvantaged by delayed germination in comparison to the pollen grains containing only a single knock-out (50% of the population). Assuming that only wild type and single knock out pollen tubes would succeed in fertilizing the ovules, the expected theoretical ratios would be very close to those that were obtained: 8.34% wild type (8.1% obtained), 25% double heterozygous (33% obtained), 50% homozygous for one gene and heterozygous for the other (48.7% obtained), 16.67% homozygous or one gene and wild type for the other (10.2% obtained) and 0% double homozygous (0% obtained). Although the double knock-out pollen grains might eventually germinate, all available ovules would be fertilized by the time the tubes reach the ovary. Moreover, pollen tube growth through the pistil maybe slower in the double knock-out pollen because of reduced overall amounts of PLs being secreted to soften the transmitting tissue.

7.5.2 Pectate lyase is secreted by the pollen tube to digest the transmitting tissue

During pollen tube elongation, PL localization is strictly confined to the tip of the pollen tube. No accumulation was visible in the distal maturing cell wall. Confocal laser scanning microscopy and FRAP experiments showed that newly synthesized PLs are continuously delivered to the tip of the pollen tube without accumulating in the wall, suggesting that PLs are secreted into the extracellular environment. This was corroborated by evidence from Western blot analysis that GFP labelled PL2 was found in the liquid *in vitro* growth

medium. Moreover, as a result of plasmolysis, the PLs accumulated in the periplasmic region, indicating that the enzymes are highly soluble and are meant to be continuously secreted during pollen tube growth.

When growing inside the pistil, the pollen tube has to invade the apoplastic space of the transmitting tract. Because of the expansive growth activity being located in the shoulder of the hemisphere shaped apex, this region is most exposed to friction forces created by the contact of the elongating pollen tube with the surrounding cells of the transmitting tract. To minimize these friction forces and to facilitate pollen tube elongation within the pistil environment, plants have developed two major strategies: (1) the activation of programmed cell death of the transmitting tissue and/or (2) the induction of secretion of auto-digesting enzymes by the style. Both of these strategies allow the loosening of the transmitting tract which facilitates pollen tube elongation. In tobacco styles, the programmed cell death of the transmitting tissue is triggered by the landing of compatible pollen on the pistil. This leads to a change in the RNA stability and to significant morphological changes in the stylar cells ultimately leading to the death of the transmitting tissue (Wang *et al.* 1996b; Wu and Cheung 2000). Cell death has been hypothesized to be necessary to provide nutrients to growing pollen tubes but also to facilitate the pollen tube penetration. Auto-digestion of the stylar tissues by hydrolytic enzymes is involved in the degradation and remodelling of the apoplast of the transmitting tract shortly prior to and during pollen tube growth. The style specific *β*-glucanase SP41 in tobacco reaches its peak 2 days before anthesis and remains high until style senescence (Ori *et al.* 1990; Sessa and Fluhr 1995). Aspartic proteinases in *Arabidopsis thaliana* transmitting tissue (Chen *et al.* 2002b) and in *Cynara cardunculus* transmitting tissue, stigmatic papilla and epidermal cells of the style (Cordeiro *et al.* 1994; Ramalho-Santos *et al.* 1997; Vieira *et al.* 2001) degrade the transmitting tract and facilitate pollen tube penetration.

The auto-digestive activity of the transmitting tract is likely to considerably aid pollen tube invasion, but it has long been hypothesized that the pollen tube ensures successful passage by adding its own enzymes to the mix. The pollen tube is known to express and therefore thought to secrete wall digesting enzymes and agents such as xylanase (Suen and Huang 2007), β-expansins (Valdivia *et al.* 2009) or polygalacturonases (Marin-Rodriguez *et al.*

2002), but the actual extrusion of these agents from the cell into the surrounding matrix has not been proven experimentally. Our findings show clearly that the *Arabidopsis* pollen tube extrudes PLs into the *in vitro* growth medium. This is consistent with bio-informatics studies using SignalP 4.0 (Petersen *et al.* 2011) and Pfam databases (Punta *et al.* 2012) showing that once exocytosed, the PL's N-terminal domain is cleaved. This suggests that PLs are not attached to the plasma membrane but rather relocated into the cell wall or, as suggested by our findings, into the extracellular space. It is therefore reasonable to presume that *in planta* these enzymes are meant to cause the 'liquefication' of the apoplast of the transmitting tissue. We predict that this process decreases the friction forces between the advancing tube and the style and facilitates invasion similar to a lubricant.

When expressing the fluorescently tagged PLs under the strong LAT52 promoter, PL1 and PL3 were not restricted to the apical cell wall, but were also localized inside cytoplasmic organelles. The mis-localization of a protein expressed under a strong promoter is a common phenomenon that was observed for example for the pectin methyl esterase inhibitor expressed under LAT52 instead of its native promoter (Röckel *et al.* 2008). Given that PLs are pectin degrading enzymes and highly soluble, excess amounts may be toxic to the pollen tube if secreted in excess because it might damage its own cell wall. The relocalization of excess PLs into cytoplasmic organelles (possibly endosomes) may therefore be a strategy to prevent the auto-destruction of the pollen tube's own wall.

7.5.3 Digested pectins could act as signaling molecules

The role of PL mediated digestion of the apoplast of the transmitting tract may not be limited to a mechanical role of lubrification, but could be further reaching. PLs cleave long pectin chains into oligogalacturonides. Oligogalacturonides play the role of signaling molecules; they are known to induce plant defense mechanisms, to regulate plant growth and development, and to be implicated in the molecular communication between rhizobia and legumes (Ridley *et al.* 2001; Field 2009; Hématy *et al.* 2009; Moscatiello *et al.* 2012; Wolf *et al.* 2012). One could therefore argue that oligogalacturonides resulting from PL activity serve as signals that lead the pollen tube through the most 'liquefied' path of the style. Though further investigation is required to reveal whether and how the

oligogalacturonides resulting from pectin digestion may be involved in pollen tube guidance, the idea that sugar rich components (such as arabinogalactan proteins) contribute to guiding the pollen tube throughout the style has been brought forward earlier (Coimbra and Pereira 2012). The novel concept here would be that the pollen tube itself actually causes these signaling molecules to be produced, and might play a pivotal role in its own guidance. How these signals are integrated with other external cues provided by the ovary and ovule tissues remains to be investigated. Only few guiding molecules have been identified so far, these include chemocyanin in *Lilium*, calcium, EA1 in maize and LURE in *Torenia fournieri* (Cheung and Wu 2001; Higashiyama *et al.* 2003; Geitmann and Palanivelu 2007; Higashiyama and Hamamura 2008; Dresselhaus and Márton 2009; Higashiyama 2010; Palanivelu 2011; Palanivelu and Tsukamoto 2012).

7.6 Conclusion

To our knowledge, this is the first time that protein secretion into the extracellular environment is proven to take place during pollen tube elongation. We showed that pectate lyases play two major roles during pollen tube development: PLs initiate pollen germination and are secreted by the elongating tube, likely to facilitate its invasive growth by digesting the pectins composing the apoplast of the transmitting tissue. Figure 7.8 summarizes our model for PL localization and dynamics during pollen tube development. Our findings open the door to a better understanding of the interaction between the male gametophyte and the female transmitting tract.

7.7 Acknowledgment

We would like thank Jonathan Soulard and Mario Cappadocia (Université de Montréal, Montréal, Qc, Canada) for kindly providing the pMDC107 and the modified pMDC107 with pLAT52 and GFP.

We would like to thank Natasha Raikhel (University of California Riverside, CA, USA) for kindly providing the pBIN-GW, p-Citrine3 and p-CFP plasmids.

We would like to thank Dr. Ravi Palanivelu (University of Arizona, AZ, USA) for kindly providing the *Arabidopsis* male sterile line.

Research in the Geitmann lab is supported by grants from the Natural Sciences and Engineering Research Council of Canada (NSERC) and the *Fonds Québécois de la Recherche sur la Nature et les Technologies* (FQRNT). Youssef Chebli is funded by the Ann Oaks doctoral scholarship of The Canadian Society of Plant Biologists / La Société canadienne de biologie végétale.

7.8 Figures

Figure 7.1

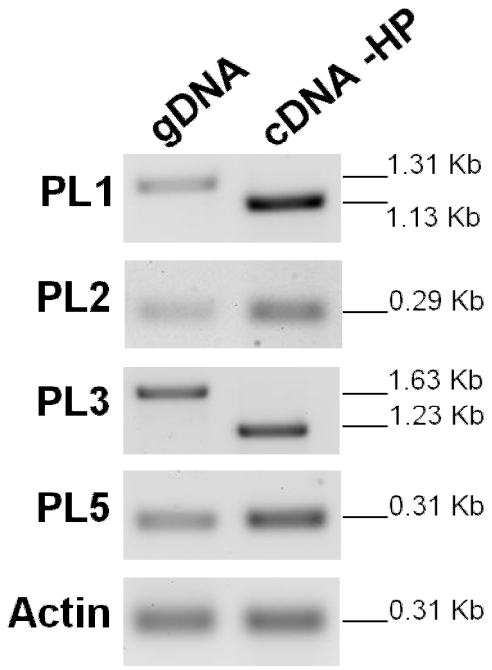

Figure 7.1: Expression of pectate lyases in pollen tubes and hydrated pollen grains.

RT-PCR was performed on cDNA from wild type hydrated pollen grains and pollen tubes. As a positive control, PCR on genomic DNA was also performed with the same sets of primers. Each gel represents the amplification of one PL or actin. Values of the molecular weight markers are indicate at the right of each gel.

Figure 7.2

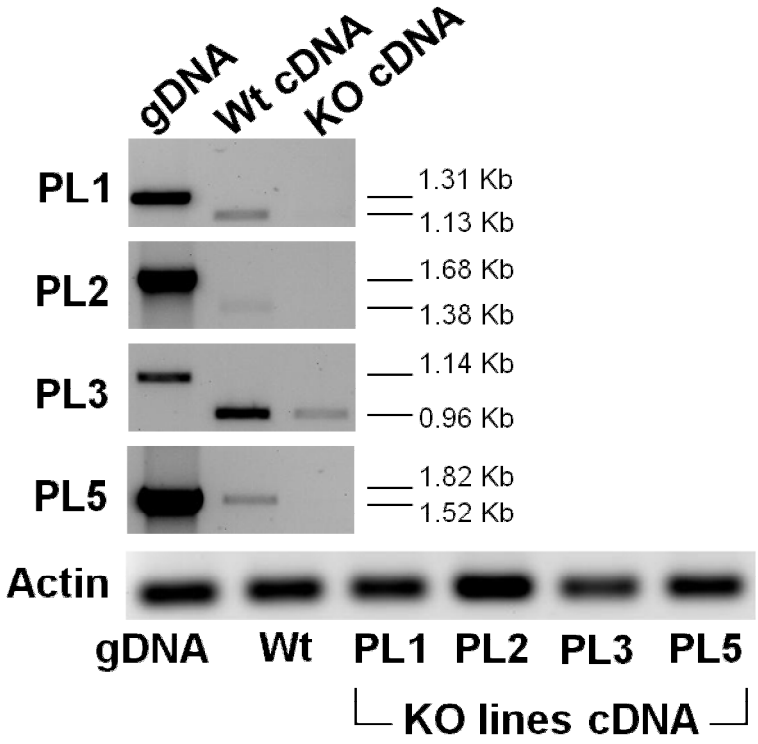

Figure 7.2: Expression of pectate lyases in wild type and knock out lines.

Semi-quantitative RT-PCR was performed on leaf cDNA from wild type and knock-out lines. As a positive control, PCR on genomic DNA was also performed with the same sets of primers. Each gel represents the amplification of one PL or actin. Values of the molecular weight markers are indicate at the right of each gel.

Figure 7.3

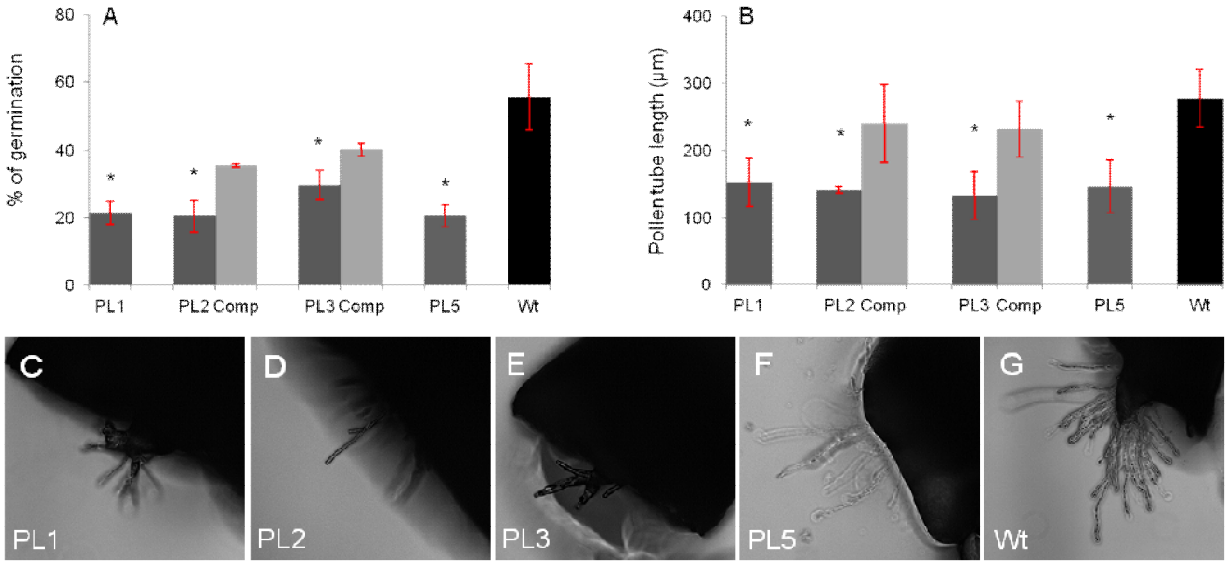

Figure 7.3: Percentage of germination and pollen tube length in knock out lines, complemented lines and wild type grown in *in vitro* conditions.

Percentage of germination (A) and pollen tube length at 6 h (B) in knock out lines (dark grey), complemented lines (light grey) and wild type (black) grown in *in vitro* conditions. Red bars represent the standard error from five repeats. Asterisks (*) show that the corresponding sample is statistically different from the wild type (two way t-test, $p<0.0001$ all samples). Pollen tubes from knock out lines grown in semi *in vivo* conditions (C to G). The images were taken after 6 hours of contact with the stigma. Bar = 10 µm.

Figure 7.4

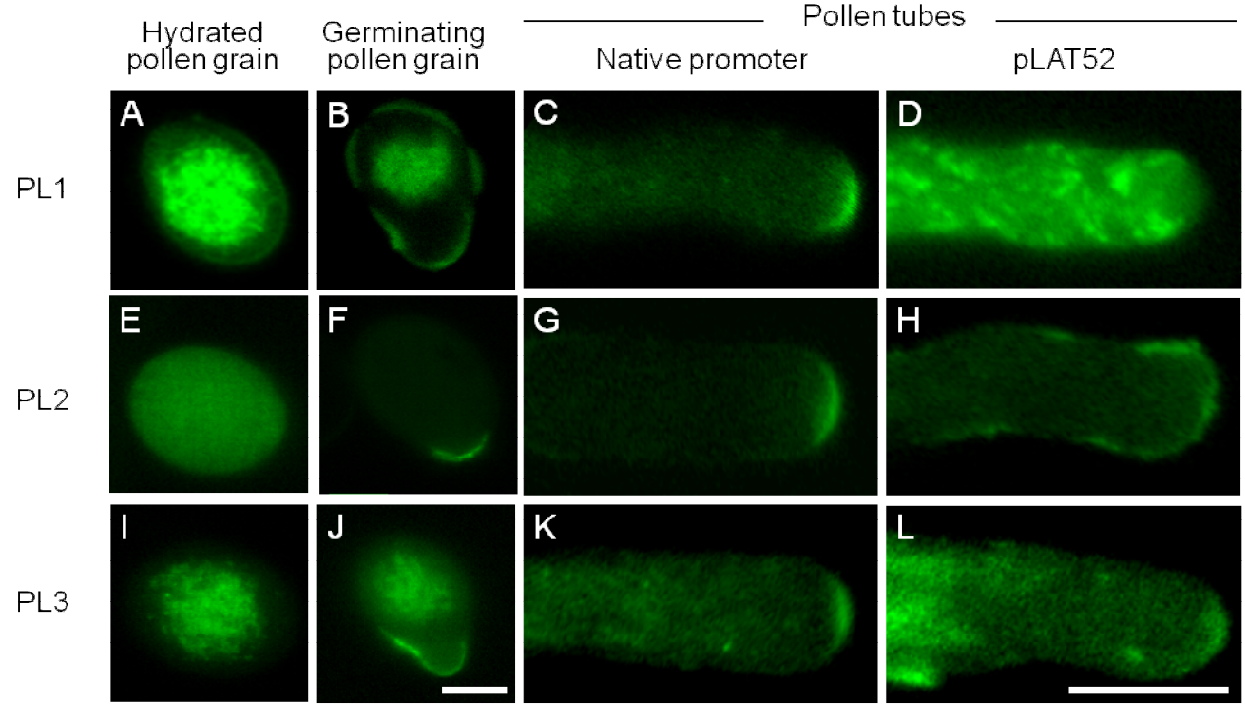

Figure 7.4: Localization of PLs in pollen grains and tubes.

Single confocal sections of hydrated pollen grains (A,E,I), germinating pollen grains (B,F,J), and pollen tubes (C,D,G,H,K,L) expressing fluorescently tagged pectate lyases PL1 (A,B,C,D), PL2 (E,F,G,H) and PL3 (I,J,K,L) under the native promoter (A,B,C,E,F,G,I,J,K) or pLAT52 (D,H,L). Scale bar in J is the same for all pollen grains (A,B,E,F,I,J) and scale bar in L is the same for all pollen tubes (C,D,G,H,K,L). Scale bars = 10 µm.

Figure 7.5

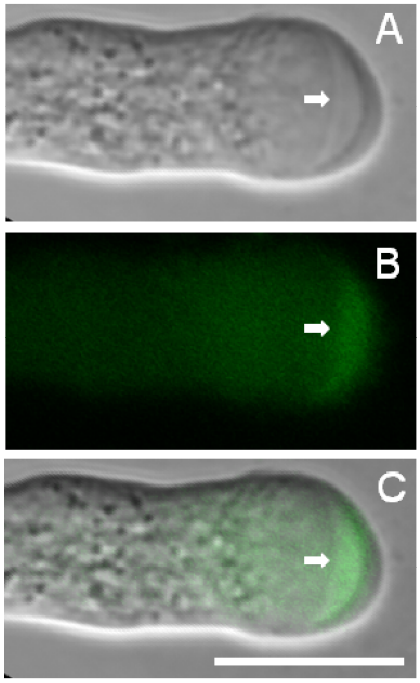

Figure 7.5: Periplasmic localization of *PL2-YFP* in plasmolysed pollen tubes.

(A) Differential interference contrast micrograph, (B) confocal laser scanning micrograph of *PL2-YFP*, (C) merged image. Arrow indicates the localization of the retracted plasma membrane. Bar = 10 µm.

Figure 7.6

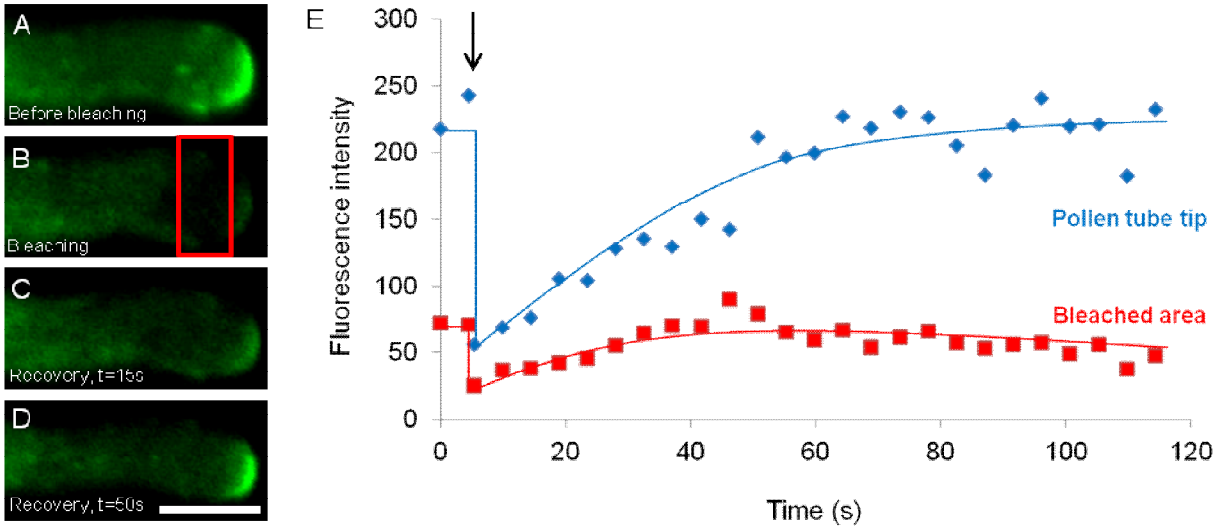

Figure 7.6: FRAP analysis of *PL1-CFP* dynamics in the apex of a growing pollen tube.

Single optical sections of a bleached pollen tube (A to D) taken before bleaching (A), immediately after bleaching (B), 15 s (C) and 50 s (D) after bleaching. (E) Relative fluorescence intensity in the bleached area (red curve) and at the tip of tube (blue curve). Red frame in B identifies the bleached area. Black arrow in (E) indicates the time of bleaching. Bar = 10 µm.

Figure 7.7

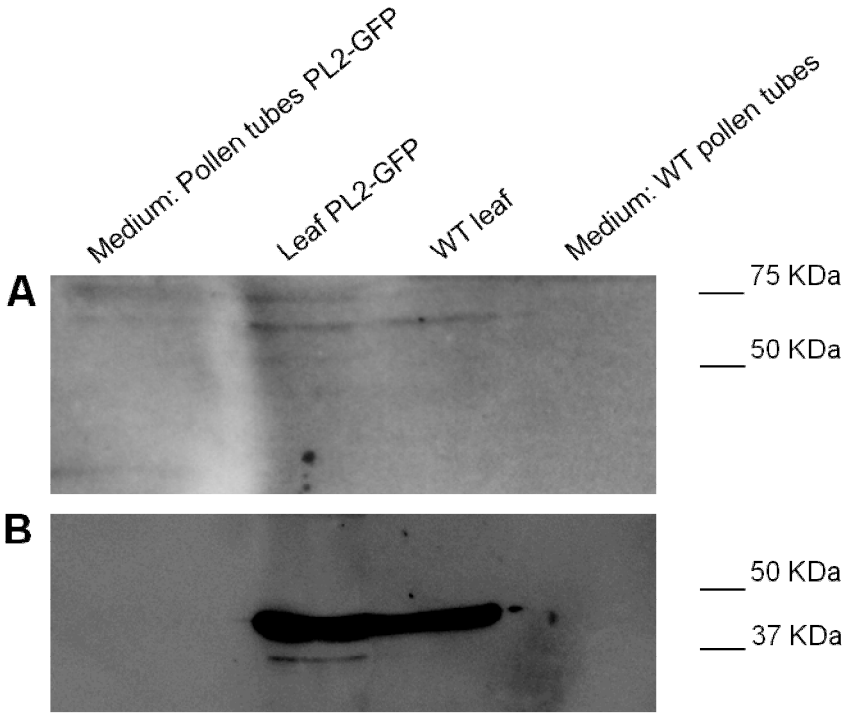

Figure 7.7: Immuno-detection of *PL2-GFP* in the pollen tube growth medium.

Immuno-detection of *PL2-GFP* in the pollen tube growth medium by Western blot using an anti-GFP. (A*) PL2-GFP* detection and (B) actin detection in PL2-GFP pollen tube growth medium (1), in whole protein extract from PL2-GFP (2) and wild type (3) leaves and wild type pollen tube growth medium (4).

Figure 7.8 Conceptual model for the localization and dynamics of PLs during pollen tube development. (legend on next page)

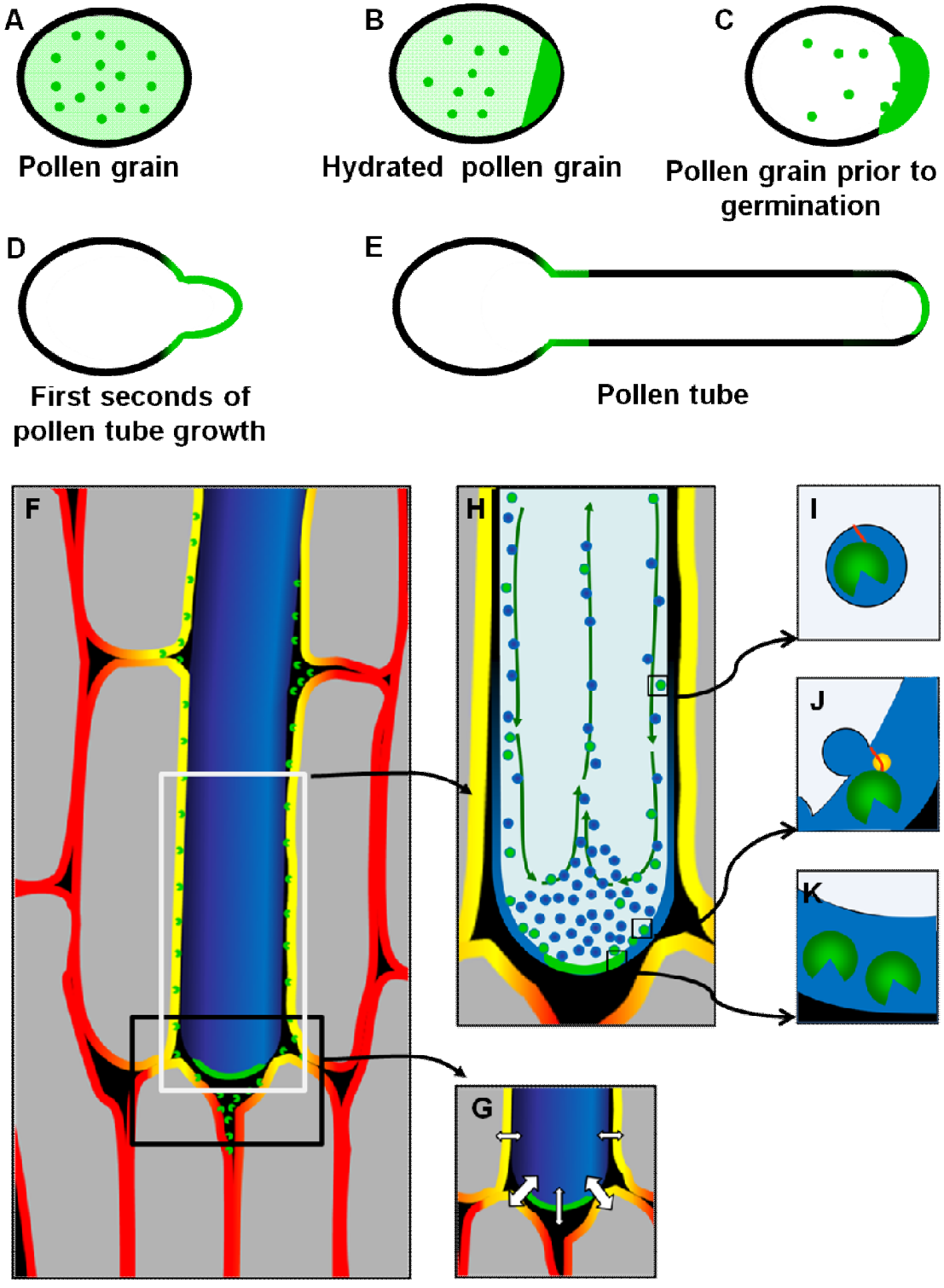

Figure 7.8: Conceptual model for the localization and dynamics of PLs during pollen tube development.

Schematic of the localization (A to E) of PLs (green) in non hydrated pollen grains (A) in hydrated pollen grains (B), in pollen grains few seconds prior to germination (C), during the first minute of pollen tube elongation (D) and during pollen tube growth. (F to K) Schematic of PL dynamics during pollen tube growth. (F) The pollen tube (blue) invades the transmitting tract and is in physical contact with the surrounding walls (yellow and red) of the transmitting tissue cells. PLs (green) are secreted at the pollen tube tip and contribute to loosening the transmitting tract cell wall, thus decreasing its stiffness. The relative stiffness of the walls is color coded with red representing stiffer walls and yellow softer walls. (G) Close up showing the relative forces applied on the pollen tube cell wall (white arrows) while elongating in the transmitting tract. Because the shoulders of the growing pollen tubes have to separate the cell walls of the transmitting tissue, they are likely subject to significant mechanical stress (arrows). This invasion of the apoplastic space would therefore be facilitated by a softened wall (red to yellow color shift). (H) Vesicles containing cell wall precursors (blue) and pectate lyases (green) are delivered to the apical plasma membrane of the pollen tube where they fuse and deliver their content (green arrows). PLs are anchored to the vesicle membrane by their N-terminal (red line in I) and when exocytosed, the N-terminal domain is cleaved (yellow circle in J) and PLs are released into the periplasmic space and cell wall (K) prior to their release into the extracellular medium (green dots in F). Objects are not drawn to scale.

7.9 Supplemental data

Supplemental Table 7.1 Sequence of the primers used in this study

Experiment	Gene	Primer name	Primer sequence
Genotying		T-DNA_primer	5'-atattgaccatcatactcattgc-3'
	PL1: At1g14420	GK074A12-Fwd	5'-ctgtctttgatagctactg-3'
		GK074A12-Rev	5'-agctccgttgagaaagtaatct-3'
	PL2: At2g02720	GK557E02-Fwd	5'-tctctcaccactgctgatt-3'
		GK557E02-Rev	5'-caaatagcatcacctgcattaaga-3'
	PL3: At3g01270	GK703E09-Fwd	5'-ttctgaagcataatccctctttgt-3'
		GK703E09-Rev	5'-gatgatttctagtccgaca-3'
	PL5: At5g15110	GK868E06-Fwd	5'-tttgtttaccagcatgttttatgc-3'
		GK868E06-Rev	5'-gacaaacatatgcaagtcac-3'
Fluorescent tagging – Native promoter	PL1: At1g14420	P1-PL1	5'-gctcgatccacctaggctgccgggaatctgtggaaactcct-3'
		P2-PL1	5'-cacagctccacctccacctccaggccggccgcaagcttcaccaagtttgcag-3'
		P3-PL1	5'-tgctggtgctgctgcggccgctggggcctgattacataaccattttgccccttcca-3'
		P4-PL1	5'-cgtagcgagaccacaggactctggtgctcttgggtccac-3'
	PL2: At2g02720	P1-PL2	5'-gctcgatccacctaggctgtggctatcggaagaggacgattggt-3'
		P2-PL2	5'-cacagctccacctccacctccaggccggccgcaggacttgccaggtttgcag-3'
		P3-PL2	5'-tgctggtgctgctgcggccgctggggcctgagaaaagcttgtgcgtgtgtgttc-3'

		P4-PL2	5’-cgtagcgagaccacaggagcatagcatctttggtggtatggtgc-3’
	PL3: At3g01270	P1-PL3	5’-gctcgatccacctaggctccggcaggagagaaagtggtgat-3’
		P2-PL3	5’-cacagctccacctccacctccaggccggccatccaatgctccggcgtatttggt-3’
		P3-PL3	5’-tgctggtgctgctgcggccgctggggcctgccgggtcggaaaagcatgctaa-3’
		P4-PL3	5’-cgtagcgagaccacaggaggagagacatgatagaagcaccccggt-3’
		attB1-Fwd	5’-ggggacaagtttgtacaaaaaagcaggctgctcgatccacctaggct-3’
		attB2-Rev	5’-ggggaccactttgtacaagaaagctgggtcgtagcgagaccacagga-3’
Fluorescent tagging – LAT52 promoter	PL1: At1g14420	PL1-Fwd	5’-caccatggcagcagctttcttgaatct-3’
		PL1-Rev	5’-gcaagcttcaccaagtttgca -3’
	PL2: At2g02720	PL2-Fwd	5’-caccatggtgaatcttgggagctacg-3’
		PL2-Rev	5’-gcaggacttgccaggtttgca -3’
	PL3: At3g01270	PL3-Fwd	5'-caccatggagacggctaggcttttca-3’
		PL3-Rev	5’-gcatgcttttccgacccggca-3’
RT-PCR (1) knock-out lines	PL1: At1g14420	PL1-KOFwd	5’-ctgtctttgatagctactg-3’
		PL1-KORev	5’-agctccgttgagaaagtaatct-3’
	PL2: At2g02720	PL2-KOFwd	5’-cactgctgattcaaatggtg-3’
		PL2-KORev	5’-gcaggacttgccaggtttgca-3’
	PL3: At3g01270	PL3-KOFwd	5’-ttctgaagcataatccctctttgt-3’
		PL3-KORev	5’-gatgatttctagtccgaca-3’
	PL5: At5g15110	PL5-KOFwd	5’-cttaacccctaagaaaacaag-3’
		PL5-KORev	5’-acagcgtctcccgactctg-3’
RT-PCR (2) transgenic fluorescent lines	PL1: At1g14420	CFP-Fwd	5’-acaacatcgaggacggca-3’
		PL1Ft-Fwd	5’- gctcccaaacaagtttaca-3’
		PL1Ft-Rev	5’- tttgttggaaggggggcaa-3’
	PL2: At2g02720	YFP-Fwd	5’-acaacatcgaggacggca-3’
		PL2Ft-Fwd	5’-cattgctcctcctattgaaga-3’
		PL2Ft-Rev	5’- acacgcacaagcttttctca-3’
	PL3: At3g01270	YFP-Fwd	5’-acaacatcgaggacggca-3’
		PL3Ft-Fwd	5’- cgtccacgttgtcaacaat-3’
		PL3Ft-Rev	5’- tgcttttccgacccggca-3’
RT-PCR (3) hydrated pollen grains and pollen tubes	PL1: At1g14420	PL1P-Fwd	5’-ctgtctttgatagctactg-3’
		PL1P-Rev	5’-agctccgttgagaaagtaatct-3’
	PL2: At2g02720	PL2P-Fwd	5’-cactgctgattcaaatggtg-3’
		PL2P-Rev	5’-ctccatagctaaggcggca-3’
	PL3: At3g01270	PL3P-Fwd	5’-ttctgaagcataatccctctttgt-3’
		PL3P-Rev	5’-atggagacggctaggctt-3’
	PL5: At5g15110	PL5P-Fwd	5’-cttaacccctaagaaaacaag-3’
		PL5P-Rev	5’-agttgtcgtagtgacgctc-3’
	Actin	Fwd	5’-aacgaccttaatcttcatgctgc-3’
		Rev	5’-ggtaacattgtgctcagtggtgg-3’

Supplemental Table 7.2: Experimental details of the semi-quantitative RT-PCRs

Experiment	RNA quantity (µg)	Annealing temperature (°C)	Number of cycles
1-Knockout lines	5	60.5	25
2-Transgenic fluorescent lines	5	56	25
3-Pollen grains and tubes	2	55	26

Supplemental Figure 7.1

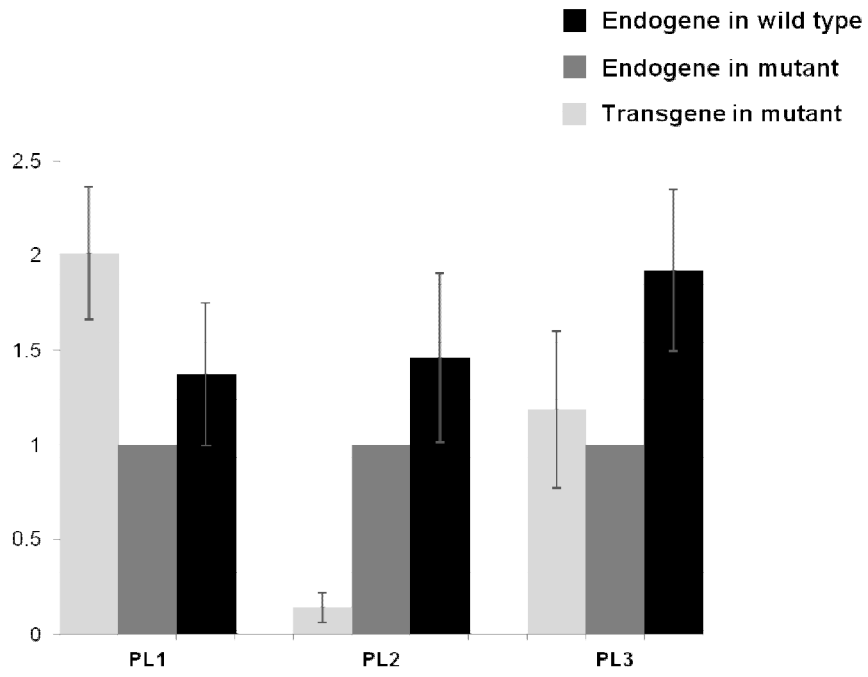

Supplemental Figure 7.1 : Relative expression levels of endogenes and transgenes assessed by semi-quantitative RT-PCR in whole *Arabidopsis* flowers.

Light grey - transgene (PL1, PL2 or PL3) in mutant, dark grey -endogene (PL1, PL2 or PL3) in mutant, black - endogene (PL1, PL2 or PL3) in wildtype. Expression levels were normalized to actin levels. Values represent the mean (n=3) and vertical bars represent the standard deviation.

Supplemental Movie 7.1: Localisation of *pPL2:PL2-YFP* expressed in *Arabidopsis* pollen tube. 3D reconstruction from stacks taken at 0.5 µm interval in false colors where higher fluorescence intensity in green and lower intensity in purple. Width of the frame equals 55 µm.

Supplemental Movie 7.2: *Arabidopsis* pollen grain expressing *pPL2:PL2-YFP* during the first stages of germination and during pollen tube growth. Images were acquired at a rate of 60 frames.s^{-1}. The video was reconstructed from 4 separate videos of the same tube. Width of the frame equals 55 µm.

8 Gravity research on plants: use of single cell experimental models

With the current development of new projects to implement permanent habitable bases on the Moon, Mars or on terrestrial orbits, it has become important to understand how plants develop and behave in conditions that are different from those on Earth. Important factors such as the presence of air convection, the relatively constant amount of space radiation and the constant gravity levels change drastically when passing the stratosphere. In the next two chapters, we review first the role played by gravity on plant cells and tissue development and show the importance of the use of single cell system to study the effect of gravity on growth and metabolism. We then study the effects of omnidirectional gravity and hyper-gravity conditions on *in vitro* pollen tube growth. This study was done in collaboration with the European Space Agency (ESA). ESA funded this research and allowed us to use the 3-D Random Position Machine and Large Diameter Centrifuge (LDC) at the European Space Research and Technology Centre (ESTEC) located in The Netherlands. By placing a fluorescent microscope on board the LDC, we were able to acquire live images of vesicle trafficking in growing pollen tubes at different *g*-levels. We also studied the effect of altered gravity on the geometry of the pollen tube and on the deposition and distribution of the different cell wall components. We show that in altered gravity conditions, pollen tube metabolism is altered.

This manuscript entitled “Gravity research on plants: use of single cell experimental models” was published in 2011 in *Frontiers in plant science* volume 2.

Youssef Chebli, Anja Geitmann

8.1 Abstract

Future space missions and implementation of permanent bases on Moon and Mars will greatly depend on the availability of ambient air and sustainable food supply. Therefore, understanding the effects of altered gravity conditions on plant metabolism and growth is vital for space missions and extra-terrestrial human existence. In this mini-review we summarize how plant cells are thought to perceive changes in magnitude and orientation of the gravity vector. The particular advantages of several single celled model systems for gravity research are explored and an overview over recent advancements and potential use of these systems is provided.

Key words

Gravity, gravitropism, gravimorphogenesis, hypergravity, microgravity, pressure model, statolith, statocyte

8.2 Introduction

Long term space missions will greatly depend on the availability of ambient air, sustainable food supply and treatment of human waste, all of which can be enhanced and improved through the cultivation of plants on board the space craft (Musgrave 2007; Wheeler 2010). Plants also provide calming effects and emotional benefits that can be pivotal in the confined environment of a space craft or orbital platform as they help astronauts to fight loneliness and depression. The positive psychological effects on the crew have the potential to reduce stress resulting from the living and working conditions during a mission (Williams 2002; Zimmermann 2003). Because of their multiple roles, plants will play a primordial role in future space missions and understanding the plant metabolic and morphogenetic responses to altered gravity conditions is indispensable for the development of space craft ecosystems or long term planetary colonization at the fractional gravity levels found on the Moon (1/6 Earth's *g*) or Mars (3/8 Earth's *g*).

Cultivation of plants on orbital platforms affects growth of organs and individual cells as was shown in many plant species (Cowles *et al.* 1984; Kuang *et al.* 1996; Wolverton and Kiss 2009; Matsumoto *et al.* 2010) although in many of these experiments the observed phenomena were a result of the combination of the direct effect of the absence of gravity on the plant and of other environmental factors such as increased radiation or absence of convection. Unlike most biotic and abiotic types of stress to which plants have been exposed to during their evolution, gravity is the only constant factor, both in direction and magnitude, to which plants had to adapt in a permanent manner. To withstand the mechanical load imposed by gravity on terrestrial organisms, plants developed mainly two strategies. The first is based on the generation of a hydroskeleton which creates an erectile force based on the balance between the internal turgor pressure and the mechanical constraint by a highly tensile resistant extracellular matrix, the cell wall. The second is based on the fortification of the cell wall through hardening that even in the absence of internal turgor allows the individual cells to stay upright against the effect of compressive forces caused by gravity (Volkmann and Baluška 2006). Modification of cell wall composition is, therefore, a readily observed phenomenon in plants exposed to a change in

g-force (Waldron and Brett 1990). This type of response has been termed **gravity resistance** (Hoson and Soga 2003). Experiments that are performed to study these architectural responses of plants to the effect of *g*-force are generally based on increasing its magnitude through placing the specimen into a centrifuge, or by decreasing it through exposure to omnilateral or true micro-gravity conditions (Hemmersbach *et al.* 1999; Hoson and Soga 2003) (Figs 8.1a,b). Omnilateral micro-gravity conditions can be produced in a clinostat or a random positioning machine by turning the specimen in rotary 2D motion or randomly in 3D, either at slow or rapid speed (Skagen and Iversen 1999) (Fig 8.1c). This does not actually alter the magnitude of the gravity force but it minimizes the effect associated with a unidirectional stimulus. True micro-gravity conditions can be achieved either on orbital platforms or during the free fall phase of sounding rocket and parabolic flights.

Plants do not only respond to a change in magnitude but also to a change in orientation of the *g*-vector. These responses are termed **gravimorphogenetic** and are typically expressed in form of a **gravitropic** behavior that is oriented in the direction of the *g*-vector (positive gravitropic) or opposed to it (negative gravitropic) (Kiss 2000; Hoson and Soga 2003). Typical responses include the reorientation of the root and the shoot of a plant that has been turned on its side. Numerous studies have investigated these gravitropic responses both in multicellular organisms and single cells (Baluška and Hasenstein 1997; Braun and Sievers 2000; Kiss 2000; Perbal and Driss-Ecole 2003; Morita 2010). Typical experiments include simple changes in the direction of the gravity vector by reorienting the sample (Fig 8.1d). However, these experiments are frequently also conducted under micro- or hyper-gravity conditions to enhance the response and analyze dose-effect relationships. Intriguingly, in multicellular organisms, the gravitropic response typically occurs at a location that is spatially separated from the cells that are responsible for the perception of the directional signal and thus requires long-distance signaling processes about which our understanding has significantly improved in recent years (Haswell 2003; Morita 2010). Auxin is an important mediator of gravity response in roots and shoots (reviewed by Morita, 2010). Gravitropism in *Arabidopsis* roots is controlled by basipetally transported auxin (Rashotte *et al.* 2000). Consistent with the important role of the hormone, transcriptomic studies have

shown that the expression of genes related to auxin biosynthesis is altered by a change in gravity level (Tamaokiet al 2009). Several auxin transporters from the PIN and PGP families are known to be involved in the distribution and the direction of auxin fluxes. The involvement of auxin and auxin transporters in gravisensing and graviresponse emphasize the importance of investigations into the regulatory mechanisms of the action of this hormone. For a thorough and up-to-date overview of auxin signaling, we refer to recently published reviews (Zhao 2010; Wu *et al.* 2011).

The challenges of cultivating plants or plant cells at micro- or hyper-*g* are manifold ranging from the complexity and spatial limitations of experimental setups in space flight conditions and centrifuges (Musgrave 2007) to the limited time of exposure that is possible during sounding rocket (duration of 10 to 12 minutes) and parabolic flight experiments (duration of tens of seconds) (Luttges 1992). The limited duration of these experimental setups highlights the advantage of biological systems that respond within the given time frame of the respective experimental device. While intracellular signaling cascades are triggered within 1 second upon the perception of an external mechanical signal (Hejnowicz *et al.* 1998), metabolic cellular responses in most plants can take up to several hours or days to be measurable thus providing a critical lower time limit for the duration of experimentation (Dutcher *et al.* 1994; Mullen *et al.* 2000).

While using entire plants is necessary to study the effects on plant growth, architecture and reproduction, studies on cellular metabolism can potentially take advantage of single cell experimental systems. These have the advantage of being easier to observe microscopically and other experimental conditions are easier to control. In the present review we present several single cell plant systems that have been used in the past years and that present great potential for gravity research, in particular for the investigation of the effects of gravity on plant cellular functioning and metabolism. To introduce the open questions in this field of research, it is worth summarizing how plant cells are thought to perceive the orientation and magnitude of the gravity vector. Several conceptual models have been proposed on how plant cells perceive gravity stimulation.

8.3 Concepts of cellular gravisensing in plants

8.3.1 Statolith-based gravisensing

In the statolith-based model, the gravity signal is triggered by the movements of small bodies inside the cytoplasm that are of higher density than the surrounding cytosol - the statoliths. The cells equipped with such statoliths are called statocytes. Statoliths typically consist of starch-containing amyloplasts or crystals such as those made of barium sulfate found in *Chara* rhizoids (Sievers *et al.* 1996; Kuznetsov *et al.* 2001; Perbal and Driss-Ecole 2003). A change in the orientation of the gravity vector relative to the orientation of the organism causes the statoliths to sediment towards the new downward facing side of the cell and their movement results in the deformation of other sub-cellular structures (Fig 8.2a). It was thought for a long time that the moving particles exert a tensile stress on actin arrays which in turn influence the activity of membrane located mechano-sensitive ion channels (Baluška and Hasenstein 1997; Hejnowicz *et al.* 1998; Morita and Tasaka 2004). However, drug-induced disruption of the actin arrays enhances the gravity response in the roots of *Arabidopsis* and rice (Staves 1997; Hou *et al.* 2003; Hou *et al.* 2004) as well as in *Arabidopsis* inflorescence stems and hypocotyls (Yamamoto and Kiss 2002). Moreover, *Arabidopsis* mutants with reduced levels of starch-content are nevertheless able to perceive gravity signals (reviewed by (Morita 2010)). Rather than the sedimenting motion it may therefore be the direct contact of amyloplasts with the endoplasmic reticulum (ER) located in the periphery of the cell that triggers the signal (Perbal and Driss-Ecole 2003; Morita 2010). High resolution electron tomography has revealed that the force of gravity on the mass of statoliths is sufficient to locally deform the membranes of the cortical ER (Leitz *et al.* 2009). Clear evidence for the action of statoliths was provided by the fact that magnetophoretic displacement of statoliths in roots and shoots of higher plants as well as *Chara* rhizoids was able to induce gravitropic curvature (Kuznetsov and Hasenstein 1996; Kuznetsov and Hasenstein 1997; Weise *et al.* 2000; Kuznetsov and Hasenstein 2001). These studies highlight the usefulness of micromanipulatory strategies for gravitational research (Geitmann 2006a; Geitmann 2006b; Geitmann 2007). While a local membrane bending by statoliths was proposed to act in gravisensing of root columella cells (Leitz *et*

al. 2009), it has been shown that in moss protonemata, statoliths do not need to exert pressure. The simple contact with a receptor located at the susceptible membrane (in this case the plasma membrane) suffices to elicit the response (Limbach *et al.* 2005). Whatever the precise biochemical signaling pathway will turn out to be, according to the statolith-based gravisensing model the cellular response depends on the intracellular motion or displacement of some sort of particle or organelle that has a higher density than the surrounding cytoplasm and that therefore sediments to the lowest region of the cell upon the reorientation of the latter relative to the gravity vector.

8.3.2 The gravitational pressure model

Most plant cells are not equipped with statoliths and a second type of gravity perception mechanism needs to be in place to explain the fact that these cells nevertheless respond to changes in *g*-force. Evidence for the presence of an alternative mechanism stems from studies on mosses, fungi, and algae which show gravity dependent growth and differentiation without the presence of statoliths (Staves 1997). In higher plants as well, a statolith-independent pathway seems to operate. Carefully adjusted rotation of roots that maintains the statolith-equipped root cap vertical during gravitropic bending does not cause the root to abolish the bending process. This supports the view that there is a second, statocyte-independent location in the root where the gravi-stimulus is perceived (Wolverton *et al.* 2002). While at times considered a controversy, it became clear that several mechanisms of gravisensing seem to operate, possibly even in the same cell (Barlow 1995; Sack 1997; Hasenstein 1999; Kiss 2000). The presence of an alternative mechanism can explain why *Arabidopsis* mutants unable to synthesize starch display an operating gravitropic response in roots and shoots albeit diminished (Caspar *et al.* 1985; Hatakeda *et al.* 2003; Soga *et al.* 2005; Buizer 2007). The gravitational pressure model provides a possible but not necessary the only explanation for this phenomenon. It suggests that the entire mass of the protoplast acts as a gravity sensor that behaves similar to a water-filled balloon that flattens when placed on a surface due to its own weight. In this model the role of starch-filled amyloplasts would be that of increasing the overall density of the protoplast (Wayne and Staves 1996). It is postulated that membrane proteins located at the top and

bottom of cell may be activated through the action of differential tensile forces as they interact with the lower and upper cell walls, respectively (Wayne *et al.* 1992; Wayne and Staves 1996) (Fig 8.2b). Hitherto, the gravitational pressure model has been based on experimentation on the internodal cells of Characean algae and its relevance for graviperception in higher plants has yet to be demonstrated.

8.3.3 Tensegrity model

An alternative, but not mutually exclusive view, on how deforming forces acting on the cell as a whole could be perceived, is through the effect of cellular distortion on the mechanics or flexibility of the cytoskeletal arrays as explained by the tensegrity model of cell functioning. Although this model was developed for animal cells (Ingber 1999), it could doubtless be transferred to plant cells. In this model, the exposure to micro-gravity decreases the internal pre-stress in the cytoskeletal array consisting of elements that resist compressive (microtubules) and tensile stresses (actin filaments). This conceptual model of cell functioning is based on the architectural principles by Buckminster Fuller (Ingber 1993). The distortion-induced change in preexisting force balance is supposed to affect local thermodynamic or kinetic parameters and thus biochemical activities (Fig 8.2c). How mechanical signals perceived at the cell surface could influence intracellular processes has been reviewed in detail (Ingber 2006; Orr *et al.* 2006). However, the change in prestress of the cytoskeletal arrays does not necessarily need to be caused by the distortion of the outer shape of the cell but could also result from the gravity force acting on organelles attached to this network ((Yang *et al.* 2008), Fig 8.2d). Finite element modeling has shown that the difference in density between the nucleus and the cytoplasm would be sufficient to cause a change in tensile stress that is significant enough to deform the cytoskeletal array upon application or removal of gravity (Yang *et al.* 2008).

While according to the tensegrity model the activities of numerous cytoplasmic enzymes are affected directly, the crucial mechanotransductive step in the statolith and pressure models is the deformation of a membrane (plasma membrane, tonoplast, mitochondria, endoplasmic reticulum) which in turn influences transmembrane Ca^{2+} fluxes and consequently the cytosolic concentration of the ion (Fasano *et al.* 2002; Toyota *et al.* 2008).

Although in statocytes and gravitactic unicellular organisms, calcium was shown to be involved in graviperception as well as in signaling processes leading to a graviresponse, in non statocyte cells in higher plants, knowledge on calcium signaling involvement in graviresponse is scant (Sinclair and Trewavas 1997; Kordyum 2003) and warrants further investigation.

8.4 Single cell systems useful for understanding statolith independent graviperception

Immediate and short term responses can be difficult to assess in multicellular systems, and therefore the use of single cells in culture has been a successful alternative approach that complements our understanding of graviperception and responses in plants. Handling of single cells is generally easier (although generally sterile conditions have to be ensured) and depending on the parameter of interest, the response can often be observed shortly after application of the environmental trigger. Moreover, microscopy is facilitated since no neighboring cells obstruct the view, thus allowing for high spatial and temporal resolution imaging. Finally, reproducible growth conditions are more readily achieved in cell cultures since parameters such as temperature, nutrient concentrations, and pH can be tightly controlled.

Among the most intensively studied single cell systems investigated in micro-gravity research are the protonemata and rhizoids of mosses and *Chara*, a freshwater alga. Although these cells are part of a multicellular organism, they are tip growing individual cells which makes them readily accessible to microscopic observation. Furthermore, gravity perception and response occur in the same cell. Both protonemata and rhizoids are equipped with statoliths and important information has been gained from numerous studies on these organisms which have been exhaustively reviewed (Schwuchow *et al.* 1990; Schwuchow *et al.* 1995; Sievers *et al.* 1996; Braun 1997; Sack 1997; Demkiv *et al.* 1999; Braun and Sievers 2000; Braun and Wasteneys 2000; Braun and Limbach 2006). In the following, we will confine our overview to studies performed on single plant cell systems that are not equipped with statoliths and that offer the possibility to assess how gravity or the absence thereof affect basic plant cell functioning and metabolism.

8.4.1 Cell wall assembly in protoplasts

The molecular architecture of the cell wall and, by consequence, its mechanical behavior are known to be affected in many but not all plants grown under micro- and hyper-gravity conditions (Cowles *et al.* 1984; Waldron and Brett 1990; Nedukha *et al.* 1994; Hoson *et al.* 1996; Nedukha 1996; Soga *et al.* 1999a; Soga *et al.* 1999b; Levine *et al.* 2001; Soga *et al.* 2001). Therefore, the investigation of altered *g*-force on the kinetics of the cell wall assembly process is of considerable interest. Single-cell studies to this end have been conducted on protoplasts generated from different plant systems. After the enzymatic removal of the cell wall, protoplasts generally start to regenerate a new cell wall. This is followed by cell division and formation of small cell aggregates few days later. These aggregates develop into callus tissue and, under suitable conditions, into mature plants. It is in particular the ability to regenerate mature plants from protoplast cultures that makes this experimental system interesting for applications in space exploration. Under microgravity conditions, cell wall formation in protoplasts isolated from *Brassica napus, Daucus carota* and *Solanum tuberosum* is significantly delayed compared with the control samples at 1-*g* (Rasmussen *et al.* 1992; Nedukha *et al.* 1994; Rasmussen *et al.* 1994). In particular, the content of structural components such as cellulose and hemicellulose is reduced whereas pectin is unaltered (Nedukha 1998; Skagen and Iversen 2000). These micro-gravity induced delays in protoplast regeneration also slow callus formation but do not prevent the process. However, under micro-*g* conditions development of intact plants is hampered, since calluses develop either roots or shoots, but not both (Iversen *et al.* 1999).

In these studies, peroxidase activity was measured in the regenerating protoplasts and revealed a decrease in enzyme activity compared to the ground control (Rasmussen *et al.* 1992). Since peroxidase activity is involved in cell wall metabolism and cross-linking of microfibrils, this reduced activity was proposed to provide a possible explanation for the observed slow-down in cell wall regeneration. However, later experiments showed that factors other than weightlessness (such as cosmic radiation) may have contributed to or even caused this change in peroxidase activity (Skagen and Iversen 2000).

Interestingly, another cellular feature may be the reason for retarded cell wall deposition, in particular reduced cellulose deposition: the cortical microtubule cytoskeleton. The amount

of cortical microtubules at 24h after protoplast isolation is greater in protoplasts cultured at 1-*g* than under microgravity (Skagen and Iversen 2000). Moreover, while cortical microtubules assessed at 24h after cell wall removal in recovering rapeseed protoplasts are organized in parallel arrays, they are randomly oriented in the 0-*g* sample and hence unaltered from those of the protoplast immediately after cell wall removal. Since cortical microtubules play an important role in cellulose microfibril deposition (Emons *et al.* 2007), the failure to reorganize may certainly influence the capacity of the cell to fully regenerate its wall and, subsequently, to divide.

8.4.2 Calcium fluxes in polar fern spores

One of the single cell systems capable of a gravitropic response is the gametophyte of the fern *Ceratopteris richardii*. During the first 24h of germination, the gravity vector determines the axis of development of the spore by setting an asymmetrical growth polarity creating two asymmetrical cells that will grow parallel to gravity in opposite directions (Edwards and Roux 1998; Chatterjee and Roux 2000). When developed in microgravity conditions, the spores are able to germinate but lose the spatial polarity (Roux *et al.* 2003). The same pattern was observed when calcium channel blockers or inhibitors such as nifedipine and eosin yellow were added to the culture medium after germination initiation (Chatterjee *et al.* 2000). Efflux of calcium at different cellular regions was recorded using ion selective electrodes on spores grown at 1-*g* and spores grown during parabolic flights (the *g* level fluctuated between micro-*g* and 1.8-*g*). The results revealed that the specific activation of mechanosensitive calcium channels at the bottom of the cell is required for graviperception (Chatterjee and Roux 2000; Salmi *et al.* 2011). These data confirm the notion that calcium fluxes are involved in graviperception in multicellular plants (Sinclair and Trewavas 1997; Fasano *et al.* 2002; Soga *et al.* 2002; Hoson *et al.* 2010). Use of the fern spore system allowed for facilitated microscopical access and measurement of ion fluxes compared to the multicellular root cell systems. However, the mechanism by which the channels are activated and the pathways that are involved in the transduction of the gravity-dependent response are yet to be determined. Progress on the understanding of the

molecular mechanism will certainly profit from advances made on other mechanoperceptive cellular systems (Orr *et al.* 2006; Poirier and Iglesias 2007).

8.4.3 Microtubule cytoskeleton in BY-2 cells

The microtubule cytoskeleton has multiple functions in plant cells including the guidance of the intracellular motion of organelles, the targeting of enzymes involved in cell wall assembly, chromosome separation and cell plate formation during mitosis. When and where microtubules are assembled from tubulin and disassembled, therefore, is pivotal for cellular functioning. In weightlessness, isolated tubulin does not self-organize into parallel microtubule bands as it does in the same *in vitro* conditions on the ground (Papaseit *et al.* 2000). Similarly, in different types of cultured mammalian cells, the organization of the microtubule cytoskeleton is affected under real or omnilateral micro-gravity conditions (Lewis *et al.* 1998; Rösner *et al.* 2006). The finding that microtubules in regenerating protoplasts cultured under micro-gravity conditions were less organized than in the ground control provided a motivation for investigating the microtubule cytoskeleton in cultures of other single plant cell types. Similar to the protoplasts, microtubules in cultured cells dedifferentiated from tobacco hypocotyls at 1-*g* were more abundant than their counterpart grown in micro-gravity (Sato *et al.* 1999). The microtubules of a third single celled system, tobacco BY-2 cells, were found to be less susceptible to a change in *g*-force, on the other hand. The BY-2 cell line was established from a callus induced on a seedling of *Nicotiana tabacum* cultivar Bright Yellow-2. Tobacco BY-2 cells grow rapidly in suspension culture and can multiply their numbers up to 100-fold within one week in adequate culture medium. Remarkably, exposure of BY-2 cells to microgravity conditions did not have any effect on cell division or cell growth. The organization of cortical microtubules was identical to that in cells cultured on Earth, and the orientation of newly deposited cellulose microfibrils was unaltered (Sieberer *et al.* 2009). Therefore, the tissue context does not seem to be a prerequisite for these cells to ensure cytoskeletal ordering under weightlessness. Rather it seems that the absence of a cell wall hampers microtubule organization during the initial phase of protoplast regeneration. This is consistent with the observation that microtubules in plant cells tend to align parallel to the principal direction

of stress and thus respond to mechanical cues (Hush and Overall 1991; Geitmann *et al.* 1997; Hamant *et al.* 2008). In line with this, the expression of tubulin genes is upregulated by hypergravity in *Arabidopsis* hypocotyls (Matsumoto *et al.* 2007) and cortical microtubules are reoriented from transverse to longitudinal (Soga *et al.* 2006). In tubulin mutants of *Arabidopsis* displaying twisted growth, hypergravity caused a more pronounced twisting phenotype and microtubule reorientation was more prominent (Matsumoto *et al.* 2010). This led to the hypothesis that by influencing cellulose deposition, microtubules play an important role in the maintenance of a normal growth phenotype against the gravitational force (Hoson *et al.* 2010).

8.4.4 Endomembrane trafficking in the pollen tube

Experiments placed on parabolic flight and sounding rockets only make sense if the organism or cell displays a response to microgravity that appears within the short duration of weightlessness achieved during the flight. Assessment of both cellular growth and metabolism using these devices can therefore be exploited with cell systems in which both parameters are highly active and change rapidly upon exposure to a trigger. The fastest growing plant cell is the pollen tube, a cellular protrusion formed by the pollen grain upon contact with the receptive stigma. The pollen tube is responsible for fertilization in higher plants and hence crucial for seed and fruit formation. Pollen tubes, like protonemata, rhizoids, root hairs, fungal hyphae and neurons, are tip-growing cells. The growth rates of pollen tubes can be up to hundreds of micrometers per minute and sustaining this process requires the continuous deposition of cell wall material in highly controlled manner to ensure morphogenesis of a perfectly cylindrical shape (Fig 8.3).

The development of the pollen grain, or microgametophyte, occurs in the anther and comprises several, precisely regulated cell divisions (meiotic and mitotic), the assembly of a highly structured and extremely resistant cell wall, and the coordinated activation of the cytoskeleton (Liu *et al.* ; Honys *et al.* 2006; Bou Daher and Geitmann 2011). Long term studies on orbital platforms have shown that pollen formation was aborted at early stages and young microspores were deformed and empty. In late developmental stages, the pollen exine was able to form but the cytoplasm seemed contracted and became disorganized

(Kuang *et al.* 1995). However, rather than an effect of micro-gravity, these phenomena were found to be a consequence of the reduced carbon dioxide environment due to lack of convective air movement. When plants were grown in high CO_2 atmosphere, pollen with normal outer morphology could be obtained from *Arabidopsis* and *Brassica*. However, although the percentage of viable pollen was much higher than during the earlier experiment, fertilization did not occur (Kuang *et al.* 1996). Optical and electron microscopy showed that pollen grains developed in micro-gravity displayed differences in size, shape, number of mitochondria as well as an abundant presence of large starch grains absent in the pollen that developed on the ground (Kuang *et al.* 1995; Kuang *et al.* 2005). When environmental conditions at micro-*g* such as CO_2, light and convection were more carefully controlled, it was possible to obtain viable embryos, seeds and siliques in *Arabidopsis* and *Brassica* proving that pollen tube growth was indeed possible at micro-*g* (Musgrave *et al.* 1997; Popova *et al.* 2009).

At hyper-gravity the effects on pollen and fertilization vary significantly between species. While at 4-*g* seed set in *Brassica* was not affected (Musgrave *et al.* 2009a), the formation of siliques was significantly reduced in *Arabidopsis* (Musgrave *et al.* 2009b). The authors found this to be due to a reduced ability of *Arabidopsis* pollen tubes to germinate at 4-*g*. They propose that the increasing *g*-force caused the cytoplasm to exert higher than normal pressure on the cell wall disturbing the tip growth process (Musgrave *et al.* 2009b). The main metabolic activity of the pollen tube is the synthesis and the deposition of cell wall precursors which are indispensable for the continuing assembly of the elongating cell (Geitmann and Steer 2006). The principal phenomenon responsible for the tube expansion is the exocytosis of vesicles containing pectins which occurs at high rates and is spatially and temporally regulated by a multitude of parameters (Chebli and Geitmann 2007). Other cell wall components such as cellulose, xyloglucans and callose are either deposited by exocytosis or directly synthesized at the plasma membrane. Each of these components plays a defined mechanical role during pollen tube growth and in each plant species these components are distributed differently forming a characteristic spatial profile (Geitmann and Dumais 2009; Fayant *et al.* 2010) (Fig 8.3). Intriguingly, the pollen tube is able to compensate for the lack of one of the components by overproduction of another (Aouar *et*

al. 2010), demonstrating that sophisticated mechanical control mechanisms must be in place to ensure that the final product is functional.

Very conveniently, pollen tubes are easily cultured *in vitro* thus allowing high resolution microscopic observations. Crucial in the present context, the high growth rate entails rapid and easily visible cellular responses upon mechanical or chemical manipulation (Geitmann and Steer 2006; Chebli and Geitmann 2007). The responses of *in vitro* growing pollen tubes developing under micro-*g* conditions or during clinostat rotation vary between plant species. In *Prunus persica* pollen tubes grown in a clinostat, callose plugs were four times longer than those in the control tubes and callose was spread along throughout the tube (De Micco *et al.* 2006a; De Micco *et al.* 2006b) indicating that cell wall assembly under altered gravity conditions was affected. Unlike somatic plant cells in which an altered cell wall assembly clearly fulfills a structural purpose since it reinforces the cell wall against the mechanical stress to which it is exposed, the performance of a pollen tube would not really be improved by a stiffer cell wall. The cellular response is therefore likely unspecific and offers the unique possibility to study the fundamental effect of altered gravity conditions on plant cell metabolism.

Cell wall assembly in the pollen tube is ensured by a high rate of intracellular trafficking targeted towards the growing end of the cell (Bove *et al.* 2008; Kroeger *et al.* 2009; Bou Daher and Geitmann 2011). Temporal and spatial control of the vesicle fusion responsible for cell wall assembly at the growing tip is required to determine the rate and direction of growth (Fayant *et al.* 2010). The influx of calcium through plasma membrane located calcium channels at the tip of the cells plays an important role in the temporal and spatial regulation of the growth process (Hepler 1997; Feijó *et al.* 2001; Chebli and Geitmann 2007). Exocytosis in the tip region is accompanied by membrane endocytosis to ensure a balanced deposition rate of cell wall and membrane material. The delicate equilibrium between exocytosis and endocytosis is disturbed when *in vitro* growing pollen tubes are exposed to micro- and hyper-*g* conditions. In micro-gravity, the uptake of a fluorescent phospholipid into pollen tubes, an indication for endocytosis, was increased, whereas the contrary was true for hyper-gravity conditions (Lisboa *et al.* 2002). Since pollen tubes are not gravitropic (De Micco *et al.* 2006b), they can therefore serve as model systems that

allow the investigation of statolith-independent, non-gravitropic responses of plant cells upon altered gravity conditions. Moreover, understanding the performance of this cell is crucial for future applications in space flight as successful fertilization is essential for on-board production of plant-based food.

8.5 Conclusion

Experiments based on entire plants are inevitable to understand plant functioning under altered gravity conditions. Nevertheless, single cell experimental systems have emerged as excellent tools that allow for in-depth studies of individual processes that are altered as a consequence of exposure to micro- or hypergravity conditions. It becomes increasingly clear that statolith mediated effects are not the only responses that contribute to plant behavior under altered gravity conditions. So far, each of the cellular systems mentioned above has been used to investigate particular aspects of cellular functioning. An important step forward will be the combined analysis of different processes on a single system to obtain a more holistic view of the involved mechanisms and to connect the dots. Secondly, identifying common principles shared by different cellular systems, as well as distinctive features that can be explained by the particular functionality of the cell wall will allow making conclusions for general plant cell functioning. By way of example, cell wall regeneration was investigated in recovering protoplasts, but elongating tip growing cells represent alternative systems that provide complementary information. The effect of gravity on the cytoskeleton has mostly been studied on comparably slowly developing cells such as BY-2 cells, but important information could probably gained from and short term experimental devices could be exploited for systems in which these cellular features are highly dynamic such as growing pollen tubes. Ion fluxes, so far only studied in fern spores in the context of gravity research, could and should equally be studied in other growing cells in which ion flux profiles have been established. Single cell systems allow for the use of imaging methods that operate at high spatial and temporal resolution and will therefore enable us to determine the roles of subcellular features such as targeted transport processes and ion fluxes that lead to a tropic response or a change in metabolic homeostasis. It will then be possible to link these results to those obtained from transcriptomic and proteomic

approaches, thus making sense of the overwhelming wealth of data that these types of studies produce (Martzivanou and Hampp 2003; Martzivanou *et al.* 2006; Wang *et al.* 2006a; Babbick *et al.* 2007; Barjaktarović *et al.* 2007; Barjaktarović *et al.* 2009). An integration of cell biological and imaging approaches with quantitative information on the expression of proteins involved in cell wall synthesis, lipid metabolism, cell division etc. will help to validate existing models and inform future models. Crucially, a multifaceted view will guide the development of new biomechanical and structural approaches to decipher the pathways of gravisensing and graviresponse.

8.6 Acknowledgments

Research in the Geitmann lab is supported by grants from the Natural Sciences and Engineering Research Council of Canada (NSERC) and the Fonds Québécois de la Recherche sur la Nature et les Technologies (FQRNT). Youssef Chebli is funded by the Ann Oaks doctoral scholarship of the Canadian Society of Plant Physiologists.

8.7 Glossary

Gravimorphogenetic	Developmental change in response to the presence or the change in the orientation or magnitude of the *g*-vector
Graviperception	The ability of a cell to become aware of the orientation or magnitude of the gravity vector
Graviresponse	Physiological or morphogenetic response of a cell or a tissue to gravity induced trigger. The responding cell does not need to be identical to the perceiving cell
Gravisensing	Perception of gravity stimulus
Gravistimulus	Mechanical process caused by the presence or change in magnitude or orientation of gravity
Gravitropism	Ability of a plant, organ or cell to orient its growth in the direction of the gravity vector
Gravity resistance	Gravimorphogenetic response that serves to reinforce the organism or organ against the effect of gravity. Typically a reinforcement of the cell wall
Mechanotransduction	Conversion of a mechanical stimulus into a chemical intracellular signaling pathway
Omnilateral	From all sides
Statocyte	Cell specialized in graviperception and typically equipped with statoliths
Statolith	Intracellular body with density higher than the surrounding cytosol causing the body to sediment in the direction of the gravity vector. Either the sedimenting motion or the new position of the statolith provides the cell with information on magnitude and orientation of the gravity vector

8.8 Figures

Figure 8.1

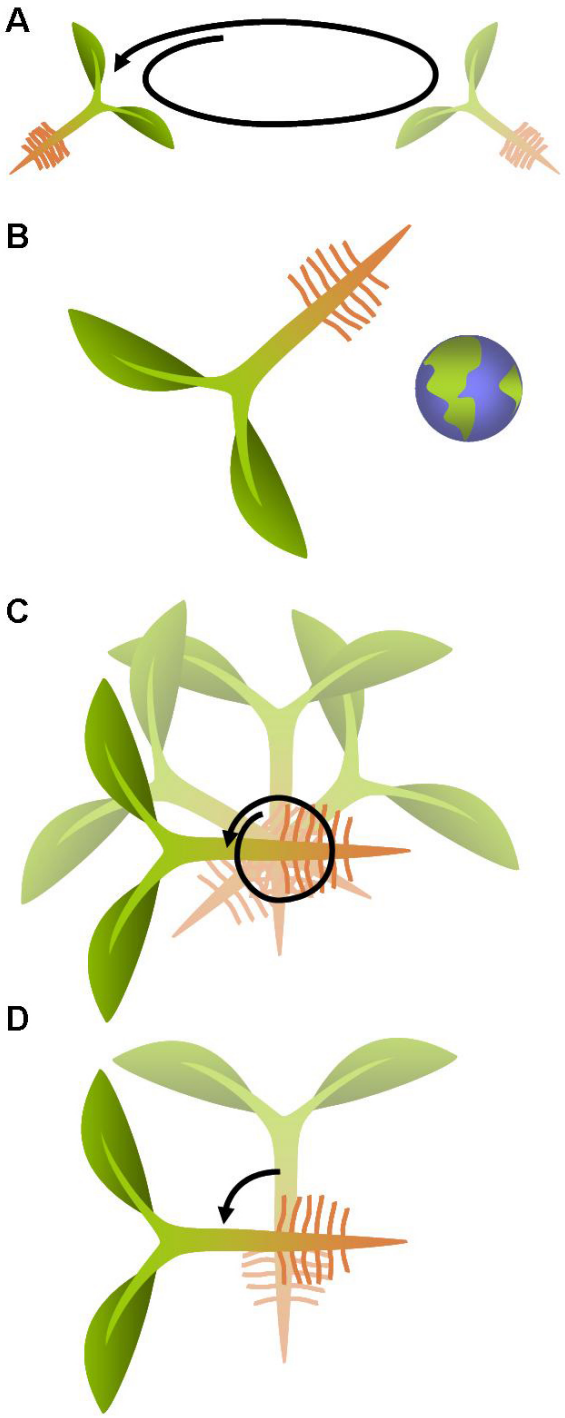

Figure 8.1: General principles used in gravity research.

(A) Centrifugation increases the magnitude of the *g*-vector resulting in a hyper-gravity stimulus. (B) True micro-gravity conditions can be obtained on orbital platforms or during the free-fall phases of sounding rockets and parabolic flights. (C) Omnilateral micro-gravity is achieved by continuously rotating the specimen, either in 2D or 3D. This does not change the magnitude of the *g*-force, but it eliminates the effect of the unidirectional stimulus caused by the *g*-vector. (D) Turning a specimen changes the orientation of the *g*-vector relative to the specimen.

Figure 8.2

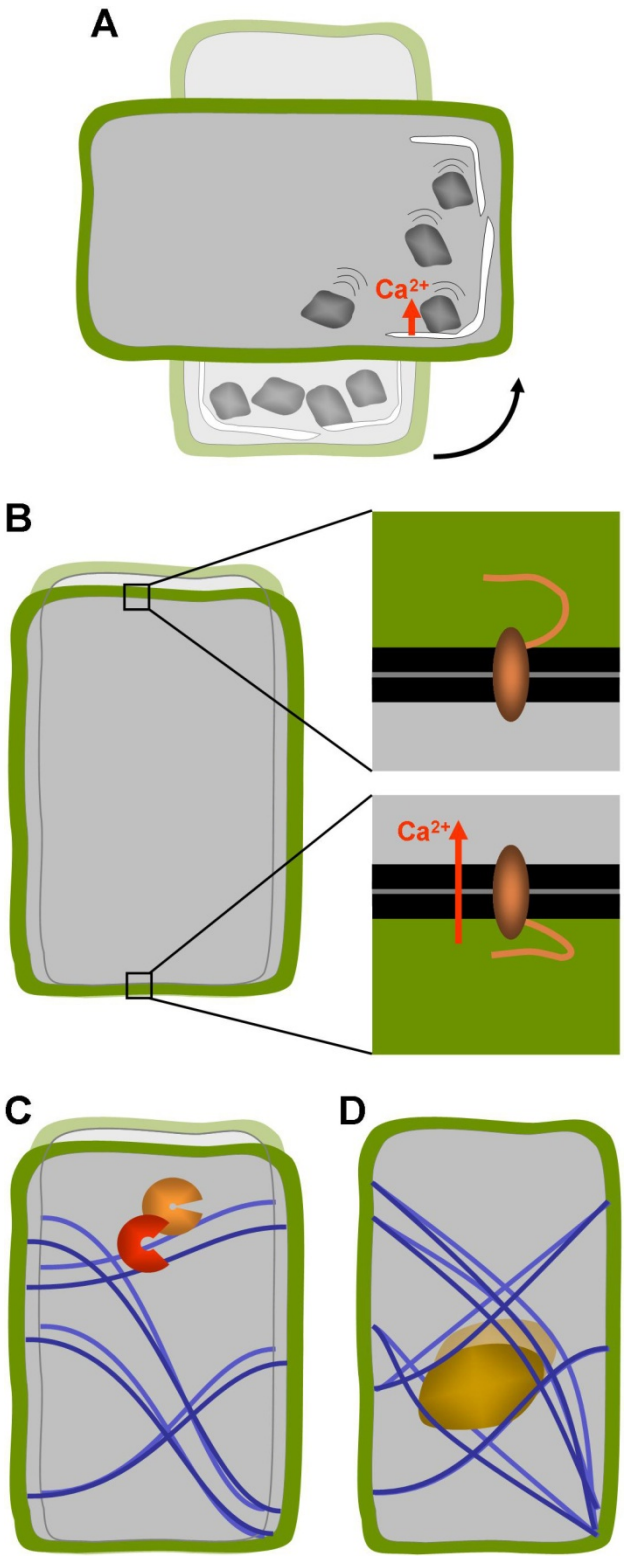

Figure 8.2: Concepts of cellular gravisensing in plants.

(A) In statolith-based gravisensing the sedimentation or change of position of intracellular organelles with higher density triggers a signal most likely based on a change in trans-membrane ion fluxes. (B) According to the gravitational pressure model the weight of the protoplast causes the forces acting on the membrane-cell wall connections at the upper and lower sides of the cells to be different. (C) The tensegrity model predicts that cellular distortion due to a change in *g*-force affects the prestress in the cytoskeletal array of the cell which in turn changes biochemical activities. (D) A variation of the tensegrity model is based on a change in cytoskeletal prestress being caused by the weight of heavy organelles that are tethered to the cytoskeletal filaments such as the nucleus.

Figure 8.3

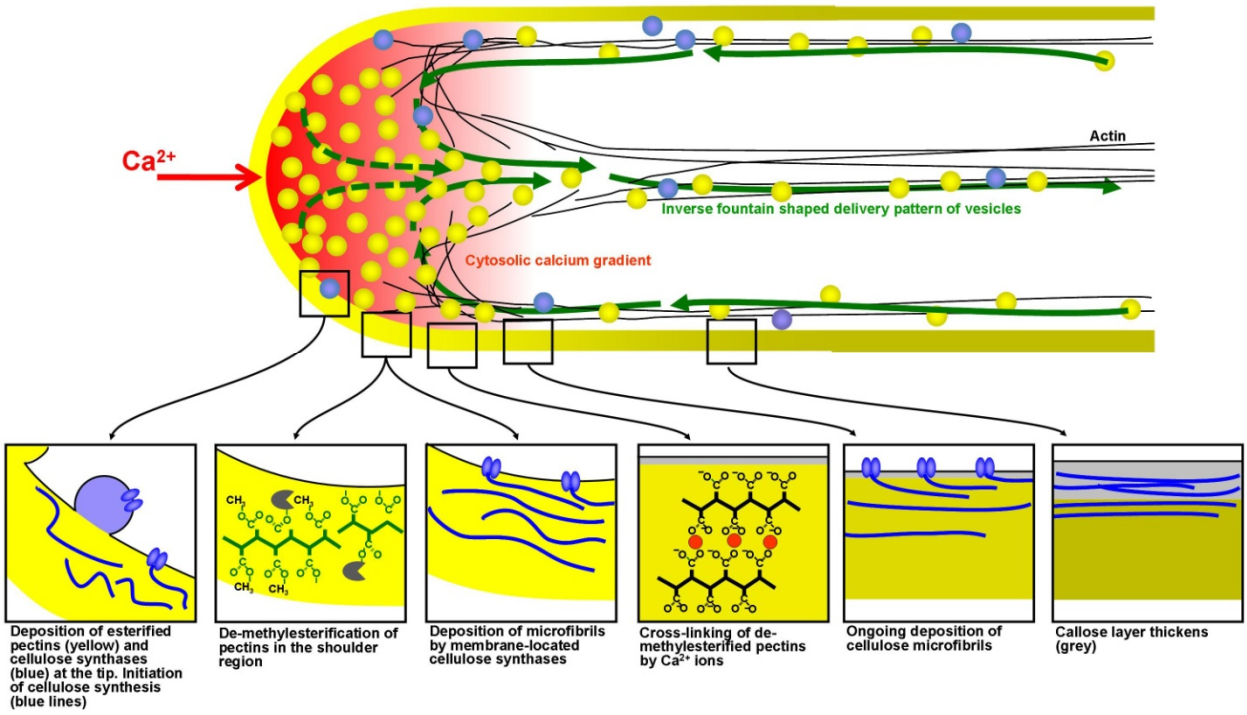

Figure 8.3: Spatial profile of mechanical properties and biochemical processes in the cell wall of growing pollen tubes

Mechanical modeling has shown that the precise spatial distribution of endomembrane trafficking, cell wall assembly processes and cross-linking of cell wall polymers determines the cellular morphogenesis and the resulting shape in growing plant cells. These processes occur particularly rapidly in pollen tubes making them an ideal model system for experiments based on short term exposure to micro-gravity.

9 Cell wall assembly and intracellular trafficking in plant cells are directly affected by changes in the magnitude of the gravitational force

This manuscript was submitted to *PlosOne* and is currently under review.

Youssef Chebli, Lauranne Pujol, Anahid Shojaeifard**,** Iman Brouwer, Jack van Loon and Anja Geitmann

I contributed to this work by developing and submitting the project to ESA, planning the experiments in collaboration with ESA, and performing all the experiments (at the IRBV and at the ESA), analyzing the data and writing the current manuscript. Lauranne Pujol and Anahid Shojaeifard were two internship students; they worked on the spatial distribution of the cell components in hyper-gravity conditions. They contributed to Figures 9.2, 9.3 and Supplemental Figure 9.1. Iman Brouwer contributed by building the low RPM centrifuge in the Geitmann lab. Jack van Loon contributed by providing assistance, guidance and expertise for the execution of the experiment on the Large Diameter Centrifuge at the European Space Agency and he also contributed to the writing of this manuscript.

9.1 Abstract

Plants are able to sense the magnitude and direction of gravity. This capacity is thought to reside in selected cell types within the plant body that are equipped with specialized organelles called statoliths. However, most plant cells do not possess statoliths, yet they respond to changes in gravity levels. To understand the effect of gravity on the metabolism and cellular functioning of non-specialized plant cells, we investigated a rapidly growing plant cell devoid of known statoliths and without gravitropic behavior, the pollen tube. The effects of hyper-gravity and omnidirectional gravity on intracellular trafficking and on cell wall assembly were assessed in *Camellia* pollen tubes, a model system with highly reproducible growth behavior *in vitro*. Using an epi-fluorescence microscope mounted on the Large Diameter Centrifuge at the European Space Agency, we were able to demonstrate that vesicular trafficking is reduced under hyper-*g* conditions. Immuno-cytochemistry confirmed that both in hyper and omnidirectional gravity conditions, the characteristic spatial profile of cellulose and callose distribution in the pollen tube wall was altered, in accordance with a dose-dependent effect on pollen tube diameter. Our findings suggest that in response to gravity induced stress, the pollen tube responds by modifying cell wall assembly to compensate for the altered mechanical load. The effect was reversible within few minutes demonstrating that the pollen tube is able to quickly adapt to changing stress conditions.

9.2 Introduction

The evolution of plants has been driven by different biotic and abiotic stresses that have varied in time and space. Gravity is the only constant factor to which plants had to adapt in permanent manner. The first plants to appear on Earth were mostly composed of soft tissues, devoid of any hard vascular tissue and plant life was therefore limited to buoyant environments. The colonization of terrestrial environments was accompanied by the development of robust vascular systems and stiff cell walls, which enabled plants to build aerial organs rising in the direction opposite to the gravity vector. Since the appearance of vascular terrestrial plants around 440 million years ago, plants have evolved by adapting permanently to this constant force (Morita 2010). To withstand the mechanical load imposed by gravity, plants developed two strategies, one being based on the erectile force created by the balance between the internal turgor pressure and the tensile resistance of the primary cell wall, the second consisting in the production of stiff secondary walls (Volkmann and Baluška 2006). For both mechanisms, the cell wall, its timely assembly and its mechanical properties are essential regulatory factors. The plant cell wall (or extracellular matrix) is made of interlinked networks of polysaccharide polymers with distinctive and modifiable mechanical properties. The relative abundance and the types of polymers as well as the interpolymer linkages are controlled to ensure functional growth of plant organs and differentiation of the individual cell. Therefore, the polymers composing the cell wall have to be delivered to or synthesized directly at the cell surface under tight spatial and temporal control (Cosgrove 2005). Any environmental change has the potential to disrupt this process, resulting in abnormal morphological phenotypes and/or dysfunctional growth and differentiation. Changes in the magnitude of the gravitational force have been shown to disrupt growth of organs and cells, for example during *Arabidopsis* hypocotyl growth (Matsumoto *et al.* 2010), root elongation (Baluška and Hasenstein 1997) and seed formation (Kuang *et al.* 1996) and many of these phenotypes have been related to defects in cell wall assembly.

In order to respond to gravity-related stress, the cell or organism must actually be able to perceive it. Two major models have been proposed to explain how plant cells perceive gravity stimulation, the statolith model and the gravitational pressure model (reviewed in

(Morita 2010; Chebli and Geitmann 2011)). Statolith-based mechanisms have been studied in great detail (Morita 2010), but most plant cells are not equipped with these specialized organelles. Cells devoid of statoliths do nevertheless respond to a gravi-stimulus, however, and hence the gravitational pressure model or alternative concepts that explain gravi-perception in the absence of statoliths warrant further research to understand how plants are affected by and respond to gravity or the absence thereof (Chebli and Geitmann 2011).

In order to understand how non-statocyte plant cells are affected by gravity, we analyzed the effect of altered *g*-force on intracellular transport and cell wall assembly in a non-statocyte and non-gravitropic plant cell system. In most plant cell systems, cell wall deposition occurs over days or even weeks and effects of altered *g*-force are only visible after long term exposure to the stress. We therefore opted to study the fastest growing cell in the plant kingdom, the pollen tube. The pollen tube is a cellular protrusion formed by the pollen grain upon contact with a receptive stigma, the landing platform on top of the pistil. The pollen tube is responsible for fertilization in higher plants and hence crucial for seed and fruit formation. Pollen tubes, similar to root hairs, fungal hyphae and neurons, are tip-growing cells. The growth rates of pollen tubes can be up to hundreds of micrometers per minute. Sustaining this process requires continuous synthesis of cell wall precursors and their delivery to the cell surface by exocytosis. To ensure morphogenesis of a perfectly cylindrical shape, vesicle exocytosis occurs at high rates and is spatially and temporally controlled by a multitude of parameters (Geitmann and Steer 2006; Chebli and Geitmann 2007). Importantly, the pollen tube does not have any known statoliths, nor does it display a gravitropic response (De Micco *et al.* 2006a). This is in accordance with its physiological behavior as flowers in many plant species are oriented arbitrarily relative to the gravity vector. To find their target, the female gametophyte, the elongating pollen tube has to follow chemical and mechanical cues presented by the pistillar tissues and the female gametophyte. A gravitropic response would interfere with the chemotropic and thigmotropic behavior necessary for target finding.

While intracellular signalling cascades are triggered immediately upon the perception of an external mechanical signal, metabolic cellular responses in most plant cells can take up to several hours or days to be measurable thus providing a critical lower time limit for the duration of experimentation. The use of rapidly growing cells such as pollen tubes with

high metabolism reduces this delay between signal and response to make experiments fit into the time frame of several hours. Moreover, it has been shown that pollen tube metabolism is altered within few minutes or seconds (*i.e.* the change of the distribution of cell wall components, lower percentage of fertilization per hour) when subjected to micro-gravity (Lisboa *et al.* 2002; Lisboa *et al.* 2008). This rapid response makes it an optimal model system to study the direct effects of gravity changes on plant cell metabolism. Very importantly, the rapid growth rate of the pollen tube entails rapid and easily visible cellular responses upon mechanical or chemical manipulation (Geitmann and Steer 2006; Chebli and Geitmann 2007).

Here, we studied the effects of changes in gravity levels on the behaviour of pollen tube growth, cell wall assembly and vesicle trafficking. We grew *Camellia japonica* pollen tubes in omnidirectional microgravity (also known a simulated microgravity) and in hyper-gravity (hyper-*g*) conditions at the facilities of the European Space Research and Technology Centre (ESTEC) of the European Space Agency (ESA) located in The Netherlands. Using immuno-cytochemical labelling coupled with epi-fluorescence microscopic techniques, we quantitatively analyzed the biochemical composition and spatial distribution of the different cell wall components in pollen tubes grown at different *g*-levels ranging from omnidirectional gravity to hyper-*g*. To further understand the effect of altered gravity on cell wall assembly and morphogenesis, we assessed how intracellular vesicle trafficking is modulated by changes in *g*-force. This approach required live cell fluorescence imaging, which was performed with an inverted microscope equipped for epi-fluorescence imaging installed as payload on the Large Diameter Centrifuge (LDC) at ESTEC-ESA.

9.3 Material and Methods

9.3.1 Plant material

Camellia japonica plants were grown in the greenhouses of the Montreal Botanical Garden. Pollen was collected from the flowers directly after anthesis. To minimize artefacts due to varying maturity of pollen grains, only batches collected during the same week were used

for any given series of experiments. Pollen grains were then dehydrated over silica gel for 24 hours and stored at -20°C until use.

9.3.2 Pollen culture

Pollen grains were hydrated for 30 min and suspended in a modified Brewbaker and Kwack germination medium (100 $\mu g.ml^{-1}$ H_3BO_3, 300 $\mu g.ml^{-1}$ $Ca(NO_3)_2$, 100 $\mu g.ml^{-1}$ KNO_3, 200 $\mu g.ml^{-1}$ $MgSO_4$, 50 $mg.ml^{-1}$ sucrose). Unless stated otherwise, the pollen grain suspension was deposited in the wells of a 0.4 µm Ibidi® plates and incubated under omnidirectional gravity and different levels of hyper-*g* ranging from 1*g* to 20*g*.

9.3.3 Viability test

Pollen grain viability was assessed using fluorescein diacetate (FDA) from a stock solution dissolved in acetone at 10 mg mL^{-1} and stored at -20°C. FDA was diluted in a 6% sucrose solution to a final concentration of 0.2 mg mL^{-1}. Hydrated pollen was dipped in 250 µL of the FDA solution on a glass slide and kept in the dark for 5 min. Observations were made with a Zeiss Imager-Z1 microscope with excitation light at 470 nm and a 515–565 nm band pass emission filter. Under these conditions, only viable pollen grains emit a fluorescence signal.

9.3.4 Omnidirectional gravity conditions

To expose pollen to omnidirectional-*g* conditions (also called simulated microgravity), pollen grains were germinated in Ibidi® cells fixed to the stage of a Random Positioning Machine (RPM) (van Loon 2007) at the European Space Research and Technology Centre (ESTEC) of the European Space Agency (ESA). The RPM was operated in random modes of speed direction and interval. The maximum acceleration was set at $60°{\cdot}s^{-1}$ via a computer user interface with dedicated control software. The samples were fixed in the centre of the inner frame with a resulting largest radius of 70 mm to the outermost wells. This results in a maximum residual g due to rotation of less then $10^{-4}g$ (van Loon 2007). After 3 hours, pollen tube growth was stopped by adding a 37% formaldehyde solution (Sigma-Aldrich) and subsequently labelled as mentioned below.

9.3.5 Hyper-gravity conditions for pollen tube cell wall labeling

Hyper-*g* was simulated by centrifugation using a centrifuge built in-house. Briefly, Ibidi® cells were fixed on a circular plate attached to a rotor turning at an adjustable, computer-controlled speed. Different *g*-levels were applied by modifying *RPM* (revolutions per minute) of the plate and taking into account the distance *r* from the center of the plate to the sample using $RPM = \sqrt{\frac{g}{r * 1.118.10^{-5}}}$. The *g*-level values mentioned in this paper are those imposed in centrifugal direction by the rotation. Pollen tubes were grown for 2 to 3 hours at hyper-*g* conditions and subsequently fixed and labelled as detailed below.

9.3.6 Fixation and fluorescence label

All steps were carried out in a microwave oven (Pelco BioWave® 34700 equipped with a Pelco Cold Spot®) operating at 150 W under 53.34 cm of Hg vacuum at a controlled temperature of 30±1°C. Pollen tubes where fixed after 2 hours of germination under hyper-*g* conditions. Fixative was added directly to the growing tubes immediately after the centrifugation or after a recovery period on the bench of 5, 10 and 15 min. Fixation was performed in 3.5% w/v freshly prepared formaldehyde and 0.3% v/v glutaraldehyde in Pipes buffer (50 mM Pipes, 1 mM EGTA 0.5 mM, $MgCl_2$, pH = 6.9) for 40 seconds followed by 3 washes in Pipes buffer. For immuno-labelling pollen tubes were then washed 3 times with phosphate buffer saline (PBS) (135 mM NaCl, 6.5 mM Na_2HPO_4, 2.7 mM KCl, 1.5 mM KH_2PO_4, pH 7.3) with 5% w/v bovine serum albumine (BSA). All subsequent washes were done with PBS buffer with 5% w/v BSA for 40 seconds. All antibodies were diluted in PBS buffer with 5% w/v BSA and incubations were done for 7 min followed by three washes in buffer. Controls were performed by omitting incubation with the primary or the secondary antibody. Pectins with low and high degree of esterification were labelled with monoclonal antibodies JIM5 and JIM7, respectively (diluted 1:50; Paul Knox, University of Leeds, United Kingdom), followed by Alexa Fluor 594 anti-rat IgG (diluted 1:100; Molecular Probes). Callose was labelled with a monoclonal IgG antibody to (1→3)-β-glucan (diluted 1:200; Biosupplies Australia Pty Ltd) followed by Alexa Fluor 594 anti-mouse IgG (diluted 1:100; Molecular Probes). Label for crystalline cellulose was performed with Cellulose Binding Module 3a (diluted 1:200; Paul Knox,

University of Leeds, United Kingdom) followed by a monoclonal mouse-anti-polyhistidine antibody (diluted 1:12; Sigma) and subsequent incubation with Alexa Fluor 594 anti-mouse IgG (diluted 1:100; Molecular Probes).

9.3.7 Fluorescence microscopy

Differential interference contrast (DIC) and fluorescence micrographs were acquired with a Zeiss LSM 510 META / LSM 5 LIVE / Axiovert 200M system. Localization of Alexa 594 was done with a 561 nm laser and an emission filter LP 575. To ensure image acquisition in the linear range, exposure times were adjusted for each image so that only one or two pixels were saturated. Z-stacks of 1 µm interval were acquired for image reconstruction using the Zeiss LSM 5 Duo software.

9.3.8 Image processing and fluorescence quantification

ImageJ software (Rasband, W.S., ImageJ, U. S. National Institutes of Health, Bethesda, Maryland, USA, http://rsb.info.nih.gov/ij/, 1997-2008) was used for quantification of fluorescence intensity based on maximum projections of Z-stacks. Pixel intensity was measured along the periphery of each pollen tube, beginning from the pole. Values for fluorescence intensity were normalized to the highest value present on an individual tube before averaging over all tubes (n>10 for each sample). Values on the x-axis in the graphs represent the meridional distance from the pole of the cell. Given a typical tube diameter of 14 µm and an approximately hemisphere-shaped apex for *Camellia*, a distance of 14 µm on the meridional curvature corresponds to a tube length of 10 µm measured along the longitudinal axis. For each treatment, at least 10 tubes were analysed. Each experiment was repeated at least 3 times.

9.3.9 Live imaging of vesicle trafficking in pollen tubes grown in hyper-gravity

To allow for live cell imaging at hyper-*g* levels, the Large Diameter Centrifuge (LDC) housed at the ESTEC-ESA (van Loon *et al.* 2008) was used. The LDC has four arms supporting up to 6 gondolas with a maximum payload of 80 kg each. The total diameter of the device is 8 m and *g*-forces of up to 20*g* can be achieved. An inverted Zeiss Axiovert-

100 microscope equipped for epi-fluorescence imaging was fixed in one of the gondolas using elastic strings (Fig 9.1). The x-y position of the stage and the focus of the microscope were remote controlled. The microscope was equipped with a Leica DFC 300 FX digital camera for brightfield and fluorescence imaging.

For the visualization of vesicle trafficking, the styryl dye FM1-43 was added at a final concentration of 1 $\mu g.mL^{-1}$ to each Ibidi® well containing growing *Camellia* pollen tubes. For FM1-43 imaging, a filter set with excitation BP 450-490 nm, beam splitter FT 510 nm and emission LP 515 nm was used. Imaging was performed on growing pollen tubes at 1, 2, 5, 7, 10 and 12 *g*. Images were acquired at 1 $frame.s^{-1}$.

9.4 Results

9.4.1 A change in gravity levels affects pollen germination, pollen tube diameter, growth rate and volume

In previous studies, *Arabidopsis* and *Brassica rapa* pollen tubes grown under hyper-*g* conditions were found to display drastically reduced growth rates and aberrant tube morphologies (Musgrave *et al.* 2009b). To assess the general effect of hyper-*g* on *Camellia* pollen performance we quantified the percentage of pollen germination, pollen tube growth rate, and pollen tube diameter in pollen germinating under various hyper-*g* and under omnidirectional-*g* conditions. In the control experiments at 1*g*, an average of 80% of the *Camellia* pollen grains was able to germinate. This value was close to the viability of the grains tested using FDA of 90% ± 3.4%, demonstrating that our *in vitro* growth conditions are close to optimal. The effect of both increased gravity level and omnidirectional-*g* was dramatic as germination percentage decreased by more than half in both situations (Fig 9.2a).

In our *in vitro* growth conditions, *Camellia* pollen tubes germinated at 30 mins after contact with the growth medium and elongated at an average rate of 290 $\mu m.h^{-1}$ as calculated from pollen tube length of germinated pollen at 3 hours after imbibition. *Camellia* pollen tubes growing at 1*g* had an average diameter of 14±0.92 µm. When tubes were grown under omnidirectional-*g* conditions, the diameter of the pollen tubes was reduced by 8% and

under hyper-*g* conditions the diameter of the pollen tubes increased by 8% at 5*g* and 38% at 20*g* (Fig 9.2b) as measured in the cylindrical shank of the tube.

Quantification of pollen tube length at hyper-*g* showed that those pollen tubes that were able to germinate under these conditions, were somewhat affected in their ability to elongate, but not dramatically so. Only at *g*-levels as high as 20*g* was the growth rate reduced to half of that of the bench control. Under omnidirectional-*g* conditions, reduction of the growth rate was significant to less than half of the control value (Fig 9.2c).

Since both growth rate and diameter were altered by changed gravity conditions, we determined the overall rate of cell wall volume to be delivered by calculating the rate at which the surface of the cellular envelope (plasma membrane and cell wall) increases. At 1*g* the surface of *Camellia* pollen tubes increased by 13 377±2 783 $\mu m^2.h^{-1}$. Whereas under hyper-gravity this surface addition rate did not change significantly, under omnidirectional gravity it was reduced by 39% (Fig 9.2d).

9.4.2 A change in gravity value does not affect the spatial profile of pectin distribution

Pollen tubes are characterized by a precisely controlled, spatially defined distribution of cell wall components which is responsible for the shape formation in this cell (Fayant *et al.* 2010). Notably, pectins change from highly methyl-esterified to primarily acidic configuration at the transition region between the hemisphere shaped apex and the tubular shank. This is achieved by the apical secretion of pectins in highly methyl-esterified form and subsequent deesterification by pectin methyl esterase in the shank of the tube (Bosch *et al.* 2005). This change in chemical configuration is thought to allow gelation by calcium ions and has been linked to a stiffening of the wall (Geitmann and Parre 2004; Parre and Geitmann 2005b; Zerzour *et al.* 2009). The tubular shank of the tube is furthermore rigidified by the deposition of callose (Parre and Geitmann 2005). The role of cellulose is less well understood. It is present in low concentrations in the shank of all pollen tube species (Aouar *et al.* 2010), but can also be present in the apex of some (Fayant *et al.* 2010). These precisely defined spatial changes in chemical configuration and relative abundance of cell wall components have been postulated to determine the pollen tube diameter (Fayant *et al.* 2010; Eggen *et al.* 2011). In particular, the cross-over point between

methyl-esterified and non-esterified pectins has been proposed to define the transition region between the hemisphere shaped tip and the cylindrical shank of the tube and to result from endocytosis of a pectin methyl esterase inhibitor at this location (Röckel *et al.* 2008; Fayant *et al.* 2010). Therefore, the observed change in tube diameter upon modulation of the *g*-force motivated us to assess whether the spatial distribution of the cell wall components was affected in these tubes. We hypothesized that in larger tubes formed under hyper-*g* conditions the cross-over point between the two configurations of pectin would be further away from the pole, whereas in smaller tubes resulting from omnidirectional-*g* conditions this cross-over point was expected to be closer to the tip. However, immunohistochemical label with JIM5 and JIM7, specific antibodies against pectins with low and high degree of esterification, respectively, revealed that the characteristic spatial profile of pectin was not visibly affected by the *g*-level tested here (Figs 9.3a-f). Quantification of relative fluorescence levels along the tube periphery did not yield any difference in the spatial distribution of either type of pectin between the pollen tubes grown at 1*g* and pollen tubes exposed to hyper-*g*.

9.4.3 A change in gravity conditions causes the relocalization of cellulose towards the apex of the tube

Since the spatial profile of pectins was not altered as a result of increased gravity-stress, we hypothesized that one of the other cell wall components might be affected in their distribution. Although crystalline cellulose is not generally present in high quantities in the pollen tube cell wall (van der Woude *et al.* 1971; Schlüpmann *et al.* 1994), it was found to play a crucial role in determining the pollen tube shape of *Petunia hybrida, Lilium auratum, Lilium orientalis, Solanum chacoense* and *Picea abies* (Anderson *et al.* 2002; Lazzaro *et al.* 2003; Aouar *et al.* 2010). Crystalline cellulose was labelled with cellulose binding module 3a (CBM3a) (Blake *et al.* 2006). After two hours of growth at 1*g*, crystalline cellulose was only detected in the distal region of *Camellia* pollen tubes starting at 10 µm from the pollen tube tip. Along the tube, the abundance increased steeply with half-maximum fluorescence intensity at 12 µm and reaching a plateau at 20 µm (Figs 9.3g,i). When pollen tubes were subjected to omnidirectional-*g* or hyper-*g* conditions of 5*g* and higher, crystalline cellulose deposition changed dramatically. In both situations

the fluorescence label was uniform around the entire cell perimeter, including the tip (Figs 9.3g,h,j). No noticeable differences in this ectopic cellulose localization were observed between various hyper-*g* levels (Supplemental Fig 9.1a).

9.4.4 Callose is closer to the tip in tubes grown in hyper-gravity

Callose is the most abundant polymer in pollen tube cell wall (Schlüpmann *et al.* 1994) and plays an important mechanical role in reinforcing the pollen tube cell wall against compression and tension stresses in the distal part of the tube (Parre and Geitmann 2005). In *Camellia* pollen tubes grown at 1*g*, visible deposition of callose appeared at 15 µm from the pole with the half-maximum fluorescence intensity at 30 µm meridional distance from the tip and a steep increase to a plateau at 40 µm (Figs 9.3l,n). When pollen tubes were subjected to omnidirectional-*g* conditions, callose deposition along the longitudinal axis increased more gradually with a half-maximum at 30 µm and a very gradual increase to a plateau at approximately 80 µm (Figs 9.3l,m). Remarkably, the callose layer was not smooth as in the 1*g* control, but irregular with a speckled appearance (Supplemental Fig 9.2, Movie 9.1). By contrast, in the 5*g* sample, callose deposition appeared as a smooth layer starting closer to the tip beginning at 7 µm with a half-maximum at 17 µm and a plateau at 21 µm. (Figs 9.3l.o). No noticeable difference in callose localization was observed between different hyper-*g* levels (Supplemental Fig 9.1b).

To further confirm that the mis-localization of cellulose and callose was due to a change in hyper-*g* conditions and that the effect was reversible, pollen tubes were grown at 5*g* for 2 hours, removed from the centrifuge and then left to grow at 1*g* for 5, 10 or 15 mins before fixation and immunolabel. As few as 5 mins at 1*g* were sufficient for cellulose and callose profiles to return to the characteristic distances from the apex that were observed in samples grown in parallel at 1*g* for the entire time (Figs 9.3k,p).

9.4.5 Vesicle trafficking is reduced at hyper-gravity levels

The principal process responsible for pollen tube expansion is the continuous and extremely high exocytosis rate of vesicles containing cell wall precursors and enzymes responsible for cell wall synthesis. Exocytosis is accompanied by membrane endocytosis to ensure a balanced deposition rate of extracellular matrix and membrane material. Pollen tube growth

is thus characterized by a tight temporal and spatial control of the dynamic vesicular trafficking (Bove *et al.* 2008). Since the spatial profiles of cellulose and callose were affected by altered *g*-levels, and since these cell wall components are assembled by synthases delivered to the plasma membrane by exocytosis, we wanted to understand how hyper-*g* affects intracellular trafficking. To this end, pollen tubes were grown in the presence of the styryl dye FM1-43 and exposed to increased *g*-levels in a Large Diameter Centrifuge allowing for live cell imaging in brightfield and fluorescence mode. In *Camellia* pollen tubes grown at 1*g*, vesicles tended to aggregate in the apical cytoplasm in a volume with the shape of an inverted cone. This phenomenon has been described in many other angiosperm species (Bove *et al.* 2008; Zonia and Munnik 2008; Bou Daher and Geitmann 2011) and is generated by an inverse fountain shaped transport pattern mediated by the actin cytoskeleton (Lovy-Wheeler *et al.* 2005; Kroeger *et al.* 2009). Previously, we had quantified this streaming pattern using spatio-temporal image correlation spectroscopy (STICS) to circumvent the fact that the sub-diffraction size of the vesicles precludes their tracking when densely packed and moving rapidly (Bove *et al.* 2008). However, STICS requires high temporal resolution image series acquired by confocal laser scanning microscopy. The present setup in the LDC only allowed for conventional epi-fluorescence imaging making the quantification of vesicle movement using STICS impossible. To quantitatively assess the intensity of vesicle trafficking, we therefore determined the size of the inverted vesicle cone as well as its fluorescence intensity. The inverted vesicle cone occupied an average surface of 62±10.0 μm^2 at 1g. The width of the cone measured as arc length at the tip was 9.7±1.9 µm. In hyper-*g* conditions, the surface of the cone was reduced by 25.6% with small, non significant variations between the different hyper-*g* levels tested (between 5*g* and 10*g*) (Figs 9.4a,b). The width of the cone did not vary significantly between different hyper-*g* levels or compared to the 1*g* control.

To quantitatively determine the relative density of vesicles within the cone while excluding potential artifacts due to bleaching, we calculated the ratio between fluorescence intensities in the cone and in the distal cytoplasm of individual pollen tubes (Figs 9.4a,c). Tubes growing at 1*g* showed a cone/cytoplasm ratio of 2.1 whereas their counterparts grown in hyper-*g* showed a ratio close to 1.1 (with insignificant variations between the different tested g levels). This corresponds to a decrease of 48.5% of the cone/cytoplasm

fluorescence ratio of the tubes grown in hyper-*g* compared to the tubes grown at 1*g* (Fig 9.4c).

9.5 Discussion

Non-statocyte single plant cells have no known anatomical feature that equips them to sense gravity, but a change in gravity level has an effect on cellular metabolism and structure (Morita and Tasaka 2004; Chebli and Geitmann 2011). We investigated the role of altered gravity on pollen tube growth behaviour. The pollen tube (or male gametophyte) is an ideal model for this kind of study because of its rapid and quantifiable response (within few seconds) to stress (Chebli and Geitmann 2011) and because it does not have any known statoliths and does not display gravitropic response (De Micco *et al.* 2006a). Pollen tubes, similar to neurons, fungal hyphae and root hairs are tip-growing cells. To sustain its rapid growth rate, constant vesicle exocytosis is required. These vesicles contain cell wall precursors, mainly pectins and hemicelluloses, as well as membrane-bound enzymes responsible for the synthesis of cellulose and callose. Furthermore, cell wall modifying enzymes and proteins are secreted, such as pectin methyl esterase (PME) or the PME inhibitor. Pectins are deposited at the apex in a highly esterified form, a material that is fluid-like (Geitmann 2010b) and PME activity is responsible of de-methyl esterifying the polymer during cell wall maturation allowing for pectin to be gelated by calcium ions in the shank of the tube (Chebli and Geitmann 2007; Röckel *et al.* 2008). Other cell wall components are either deposited by exocytosis (xyloglucans) or synthesized directly at the plasma membrane (cellulose, callose) (Chebli and Geitmann 2007). The main question we wanted to answer is how gravity affects the delivery of cell wall material during plant cell growth and how this material is assembled once deposited during cell wall maturation.

9.5.1 Altered gravity affects pollen performance

Our data showed that in *Camellia* pollen tubes grown under altered gravity conditions both germination percentage and growth rate were reduced. This is in accordance with observations made in pollen grains from *Arabidopsis* (Musgrave *et al.* 2009b), *Pyrus* and *Prunus* (De Micco *et al.* 2006a) germinated in hyper-*g* conditions and suggests that despite an absence of an obvious gravity perception mechanism, certain cellular functions are

affected when these cells are exposed to altered gravity levels. Interestingly, the germination percentage was reduced more dramatically, whereas those tubes that succeeded to germinate did grow relatively well, even at *g*-forces up to 20*g*. This indicates that the mechanism of germination might require cellular processes that are more susceptible to mechanical stress than those governing pollen tube growth. Whether this is related to the critical step of the initial polarization of the cell (Heslop-Harrison 1987) or to the processes that lead to the softening of the aperture cell wall required for pollen tube outgrowth (Geitmann 2010a) remains to be investigated.

9.5.2 Gravity stress affects cell wall assembly and morphogenesis

As a consequence of gravity stress, the diameter of *Camellia* pollen tubes was altered and this effect was clearly dose-dependent. Omnidirectional-*g* conditions resulted in a reduced diameter, whereas increasing hyper-*g* lead to an increasingly large pollen tube diameter. The diameter of the pollen tube is determined by the kinetics of rigidification of the cell wall material once it is deposited at the apex (Geitmann and Ortega 2009; Fayant *et al.* 2010; Eggen *et al.* 2011). The stiffening is caused by calcium gelation of de-methyl-esterified pectins. Pectin de-methyl esterification is accomplished by PME that is equally secreted at the apex, but whose activity is inhibited in the apical dome by the PME inhibitor (Röckel *et al.* 2008). It is thought that endocytosis of the inhibitor at the transition region between apex and shank allows the enzyme to act and hence the spatial location of this endocytotic activity might be a critical determinant for pollen tube diameter and shape generation. A disturbance either in the spatial or temporal control of the secretion of the amount of pectin, the amount of PME or of the efficiency or location of endocytosis of PMEI could provide an explanation for a change in cellular diameter.

If an altered kinetics in pectin de-esterification were the principal reason for the observed altered tube diameter, one would predict that the pectin profiles (both esterified and non-esterified) should be shifted slightly - towards the apex to explain the smaller pollen tube diameter at omnidirectional-*g* and away from the apex at hyper-*g*. The latter shift would be expected to be as small as 3.1 µm at 20*g* in accordance with the observed 4 µm increase in cellular diameter compared to the 1*g* control. However, the high variability in the pectin distribution profiles between individual pollen tubes, and the fact that these profiles only

represent relative distributions, rather than absolute pectin abundance, did not allow us to discern such a small shift.

9.5.3 Intracellular trafficking is reduced at hyper-gravity

The delivery of material to the growing apex relies on an exquisitely regulated balance between exocytosis and endocytosis both of which need to be precisely controlled in time and space (Bove *et al.* 2008). Intracellular trafficking is therefore of crucial importance for proper pollen tube elongation and the process is governed by a characteristic actin array (Kroeger *et al.* 2009) that directs vesicles to the expanding apical cell surface (Bou Daher and Geitmann 2011). Past studies relied on a combination of high spatial and temporal resolution imaging using a confocal laser scanning microscope and spatio-temporal image correlation spectroscopy. This allowed for the identification and quantification of the intracellular trafficking patterns in the pollen tube. However, this type of imaging or quantitative analysis was not feasible in the Large Diameter Centrifuge and we had to resort to conventional epi-fluorescence microscopy. Using fluorescence intensity of vesicles labelled by the styryl-dye FM1-43 as a proxy for trafficking, we observed a significant reduction in the number of vesicles present in the apical cone at hyper-*g* compared to the 1*g* control. This is consistent with findings by Lisboa and colleagues (Lisboa *et al.* 2002) who used samples fixed after exposure to temporary hyper-*g* stress and showed that endocytotic retrieval of plasma membrane in tobacco pollen tubes was reduced compared to the 1*g* control. At the hyper-*g*-values tested here, there was no significant dose-dependent effect, however. Whether the reduction of vesicles in the apex in our setup is due to a slower rate of overall transport or a reduced number of secretory vesicles produced cannot be deduced from the present data. A reduced number of vesicles in the apical cone could also mean that the equilibrium between the forward and rearward transport rates within the tube is altered. If the rearward vesicle transport by the central actin array is accelerated, or the forward transport in the periphery is slowed, the accumulation of vesicles in the apex would be reduced (Kroeger *et al.* 2009). The fact that the surface expansion rate of pollen tubes grown at hyper-*g* was comparable to their counterparts grown at 1*g* shows that despite the difference in the rate of longitudinal elongation, the same amount of cell wall material is deposited at the apex over time (assuming that cell wall thickness is constant). This

suggests that the number of exocytosis events is not affected by the hyper-gravity stress, but rather that the location of these events, and thus the resulting morphogenetic process are altered. The wider tube diameter at hyper-*g* is indicative either for a less focused distribution of exocytosis events or for the subcellular localization of endocytosis being shifted further distal. Remarkably, the unaltered rate of surface growth suggests that the vesicle fusion rate is indeed a rate limiting factor for pollen tube expansion - independently of the degree of polarity and precise morphology of the resulting cell.

9.5.4 Hyper-gravity affects cellulose assembly

In normal growing *Camellia* pollen tubes, both cellulose and callose are absent from the apical region of the cell. This characteristic profile was changed dramatically as cellulose appeared in the tip both at hyper-*g* and omnidirectional-*g*. In general, cellulose is known to stiffen the cell wall and its absence from the tip was thought to be consistent with the rapid expansion activity occurring in this cellular region. The fact that the gravity stressed tubes displaying apical cellulose only showed moderately reduced growth rates raises questions about the concept of wall stiffening. As long as the cellulose microfibrils are short or not cross-linked, their presence does not necessarily imply a stiffening of the wall. This would be consistent with the fact that not all pollen tubes growing under normal *in vitro* conditions are devoid of cellulose at the apex. Those of *Arabidopsis thaliana* and *Lilium orientalis*, for example, display crystalline cellulose in the apex (Fayant *et al.* 2010; Chebli *et al.* 2012) suggesting that the role of this polymer for the morphogenetic process may be more subtle. It remains to be elucidated how the gravity-trigger causes cellulose to appear at the apex in *Camellia* pollen tubes. The explanation may be simply in the kinetics of the cellulose synthase activity that could be argued to be time-dependent rather than position-dependent. Since the tubes grow slower under gravity-induced stress, the amount of cellulose formed at a given location from the pole of the cell may be higher as a result of this location being distanced from the advancing pole at a reduced rate. In this scenario, the altered cellulose profile is a passive consequence of a lower growth rate. Alternatively, one can hypothesize that additional deposition of cellulose at the apex serves to stabilize an otherwise weakened cell wall. This weakening might for example be induced by a reduced supply with pectin, consistent with the reduced trafficking. It is known that pollen tubes are

able to compensate for the lack of one cell wall component by increased deposition of another (Aouar *et al.* 2010). This scenario would therefore represent an active response of the cell to a modulation in cell wall mechanics. As a third hypothesis one could argue that rather than affecting cell wall assembly directly, because of a cellular flattening induced by the centrifugal force the hyper-*g* induced stress simulates an increase in turgor leading to an increase in tensile stress in the wall. An effort to strengthen the apical wall could therefore be interpreted to serve to counteract the increased turgor and prevent bursting. In this latter scenario, it is difficult to explain why cellulose would equally appear at the tip at omnidirectional-*g*, which is generally interpreted to correspond to simulated microgravity. The finding could be reconciled with this hypothesis, on the other hand, if one accepts that omnidirectional-*g* is, in fact, not the removal of gravity, but simply a continuous change of the orientation of the 1*g* gravity force that might result in more overall stress than the stable positioning of the cell versus the orientation of the gravity vector.

The rapid reversibility of the altered spatial profiles of cellulose and callose after removal of the hyper-*g* induced stress confirms that the phenomenon is caused by a direct effect of gravity stress on the cellular processes involved in cell wall delivery and assembly rather than an effect mediated by a change of gene expression or synthesis of cell wall material. Full recovery was achieved within 5 min, a time period that is unlikely to involve any processes that are significantly upstream of the growth machinery, such as signaling to the nucleus.

9.5.5 Omnidirectional gravity disrupts callose deposition

In normally growing pollen tubes, callose is deposited in the distal portion of the tube and plays a role of reinforcement against compression and tension stresses (Parre and Geitmann 2005). At hyper-*g*, although the apex was still devoid of this polymer, the callose layer was visible closer to the tip than at the 1*g* control. A similar kinetics-based argument could be brought forward for this phenomenon, as that proposed for cellulose. At lower growth rate, a given location on the cell surface is being distanced from the advancing pole at a slower rate, and hence accumulation starts at a closer distance from the tip if callose synthesis rates by individual synthases are otherwise unaltered. If this hypothesis holds true for both, callose of cellulose, the question arises why the two components are affected to a different

degree. This difference could be explained with different basal rates of the synthesis activity. On the other hand, similar to cellulose, callose deposition might also be enhanced to compensate for the perceived increased turgor resulting from compression stressed caused by the centrifugal force.

The more puzzling phenomenon is the fact the callose layer becomes irregular and speckled at omnidirectional-*g*. Clearly, there is a disturbance in the deposition of this layer upon this supposedly gentler type of gravity-stress. Whether the irregular patches are a result of a reduced number of callose synthases being supplied, or their clustering within the plasma membrane, or yet another mechanism remains to be elucidated.

9.6 Conclusion

To our knowledge, this is the first time fluorescence microscopy has been used to monitor live sub-cellular events in hyper-*g* conditions. Our novel approach allowed to shed light on the behaviour of non-statocyte plant cells in response to changes in gravity force, suggesting that cell wall assembly and intracellular trafficking are affected to compensate for the altered mechanical load imposed by omnidirectional and hyper-*g*. Although complementary experiments are required to understand the causality link between the different effects of altered gravity, this approach proved the feasibility of live cell fluorescence imaging.

9.7 Acknowledgment

This project was financed by the European Space Agency *Spin Your Thesis!* program. Research in the Geitmann lab is supported by grants from the Natural Sciences and Engineering Research Council of Canada (NSERC) and the Fonds Québécois de la Recherche sur la Nature et les Technologies (FQRNT). Youssef Chebli is funded by the Ann Oaks doctoral scholarship of The Canadian Society of Plant Biologists / La Société canadienne de biologie végétale.

9.8 Figures

Figure 9.1

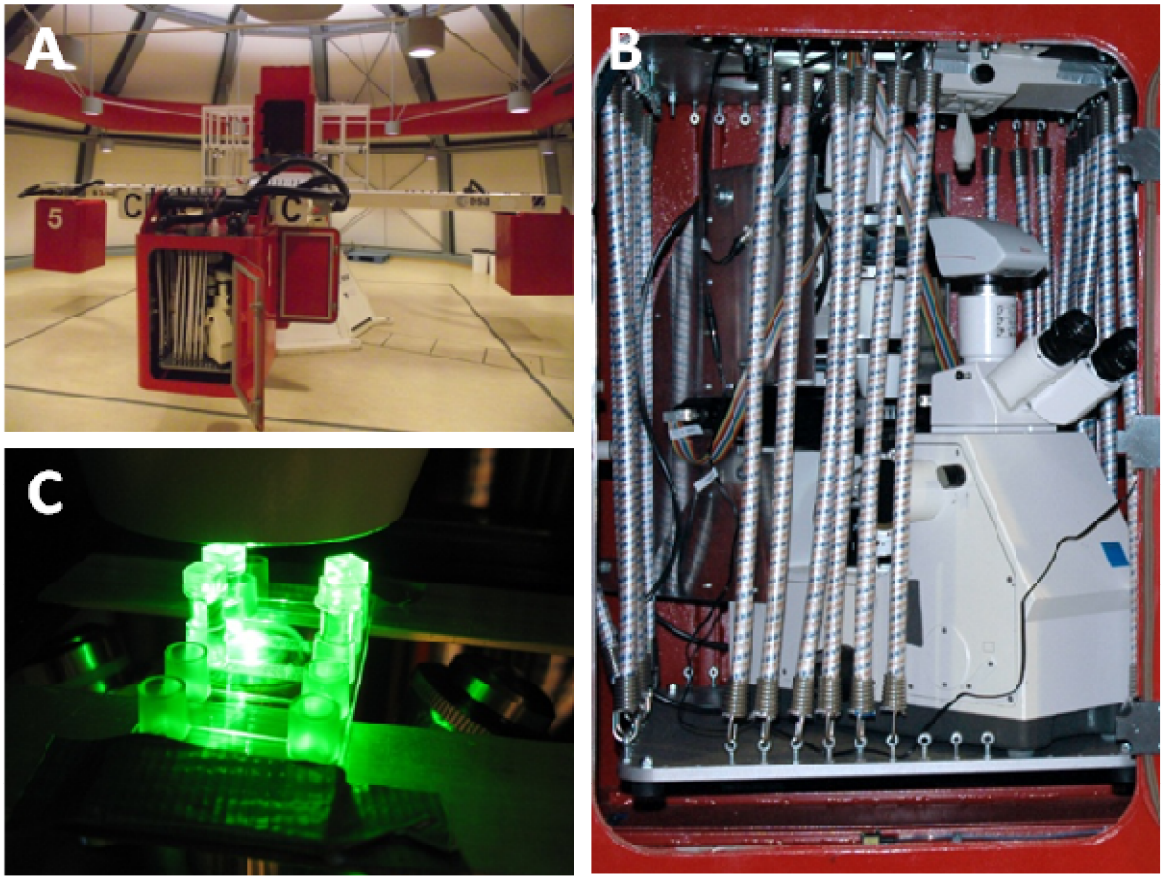

Figure 9.1: Large Diameter Centrifuge at the research facilities of the European Space Research and Technology Centre of the European Space Agency in Noordwijk, The Netherlands.

(A) The LDC is composed of four arms supporting a total of up to 6 gondolas. (B) An inverted Zeiss Axiovert 100 microscope equipped with a mercury lamp was fixed inside one of the gondolas allowing live observations of growing pollen tubes in Ibidi® cells (C).

.

Figure 9.2

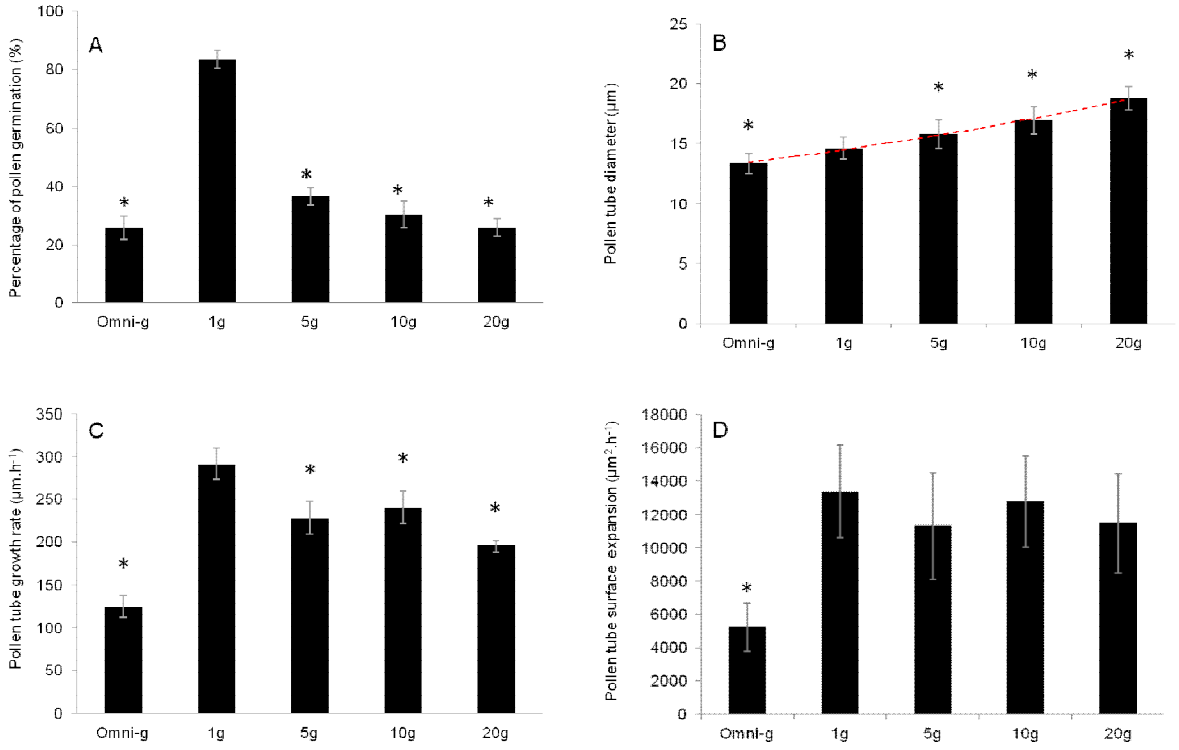

Figure 9.2: Response of Camellia pollen tube morphology to altered gravity conditions.

(A) Germination percentage of pollen grains. Pollen grains were considered germinated when the length of the pollen tube exceeded the diameter of the pollen grain. (B) Pollen tube diameter was measured at approximately 20 µm from the pole. The red line shows a dose-dependent increase in the pollen tube diameter with the smallest diameter observed at omnidirectional-*g* and the largest at 20*g*. (C) Pollen tube elongation rate as calculated from pollen tube length after 2 to 3 hours following imbibition. (D) Rate of surface expansion as calculated from pollen tube diameter and elongation rate. Asterisks (*) indicate statistically significant difference between samples grown in altered gravity conditions compared to the samples grown at 1*g* (Two way t-test yielded $p < 0.001$).

Figure 9.3

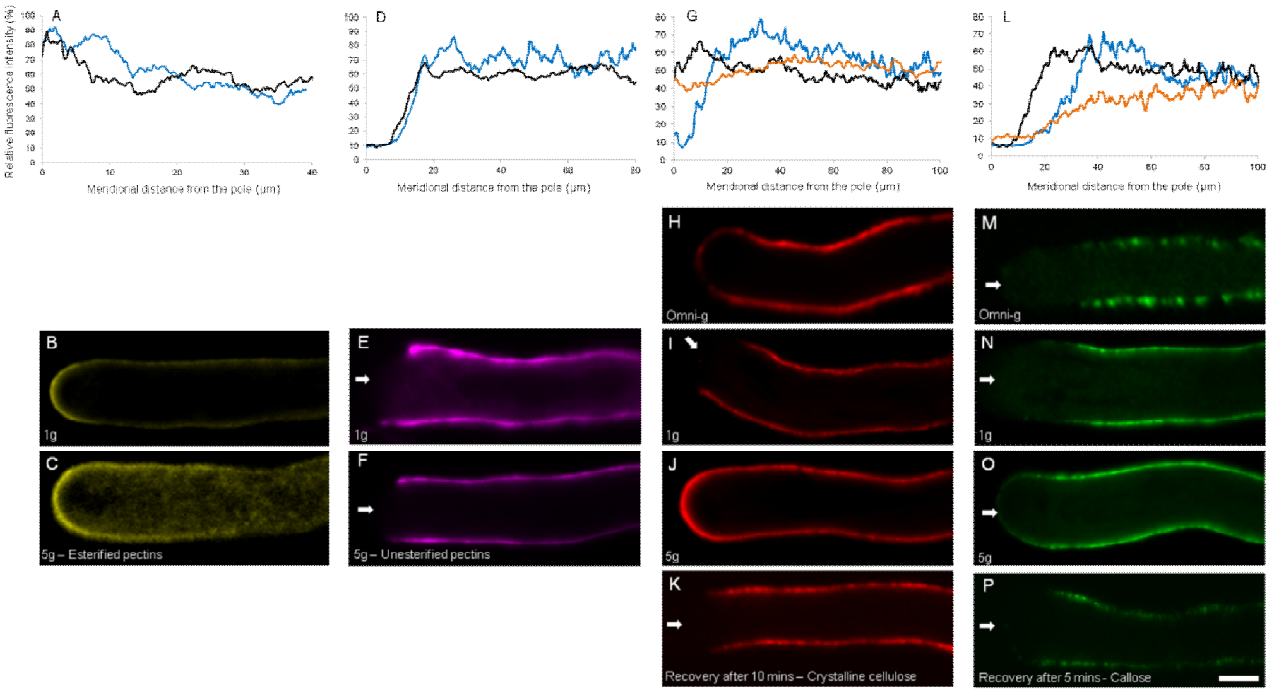

Figure 9.3: Relative spatial distribution of the cell wall components in *Camellia* pollen tubes grown in omnidirectional-*g*, at 1*g* and in 5*g* conditions

Relative spatial distribution of esterified pectins (A,B,C), unesterified pectins (D,E,F), cellulose (G,H,I,J,K), and callose (L,M,N,O,P) in *Camellia* pollen tubes grown in omnidirectional-*g* (orange curve), at 1*g* (blue curve) and in 5*g* conditions (black curve). Relative label intensities were quantified along the meridional tube surface measured on z-stack projections (A,D,G,L). Corresponding fluorescence micrographs of median optical sections (B,C,E,F,H,IJ,M,N,O) are displayed for the different gravity levels. Recovery of the typical spatial profile observed at 1*g* for cellulose and callose is observed 5 mins after removal from the centrifuge (K,P). Specific label was performed using JIM7 and JIM5 antibodies, directed against highly esterified and unesterified pectins, respectively, Cellulose Binding Module 3A against crystalline cellulose and anti (1→3)-β-glucan against callose. Graphs represent the average of n> 10 pollen tubes. Arrows mark the position of the pollen tube tip. Bar = 10 µm.

Figure 9.4

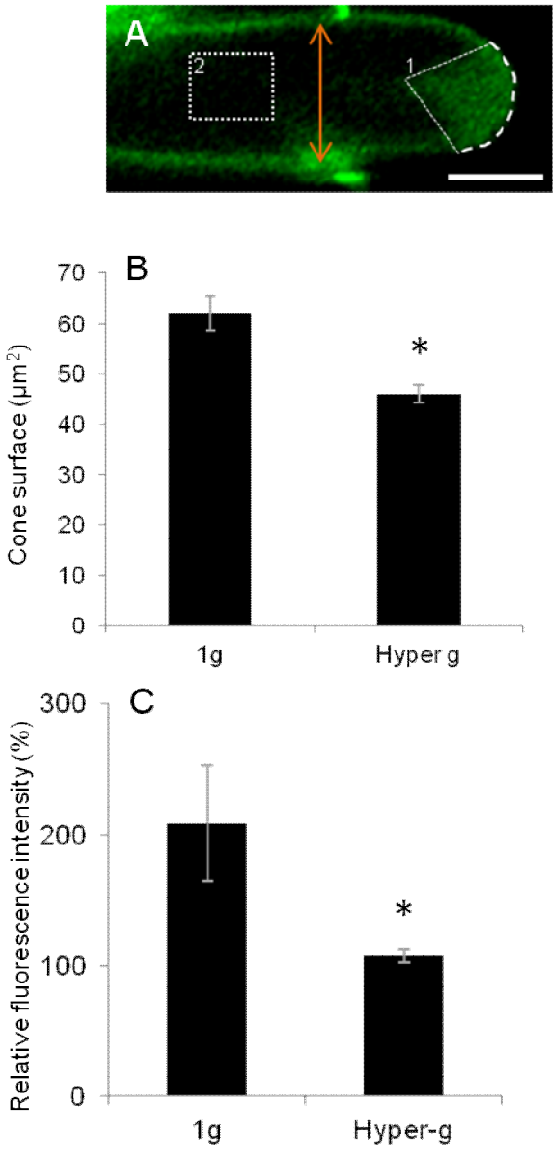

Figure 9.4: Geometry and fluorescence intensity of the apical vesicle cone.

Geometry (A,B) and fluorescence intensity (A,C) of the apical vesicle cone. Vesicles were labeled by the styryl dye FM1-43 taken up by endocytosis. At the time of imaging the dye had been incorporated into most of the endomembrane system including exocytotic vesicles. (A) represents a pollen tube marked with FM1-43, the orange arrow represents the diameter of the pollen tube. Vesicular surface (B) and fluorescence intensity (area 1 in A) as well as the fluorescence intensity of the distal cytoplasm (area 2 in A) were measured in pollen tubes grown at 1 g and in hyper-*g* conditions. Relative fluorescence intensity (C) was expressed as a ratio between the fluorescence of the vesicle cone over the fluorescence of the distal cytoplasm fluorescence of the same tube. Asterisks (*) indicate statistically significant difference between samples grown in hyper-*g* and control samples grown at 1*g* (Two way t-test. $p < 5.10^{-4}$ for the three graphs). Bar = 10 µm.

9.9 Supplemental data

Supplemental Figure 9.1

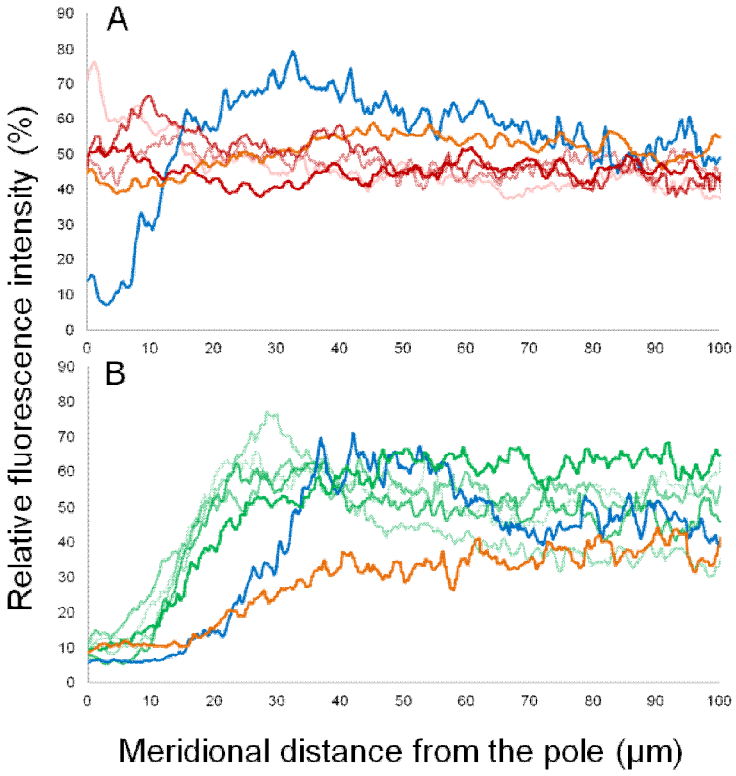

Supplemental Figure 9.1: Relative spatial distribution of cellulose and callose in *Camellia* pollen tubes grown in omnidirectional-*g*, at 1*g*, and hyper-*g*.

Relative spatial distribution of cellulose (A) and callose (B) in *Camellia* pollen tubes grown in omnidirectional-*g* (orange), at 1*g* (blue), and hyper-*g* (2*g*, 5*g*, 7*g*, 10*g* and 14*g*) represented by shading colors of red (cellulose) and green (callose) with darkes shade for highest *g*-value. Relative label intensities were quantified along the meridional tube surface measured on z-stack projections. All samples grown in hyper-*g* were significantly different from the samples grown in omnidirectional-*g* or at 1*g* but no difference was observed between the individual levels of hyper-*g*.

Supplemental Figure 9.2

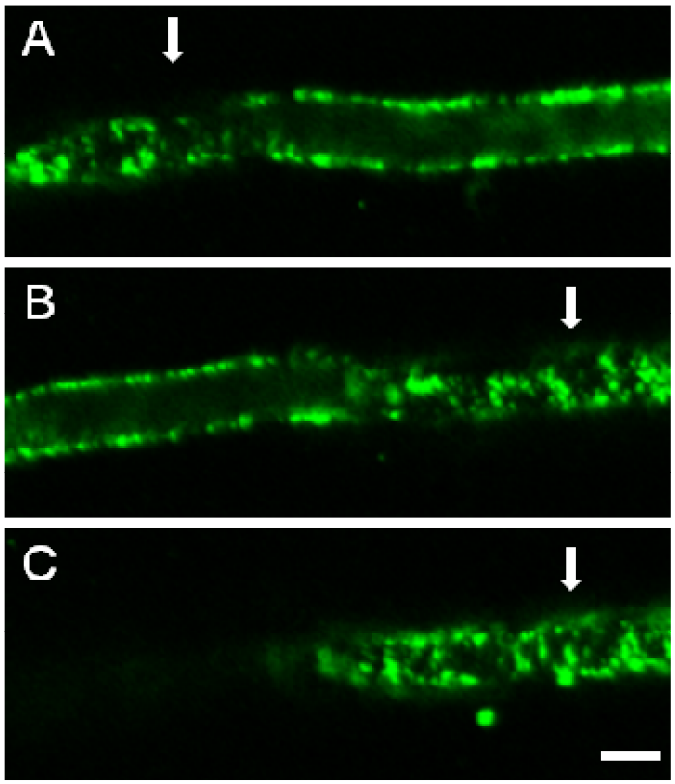

Supplemental Figure 9.2: Confocal laser scanning micrographs of a pollen tube grown in omnidirectional-*g* labelled with (1→3)-β-glucan against callose.

The three micrographs were taken from the same region of the pollen tube at different focal depths. Because of the oblique positioning of the tube, the optical sections show the median position of the tube (arrowheads) and the peripheral position (arrows) illustrating the patchy distribution of callose. Bar = 10 µm.

Supplemental Movie 9.1: Immuno-localization of callose in *Camellia* pollen tubes grown in omnidirectional-*g* conditions. 3D reconstruction from z-stack of confocal laser scanning micrographs acquired at 0.5 µm interval. Width of the frame equals 225 µm.

10 Conclusion and perspectives

Growth, morphogenesis and differentiation are the three fundamental processes leading to the formation of a biologically functional organism. Cells, tissues and organs undergo numerous morphological, structural and metabolic modifications before reaching their functional stages. These modifications are triggered and regulated by genetic and environmental cues which forge their final shape and physiological roles. Unlike animal cells, plant cell shaping relies greatly on the development and maturation of the cell wall. As detailed in the introduction, the primary cell wall is formed of a visco-elastic material predominantly composed of a cellulose/xyloglucans network embedded in a matrix of pectin. This simplistic view of the cell wall composition hides a much more intricate network where each component, each enzyme, each molecule and each ion plays a crucial role in determining the physiological and mechanical behaviour of the differentiating cell or tissue. To be able to achieve their final shape, plant cells constantly remodel their cell walls. The remodelling process involves tightly monitored changes of the chemical composition which in turn entails changes to the local mechanical properties of the cell wall. Because plant cells are constantly pressurized (due to their hydrostatic turgor pressure), the cell wall will always yield and grow at the softest spot whereas at the stiffer surface locations, growth will be reduced or arrested. Therefore, the chemical nature, the structure and the amount of each cell wall component have to be precisely regulated to guarantee proper growth, morphogenesis and differentiation.

The goal of this thesis is to understand the role played by the different cell wall components in shaping the plant cell and controlling the growth behaviour. Because of its high growth rate, its uni-directional growth, its relative simple cell wall composition and its easy *in vitro* germination, the male gametophyte emerged as the ideal biological model for this study.

During sexual plant reproduction, the pollen tube has to emerge through the thick intine of the pollen grain, elongate through the style between the transmitting tract cells, find its way to the ovary and then burst to deliver the sperm cells for double fertilization to occur. During all these steps the pollen tube is subjected to high mechanical and physiological stresses and it is crucial that it maintains its tubular invasive shape at all times. The first

barrier to be affected by these stresses is the pollen tube cell wall which has to (1) control the pollen tube shape, growth direction and growth rate, (2) regulate its own mechanics and (3) protect the sperm cells. Deciphering how the chemical composition and the structure of the different cell wall components influence the mechanical behaviour of the cellular envelope is therefore essential to understand how the pollen tube is able to sustain and regulate its constant elongation process while interacting with the extracellular environment. On the technical level, several methods ranging from cellular and molecular biology, to high performance microscopical imaging were used to assess the role of each cell wall component in shaping the pollen tube geometry.

10.1 Optimizing the protocols

The first step of my thesis was to optimize the protocols for pollen germination and for the processing of pollen tubes for microscopical observations. For *Lilium*, *Camellia* and *Solanum* pollen, the adequate germination protocols were already available, but for *Arabidopsis* pollen, we lacked a reliable and reproducible germination protocol. My colleague Firas Bou Daher and I optimized the different conditions of temperature, pH, sugar and salt concentrations that have to be used in different experimental setups to obtain a high and reproducible germination rate as well as healthy growing pollen tubes. In our hands, this method, published in *Plant Cell Reports*, worked better than those available in the literature at that time. The second step was to optimize the conditions of sample preparation for microscopical observations. Sample preparation is always a critical step and any flaw during this process can lead to the formation of artefacts. This can be caused by the different chemicals used to fix and treat the cells but also by the environmental conditions such as temperature that have the potential to alter tissue ultrastructure or antigenic properties. The method we optimized is based on the use of microwaves and on the control of the sample temperature. Microwaves cause the molecules of the sample to vibrate, thus facilitating the diffusive penetration and fixation of the chemicals, antibodies and salt into the cells in a much faster and efficient way when compared to bench-top treated samples. Moreover, preparation time is reduced at least by half.

10.2 Cellulose: the unexpected roles during pollen growth

Cellulose is the most abundant polymer in plant cell walls. On the cellular level, the spatial arrangement and abundance of the cellulosic microfibrils determine the rate and direction of cell expansion. Taken together with the fact that the pollen tube is an anisotropically growing cell, the initial hypothesis was that cellulose might play a reinforcing role against the turgor induced tensile stress in the pollen tube shank. In pollen tubes, cellulose is not very abundant and is thought to comprise roughly 10% of the pollen tube total neutral polysaccharides (Schlüpmann *et al.* 1994). Nevertheless, the experiments conducted to understand its mechanical role during pollen tube growth showed that the cellulosic network does not reinforce the pollen tube cell wall against compression stresses. The most efficient orientation of microfibrils for reinforcing the cell wall against circumferential tensile stress would be perpendicular to the main axis of growth, but when investigated in *Solanum*, *Lilium* and *Arabidopsis* pollen tubes, the net microfibril orientation was helical, not transverse. This is not consistent with a strong role in reinforcing the cell wall against turgor induced tensile stress in pollen tubes. Moreover, our findings show that cellulose is crucial in maintaining the pollen diameter. When a cellulose synthesis inhibitor (CGA) was added to growing *Lilium* pollen tubes, growth was not inhibited and pollen tubes responded by an increase in their diameter and by secreting more pectins (Aouar *et al.* 2010). On another hand, when *Camellia* pollen tubes were subjected to hyper-*g* levels or omnidirectional-*g*, the diameter of the pollen tube changed and cellulose was relocalized at the apex. In both cases, the exocytosis of abnormally higher (in hyper-*g*) or lower (in omni-*g*) amounts of esterified pectin lead to a modification in the cell wall Young's modulus as predicted by the FE model (Fayant *et al.* 2010). We speculate that to avoid swelling like a balloon (Fayant *et al.* 2010), cellulose was added to the pollen tube apex to rebalance the wall mechanical properties at the tip and keep the pollen tube diameter in a range allowing functional growth. These two findings could at first seem to be contradictory: Why when pollen tubes were treated with CGA, they continued growing and did not swell to make a sphere as predicted by the FE model? In theory this would have been the normal behavior since cellulose is not present anymore in the supapical region to determine the pollen tube diameter. One would have to point out that the pollen tubes did indeed swell like a sphere at

the apex before resuming a functional growth with a wider diameter. The continuous growth of the tube in these conditions could be explained by the fact that pectin metabolic enzymes such as PME would have been required in a higher number and/or greater activity in order to stiffen the wall and insure that the cell wall Young's modulus stays in a range allowing the pollen tube to grow and keep its tubular shape. This would have to be proven by assessing the activity and following the localization of PME and PMEI in pollen tubes growing in the presence of CGA. In light of this conclusion, the next question would then be: Why in altered gravity conditions, do the pollen tubes respond by adding more cellulose at the tip and not just modifying the pectin related enzymes activities? The answer is that the pollen tubes probably do modify the activity of these enzymes, but taking into account that the exocytosis rates are modified, these activity changes would probably not be sufficient to stabilize the pollen tube geometry. Moreover, from an energetic point of view, it may be more efficient for the pollen tube to deliver to the apex vesicles containing cellulose synthases that have begun synthesizing cellulose or to activate CESAs already present at the apical membrane, than to upregulate the synthesis of new pectin metabolic enzymes. This raises the question of the kinetics of the cellulose synthases, and whether they are activated in a time or position dependent manner in pollen tubes.

Cellulose synthesis is thought to be initiated at the plasma membrane. However, using immunogold labeling of chemically and cryo-fixed pollen tubes, we were able to show that crystalline cellulose was present inside *Arabidopsis* pollen tube vesicles. Although this constitutes only an indirect proof of the possible early synthesis of cellulose inside vesicles, it could explain how the fastest growing cell of the plant kingdom is able to rapidly adapt to a (sudden) change in its cell wall mechanical properties. As detailed in chapter 4, the idea of cellulose synthesis in pollen tube vesicles is not new and we think this mechanism might provide the cell wall assembly machinery with a head start necessary to sustain the rapid elongation of the pollen tube. Further direct evidence is required to unequivocally prove that cellulose synthesis is initiated in vesicles. One way would be to isolate vesicles from pollen tubes, analyse their content and detect any glucan synthase activity. Of course, differentiating whether the glucan synthase activity originates from cellulose or xyloglucan synthases might be difficult but could probably be overcome by putting in place a pull

down experiment where only chains of β-1,4-glucose (present in vesicles) would be pulled down with their respective β-glucan synthase.

Proving indubitably that cellulose synthesis is initiated in vesicles would open the way to a better understanding of the regulation of this process and its initiating factors. More questions concerning the regulation of each CESA in the rosette would have to be answered: Do the different CESA work in tandem or are they activated sequentially in the vesicles and in the cell wall? And how is their activity triggered and regulated? What are the mechanical properties of the cellulosic microfibrils synthesized in vesicles? And how do they integrate into the cell wall?

10.3 Tight regulation of pectin chemistry, a *sine qua non* condition for functional growth

Pectins are the first cell wall components to be secreted by the pollen tube. They are exocytosed in a highly methyl-esterified form at the apex of the tube and are subsequently de-esterified and cross-linked with calcium in the sub-apical part of the tube. The gradient of pectin esterification confers to the pollen tube cell wall its specific mechanical properties allowing it to maintain a regular tubular shape. As for any elastic or visco-elastic material, the cell wall is able to keep its geometry and resist deformation forces in a certain range determined by the chemical properties of its structural components. Since pectins constitute the majority of the apical cell wall material in the pollen tube, any imbalance in the amount exocytosed or in the *in muro* esterification gradient can lead to a deformation of the pollen tube geometry and/or a change in the amount and localization of other secreted cell wall components. This was proven theoretically and experimentally throughout the different chapters of this thesis. When using a set of selective enzymatic treatments (pectinase or PME) to induce specific chemical changes to the outer pectic layer, the pollen tube growth behavior changed in accordance with the modifications of the mechanical properties of the cell wall. At the same time, subjecting pollen tubes to altered gravity resulted in the disruption of the normal vesicle flow and consequently in the delivery of the proper amount of pectin and cell wall material to the apex. In all these cases a change in the pectin distribution profiles leads to the deformation of the pollen tube geometry because of an

alteration in the cell wall mechanical properties expressed by a drastic change in Young's modulus. In order to better understand the effects of the above mentioned factors on the mechanical properties of the apical cell wall, measurements of the mechanical properties should be assessed by micro-indentation or atomic force microscopy. Both techniques would allow the direct assessment of the mechanical behavior of the pollen tube cell wall under stress at subcellular resolution. Using an atomic force microscope to measure *in situ* the local mechanical properties of the pollen tubes growing in hyper-*g* conditions would be possible. The setup that was used in the LDC (chapter 9) was based on a set of elastic strings supporting a fluorescent microscope inside a payload gondola. Although there is room for improvement - especially for gravity forces greater than 10*g* - the system was very stable below 10*g* and capturing videos of growing pollen tubes was performed without significant vibrations. The technical challenges of building such a system are huge, since the weight of the whole system increases linearly with the applied *g*-level. This stresses the optical and electronic equipment that has to be firmly attached and reinforced. Nevertheless -and despite the many obstacles one could face when using an AFM in hyper-*g* conditions- the data obtained by such an experiment on growing pollen tubes, protoplasts or meristematic cells could enormously benefit our knowledge on the mechanical requirements of plant cells when growing and differentiating in a non-terrestrial environment. Linking these findings to the chemical composition of the cell wall and the vesicular trafficking would be a requirement to understand the plant metabolic and morphogenetic responses to altered gravity conditions. This could be done by using a laser scanning confocal microscope instead of a regular epi-fluorescence microscope. The resulting tremendous enhancement in the resolution and imaging quality would allow looking into the details of organelle and vesicle dynamics and, more importantly, to the changes in the actin cytoskeleton behaviour. The combined results of such an investigation would be indispensable for the development of spacecraft ecosystems or long term planetary colonization.

A deformation of the pollen tube shape can be produced by a change in its own cell wall properties, but because the tube is an invading cell, deformation can also be induced by the surrounding tissues. To reach the ovary, the pollen tube has to invade the pistillar tissue (in

solid style species like *Arabidopsis*) and forge its way between the transmitting tract cells. As in all plant tissues, the transmitting cells are connected by the middle lamella that is principally formed of pectins. Although no direct assessment was done to determine the exact mechanical properties of the stylar middle lamella, its chemical composition and biological function suggest that it is made of a stiff elastic material. During siphonogamy, to prevent the yielding pollen tube cell wall from being ruptured by the friction created during the elongation, the pectins composing the middle lamella have to be "liquefied". Several enzymes and processes specific to the style or to the pollen tube are implicated in this process (please refer to chapter 7 for more details). We showed that secreted pectate lyases are required to facilitate the pollen tube penetration process. More importantly, we directly proved for the first time that the pollen tube secretes enzymes into the surrounding growth matrix. This opens the way to a better understanding of the interaction between the male gametophyte and the pistil. Several studies showed that signaling pathways are implicated in the targeting of the pollen tube to the ovary. A calibrated guidance mechanism based on communication between the pistil and the pollen tube is necessary for the latter to follow the right path and reach the ovary (Cheung *et al.* 1995; Palanivelu and Preuss 2000; Higashiyama *et al.* 2003; Palanivelu *et al.* 2003; Palanivelu and Preuss 2006; Geitmann and Palanivelu 2007; Higashiyama and Hamamura 2008; Higashiyama 2010; Márton and Dresselhaus 2010). The digested pectins in the transmitting tract could therefore serve as signaling molecules in guiding the pollen tube through the style. The signaling effects of digested pectins could work either on the pollen tube *per se* by guiding it through the softest path and/or on the female transmitting tract by indirectly triggering pathways activating early cell death or middle lamella digestion downstream of the pollen tube path. If the digested pectins play a guiding role, they must be 'sensed' and recognized by the pollen tube as extracellular digested pectins. One way the pollen tube is able to exchange information with the extracellular media is through its very active endocytotic/exocytotic process. Therefore, internalizing digested pectins could be required for or involved in leading the pollen tube throughout its path. One way of proving this hypothesis would be to combine a set of two experiments: (1) germinating pollen grain *in vitro* in a pectin gel labelled with ^{14}C and (2) allowing the pollen grains to germinate in a regular gellified medium before giving the tubes the "choice" to remain in the same

gellified medium or to follow a path made of predigested pectins. If the ^{14}C is found inside the growing pollen tubes and if the tubes follow the path of the predigested pectins, it would mean that the digested pectins can lead the pollen tube through a specific route by regulating intracellular guidance pathways.

10.4 Pectin, cellulose and callose: the three vertices of the pollen tube cell wall

Although each cell wall component plays a specific role during pollen tube elongation, our experiments show that they are all bound together (chapter 4) and more importantly, act in synergy to ensure the continual functional growth of the pollen tube. Taken individually, pectin regulates growth rate and pollen tube diameter in the apical part (chapters 4, 6 and 9), cellulose is crucial for determining the pollen tube diameter in the sup-apical region (chapters 4, 5 and 9) and callose is essential for reinforcing the cell wall against compression and tension stresses in the distal part of the tube (Parre and Geitmann 2005a). But, when one of the component's synthesis, deposition, regulation, structure or distribution is altered, the pollen tube reacts immediately (within a time interval of seconds) to remedy the modifications of its mechanical properties in order to safeguard its biological function. A mis-regulation of any of the three major cell wall components leads to the reorganization of the others showing that through the different regulatory pathways, pectin, cellulose and callose act synergistically to provide the proper mechanical properties to the pollen tube cell wall. This pushes us to look at the cell wall as a whole dynamic entity where backup systems can be rapidly put in place to ensure proper growth and morphogenesis.

References

Acebes, J. L., Ester P. Lorences, Gloria Revilla and Ignacio Zarra (1993). "Pine xyloglucan. Occurrence, localization and interaction with cellulose." Physiologia Plantarum **89**(3): 417-422.

Al-Qsous, S., E. Carpentier, D. Klein-Eude, C. Burel, A. Mareck, H. Dauchel, V. Gomord and A. Balangé (2004). "Identification and isolation of a pectin methylesterase isoform that could be involved in flax cell wall stiffening." Planta **219**(2): 369-378.

Alonso-Simón, A., J. B. Kristensen, J. Øbro, C. Felby, W. G. T. Willats and H. Jørgensen (2010). "High-throughput microarray profiling of cell wall polymers during hydrothermal pre-treatment of wheat straw." Biotechnology and Bioengineering **105**(3): 509-514.

Anderson, J. R., W. S. Barnes and P. Bedinger (2002). "2,6-Dichlorobenzonitrile, a cellulose biosynthesis inhibitor, affects morphology and structural integrity of petunia and lily pollen tubes." Journal of Plant Physiology **159**(1): 61-67.

Antosiewicz, D. M., M. M. Purugganan, D. H. Polisensky and J. Braam (1997). "Cellular localization of *Arabidopsis* xyloglucan endotransglycosylase-related proteins during development and after wind stimulation." Plant Physiology **115**(4): 1319-1328.

Aouar, L., Y. Chebli and A. Geitmann (2010). "Morphogenesis of complex plant cell shapes - the mechanical role of crystalline cellulose in growing pollen tubes." Sexual Plant Reproduction **23**(1): 15-27.

Arabidopsis Genome Initiative (2000). "Analysis of the genome sequence of the flowering plant *Arabidopsis thaliana*." Nature **408**: 796-815.

Arioli, T., L. Peng, A. S. Betzner, J. Burn, W. Wittke, W. Herth, C. Camilleri, H. Höfte, J. Plazinski, R. Birch, A. Cork, J. Glover, J. Redmond and R. E. Williamson (1998). "Molecular analysis of cellulose biosynthesis in *Arabidopsis*." Science **279**(5351): 717-720.

Arsovski, A. A., G. W. Haughn and T. L. Western (2010). "Seed coat mucilage cells of *Arabidopsis thaliana* as a model for plant cell wall research." Plant Signaling & Behavior **5**(7): 796-801.

Augustin, S., M. Stock, O. Cromwell, A. Nandy and G. Reese (2012). "18 proteomic and immunological characterization of ragweed allergens." World Allergy Organization Journal **5**: S23-S24 10.1097/1001.WOX.0000411763.0000428401.0000411742.

Babbick, M., C. Dijkstra, O. Larkin, P. Anthony, M. Davey, J. Power, K. Lowe, M. Cogoli-Greuter and R. Hampp (2007). "Expression of transcription factors after short-term exposure of *Arabidopsis thaliana* cell cultures to hypergravity and simulated microgravity (2-D/3-D clinorotation, magnetic levitation)." Advances in Space Research **39**: 1182–1189.

Baluška, F. and K. H. Hasenstein (1997). "Root cytoskeleton: its role in perception of and response to gravity." Planta **203**: S69-S78.

Baluška, F., A. Hlavacka, J. Samaj, K. Palme, D. G. Robinson, T. Matoh, M. D.W., D. Menzel and D. Volkmann (2002). "F-Actin-dependent endocytosis of cell wall

pectins in meristematic root cells. Insights from brefeldin A-induced compartments." Plant Physiology **130**(422-431).

Baluška, F., J. Salaj, J. Mathur, M. Braun, F. Jasper, J. Šamaj, N. H. Chua, P. W. Barlow and D. Volkmann (2000). "Root hair formation: F-actin-dependent tip growth is initiated by local assembly of profilin-supported F-actin meshworks accumulated within expansin-enriched bulges." Developmental Biology **227**(2): 618-632.

Banik, M., T. P. J. Garrett and G. B. Fincher (1996). "Molecular cloning of cDNAs encoding (1→4)-β-xylan endohydrolases from the aleurone layer of germinated barley (<i>Hordeum vulgare</i>)." Plant Molecular Biology **31**(6): 1163-1172.

Barceló, A. R. and V. G. R. Laura (2009). *Reactive oxygen species in plant cell walls*
In: Reactive Oxygen Species in Plant Signaling. L. A. Rio and A. Puppo, Springer Berlin Heidelberg**:** 73-93.

Barjaktarović, Ž., A. Nordheim, T. Lamkemeyer, C. Fladerer, J. Madlung and R. Hampp (2007). "Time-course of changes in amounts of specific proteins upon exposure to hyper-g, 2-D clinorotation, and 3-D random positioning of *Arabidopsis* cell cultures." Journal of Experimental Botany **58**(15-16): 4357-4363.

Barjaktarović, Ž., W. Schütz, J. Madlung, C. Fladerer, A. Nordheim and R. Hampp (2009). "Changes in the effective gravitational field strength affect the state of phosphorylation of stress-related proteins in callus cultures of *Arabidopsis thaliana*." Journal of Experimental Botany **60**(3): 779-789.

Barlow, P. W. (1995). "Gravity perception in plants: a multiplicity of systems derived by evolution?" Plant Cell and Environment **18**: 951-962.

Bartnicki-Garcia, S. (2002). Hyphal tip growth: outstanding questions. Molecular biology of fungal development. H. D. Osiewacz. New York, Marcel Dekker**:** 29-58.

Bartnicki-Garcia, S., C. E. Bracker, G. Gierz, R. Lopez-Franco and H. Lu (2000). "Mapping the growth of fungal hyphae: orthogonal cell wall expansion during tip growth and the role of turgor." Biophysical Journal **79**: 2382-2390.

Bartnicki-Garcia, S., F. Hergert and G. Gierz (1989). "Computer simulation of fungal morphogenesis and the mathematical basis for hyphal (tip) growth." Protoplasma **153**: 46-57.

Baskin, T. (2005). "Anisotropic expansion of the plant cell wall." Annual Review of Cell and Developmental Biology **21**: 203-222.

Baskin, T. I., H. T. H. M. Meekes, B. M. Liang and R. E. Sharp (1999). "Regulation of growth anisotropy in well-watered and water-stressed maize roots. II. Role of cortical microtubules and cellulose microfibrils." Plant Physiology **119**: 681-692.

Battey, N. H., N. C. James, A. J. Greenland and C. Brownlee (1999). "Exocytosis and endocytosis." Plant Cell **11**: 643-659.

Becker, J. D., L. C. Boavida, J. Carneiro, M. Haury and J. A. Feijó (2003). "Transcriptional profiling of *Arabidopsis* tissues reveals the unique characteristics of the pollen transcriptome." Plant Physiology **133**(2): 713-725.

Benkert, R., G. Obermeyer and F. W. Bentrup (1997). "The turgor pressure of growing lily pollen tubes." Protoplasma **198**: 1-8.

Beutner, D., T. Voets, E. Neher and T. Moser (2001). "Calcium dependence of exocytosis and endocytosis at the cochlear inner hair cell afferent synapse." Neuron **29**: 681-690.

Bih, F. Y., S. S. H. Wu, C. Ratnayake, L. L. Walling, E. A. Nothnagel and A. H. C. Huang (1999). "The predominant protein on the surface of maize pollen is an endoxylanase synthesized by a tapetum mRNA with a long 5′ leader." Journal of Biological Chemistry **274**(32): 22884-22894.

Blackbourn, H. D., P. J. Barker, N. S. Huskisson and N. H. Battey (1992). "Properties and partial protein sequence of plant annexins." Plant Physiology **99**: 864-871.

Blake, A. W., L. McCartney, J. E. Flint, D. N. Bolam, A. B. Boraston, H. J. Gilbert and J. P. Knox (2006). "Understanding the biological rationale for the diversity of cellulose-directed carbohydrate-binding modules in prokaryotic enzymes." Journal of Biological Chemistry **281**(39): 29321-29329.

Blevins, D. G. and K. M. Lukaszewski (1998). "Boron in plant structure and function." Annual Review of Plant Physiology and Plant Molecular Biology **49**: 481-500.

Boavida, L. C. and S. McCormick (2007). "Temperature as a determinant factor for increased and reproducible in vitro pollen germination in *Arabidopsis thaliana*." The Plant Journal **52**(3): 570-582.

Boldogh, I., A. Bacsi, B. K. Choudhury, N. Dharajiya, R. Alam, T. K. Hazra, S. Mitra, R. M. Goldblum and S. Sur (2005). "ROS generated by pollen NADPH oxidase provide a signal that augments antigen-induced allergic airway inflammation." The Journal of Clinical Investigation **115**(8): 2169-2179.

Bolduc, J. F., L. Lewis, C. E. Aubin and A. Geitmann (2006). "Finite-element analysis of geometrical factors in micro-indentation of pollen tubes." Biomechanics and Modeling in Mechanobiology **5**: 227-236.

Bonin, C. P., I. Potter, G. F. Vanzin and W.-D. Reiter (1997). "The MUR1 gene of *Arabidopsis thaliana* encodes an isoform of GDP-d-mannose-4,6-dehydratase, catalyzing the first step in the de novo synthesis of GDP-l-fucose." Proceedings of the National Academy of Sciences **94**(5): 2085-2090.

Bordenave, M., C. Breton, R. Goldberg, J.-C. Huet, S. Perez and J.-C. Pernollet (1996). "Pectinmethylesterase isoforms from *Vigna radiata* hypocotyl cell walls: kinetic properties and molecular cloning of a cDNA encoding the most alkaline isoform." Plant Molecular Biology **31**(5): 1039-1049.

Bordenave, M. and R. Goldberg (1994). "Immobilized and free apoplastic pectinmethylesterases in mung bean hypocotyl." Plant Physiol. **106**(3): 1151-1156.

Bosch, M., A. Y. Cheung and P. K. Hepler (2005). "Pectin methylesterase, a regulator of pollen tube growth." Plant Physiology **138**(3): 1334-1346.

Bosch, M. and P. K. Hepler (2005). "Pectin methylesterases and pectin dynamics in pollen tubes." Plant Cell **17**(12): 3219-3226.

Bou Daher, F., Y. Chebli and A. Geitmann (2009). "Optimization of conditions for germination of cold-stored *Arabidopsis thaliana* pollen." Plant Cell Reports **28**(3): 347-357.

Bou Daher, F. and A. Geitmann (2011). "Actin is involved in pollen tube tropism through redefining the spatial targeting of secretory vesicles." Traffic **12**(11): 1537-1551.

Bourquin, V., N. Nishikubo, H. Abe, H. Brumer, S. Denman, M. Eklund, M. Christiernin, T. T. Teeri, B. Sundberg and E. J. Mellerowicz (2002). "Xyloglucan endotransglycosylases have a function during the formation of secondary cell walls of vascular tissues." The Plant Cell Online **14**(12): 3073-3088.

Bove, J., B. Vaillancourt, J. Kroeger, P. K. Hepler, P. W. Wiseman and A. Geitmann (2008). "Magnitude and direction of vesicle dynamics in growing pollen tubes using

spatiotemporal image correlation spectroscopy and fluorescence recovery after photobleaching." Plant Physiology **147**(4): 1646-1658.

Boynton, R. (2001). Precise measurement of mass. 60th annual conference of the society of allied weight engineers. Arlington, Texas, Space Electronics, Inc, Berlin, Connecticut.

Braun, M. (1997). "Gravitropism in tip-growing cells." Planta **203**: S11-S19.

Braun, M. and C. Limbach (2006). "Rhizoids and protonemata of characean algae: model cells for research on polarized growth and plant gravity sensing." Protoplasma **229**: 133-142.

Braun, M. and A. Sievers (2000). "Plant cells on Earth and in Space." Korean Journal of Biological Sciences **4**: 201-214.

Braun, M. and G. Wasteneys (2000). Actin in characean rhizoids and protonemata. Tip growth, gravity sensing and photomorphogenesis. Actin: a dynamic framework for multiple plant cell functions. C. Staiger, F. Baluska, P. Volkmann and P. Barlow. Dordrecht, The Netherlands,, Kluwer Academic Publishers**:** 237-258.

Brewbaker, J. L. and B. H. Kwack (1963). "The essential role of calcium ion in pollen germination and pollen tube growth." American Journal of Botany **50**: 859-865.

Brown, R. C. and B. E. Lemmon (1992). "Control of division plane in normal and griseofulvin-treated microsporocytes of Magnolia." Journal of Cell Science **103**(4): 1031-1038.

Brown, R. M. J. (1969). "Observation on the relationship of the Golgi apparatus to wall formation in the marine Chrysophycean alga, *Pleurochrysis scherffelii* Pringsheim." Journal of Cell Biology **41**(1): 109-123.

Brummell, D. A., A. Camirande and G. A. Maclachlan (1990). "Differential distribution of xyloglucan glycosyl transferases in pea Golgi dictyosomes and secretory vesicles." J Cell Sci **96**(4): 705-710.

Bryant, V. M. and G. D. Jones (2006). "Forensic palynology: Current status of a rarely used technique in the United States of America." Forensic Science International **163**(3): 183-197.

Buckeridge, M. S., H. J. Crombie, C. J. M. Mendes, J. S. G. Reid, M. J. Gidley and C. C. J. Vieira (1997). "A new family of oligosaccharides from the xyloglucan of Hymenaea courbaril L. (Leguminosae) cotyledons." Carbohydrate Research **303**(2): 233-237.

Buizer, K. (2007). "GraPhoBox: Gravitropism and phototropism in *Arabidopsis thaliana*." Microgravity Science and Technology **19**(5): 239-243.

Bunzel, M. (2010). "Chemistry and occurrence of hydroxycinnamate oligomers." Phytochemistry Reviews **9**(1): 47-64.

Burk, D. H. and Z.-H. Ye (2002). "Alteration of oriented deposition of cellulose microfibrils by mutation of a katanin-like microtubule-severing protein." Plant Cell **14**: 2145-2160.

Burton, R. A., M. J. Gidley and G. B. Fincher (2010). "Heterogeneity in the chemistry, structure and function of plant cell walls." Nat Chem Biol **6**(10): 724-732.

Cai, G., C. Del Casino, S. Romagnoli and M. Cresti (2005). "Pollen cytoskeleton during germination and pollen tube growth." Current Science **89**: 1853-1860.

Cai, G., C. Faleri, C. Del Casino, A. M. C. Emons and M. Cresti (2011). "Distribution of callose synthase, cellulose synthase, and sucrose synthase in Tobacco pollen tube

is controlled in dissimilar ways by actin filaments and microtubules." Plant Physiology **155**(3): 1169-1190.

Cai, G., A. Moscatelli and M. Cresti (1997). "Cytoskeletal organization and pollen tube growth." Trends in Plant Science **2**: 86-91.

Cai, G., A. Moscatelli, C. DelCasino and M. Cresti (1996). "Cytoplasmic motors and pollen tube growth." Sexual Plant Reproduction **9**: 59-64.

Callister, W. D. (1994). Materials science and engineering: An introduction - 3rd edition. New York, John Wiley & Sons Inc.

Camacho, L., R. Parton, A. J. Trewavas and R. Malho (2000). "Imaging cytosolic free calcium distribution and oscillations in pollen tubes with confocal microscopy: a comparison of different dyes and loading methods." Protoplasma **212**: 162-173.

Camardella, L., V. Carratore, M. A. Ciardiello, L. Servillo, C. Balestrieri and A. Giovane (2000). "Kiwi protein inhibitor of pectin methylesterase." European Journal of Biochemistry **267**(14): 4561-4565.

Campàs, O. and L. Mahadevan (2009). "Shape and dynamics of tip-growing cells." Current Biology **19**: 2102-2107.

Cantarel, B. L., P. M. Coutinho, C. Rancurel, T. Bernard, V. Lombard and B. Henrissat (2009). "The Carbohydrate-Active EnZymes database (CAZy): an expert resource for glycogenomics." Nucleic Acids Research **37**(suppl 1): D233-D238.

Cárdenas, L., S. T. McKenna, J. G. Kunkel and P. K. Hepler (2006). "NAD(P)H oscillates in pollen tubes and is correlated with tip growth." Plant Physiology **142**(4): 1460-1468.

Carol, R. J. and L. Dolan (2006). "The role of reactive oxygen species in cell growth: lessons from root hairs." Journal of Experimental Botany **57**(8): 1829-1834.

Caspar, T., S. C. Huber and C. Somerville (1985). "Alterations in growth, photosynthesis, and respiration in a starchless mutant of *Arabidopsis thaliana* (L.) deficient in chloroplast phosphoglucomutase activity." Plant Physiol. **79**(1): 11-17.

Chanliaud, E., K. M. Burrows, G. Jeronimidis and M. J. Gidley (2002). "Mechanical properties of primary plant cell wall analogues." Planta **215**: 989-996.

Chanliaud, E. and M. J. Gidley (1999). "*In vitro* synthesis and properties of pectin / *Acetobacter xylinus* cellulose composites." Plant Journal **20**(1): 25-35.

Charras, G. T., J. C. Yarrow, M. A. Horton, L. Mahadevan and T. J. Mithcison (2005). "Non-equilibration of hydrostatic pressure in blebbing cells." Nature **435**: 365-369.

Chatterjee, A., D. M. Porterfield, P. J. S. Smith and S. J. Roux (2000). "Gravity directed calcium current in germinating spores of *Ceratopteris richardii*." Planta **210**: 607-610.

Chatterjee, A. and S. J. Roux (2000). "*Ceratopteris richardii*: A productive model for revealing secrets of signaling and development." Journal of Plant Growth Regulation **19**(3): 284-289-289.

Chebli, Y. and A. Geitmann (2007). "Mechanical principles governing pollen tube growth." Functional Plant Science and Biotechnology **1**(2): 232-245.

Chebli, Y. and A. Geitmann (2011). "Gravity research on plants: use of single cell experimental models." Frontiers in Plant Science **2**(56): 1-10.

Chebli, Y., M. Kaneda, R. Zerzour and A. Geitmann (2012). "The cell wall of the *Arabidopsis thaliana* pollen tube - spatial distribution, recycling and network formation of polysaccharides." Plant Physiology **160**: 1-16.

Chen, C. Y., E. I. Wong, L. Vidali, A. Estavillo, P. K. Hepler, H. Wu and A. Y. Cheung (2002a). "The regulation of actin organization by actin-depolymerising factor in elongating pollen tubes." The Plant Cell **14**: 2175- 2190.

Chen, X., J. E. Pfeil and S. Gal (2002b). "The three typical aspartic proteinase genes of *Arabidopsis thaliana* are differentially expressed." European Journal of Biochemistry **269**(18): 4675-4684.

Cheung, A. Y., H. Wang and H.-m. Wu (1995). "A floral transmitting tissue-specific glycoprotein attracts pollen tubes and stimulates their growth." Cell **82**(3): 383-393.

Cheung, A. Y. and H.-m. Wu (2007). "Structural and functional compartmentalization in pollen tubes." Journal of Experimental Botany **58**: 75-82.

Cheung, A. Y. and H. Wu (2001). "Pollen tube guidance - Right on target." Science **293**: 1441-1442.

Cho, H.-T. and D. J. Cosgrove (2002). "Regulation of root hair initiation and expansin gene expression in *Arabidopsis*." The Plant Cell Online **14**(12): 3237-3253.

Cho, H. T. and H. Kende (1997). "Expression of expansin genes is correlated with growth in deepwater rice." The Plant Cell Online **9**(9): 1661-1671.

Clarke, J. T., R. C. M. Warnock and P. C. J. Donoghue (2011). "Establishing a time-scale for plant evolution." New Phytologist **192**(1): 266-301.

Cleemput, G., K. Van Laere, M. Hessing, F. Van Leuven, S. Torrekens and J. A. Delcour (1997). "Identification and characterization of a novel arabinoxylanase from wheat flour." Plant Physiology **115**(4): 1619-1627.

Coelho, S. M., A. R. Taylor, K. P. Ryan, I. Sousa-Pinto, M. T. Brown and C. Brownlee (2002). "Spatiotemporal patterning of reactive oxygen production and Ca^{2+} wave propagation in *Fucus* rhizoid cells." Plant Cell **14**(10): 2369-2381.

Coimbra, S. and L. G. Pereira (2012). Arabinogalactan proteins in *Arabidopsis thaliana* pollen development. Transgenic Plants - Advances and Limitations. Y. Ö. Çiftçi, In Tech**:** 329-352.

Cole, R. A. and J. E. Fowler (2006). "Polarized growth: maintaining focus on the tip." Current Opinion in Plant Biology **9**: 579-588.

Cole, R. A., L. Synek, V. Zarsky and J. E. Fowler (2005). "SEC8, a subunit of the putative *Arabidopsis* exocyst complex, facilitates pollen germination and competitive pollen tube growth." Plant Physiology **138**: 2005-2018.

Collmer, A. and N. T. Keen (1986). "The role of pectic enzymes in plant pathogenesis." Annual Review of Phytopathology **24**(1): 383-409.

Cordeiro, M. C., M. S. Pais and P. E. Brodelius (1994). "Tissue-specific expression of multiple forms of cyprosin (aspartic proteinase) in flowers of *Cynara cardunculus*." Physiologia Plantarum **92**(4): 645-653.

Cosgrove, D. J. (1989). "Characterization of long-term extension of isolated cell walls from growing cucumber hypocotyls." Planta **177**(1): 121-130.

Cosgrove, D. J. (1999). "Enzymes and other agents that enhance cell wall extensibility." Annual Review of Plant Physiology and Plant Molecular Biology **50**(1): 391-417.

Cosgrove, D. J. (2000a). "Expansive growth of plant cell walls." Plant Physiology and Biochemistry **38**(1-2): 109-124.

Cosgrove, D. J. (2000b). "Loosening of plant cell walls by expansins." Nature **407**(6802): 321-326.

Cosgrove, D. J. (2005). "Growth of the plant cell wall." Nat Rev Mol Cell Biol **6**(11): 850-861.

Cowles, J. R., H. W. Scheld, R. Lemay and C. Peterson (1984). "Growth and lignification in seedlings exposed to eight days of microgravity." Annals of Botany **54**: 33-48.

Curtis, M. D. and U. Grossniklaus (2003). "A Gateway cloning vector set for high-throughput functional analysis of genes in planta." Plant Physiology **133**(2): 462-469.

D'Amato, G., L. Cecchi, S. Bonini, C. Nunes, I. Annesi-Maesano, H. Behrendt, G. Liccardi, T. Popov and P. Van Cauwenberge (2007). "Allergenic pollen and pollen allergy in Europe." Allergy **62**(9): 976-990.

Da Riva Ricci, D. and B. Kendrick (1972). "Computer modelling of hyphal tip growth in fungi." Canadian Journal of Botany **50**: 2455-2462.

Daas, P. J. H., A. G. J. Voragen and H. A. Schols (2000). "Characterization of non-esterified galacturonic acid sequences in pectin with endopolygalacturonase." Carbohydrate Research **326**(2): 120-129.

Dai, S., T. Chen, K. Chong, Y. Xue, S. Liu and T. Wang (2007). "Proteomics identification of differentially expressed proteins associated with pollen germination and tube growth reveals characteristics of germinated *Oryza sativa* pollen." Molecular & Cellular Proteomics **6**(2): 207-230.

Dardelle, F., A. Lehner, Y. Ramdani, M. Bardor, P. Lerouge, A. Driouich and J.-C. Mollet (2010). "Biochemical and immunocytological characterizations of *Arabidopsis* pollen tube cell wall." Plant Physiology **153**(4): 1563-1576.

De Micco, V., M. Scala and G. Aronne (2006a). "Effects of simulated microgravity on male gametophyte of *Prunus*, *Pyrus*, and *Brassica* species." Protoplasma **228**(1): 121-126.

De Micco, V., M. Scala and G. Aronne (2006b). "Evaluation of the effect of clinostat rotation on pollen germination and tube development as a tool for selection of plants in Space." Acta Astronautica **58**: 464-470.

de Win, A. H., E. S. Pierson and J. Derksen (1999). "Rational analyses of organelle trajectories in tobacco pollen tubes reveal characteristics of the actomyosin cytoskeleton." Biophysical Journal **76**: 1648-1658.

Delmer, D. P. (1987). "Cellulose biosynthesis." Annual Review in Plant Physiology **38**: 259-290.

Delmer, D. P., S. M. Read and G. Cooper (1987). "Identification of a receptor protein in cotton fibers for the herbicide 2,6-dichlorobenzonitrile." Plant Physiology **84**: 415-420.

Demaree, R. S. and R. T. Giberson (2001). Overview of microwave-assisted tissue processing for transmission electron microscopy. Microwave Techniques and Protocols**:** 1-11.

Demkiv, O. T., E. L. Kordyum, O. R. Kardash and O. Y. Khorkavtsiv (1999). "Gravitropism and phototropism in protonemata of the moss Pohlia nutans (hedw.) Lindb." Advances in Space Research **23**(12): 1999-2004.

Denet, B. (1996). "Numerical simulation of cellular tip growth." Physical Review **53**: 986-992.

Derbyshire, P., M. McCann and K. Roberts (2007). "Restricted cell elongation in *Arabidopsis* hypocotyls is associated with a reduced average pectin esterification level." BMC Plant Biology **7**(1): 31.

Derksen, J. (1996). "Pollen tubes: a model system for plant cell growth." Botanica Acta **109**: 341-345.

Derksen, J., G.-J. Janssen, M. Wolters-Arts, I. Lichtscheidl, W. Adlassnig, M. Ovecka, F. Doris and M. Steer (2011). "Wall architecture with high porosity is established at the tip and maintained in growing pollen tubes of *Nicotiana tabacum*." The Plant Journal **68**(3): 495-506.

Derksen, J., B. Knuiman, K. Hoedemaekers, A. Guyon, S. Bonhomme and E. S. Pierson (2002). "Growth and cellular organization of *Arabidopsis* pollen tubes *in vitro*." Sexual Plant Reproduction **15**: 133-139.

Derksen, J., Y.-Q. Li, B. Knuiman and H. Geurts (1999). "The wall of *Pinus sylvestris* L. pollen tubes." Protoplasma **208**: 26-36.

Derksen, J., T. Rutten, I. K. Lichtscheidl, A. H. N. DeWin, E. S. Pierson and G. Rongen (1995). "Quantitative analysis of the distribution of organelles in tobacco pollen tubes: implications for exocytosis and endocytosis." Protoplasma **188**: 267-276.

Desprez, T., M. Juraniec, E. F. Crowell, H. Jouy, Z. Pochylova, F. Parcy, H. Höfte, M. Gonneau and S. Vernhettes (2007). "Organization of cellulose synthase complexes involved in primary cell wall synthesis in *Arabidopsis thaliana*." Proceedings of the National Academy of Sciences **104**(39): 15572-15577.

Dhugga, K. S., R. Barreiro, B. Whitten, K. Stecca, J. Hazebroek, G. S. Randhawa, M. Dolan, A. J. Kinney, D. Tomes, S. Nichols and P. Anderson (2004). "Guar seed ß-mannan synthase is a member of the cellulose synthase super gene family." Science **303**(5656): 363-366.

Dowd, P. E., S. Coursol, A. L. Skirpan, T.-h. Kao and S. Gilroy (2006). "*Petunia* phospholipase C1 is involved in pollen tube growth." Plant Cell **18**: 1438-1453.

Downes, B. P. and D. N. Crowell (1998). "Cytokinin regulates the expression of a soybean β-expansin gene by a post-transcriptional mechanism." Plant Molecular Biology **37**(3): 437-444.

Dresselhaus, T. and M. L. Márton (2009). "Micropylar pollen tube guidance and burst: adapted from defense mechanisms?" Current Opinion in Plant Biology **12**(6): 773-780.

Dumais, J., S. R. Long and S. L. Shaw (2004). "The mechanics of surface expansion anisotropy in *Medicago truncatula* root hairs." Plant Physiology **136**: 3266-3275.

Dumais, J., S. L. Shaw, C. R. Steele, S. R. Long and P. M. Ray (2006). "An anisotropic-viscoplastic model of plant cell morphogenesis by tip growth." International Journal of Developmental Biology **50**: 209-222.

Dutcher, F., E. Hess and T. Halstead (1994). "Progress in plant research in space." Advances in Space Research **14**: 159-171.

Dutta, R. and D. G. Robinson (2004). "Identification and characterization of stretch-activated ion channels in pollen protoplasts." Plant Physiology **135**: 1398-1406.

Dyson, R. J. and O. E. Jensen (2010). "A fibre-reinforced fluid model of anisotropic plant cell growth." Journal of Fluid Mechanics **655**: 472-503.

Ebbelaar, M. E. M., G. A. Tucker, M. M. Laats, C. Dijk, T. Stolle-Smits and K. Recourt (1996). "Characterization of pectinases and pectin methylesterase cDNAs in pods of green beans (Phaseolus vulgaris L.)." Plant Molecular Biology **31**(6): 1141-1151.

Edelmann, H. G. and S. C. Fry (1992). "Kinetics of integration of xyloglucan into the walls of suspension-cultured rose cells." Journal of Experimental Botany **43**(4): 463-470.

Edwards, E. S. and S. J. Roux (1998). "Influence of gravity and light on the developmental polarity of *Ceratopteris richardii* fern spores." Planta **205**: 553-560.

Eggen, E., M. Niels de Keijzer and B. M. Mulder (2011). "Self-regulation in tip-growth: The role of cell wall ageing." Journal of Theoretical Biology **283**(1): 113-121.

Elleman, C., V. Franklin-Tong and H. Dickinson (1992). "Pollination in species with dry stigmas: the nature of the early stigmatic response and the pathway taken by pollen tubes." New Phytologist **121**(3): 413-424.

Elson, E., B. Daily, W. McConnaughey, C. Pasternak and N. Petersen (1983). Measurement of forces which determine the shapes of adherent cells in culture. Frontiers in Biochemical and Biophysical Studies of Proteins and Membranes. S. S. T-Y Liu, A Schechter, K Yagi, H Yajima, KT Yasunobu. New York, Elsevier**:** 399-411.

Emons, A. M. C., H. Höfte and B. M. Mulder (2007). "Microtubules and cellulose microfibrils: how intimate is their relationship?" Trends in Plant Science **12**(7): 279-281.

Emons, A. M. C. and B. M. Mulder (1998). "The making of the architecture of the plant cell wall: How cells exploit geometry." Plant Biology **95**: 7215-7219.

Emons, A. M. C. and B. M. Mulder (2000). "How the deposition of cellulose microfibrils builds cell wall architecture." Trends in Plant Science **5**: 35- 40.

Engels, F. M. (1973). "Function of Golgi vesicles in relation to cell wall synthesis in germinating *Petunia* pollen. I. Isolation of Golgi vesicles." Acta Botanica Neerlandica **22**(1): 6-13.

Engels, F. M. (1974). "Function of Golgi vesicles in relation to cell wall synthesis in germinating *Petunia* pollen. II. Chemical composition of Golgi vesicles and pollen tube wall." Acta Botanica Neerlandica **23**(2): 81-89.

Engels, F. M. (1974). "Function of Golgi vesicles in relation to cell wall synthesis in germinating *Petunia* pollen. IV. Identification of cellulose in pollen tube walls and Golgi vesicles by X-ray diffraction." Acta Botanica Neerlandica **23**(3): 209-215.

Essau, K. (1977). Anatomy of seed plants, John Willey & Sons, Ins.

Fagard, M., T. Desnos, T. Desprez, F. Goubet, G. Refregier, G. Mouille, M. McCann, C. Rayon, S. Vernhettes and H. Höfte (2000). "PROCUSTE1 encodes a cellulose synthase required for normal cell elongation specifically in roots and dark-grown hypocotyls of *Arabidopsis*." The Plant Cell Online **12**(12): 2409-2423.

Faik, A., M. Bar-Peled, A. E. DeRocher, W. Zeng, R. M. Perrin, C. Wilkerson, N. V. Raikhel and K. Keegstra (2000). "Biochemical characterization and molecular cloning of an α-1,2-fucosyltransferase that catalyzes the last step of cell wall xyloglucan biosynthesis in pea." Journal of Biological Chemistry **275**(20): 15082-15089.

Faik, A., N. J. Price, N. V. Raikhel and K. Keegstra (2002). "An *Arabidopsis* gene encoding an α-xylosyltransferase involved in xyloglucan biosynthesis." Proceedings of the National Academy of Sciences **99**(11): 7797-7802.

Falconer, M. M. and R. W. Seagull (1985). "Immunofluorescent and calcofluor white staining of developing tracheary elements in *Zinnia elegans* L. suspension cultures." Protoplasma **125**(3): 190-198.

Fan, L.-M., W.-W. Wu, H. Wang and W.-H. Wu (2001). "*In-vitro Arabidopsis* pollen germination and characterization of the inward potassium currents in *Arabidopsis* pollen grain protoplasts." Journal of Experimental Botany **52**: 1603-1614.

Fan, L.-M., W.-W. Wu and H.-Y. Yang (1999). "Identification and characterization of the inward K^+ channel in the plasma membrane of *Brassica* pollen protoplasts." Plant Cell Physiology **40**: 859-865.

Fanutti, C., M. J. Gidley and J. S. G. Reid (1993). "Action of a pure xyloglucan endo-transglycosylase (formerly called xyloglucan-specific endo-(1-4)-β-d-glucanase) from the cotyledons of germinated nasturtium seeds." The Plant Journal **3**(5): 691-700.

Farkas, V., Z. Sulova, E. Stratilova, R. Hanna and G. Maclachlan (1992). "Cleavage of xyloglucan by nasturtium seed xyloglucanase and transglycosylation to xyloglucan subunit oligosaccharides." Archives of Biochemistry and Biophysics **298**(2): 365-370.

Fasano, J. M., G. D. Massa and S. Gilroy (2002). "Ionic signaling in plant responses to gravity and touch." Journal of Plant Growth Regulation **21**: 71-88.

Fayant, P., O. Girlanda, Y. Chebli, C.-E. Aubin, I. Villemure and A. Geitmann (2010). "Finite element model of polar growth in pollen tubes." Plant Cell **22**: 2579-2593.

Feijó, J. (2010). "The mathematics of sexual attraction." Journal of Biology **9**(3): 1-5.

Feijó, J. A., R. Malhó and G. Obermeyer (1995a). "Ion dynamics and its possible role during *in-vitro* pollen germination and tube growth." Protoplasma **187**(1-4): 155-167.

Feijó, J. A., R. Malhó and M. S. Pais (1995b). "Electrical currents, ion channels and ion pumps during germination and growth of pollen tubes." Protoplasma **187**: 155-167.

Feijó, J. A., J. Sainhas, G. R. Hackett, J. G. Kunkel and P. K. Hepler (1999). "Growing pollen tubes possess a constitutive alkaline band in the clear zone and a growth-dependent acidic tip." Journal of Cell Biology **144**: 483-496.

Feijó, J. A., J. Sainhas, T. L. Holdaway-Clarke, M. S. Cordeiro, J. G. Kunkel and P. K. Hepler (2001). "Cellular oscillations and the regulation of growth: the pollen tube paradigm." Bioessays **23**(1): 86-94.

Feingold, D. S., E. F. Neufeld and W. Z. Hassid (1959). "Xylosyl transfer catalyzed by an asparagus extract." Journal of Biological Chemistry **234**(3): 488-489.

Ferguson, C., T. T. Teeri, M. Siika-aho, S. M. Read and A. Bacic (1998). "Location of cellulose and callose in pollen tubes and grains of *Nicotiana tabacum*." Planta **206**(3): 452-460.

Field, R. A. (2009). Oligosaccharide signalling molecules. Plant-derived natural products. A. E. Osbourn and V. Lanzotti, Springer US**:** 349-359.

Filichkin, S. A., J. M. Leonard, A. Monteros, P.-P. Liu and H. Nonogaki (2004). "A novel endo-β-mannanase gene in tomato LeMAN5 is associated with anther and pollen development." Plant Physiology **134**(3): 1080-1087.

Foissner, I., F. Grolig and G. Obermeyer (2002). "Reversible protein phosphorylation regulates the dynamic organization of the pollen tube cytoskeleton: Effects of calyculin A and okadaic acid." Protoplasma **2002**: 1-15.

Foreman, J., V. Demidchik, J. H. F. Bothwell, P. Mylona, H. Miedema, M. A. Torres, P. Linstead, S. Costa, C. Brownlee, J. D. G. Jones, J. M. Davies and L. Dolan (2003). "Reactive oxygen species produced by NADPH oxidase regulate plant cell growth." Nature **422**(6930): 442-446.

Francis, K. E., S. Y. Lam and G. P. Copenhaver (2006). "Separation of *Arabidopsis* pollen tetrads is regulated by QUARTET1, a pectin methylesterase gene." Plant Physiology **142**(3): 1004-1013.

Franklin-Tong, V. E. (1999). "Signaling and the modulation of pollen tube growth." Plant Cell **11**(4): 727-738.

Franklin-Tong, V. E. and F. C. H. Franklin (2003). "The different mechanisms of gametophytic self–incompatibility." Philosophical Transactions of the Royal Society of London. Series B: Biological Sciences **358**(1434): 1025-1032.

Franklin-Tong, V. E., G. Hackett and P. K. Hepler (1997). "Ratio-imaging of $[Ca2+]_i$ in the self-incompatibility response in pollen tubes of *Papaver rhoeas*." Plant Journal **12**: 1375-1386.

Freshour, G., C. P. Bonin, W.-D. Reiter, P. Albersheim, A. G. Darvill and M. G. Hahn (2003). "Distribution of fucose-containing xyloglucans in cell walls of the *mur1* mutant of *Arabidopsis*." Plant Physiology **131**(4): 1602-1612.

Fricker, M. D., N. S. White and G. Obermeyer (1997). "pH gradients are not associated with tip growth in pollen tubes of *Lilium longiflorum*." Journal of Cell Science **110**: 1729-1740.

Fry, S. C. (1998). "Oxidative scission of plant cell wall polysaccharides by ascorbate-induced hydroxyl radicals." Biochem. J. **332**(2): 507-515.

Fry, S. C., J. G. Miller and J. C. Dumville (2002). "A proposed role for copper ions in cell wall loosening." Plant and Soil **247**(1): 57-67.

Fry, S. C., R. C. Smith, K. F. Renwick, D. J. Martin, S. K. Hodge and K. J. Matthews (1992). "Xyloglucan endotransglycosylase, a new wall-loosening enzyme activity from plants." The Biochemical journal **282 (Pt 3)**: 821-828.

Gapper, C. and L. Dolan (2006). "Control of plant development by reactive oxygen species." Plant Physiology **141**(2): 341-345.

Geitmann, A. (1997). Growth and formation of the cell wall in pollen tubes of *Nicotiana tabacum* and *Petunia hybrida*. Egelsbach Frankfurt Washington, Hänsel-Hohenhausen**:** 181.

Geitmann, A. (1999). The rheological properties of the pollen tube cell wall. Fertilization in higher plants: Molecular and cytological aspects. M. Cresti, G. Cai and A. Moscatelli, Springer Verlag**:** 283-302.

Geitmann, A. (2006a). "Plant and fungal cytomechanics: quantifying and modeling cellular architecture." Canadian Journal of Botany **84**: 581-593.

Geitmann, A. (2006b). "Experimental approaches used to quantify physical parameters at cellular and subcellular levels." American Journal of Botany **93**(10): 1220-1230.

Geitmann, A. (2007). "Cytomechanical tools for plant gravitational biology." Gravitational and Space Biology **20**: 31-42.

Geitmann, A. (2010a). "How to shape a cylinder: pollen tube as a model system for the generation of complex cellular geometry." Sexual Plant Reproduction **23**(1): 63-71.

Geitmann, A. (2010b). "Mechanical modeling and structural analysis of the primary plant cell wall." Current Opinion in Plant Biology **13**(6): 693-699.

Geitmann, A. and M. Cresti (1998). "Ca^{2+} channels control the rapid expansions in pulsating growth of *Petunia hybrida* pollen tubes." Journal of Plant Physiology **152**: 439-447.

Geitmann, A. and J. Dumais (2009). "Not-so-tip-growth." Plant Signaling and Behavior **4**(2): 136-138.

Geitmann, A. and A. M. C. Emons (2000). "The cytoskeleton in plant and fungal cell tip growth." Journal of Microscopy **198**: 218-245.

Geitmann, A., J. M. Hush and R. L. Overall (1997). "Inhibition of ethylene biosynthesis does not block microtubule re-orientation in wounded pea roots." Protoplasma **198**: 135- 142.

Geitmann, A., Y. Q. Li and M. Cresti (1995). "Ultrastructural immunolocalization of periodic pectin depositions in the cell wall of *Nicotiana tabacum* pollen tubes." Protoplasma **187**: 168-171.

Geitmann, A., Y. Q. Li and M. Cresti (1996). "The role of the cytoskeleton and dictyosome activity in the pulsatory growth of *Nicotiana tabacum* and *Petunia hybrida*." Botanica Acta **109**: 102-109.

Geitmann, A., W. McConnaughey, I. Lang-Pauluzzi, V. E. Franklin-Tong and A. M. C. Emons (2004). "Cytomechanical properties of *Papaver* pollen tubes are altered after self-incompatibility challenge." Biophysical Journal **86**: 3314-3323.

Geitmann, A. and J. K. E. Ortega (2009). "Mechanics and modeling of plant cell growth." Trends in Plant Science **14**(9): 467-478.

Geitmann, A. and R. Palanivelu (2007). "Fertilization requires communication: signal generation and perception during pollen tube guidance." Floriculture and Ornamental Biotechnology **1**: 77-89.

Geitmann, A. and E. Parre (2004). "The local cytomechanical properties of growing pollen tubes correspond to the axial distribution of structural cellular elements." Sexual Plant Reproduction **17**: 9-16.

Geitmann, A., B. Snowman, V. E. Franklin-Tong and A. M. C. Emons (2000). "Alterations in the actin cytoskeleton of the pollen tube are induced by the self-incompatibility reaction in *Papaver rhoeas*." Plant Cell **12**: 1239-1251.

Geitmann, A. and M. W. Steer (2006). The architecture and properties of the pollen tube cell wall. The pollen tube: a cellular and molecular perspective, Plant Cell Monographs. R. Malhó. Berlin Heidelberg, Springer Verlag. **3:** 177-200.

Gibbon, B. C., D. R. Kovar and C. J. Staiger (1999). "Latrunculin B has different effects on pollen germination and tube growth." Plant Cell **11**(12): 2349-2363.

Gibeaut, D. M. and N. C. Carpita (1994). "Biosynthesis of plant cell wall polysaccharides." The FASEB Journal **8**(12): 904-915.

Giberson, R. T. (2001). Vacuum-assisted microwave processing of animal tissues for electron microscopy. Microwave Techniques and Protocols**:** 13-23.

Gierz, G. and S. Bartnicki-Garcia (2001). "A three-dimensional model of fungal morphogenesis based on the vesicle supply center concept." Journal of Theoretical Biology **208**: 151-164.

Giovane, A., L. Servillo, C. Balestrieri, A. Raiola, R. D'Avino, M. Tamburrini, M. A. Ciardiello and L. Camardella (2004). "Pectin methylesterase inhibitor." Biochimica et Biophysica Acta (BBA) - Proteins & Proteomics **1696**(2): 245-252.

Goodwillie, C. (1997). "The genetic control of self-incompatibility in Linanthus parviflorus (Polemoniaceae)." Heredity **79**(4): 424-432.

Goriely, A. and M. Tabor (2003a). "Biomechanical models of hyphal growth in actinomycetes." Journal of Theoretical Biology **222**: 211-218.

Goriely, A. and M. Tabor (2003b). "Self-similar tip growth in filamentary organisms." Physical Review Letters **90**: 1-4.

Goriely, A. and M. Tabor (2008). "Mathematical modeling of hyphal tip growth." Fungal Biology Reviews **22**: 77-83.

Gossot, O. and A. Geitmann (2007). "Pollen tube growth: coping with mechanical obstacles involves the cytoskeleton." Planta **226**(2): 405-416.

Goubet, F., A. Misrahi, S. K. Park, Z. Zhang, D. Twell and P. Dupree (2003). "AtCSLA7, a cellulose synthase-like putative glycosyltransferase, is important for pollen tube growth and embryogenesis in *Arabidopsis*." Plant Physiology **131**(2): 547-557.

Green, P. B. (1962). "Mechanism for plant cellular morphogenesis." Science **138**: 1404-1405.

Green, P. B. (1969). "Cell morphogenesis." Ann Rev Plant Physiol **20**: 365-394.

Greenberg, J. T. (1996). "Programmed cell death: a way of life for plants." Proceedings of the National Academy of Sciences **93**: 12094-12097.

Griessner, M. and G. Obermeyer (2003). "Characterization of whole-cell K^+ currents across the plasma membrane of pollen grain and tube protoplasts of *Lilium longiflorum*." Journal of Membrane Biology **193**: 99-108.

Gruppen, H., R. A. Hoffmaann, F. J. M. Kormelink, A. G. J. Voragen, J. P. Kamerlin and J. F. G. Vliegenthart (1992). "Characterisation by 1H NMR spectroscopy of enzymically derived oligosaccharides from alkali-extractable wheat-flour arabinoxylan." Carbohydrate Research **233**(0): 45-64.

Gu, Y., Y. Fu, P. E. Dowd, S. Li, V. Vernoud, S. Gilroy and Z. Yang (2005). "A Rho family GTPase controls actin dynamics and tip growth via two counteracting downstream pathways in pollen tubes." Journal of Cell Biology **169**: 127-138.

Guglielmino, N., M. Liberman, A. M. Catesson, A. Mareck, R. Prat, S. Mutaftschiev and R. Goldberg (1997). "Pectin methylesterases from poplar cambium and inner bark: localization, properties and seasonal changes." Planta **202**(1): 70-75.

Guyon, V. N., J. D. Astwood, E. C. Garner, A. K. Dunker and L. P. Taylor (2000). "Isolation and characterization of cDNAs expressed in the early stages of flavonol-induced pollen germination in *Petunia*." Plant Physiology **123**(2): 699-710.

Hamant, O., M. Heisler, H. Jönsson, P. Krupinski, M. Uyttewaaal, P. Bokov, F. Corson, P. Sahlin, A. Boudaoud, E. Meyerowitz, Y. Couder and J. Traas (2008). "Developmental patterning by mechanical signals in *Arabidopsis*." Science **322**: 1650-1655.

Handford, M., T. Baldwin, F. Goubet, T. Prime, J. Miles, X. Yu and P. Dupree (2003). "Localisation and characterisation of cell wall mannan polysaccharides in *Arabidopsis thaliana*." Planta **218**(1): 27-36.

Hart, D. A. and P. K. Kindel (1970). "Isolation and partial characterization of apiogalacturonans from the cell wall of *Lemna minor*." Biochem. J. **116**: 569–579.

Hasenstein, K. H. (1999). "Gravisensing and plants and fungi." Advances in Space Research **24**: 677-685.

Haswell, E. S. (2003). "Gravity perception: How plants stand up for themselves." Current Biology **13**: R761-R763.

Hatakeda, Y., M. Kamada, N. Goto, H. Fukaki, M. Tasaka, H. Suge and H. Takahashi (2003). "Gravitropic response plays an important role in the nutational movements of the shoots of Pharbitis nil and Arabidopsis thaliana." Physiologia Plantarum **118**(3): 464-473.

Hayashi, T. (1989). "Xyloglucans in the primary cell wall." Annual Review of Plant Physiology and Plant Molecular Biology **40**(1): 139-168.

Hayashi, T., K. i. Baba and K. Ogawa (1994a). "Macromolecular complexes of xyloglucan and cellulose obtained by annealing." Plant and Cell Physiology **35**(2): 219-223.

Hayashi, T., M. P. F. Marsden and D. P. Delmer (1987). "Pea xyloglucan and cellulose." Plant Physiology **83**(2): 384-389.

Heizmann, P., D. T. Luu and C. Dumas (2000). "Pollen-stigma adhesion in the Brassicaceae." Annals of Botany **85**(suppl 1): 23-27.

Hejnowicz, Z., C. Sondag, W. Alt and A. Sievers (1998). "Temporal course of graviperception in intermittently stimulated cress roots." Plant, Cell & Environment **21**(12): 1293-1300.

Helsper, J. P. F. G., J. H. Veerkamp and M. M. A. Sassen (1977). "Beta-glucan synthetase activity in golgi vesicles of *Petunia hybrida*." Planta **133**: 303-308.

Hématy, K., C. Cherk and S. Somerville (2009). "Host–pathogen warfare at the plant cell wall." Current Opinion in Plant Biology **12**(4): 406-413.

Hemmersbach, R., D. Volkmann and D.-P. Häder (1999). "Graviorientation in protists and plants." Journal of Plant Physiology **154**: 1-15.

Hepler, P. K. (1997). "Tip growth in pollen tubes: calcium leads the way." Trends in Plant Science **2**: 79-80.

Hepler, P. K., A. Lovy-Wheeler, S. T. McKenna and J. G. Kunkel (2006). Ions and pollen tube growth. The pollen tube: a cellular and molecular perspective. R. Malhó. Berlin Heidelberg, Springer Verlag. **3:** 47-69.

Hepler, P. K., L. Vidali and A. Y. Cheung (2001). "Polarized cell growth in higher plants." Annual Review of Cell and Developmental Biology **17**(1): 159-187.

Herbers, K., E. P. Lorences, C. Barrachina and U. Sonnewald (2001). "Functional characterisation of *Nicotiana tabacum*; xyloglucan endotransglycosylase (*Nt* XET-1): generation of transgenic tobacco plants and changes in cell wall xyloglucan." Planta **212**(2): 279-287.

Herron, S. R., J. A. E. Benen, R. D. Scavetta, J. Visser and F. Jurnak (2000). "Structure and function of pectic enzymes: Virulence factors of plant pathogens." Proceedings of the National Academy of Sciences of the United States of America **97**(16): 8762-8769.

Herron, S. R., R. D. Scavetta, M. Garrett, M. Legner and F. Jurnak (2003). "Characterization and implications of Ca^{2+} binding to pectate lyase C." J. Biol. Chem.: M209306200.

Herth, W. and E. Schnepf (1980). "The fluorochrome, calcofluor white, binds oriented to structural polysaccharide fibrils." Protoplasma **105**(1): 129-133.

Heslop-Harrison, J. (1987). "Pollen germination and pollen-tube growth." International Review of Cytology **107**: 1-78.

Higashiyama, T. (2010). "Peptide signaling in pollen–pistil interactions." Plant and Cell Physiology **51**(2): 177-189.

Higashiyama, T. and Y. Hamamura (2008). "Gametophytic pollen tube guidance." Sexual Plant Reproduction **21**(1): 17-26.

Higashiyama, T., H. Kuroiwa and T. Kuroiwa (2003). "Pollen-tube guidance: beacons from the female gametophyte." Current Opinion in Plant Biology **6**(1): 36-41.

Hill, J. P. and E. M. Lord (1987). "Dynamics of pollen tube growth in the wild radish *Raphanus raphanistrum* (Brassicaceae). II. Morphology, cytochemistry and ultrastructure of transmitting tissues, and path of pollen tube growth." American Journal of Botany **74**(7): 988-997.

Hiratsuka, R., Y. Yamada and O. Terasaka (2002). "Programmed cell death of *Pinus nucellus* in response to pollen tube penetration." Journal of Plant Research **115**(1118): 141-148.

His, I., A. Driouich, F. Nicol, A. Jauneau and H. Höfte (2001). "Altered pectin composition in primary cell walls of korrigan, a dwarf mutant of *Arabidopsis* deficient in a membrane-bound endo-1,4-β-glucanase." Planta **212**: 348-358.

Hiscock, S. J., F. M. Dewey, J. O. D. Coleman and H. G. Dickinson (1994). "An active cutinase from the pollen of *Brassica napus* closely resembles fungal cutinases." Planta **193**: 377-384.

Hiscock, S. J. and S. M. McInnis (2003). "Pollen recognition and rejection during the sporophytic self-incompatibility response: Brassica and beyond." Trends in Plant Science **8**(12): 606-613.

Holdaway-Clarke, T. L., J. A. Feijó, G. R. Hackett, J. G. Kunkel and P. K. Hepler (1997). "Pollen tube growth and the intracellular cytosolic calcium gradient oscillate in phase while extracellular calcium influx is delayed." Plant Cell **9**: 1999-2010.

Holdaway-Clarke, T. L. and P. K. Hepler (2003). "Control of pollen tube growth: role of ion gradients and fluxes." New Phytologist **159**: 539-563.

Holdaway-Clarke, T. L., N. M. Weddle, S. Kim, A. Robi, C. Parris, J. G. Kunkel and P. K. Hepler (2003). "Effect of extracellular calcium, pH and borate on growth oscillations in *Lilium formosanum* pollen tubes." Journal of Experimental Botany **54**(380): 65-72.

Honys, D., D. Renak and D. Twell (2006). Male gametophyte development and function. Floriculture, Ornamental and Plant Biotechnology: Advances and Topical Issues. J. Teixera da Silva. London, UK, Global Science Books. **1:** 76-87.

Honys, D. and D. Twell (2003). "Comparative analysis of the *Arabidopsis* pollen transcriptome." Plant Physiology **132**(2): 640-652.

Hoson, T., S. Matsumoto, K. Soga and K. Wakabayashi (2010). "Cortical microtubules are responsible for gravity resistance in plants." Plant Signaling and behavior **5**(6): 752-754.

Hoson, T., K. Nishitani, K. Miyamoto, J. Ueda, S. Kamisaka, R. Yamamoto and Y. Masuda (1996). "Effects of hypergravity on growth and cell wall properties of cress hypocotyls." Journal of Experimental Botany **47**: 513-517.

Hoson, T. and K. Soga (2003). "New aspects of gravity responses in plant cells." International Review of Cytology **229**: 209-244.

Hou, G., V. L. Kramer, Y.-S. Wang, R. Chen, G. Perbal, S. Gilroy and E. B. Blancaflor (2004). "The promotion of gravitropism in *Arabidopsis* roots upon actin disruption is coupled with the extended alkalinization of the columella cytoplasm and a persistent lateral auxin gradient." The Plant Journal **39**(1): 113-125.

Hou, G., D. R. Mohamalawari and E. B. Blancaflor (2003). "Enhanced gravitropism of roots with a disrupted cap actin cytoskeleton." Plant Physiology **131**(3): 1360-1373.

Hughes, J. and M. McCully (1975). "The use of an optical brightener in the study of plant structure." Biotechnic and Histochemistry **50**(5): 319-329.

Hülskamp, M., S. D. Kopczak, T. F. Horejsi, B. K. Kihl and R. E. Pruitt (1995). "Identification of genes required for pollen-stigma recognition in Arabidopsis thaliana." The Plant Journal **8**(5): 703-714.

Hush, J. M. and R. L. Overall (1991). "The microtubule cytoskeleton has multiple functions in plant cells including the guidance of the intracellular motion of organelles, the targeting of enzymes involved in cell wall assembly, chromosome separation and cell plate formation during mitosis." Cell Biology International Reports **15**: 551-560.

Hwang, J.-U., Y. Gu, Y.-J. Li and Z. Yang (2005). "Oscillatory ROP GTPase activation leads the oscillatory polarized growth of pollen tubes." Molecular Biology of the Cell **16**: 5385-5399.

Hwang, J.-U., G. Wu, A. Yan, Y.-J. Lee, C. S. Grierson and Z. Yang (2010). "Pollen-tube tip growth requires a balance of lateral propagation and global inhibition of Rho-family GTPase activity." Journal of Cell Science **123**(3): 340-350.

Hwang, J.-U. and Z. Yang (2006). Small GTPases and spatiotemporal regulation of pollen tube growth. The pollen tube: a cellular and molecular perspective, Plant Cell Monographs. R. Malhó. Berlin Heidelberg, Springer Verlag. **3:** 95-116.

Hyodo, H., S. Yamakawa, Y. Takeda, M. Tsuduki, A. Yokota, K. Nishitani and T. Kohchi (2003). "Active gene expression of a xyloglucan endotransglucosylase/hydrolase gene, *XTH9* in inflorescence apices is related to cell elongation in *Arabidopsis thaliana*." Plant Molecular Biology **52**(2): 473-482.

Iglesias, N., J. A. Abelenda, M. Rodiño, J. Sampedro, G. Revilla and I. Zarra (2006). "Apoplastic glycosidases active against xyloglucan oligosaccharides of *Arabidopsis thaliana*." Plant and Cell Physiology **47**(1): 55-63.

Ingber, D. (2006). "Cellular mechanotransduction: putting all the pieces together again." FASEB Journal **20**: 11-27.

Ingber, D. E. (1993). "Cellular tensegrity: defining new rules of biological design that govern the cytoskeleton." Journal of Cell Science **104**: 613-627.

Ingber, D. E. (1999). "How cells (might) sense microgravity." The FASEB Journal **13**(9001): 3-15.

Ishii, T. (1991a). "Acetylation at O-2 of arabinofuranose residues in feruloylated arabinoxylan from bamboo shoot cell-walls." Phytochemistry **30**(7): 2317-2320.

Ishii, T. (1991b). "Isolation and characterization of a diferuloyl arabinoxylan hexasaccharide from bamboo shoot cell-walls." Carbohydrate Research **219**(0): 15-22.

Ishii, T., T. Matsunaga, P. Pellerin, M. A. O'Neill, A. Darvill and P. Albersheim (1999). "The plant cell wall polysaccharide rhamnogalacturonan II self-assembles into a covalently cross-linked dimer." Journal of Biological Chemistry **274**(19): 13098-13104.

Iversen, T.-H., A. Johnsson, E. Skagen, E. Ødegaard, T. Beisvåg, G. Chinga, P. Andreassen, A. Wold, A.-I. Kittang, A. Hammervold and O. Rasmussen (1999). "Effect of a microgravity environment and influences of variations in gravity on the regeneration of rapeseed plant protoplasts flown on the S/MM-03 mission." ESA SP-1222: 103-117.

Iwai, H., T. Ishii and S. Satoh (2001). "Absence of arabinan in the side chains of the pectic polysaccharides strongly associated with cell walls of *Nicotiana*

plumbaginifolia non-organogenic callus with loosely attached constituent cells." Planta **213**(6): 907-915.

Iwano, M., H. Shiba, T. Miwa, F.-S. Che, S. Takayama, T. Nagai, A. Miyawaki and A. Isogai (2004). "Ca^{2+} dynamics in a pollen grain and papilla cell during pollination of *Arabidopsis*." Plant Physiology **136**: 3562-3571.

Jacobs, A. K., V. Lipka, R. A. Burton, R. Panstruga, N. Strizhov, P. Schulze-Lefert and G. B. Fincher (2003). "An *Arabidopsis* callose synthase, GSL5, is required for wound and papillary callose formation." Plant Cell **15**(11): 2503-2513.

Jaffe, L. F. and R. Nuccitelli (1974). "An ultrasensitive vibrating probe for measuring steady extracellular currents." Journal of Cell Biology **63**(2): 614-628.

Jarvis, M. C. (1984). "Structure and properties of pectin gels in plant cell walls." Plant Cell and Environment **7**: 153-164.

Jauh, G. Y. and E. M. Lord (1996). "Localization of pectins and arabinogalactan-proteins in lily (Lilium longiflorum L.) pollen tube and style, and their possible roles in pollination." Planta **199**: 251-261.

Jiang, L., S.-L. Yang, L.-F. Xie, C. S. Puah, X.-Q. Zhang, W.-C. Yang, V. Sundaresan and D. Ye (2005). "VANGUARD1 encodes a pectin methylesterase that enhances pollen tube growth in the *Arabidopsis* style and transmitting tract." The Plant Cell Online **17**(2): 584-596.

Jiao, Y., N. J. Wickett, S. Ayyampalayam, A. S. Chanderbali, L. Landherr, P. E. Ralph, L. P. Tomsho, Y. Hu, H. Liang, P. S. Soltis, D. E. Soltis, S. W. Clifton, S. E. Schlarbaum, S. C. Schuster, H. Ma, J. Leebens-Mack and C. W. dePamphilis (2011). "Ancestral polyploidy in seed plants and angiosperms." Nature **473**(7345): 97-100.

Jimenez-Bermudez, S., J. Redondo-Nevado, J. Munoz-Blanco, J. L. Caballero, J. M. Lopez-Aranda, V. Valpuesta, F. Pliego-Alfaro, M. A. Quesada and J. A. Mercado (2002). "Manipulation of strawberry fruit softening by antisense expression of a pectate lyase gene." Plant Physiol. **128**(2): 751-759.

Johns, S., C. M. Davis and N. P. Money (1999). "Pulses in turgor pressure and water potential: resolving the mechanics of hyphal growth." Microbial Research **154**: 225-231.

Johnson-Brousseau, S. A. and S. McCormick (2004). "A compendium of methods useful for characterizing *Arabidopsis* pollen mutants and gametophytically-expressed genes." Plant Journal **39**(5): 761-775.

Jones, R. M. (1999). Mechanics of composite materials. London, Taylor & Francis.

Kerstens, S., W. F. Decraemer and J. P. Verbelen (2001). "Cell walls at the plant surface behave mechanically like fiber-reinforced composite materials." Plant Physiology **127**: 381-385.

Kha, H., S. C. Tuble, S. Kalyanasundaram and R. E. Williamson (2010). "WallGen, software to construct layered cellulose-hemicellulose networks and predict their small deformation mechanics." Plant Physiology **152**: 774-786.

Kikuchi, A., Y. Edashige, T. Ishii and S. Satoh (1996). "A xylogalacturonan whose level is dependent on the size of cell clusters is present in the pectin from cultured carrot cells." Planta **200**(4): 369-372.

Kimura, S., W. Laosinchai, T. Itoh, X. Cui, C. R. Linder and R. M. Brown (1999). "Immunogold labeling of rosette terminal cellulose-synthesizing complexes in the vascular plant *Vigna angularis*." The Plant Cell Online **11**(11): 2075-2085.

Kiss, J. Z. (2000). "Mechanisms of the early phases of plant gravitropism." CRC Critical Reviews in Plant Science **19**: 551-573.

Klahre, U., C. Becker, A. C. Schmitt and B. Kost (2006). "Nt-RhoGDI2 regulates Rac/Rop signaling and polar cell growth in tobacco pollen tubes." Plant Journal **46**: 1018-1031.

Klahre, U. and B. Kost (2006). "Tobacco RhoGTPase ACTIVATING PROTEIN1 spatially restricts signaling of RAC/Rop to the apex of pollen tubes." Plant Cell **18**(11): 3033-3046.

Knox, J. P., S. Day and K. Roberts (1989). "A set of cell surface glycoproteins forms an early position, but not cell type, in the root apical meristem of *Daucus carota* L." Development **106**: 47-56.

Knox, J. P., P. J. Linstead, J. King, C. Cooper and K. Roberts (1990). "Pectin esterification is spatially regulated both within cell walls and between developing tissues of root apices." Planta **181**: 512-521.

Koch, A. L. (1982). "The shape of the hyphal tips of fungi." Journal of General Microbiology **128**: 947-955.

Koch, A. L. (1994). "The problem of hyphal growth in streoptomycetes and fungi." Fungal Genetics and Biology **21**: 173-187.

Konopka, C. A. and S. Y. Bednarek (2008). "Variable-angle epifluorescence microscopy: a new way to look at protein dynamics in the plant cell cortex." The Plant Journal **53**(1): 186-196.

Kordyum, E. L. (2003). "Calcium signaling in plant cells in altered gravity." Advances in Space Research **32**: 1621-1630.

Kost, B., E. Lemichez, P. Spielhofer, Y. Hong, K. Tolias, C. Carpenter and N. H. Chua (1999). "Rac homologues and compartmentalized phosphatidylinositol 4,5-bisphosphate act in a common pathway to regulate polar pollen tube growth." Journal of Cell Biology **145**: 317-330.

Kost, B., P. Spielhofer and N. H. Chua (1998). "A GFP-mouse talin fusion protein labels plant actin filaments *in vivo* and visualizes the actin cytoskeleton in growing pollen tubes." Plant Journal **16**: 393-401.

Kovar, D. R., B. K. Drøbak and C. J. Staiger (2000). "Maize profilin isoforms are functionally distinct." Plant Cell **12**: 583-598.

Kozo, K., S. Yoshiaki, K. Mariko and M. Akira (1990). "Purification and characterization of pectinesterase from *Ficus awkeotsang*." Agricultural and biological chemistry **54**(6): 1469-1476.

Kroeger, J. H., F. Bou Daher, M. Grant and A. Geitmann (2009). "Microfilament orientation constrains vesicle flow and spatial distribution in growing pollen tubes." Biophysical Journal **97**: 1822-1831.

Kroeger, J. H., A. Geitmann and M. Grant (2008). "Model for calcium dependent oscillatory growth in pollen tubes." Journal of Theoretical Biology **253**: 363-374.

Kroh, M. and B. Knuiman (1982). "Ultrastructure of cell wall and plugs of tobacco pollen tubes after chemical extraction of polysaccharides." Planta **154**: 241-250.

Kuang, A., M. E. Musgrave and S. W. Matthews (1996). "Modification of reproductive development in *Arabidopsis thaliana* under spaceflight conditions." Planta **198**: 588-594.

Kuang, A., M. E. Musgrave, S. W. Matthews, D. B. Cummins and S. C. Tucker (1995). "Pollen and ovule development in *Arabidopsis thaliana* under spaceflight condition." American Journal of Botany **82**: 585-595.

Kuang, A., A. Popova, G. McClure and M. E. Musgrave (2005). "Dynamics of storage reserve deposition during *Brassica rapa* L. pollen and seed development in microgravity." International Journal of Plant Science **166**: 85-96.

Kulikauskas, R. and S. McCormick (1997). "Identification of the tobacco and *Arabidopsis* homologues of the pollen-expressed LAT59 gene of tomato." Plant Molecular Biology **34**(5): 809-814.

Kurek, I., Y. Kawagoe, D. Jacob-Wilk, M. Doblin and D. Delmer (2002). "Dimerization of cotton fiber cellulose synthase catalytic subunits occurs via oxidation of the zinc-binding domains." Proceedings of the National Academy of Sciences **99**(17): 11109-11114.

Kuznetsov, O., C. Brown, H. Levine, W. Piastuch, M. Sanwo-Lewandowski and K. Hasenstein (2001). "Composition and physical properties of starch in microgravity-grown plants." Advances in Space Research **28**: 651-658.

Kuznetsov, O. A. and K. H. Hasenstein (1996). "Intracellular magnetophoresis of amyloplasts and induction of root curvature." Planta **198**: 87-94.

Kuznetsov, O. A. and K. H. Hasenstein (1997). "Magnetophoretic induction of curvature in coleoptiles and hypocotyls." Journal of Experimental Botany **48**: 1951-1957.

Kuznetsov, O. A. and K. H. Hasenstein (2001). "Intracellular magnetophoresis of statoliths in *Chara* rhizoids and analysis of cytoplasm viscoelasticity." Advances in Space Research **27**: 887-892.

Laloi, C., K. Apel and A. Danon (2004). "Reactive oxygen signalling: the latest news." Current Opinion in Plant Biology **7**(3): 323-328.

Lancelle, S. A. and P. K. Hepler (1992). "Ultrastructure of freeze-substituted pollen tubes of *Lilium longiflorum*." Protoplasma **167**: 215-230.

Lane, D. R., A. Wiedemeier, L. Peng, H. Hofte, S. Vernhettes, T. Desprez, C. H. Hocart, R. J. Birch, T. I. Baskin, J. E. Burn, T. Arioli, A. S. Betzner and R. E. Williamson (2001). "Temperature-sensitive alleles of RSW2 link the KORRIGAN endo-1,4-{beta}-glucanase to cellulose synthesis and cytokinesis in *Arabidopsis*." Plant Physiol. **126**(1): 278-288.

Langridge, P. D. and R. R. Kay (2006). "Blebbing of *Dictyostelium* cells in response to chemoattractant." Experimental Cell Research **312**: 2009-2017.

Lazzaro, M. D., J. M. Donohue and F. M. Soodavar (2003). "Disruption of cellulose synthesis by isoxaben causes tip swelling and disorganizes cortical microtubules in elongating conifer pollen tubes." Protoplasma **220**(3): 201-207.

Le Goff, A., C. M. G. C. Renard, E. Bonnin and J. F. Thibault (2001). "Extraction, purification and chemical characterisation of xylogalacturonans from pea hulls." Carbohydrate Polymers **45**(4): 325-334.

Lehner, A., F. Dardelle, O. Soret-Morvan, P. Lerouge, A. Driouich and J.-C. Mollet (2010). "Pectins in the cell wall of *Arabidopsis thaliana* pollen tube and pistil." Plant Signaling & Behavior **5**(10): 1282-1285.

Leitz, G., B. Kang, M. E. A. Schoenwaelder and L. A. Staehelin (2009). "Statolith sedimentation kinetics and force transduction to the cortical endoplasmi reticulum in gravity-sensing *Arabidopsis* columella cells." Plant Cell **21**: 843-860.

Lennon, K. A. and E. M. Lord (2000). "*In vivo* pollen tube cell of *Arabidopsis thaliana*. I. Tube cell cytoplasm and wall." Protoplasma **214**: 45-56.

Lennon, K. A., S. Roy, P. K. Hepler and E. M. Lord (1998). "The structure of the transmitting tissue of *Arabidopsis thaliana* (L.) and the path of pollen tube growth." Sexual Plant Reproduction **11**: 49-59.

Levine, L., A. Heyenga, H. Levine, J. Choi, L. Davin, A. Krikorian and N. Lewis (2001). "Cell-wall architecture and lignin composition of wheat development in a microgravity environmen." Phytochemistry **57**: 835-846.

Lewis, M., J. Reynolds, L. Cubano, J. Hatton, B. Lawless and E. Piepmeier (1998). "Spaceflight alters microtubules and increases apopotosis in human lymphocytes (Jurkat)." FASEB Journal **12**: 1007-1018.

Li, H., Y. K. Lin, R. M. Heath, M. X. Zhu and Z. B. Yang (1999). "Control of pollen tube tip growth by a pop GTPase-dependent pathway that leads to tip-localized calcium influx." Plant Cell **11**(9): 1731-1742.

Li, Y.-Q., H.-Q. Zhang, E. S. Pierson, F.-Y. Huang, H. F. Linskens, P. K. Hepler and M. Cresti (1996). "Enforced growth-rate fluctuation causes pectin ring formation in the cell wall of *Lilium longiflorum* pollen tubes." Planta **200**(1): 41-49.

Li, Y., C. P. Darley, V. Ongaro, A. Fleming, O. Schipper, S. L. Baldauf and S. J. McQueen-Mason (2002). "Plant expansins are a complex multigene family with an ancient evolutionary origin." Plant Physiology **128**(3): 854-864.

Li, Y. Q., F. Chen, H. F. Linskens and M. Cresti (1994). "Distribution of unesterified and esterified pectins in cell walls of pollen tubes of flowering plants." Sexual Plant Reproduction **7**(3): 145-152.

Liepman, A., R. Wightman, N. Geshi, S. Turner and H. Scheller (2010). "Arabidopsis - a powerful model system for plant cell wall research." Plant Journal **61**: 1107-1121.

Liepman, A. H., C. G. Wilkerson and K. Keegstra (2005). "Expression of cellulose synthase-like (Csl) genes in insect cells reveals that CslA family members encode mannan synthases." Proceedings of the National Academy of Sciences of the United States of America **102**(6): 2221-2226.

Lietzke, S. E., M. D. Yoder, N. T. Keen and F. Jurnak (1994). "The three-dimensional structure of pectate lyase E, a plant virulence factor from *Erwinia chrysanthemi*." Plant Physiol. **106**(3): 849-862.

Limbach, C., J. Hauslage, C. Schäfer and M. Braun (2005). "How to activate a plant gravireceptor. Early mechanism of gravity sensing studied in characean rhizoids during parabolic flights." Plant Physiology **139**: 1030-1040.

Liners, F., J.-F. Thibault and P. Van Cutsem (1992). "Influence of the degree of polymerization of oligogalacturonates and of esterification pattern of pectin on their recognition by monoclonal antibodies." Plant Physiol. **99**(3): 1099-1104.

Lintilhac, P. M., C. Wei, J. J. Tanguay and J. O. Outwater (2000). "Ball tonometry: a rapid nondestructive method for the measuring cell turgor pressure in thin-walled plant cells." Journal of Plant Growth Regulation **19**: 90- 97.

Lisboa, S., G. Scherer and H. Quader (2002). "Endocytosis in tobacco pollen tubes: visualisation and measurement of plasma membrane retrieval during different gravity conditions indicates gravity-dependence of endocytosis." Journal of Gravitational Physiology **9**: 239-240.

Lisboa, S., G. Scherer and H. Quader (2008). "Localized endocytosis in tobacco pollen tubes: visualisation and dynamics of membrane retrieval by a fluorescent phospholipid." Plant Cell Reports **27**(1): 21-28.

Liszkay, A., B. Kenk and P. Schopfer (2003). "Evidence for the involvement of cell wall peroxidase in the generation of hydroxyl radicals mediating extension growth." Planta **217**(4): 658-667.

Liszkay, A., E. van der Zalm and P. Schopfer (2004). "Production of reactive oxygen intermediates ($O_2^{\cdot -}$, H_2O_2, and $^{\cdot}OH$) by maize roots and their role in wall loosening and elongation growth." Plant Physiology **136**(2): 3114-3123.

Liu, B., C.-M. K. Ho and Y.-R. J. Lee "Microtubule reorganization during mitosis and cytokinesis: Lessons learned from developing microgametophytes in *Arabidopsis thaliana*." Frontiers in Plant Science **2**.

Lloyd, C. (2006). "Microtubules make tracks for cellulose." Science **312**: 1482-1483.

Lockhart, J. A. (1965). "An analysis of irreversible plant cell elongation." Journal of Theoretical Biology **8**: 264-275.

Longland, J. M., S. C. Fry and A. J. Trewavas (1989). "Developmental control of apiogalacturonan biosynthesis and UDP-apiose production in a duckweed." Plant Phsyiology **90**: 972–976.

Lord, E. (2000). "Adhesion and cell movement during pollination: Cherchez la femme." Trends in Plant Sciences **5**: 368- 373.

Louvet, R., E. Cavel, L. Gutierrez, S. Guénin, D. Roger, F. Gillet, F. Guerineau and J. Pelloux (2006). "Comprehensive expression profiling of the pectin methylesterase gene family during silique development in *Arabidopsis thaliana*." Planta **224**(4): 782-791.

Lovy-Wheeler, A., J. G. Kunkel, E. G. Allwood, P. J. Hussey and P. K. Hepler (2006). "Oscillatory increases in alkalinity anticipate growth and may regulate actin dynamics in pollen tubes of lily." Plant Cell **18**(9): 2182-2193.

Lovy-Wheeler, A., K. L. Wilsen, T. I. Baskin and P. K. Hepler (2005). "Enhanced fixation reveals the apical cortical fringe of actin filaments as a consistent feature of the pollen tube." Planta **221**(1): 95-104.

Luttges, M. (1992). "Recognizing and optimizing flight opportunities with hardware and life sciences limitations." Transactions of the Kansas Academy of Science **95**: 76-86.

MacKintosh, F. C., J. Käs and P. A. Janmey (1995). "Elasticity of semiflexible biopolymer networks." Physical Review Letters **75**: 4425-4428.

Madson, M., C. Dunand, X. Li, R. Verma, G. F. Vanzin, J. Caplan, D. A. Shoue, N. C. Carpita and W.-D. Reiter (2003). "The MUR3 gene of *Arabidopsis* encodes a xyloglucan galactosyltransferase that is evolutionarily related to animal exostosins." The Plant Cell Online **15**(7): 1662-1670.

Malhó, R. (2006). The pollen tube: a cellular and molecular perspective. Berlin Heidelberg, Springer Verlag.

Malhó, R., L. Camacho and A. Moutinho (2000). "Signaling pathways in pollen tube growth and reorientation." Annals of Botany **85**: 59-68.

Malhó, R., P. Castanho-Coelho, E. S. Pierson and J. Derksen (2005). Endocytosis and membrane recycling in pollen tubes. Plant Endocytosis. . J. Šamaj, F. Baluška and D. Menzel. Germany, Springer-Verlag**:** 277-292.

Malhó, R., Q. Liu, D. Monteiro, C. Rato, L. Camacho and A. Dinis (2006). "Signalling pathways in pollen germination and tube growth." Protoplasma **228**(1): 21-30.

Malhó, R., N. D. Read, M. S. Pais and A. J. Trewavas (1994). "Role of cytosolic free calcium in the reorientation of pollen tube growth." The Plant Journal **5**(3): 331-341.

Malhó, R., N. D. Read, A. J. Trewavas and M. S. Pais (1995). "Calcium channel activity during pollen tube growth and reorientation." Plant Cell **7**(8): 1173-1184.

Malhó, R. and A. J. Trewavas (1996). "Localized apical increases of cytosolic free calcium control pollen tube orientation." Plant Cell **8**(11): 1935-1949.

Marin-Rodriguez, M. C., J. Orchard and G. B. Seymour (2002). "Pectate lyases, cell wall degradation and fruit softening." J. Exp. Bot. **53**(377): 2115-2119.

Márton, M.-L. and T. Dresselhaus (2010). "Female gametophyte-controlled pollen tube guidance." Biochemical Society Transactions **038**(2): 627-630.

Martzivanou, M., M. Babbick, M. Cogoli-Greuter and R. Hampp (2006). "Microgravity-related changes in gene expression after short-term exposure of *Arabidopsis thaliana* cell cultures." Protoplasma **229**: 155–162.

Martzivanou, M. and R. Hampp (2003). "Hyper-gravity effects on the *Arabidopsis* transcriptome." Physiologia Plantarum **118**: 221–231.

Mascarenhas, J. P. (1993). "Molecular mechanisms of pollen tube growth and differentiation." Plant Cell **5**: 1303-1314.

Mathur, J. (2004). "Cell shape development in plants." Trends in Plant Science **9**: 583-590.

Mathur, J. (2006). "Local interactions shape plant cells." Current Opinion in Cell Biology **18**(1): 40-46.

Matsui, A., R. Yokoyama, M. Seki, T. Ito, K. Shinozaki, T. Takahashi, Y. Komeda and K. Nishitani (2005). "AtXTH27 plays an essential role in cell wall modification during the development of tracheary elements." The Plant Journal **42**(4): 525-534.

Matsumoto, S., S. Kumasaki, K. Soga, K. Wakabayashi, T. Hashimoto and T. Hoson (2010). "Gravity-induced modifications to development in hypocotyls of *Arabidopsis* tubulin mutants." Plant Physiol. **152**(2): 918-926.

Matsumoto, S., Y. Saito, S. Kumasaki, K. Soga, K. Wakabayashi and T. Hoson (2007). "Upregulation of tubulin genes and roles of microtubules in hypergravityinduced growth modifications in *Arabidopsis* hypocotyls." Advances in Space Research **39**: 1176-1181.

Mayers, C. P. (1970). "Histological fixation by microwave heating." Journal of Clinical Pathology **23**(3): 273-275.

McCann, M. C. and K. Roberts (1991). Architecture of the primary cell wall. The cytoskeletal basis of plant growth and form. C. W. Lloyd. London, Academic Press**:** 109-129.

McClure, B. and V. Franklin-Tong (2006). "Gametophytic self-incompatibility: understanding the cellular mechanisms involved in "self" pollen tube inhibition." Planta **224**(2): 233-245.

McCormick, S. (2004). "Control of male gametophyte development." The Plant Cell Online **16**(suppl 1): S142-S153.

McKenna, S. T., J. G. Kunkel, M. Bosch, C. M. Rounds, L. Vidali, L. J. Winship and P. K. Hepler (2009). "Exocytosis precedes and predicts the increase in growth in oscillating pollen tubes." Plant Cell **21**: 3026-3040.

McNeil, M., A. Darvill and P. Albersheim (1980). "Structure of plant cell walls: X. rhamnogalacturonan I, a structurally complex pectic polysaccharide in the walls of suspension-cultured sycamore cells." Plant Phsyiology **66**: 1128–1134.

McQueen-Mason, S. and D. J. Cosgrove (1994). "Disruption of hydrogen bonding between plant cell wall polymers by proteins that induce wall extension." Proceedings of the National Academy of Sciences **91**(14): 6574-6578.

McQueen-Mason, S., D. M. Durachko and D. J. Cosgrove (1992). "Two endogenous proteins that induce cell wall extension in plants." The Plant Cell Online **4**(11): 1425-1433.

McQueen-Mason, S. J. and D. J. Cosgrove (1995). "Expansin mode of action on cell walls (analysis of wall hydrolysis, stress relaxation, and binding)." Plant Physiology **107**(1): 87-100.

Messerli, M. and D. G. Robinson (1998). "Cytoplasmic acidification and current influx follow growth pulses of *Lilium longiflorum* pollen tubes." Plant Journal **16**: 87-91.

Messerli, M. and K. R. Robinson (1997). "Tip localized Ca^{2+} pulses are coincident with peak pulsatile growth rates in pollen tubes of *Lilium longiflorum*." Journal of Cell Science **110**: 1269-1278.

Messerli, M. A., R. Creton, L. F. Jaffe and K. R. Robinson (2000). "Periodic increases in elongation rate precede increases in cytosolic Ca^{2+} during pollen tube growth." Developmental Biology **222**(1): 84-98.

Messerli, M. A., G. Danuser and K. R. Robinson (1999). "Pulsatile influxes of H^+, K^+ and Ca^{2+} lag growth pulses of *Lilium longiflorum* pollen tubes." Journal of Cell Science **112**(10): 1497-1509.

Messerli, M. A. and K. R. Robinson (2003). "Ionic and osmotic disruption of the lily pollen tube oscillator: testing proposed models." Planta **217**: 147-157.

Messerli, M. A., P. J. S. Smith, R. C. Lewis and K. R. Robinson (2004). "Chloride fluxes in lily pollen tubes: a critical reevaluation." Plant Journal **40**(5): 799-812.

Micheli, F. (2001). "Pectin methylesterases: cell wall enzymes with important roles in plant physiology." Trends in Plant Science **6**(9): 414-419.

Micheli, F., B. Sundberg, R. Goldberg and L. Richard (2000). "Radial distribution pattern of pectin methylesterases across the cambial region of hybrid aspen at activity and dormancy." Plant Physiol. **124**(1): 191-200.

Mildenhall, D. C., P. E. J. Wiltshire and V. M. Bryant (2006). "Forensic palynology: Why do it and how it works." Forensic Science International **163**(3): 163-172.

Miller, D. D., D. A. Callaham, D. J. Gross and P. K. Hepler (1992). "Free Ca^{2+} gradient in growing pollen tubes of *Lilium*." Journal of Cell Science **101**: 7-12.

Mo, B. and J. D. Bewley (2003). "The relationship between β-mannosidase and endo-β-mannanase activities in tomato seeds during and following germination: a comparison of seed populations and individual seeds." Journal of Experimental Botany **54**(392): 2503-2510.

Moller, I., I. Sørensen, A. J. Bernal, C. Blaukopf, K. Lee, J. Øbro, F. Pettolino, A. Roberts, J. D. Mikkelsen, J. P. Knox, A. Bacic and W. G. T. Willats (2007). "High-throughput mapping of cell-wall polymers within and between plants using novel microarrays." The Plant Journal **50**(6): 1118-1128.

Money, N. P. (1997). "Wishful thinking of turgor revisited: The mechanics of fungal growth." Fungal Genetics and Biology **21**: 173- 187.

Monteiro, D., P. C. Coelho, C. Rodrigues, L. Camacho, H. Quader and R. Malhó (2005). "Modulation of endocytosis in pollen tube growth by phosphoinositides and phospholipids." Protoplasma **V226**(1): 31-38.

Mori, I. C. and J. I. Schroeder (2004). "Reactive oxygen species activation of plant Ca^{2+} channels. A signaling mechanism in polar growth, hormone transduction, stress signaling, and hypothetically mechanotransduction." Plant Physiology **135**(2): 702-708.

Morita, M. T. (2010). "Directional gravity sensing in gravitropism." Annual Review of Plant Biology **61**(1): 705-720.

Morita, M. T. and M. Tasaka (2004). "Gravity sensing and signaling." Current Opinion in Plant Biology **7**(6): 712-718.

Moscatelli, A., G. Cai, F. Ciampolini and M. Cresti (1998). "Dynein heavy chain-related polypeptides are associated with organelles in pollen tubes of *Nicotiana tabacum*." Sexual Plant Reproduction **11**: 31-40.

Moscatiello, R., B. Baldan, A. Squartini, P. Mariani and L. Navazio (2012). "Oligogalacturonides: novel signalling molecules in rhizobium-legume communications." Molecular Plant-Microbe Interactions.

Mouline, K., A. A. Very, F. Gaymard, J. Boucherez, G. Pilot, M. Devic, D. Bouchez, J. B. Thibaud and H. Sentenac (2002). "Pollen tube development and competitive ability are impaired by disruption of a Shaker K^+ channel in *Arabidopsis*." Genes and Development **16**(3): 339-350.

Mullen, J., C. Wolverton, H. Ishikawa and M. Evans (2000). "Kinetics of constant gravitropic stimulus responses in *Arabidopsis* roots using a feedback system." Plant Physiology **123**: 665-670.

Müller, K., A. Linkies, R. A. M. Vreeburg, S. C. Fry, A. Krieger-Liszkay and G. Leubner-Metzger (2009). "*In vivo* cell wall loosening by hydroxyl radicals during cress seed germination and elongation growth." Plant Physiology **150**(4): 1855-1865.

Müller, W., H. Fricke, A. N. Halliday, M. T. McCulloch and J.-A. Wartho (2003). "Origin and migration of the Alpine iceman." Science **302**(5646): 862-866.

Murfett, J., T. J. Strabala, D. M. Zurek, B. Mou, B. Beecher and B. A. McClure (1996). "S-RNase and interspecific pollen rejection in the genus Nicotiana: Multiple pollen-rejection pathways contribute to unilateral incompatibility between self-incompatible and self-compatible species." The Plant Cell Online **8**(6): 943-958.

Musgrave, M. (2007). "Growing plants in space." CAB Reviews Perspectives in Agriculture, Veterinary Science, Nutrition and Natural Resources **2**: 065.

Musgrave, M., A. Kuang, J. Allen, J. Blasiak and J. J. W. A. van Loon (2009a). "*Brassica rapa* L. seed development in hypergravity." Seed Science Research **19**: 63-72.

Musgrave, M., A. Kuang, J. Allen and J. van Loon (2009b). "Hypergravity prevents seed production in *Arabidopsis* by disrupting pollen tube growth." Planta **230**(5): 863-870.

Musgrave, M. E., A. Kuang and S. W. Matthews (1997). "Plant reproduction during spaceflight: importance of the gaseous environment." Planta (Berl) **203**: S177-S184.

Nebenführ, A. (2002). "Vesicle traffic in the endomembrane system: a tale of COPs, Rabs and SNAREs." Current Opinion in Plant Biology **5**(6): 507-512.

Nedukha, E. M. (1996). "Possible mechanisms of plant cell wall changes at microgravity." Advances in Space Research **17**: 37-45.

Nedukha, E. M. (1998). "Effects of clinorotation on the polysaccharide content of resynthesized walls of protoplasts." Advances in Space Research **21**: 1121-1126.

Nedukha, E. M., V. A. Sidorov and V. M. Samoylov (1994). "Clinostation influence on regeneration of a cell wall in *Solanum tuberosum* L. protoplasts." Advances in Space Research **14**(97-101).

Nick, P. (2010). "Stress, ROS, and actin—a volatile *menage à trois* ?" Protoplasma **239**(1): 1-2.

Nicol, F., I. His, A. Jauneau, S. Vernhettes, H. Canut and H. Hofte (1998). "A plasma membrane-bound putative endo-1,4-β-D-glucanase is required for normal wall assembly and cell elongation in *Arabidopsis*." EMBO J **17**(19): 5563-5576.

Niogret, M.-F., M. Dubald, P. Mandaron and R. Mache (1991). "Characterization of pollen polygalacturonase encoded by several cDNA clones in maize." Plant Molecular Biology **17**(6): 1155-1164.

Nishikawa, S.-i., G. Zinkl, R. Swanson, D. Maruyama and D. Preuss (2005). "Callose (beta-1,3 glucan) is essential for *Arabidopsis* pollen wall patterning, but not tube growth." BMC Plant Biology **5**(1): 22.

Nishitani, K. and R. Tominaga (1992). "Endo-xyloglucan transferase, a novel class of glycosyltransferase that catalyzes transfer of a segment of xyloglucan molecule to another xyloglucan molecule." Journal of Biological Chemistry **267**(29): 21058-21064.

Novick, P., M. D. Garrett, P. Brennwald, A. Lauring, F. P. Finger, R. Collins and D. R. TerBush (1995). "Control of exocytosis in yeast." Cold Spring Harbor Symposia on Quantitative Biology **60**: 171-177.

Nühse, T. S., A. Stensballe, O. N. Jensen and S. C. Peck (2004). "Phosphoproteomics of the *Arabidopsis* plasma membrane and a new phosphorylation site database." The Plant Cell Online **16**(9): 2394-2405.

O'Kelley, J. C. and P. H. Carr (1954). "An electron micrographic study of the cell walls of elongating cotton fibers, root hairs, and pollen tubes." American Journal of Botany **41**: 261-264.

O'Neill, M. A., S. Eberhard, P. Albersheim and A. G. Darvill (2001). "Requirement of borate cross-linking of cell wall rhamnogalacturonan II for *Arabidopsis* growth." Science **294**(5543): 846-849.

Obel, N., L. Neumetzler and M. Pauly (2007). Hemicelluloses and cell expansion. The Expanding Cell. J.-P. Verbelen and K. Vissenberg, Springer Berlin / Heidelberg. **6:** 57-88.

Obermeyer, G. and H.-A. Kolb (1993). "K^+ channels in the plasma membrane of lily pollen protoplasts." Botanica Acta **106**: 26-31.

Oechslin, R., M. V. Lutz and R. Amadò (2003). "Pectic substances isolated from apple cellulosic residue: structural characterisation of a new type of rhamnogalacturonan I." Carbohydrate Polymers **51**(3): 301-310.

Ohmiya, Y., M. Samejima, M. Shiroishi, Y. Amano, T. Kanda, F. Sakai and T. Hayashi (2000). "Evidence that endo-1,4-β-glucanases act on cellulose in suspension-cultured poplar cells." The Plant Journal **24**(2): 147-158.

Ohmiya, Y., T. Takeda, S. Nakamura, F. Sakai and T. Hayashi (1995). "Purification and properties of a wall-bound endo-1,4-β-glucanase from suspension-cultured poplar cells." Plant and Cell Physiology **36**(4): 607-614.

Okamoto-Nakazato, A. (2002). "A brief note on the study of yieldin, a wall-bound protein that regulates the yield threshold of the cell wall." Journal of Plant Research **115**(4): 309-313.

Okamoto-Nakazato, A., T. Nakamura and H. Okamoto (2000a). "The isolation of wall-bound proteins regulating yield threshold tension in glycerinated hollow cylinders of cowpea hypocotyl." Plant, Cell & Environment **23**(2): 145-154.

Okamoto-Nakazato, A., K. Takahashi, N. Kido, K. Owaribe and K. Katou (2000b). "Molecular cloning of yieldins regulating the yield threshold of cowpea cell walls: cDNA cloning and characterization of recombinant yieldin." Plant, Cell & Environment **23**(2): 155-164.

Ori, N., G. Sessa, T. Lotan, S. Himmelhoch and R. Fluhr (1990). A major stylar matrix polypeptide (sp41) is a member of the pathogenesis-related proteins superclass.

Orr, A., B. Helmke, B. Blackman and M. Schwartz (2006). "Mechanisms of mechanotransduction." Developmental Cell **10**: 11-20.

Ortega, J. K. E. (2004). A quantitative biophysical perspective of expansive growth for cells with walls. Recent Research Developments in Biophysics. S. G. Pandalai, Editor. eds.**:** 297-324.

Osborne, D. J. (2004). "Advances in pectin and pectinase research. Voragen F, Schols H and Visser R. eds. 2003. The Netherlands: Kluwer Academic Publishers. €145 (hardback). 491 pp." Annals of Botany **94**(3): 479-480.

Pagant, S., A. Bichet, K. Sugimoto, O. Lerouxel, T. Desprez, M. McCann, P. Lerouge, S. Vernhettes and H. Höfte (2002). "KOBITO1 encodes a novel plasma membrane protein necessary for normal synthesis of cellulose during cell expansion in *Arabidopsis*." The Plant Cell Online **14**(9): 2001-2013.

Palanivelu, R. (2011). "Targeted growth of pollen tubes to ovules prior to completing fertilization." Molecular Reproduction and Development **78**(12): 893-893.

Palanivelu, R., L. Brass, A. F. Edlund and D. Preuss (2003). "Pollen tube growth and guidance Is regulated by POP2, an *Arabidopsis* gene that controls GABA levels." Cell **114**(1): 47-59.

Palanivelu, R. and D. Preuss (2000). "Pollen tube targetting and axon guidance: Parallels in tip growth mechanisms." Trends in Cell Biology **10**: 517- 524.

Palanivelu, R. and D. Preuss (2006). "Distinct short-range ovule signals attract or repel *Arabidopsis thaliana* pollen tubes *in vitro*." BMC Plant Biology **6**(1): 7.

Palanivelu, R. and T. Tsukamoto (2012). "Pathfinding in angiosperm reproduction: pollen tube guidance by pistils ensures successful double fertilization." Wiley Interdisciplinary Reviews: Developmental Biology **1**(1): 96-113.

Papaseit, C., N. Pochon and J. Tabony (2000). "Microtubule self-organization is gravity-dependent." Proceedings of the National Academy of Sciences of the United States of America **97**: 8364-8368.

Paradez, A., A. Wright and D. W. Ehrhardt (2006). "Microtubule cortical array organization and plant cell morphogenesis." Current Opinion in Plant Biology **9**: 571-578.

Paredez, A. R., C. R. Somerville and D. W. Ehrhardt (2006). "Visualization of cellulose synthase demonstrates functional association with microtubules." Science **312**(5779): 1491-1495.

Parre, E. and A. Geitmann (2005). "More than a leak sealant - the physical properties of callose in pollen tubes." Plant Physiology **137**: 274-286.

Parre, E. and A. Geitmann (2005a). "More than a leak sealant. The mechanical properties of callose in pollen tubes." Plant Physiology **137**(1): 274-286.

Parre, E. and A. Geitmann (2005b). "Pectin and the role of the physical properties of the cell wall in pollen tube growth of *Solanum chacoense*." Planta **220**(4): 582-592.

Parton, R. M., S. Fischer-Parton, A. J. Trewavas and M. K. Watahiki (2003). "Pollen tubes exhibit regular periodic membrane trafficking events in the absence of apical extension." Journal of Cell Science **116**: 2707-2719.

Parton, R. M., S. Fischer-Parton, M. K. Watahiki and T. A. J. (2001). "Dynamics of the apical vesicle accumulation and the rate of growth are related in individual pollen tubes." Journal of Cell Sciences **114**: 2685-2695.

Pear, J. R., Y. Kawagoe, W. E. Schreckengost, D. P. Delmer and D. M. Stalker (1996). "Higher plants contain homologs of the bacterial celA genes encoding the catalytic subunit of cellulose synthase." Proceedings of the National Academy of Sciences **93**(22): 12637-12642.

Peaucelle, A., R. Louvet, J. N. Johansen, H. Höfte, P. Laufs, J. Pelloux and G. Mouille (2008). "*Arabidopsis* phyllotaxis is controlled by the methyl-esterification status of cell-wall pectins." Current Biology **18**(24): 1943-1948.

Pelloux, J., C. Rustérucci and E. J. Mellerowicz (2007). "New insights into pectin methylesterase structure and function." Trends in Plant Science **12**(6): 267-277.

Peña, M. J., P. Ryden, M. Madson, A. C. Smith and N. C. Carpita (2004). "The galactose residues of xyloglucan are essential to maintain mechanical strength of the primary cell walls in *Arabidopsis* during growth." Plant Physiology **134**(1): 443-451.

Perbal, G. and D. Driss-Ecole (2003). "Mechanotransduction in gravisensing cells." Trends in Plant Science **8**(10): 498-504.

Petersen, N. O., W. B. McConnaughey and E. L. Elson (1982). "Dependence of locally measured cellular deformability on position on the cell, temperature, and cytochalasin B." Proceedings of the National Academy of Sciences of the United States of America **79**(17): 5327-5331.

Petersen, T. N., S. Brunak, G. von Heijne and H. Nielsen (2011). "SignalP 4.0: discriminating signal peptides from transmembrane regions." Nat Meth **8**(10): 785-786.

Pickersgill, R., J. Jenkins, G. Harris, W. Nasser and J. Robert-Baudouy (1994). "The structure of *Bacillus subtilis* pectate lyase in complex with calcium." Nat Struct Mol Biol **1**(10): 717-723.

Picton, J. M. and M. W. Steer (1983a). "Evidence for the role of Ca^{2+} ions in tip extension in pollen tubes." Protoplasma **115**(1): 11-17.

Picton, J. M. and M. W. Steer (1983b). "Membrane recycling and the control of secretory activity in pollen tubes." Journal of Cell Science **63**: 303-310.

Picton, J. M. and M. W. Steer (1985). "The effects of ruthenium red, lanthanum, fluorescein isothiocyanate and trifluoperazine on vesicle transport, vesicle fusion and tip extension in pollen tubes." Planta **163**: 20-26.

Pierson, E. S., D. D. Miller, D. A. Callaham, A. M. Shipley, B. A. Rivers, M. Cresti and P. K. Hepler (1994). "Pollen tube growth is coupled to the extracellular calcium ion flux and the intracellular calcium gradient: effect of BAPTA-type buffers and hypertonic media." Plant Cell **6**: 1815-1828.

Pierson, E. S., D. D. Miller, D. A. Callaham, J. VanAken, G. Hackett and P. K. Hepler (1996). "Tip-localized calcium entry fluctuates during pollen tube growth." Developmental Biology **174**: 160-173.

Pierson, E. S., P. J. S. Smith, A. M. Shipley, L. F. Jaffe, M. Cresti and P. K. Hepler (1993). Ca^{2+} fluxes around pollen grains and pollen tubes of lily; Normal development and effects of thermal shock, BAPTA-type buffer microinjection and depletion of boric acid from the medium. **185:** 302-303.

Pina, C., F. Pinto, J. A. Feijó and J. D. Becker (2005). "Gene family analysis of the *Arabidopsis* pollen transcriptome reveals biological implications for cell growth, division control, and gene expression regulation." Plant Physiology **138**(2): 744-756.

Poirier, C. and P. Iglesias (2007). "An integrative approach to understanding mechanosensation." Briefings in Bioinformatics **8**: 258-265.

Popova, A., M. Musgrave and A. Kuang (2009). "The development of embryos in *Brassica rapa* L. in microgravity." Cytology and Genetics **43**(2): 89-93.

Potocký, M., M. A. Jones, R. Bezvoda, N. Smirnoff and V. Žárský (2007). "Reactive oxygen species produced by NADPH oxidase are involved in pollen tube growth." New Phytologist **174**(4): 742-751.

Potter, I. (1994). "Changes in xyloglucan endotransglycosylase (XET) activity during hormoneinduced growth in lettuce and cucumber hypocotyls and spinach cell suspension cultures." J. Exp. Bot. **45**: 1703-1710.

Pratelli, R., J.-U. Sutter and M. R. Blatt (2004). "A new catch in the SNARE." Trends in Plant Science **9**(4): 187-195.

Preuss, D., B. Lemieux, G. Yen and R. W. Davis (1993). "A conditional sterile mutation eliminates surface components from Arabidopsis pollen and disrupts cell signaling during fertilization." Genes & Development **7**(6): 974-985.

Prosser, J. I. (1994). Mathematical modelling of fungal growth. The Growing Fungus. N. A. R. Gow and G. M. Gadd. London, Chapman & Hall**:** 319-335.

Prosser, J. I. and A. P. J. Trinci (1979). "A model for hyphal growth and branching." Journal of General Microbiology **111**: 153-164.

Pua, E.-C., C.-K. Ong, P. Liu and J.-Z. Liu (2001). "Isolation and expression of two pectate lyase genes during fruit ripening of banana (*Musa acuminata*)." Physiologia Plantarum **113**(1): 92-99.

Punta, M., P. C. Coggill, R. Y. Eberhardt, J. Mistry, J. Tate, C. Boursnell, N. Pang, K. Forslund, G. Ceric, J. Clements, A. Heger, L. Holm, E. L. L. Sonnhammer, S. R. Eddy, A. Bateman and R. D. Finn (2012). "The Pfam protein families database." Nucleic Acids Research **40**(D1): D290-D301.

Radauer, C., M. Bublin, S. Wagner, A. Mari and H. Breiteneder (2008). "Allergens are distributed into few protein families and possess a restricted number of biochemical functions." Journal of Allergy and Clinical Immunology **121**(4): 847-852.e847.

Ramalho-Santos, M., J. Pissarra, P. Veríssimo, S. Pereira, R. Salema, E. Pires and C. J. Faro (1997). "Cardosin A, an abundant aspartic proteinase, accumulates in

protein storage vacuoles in the stigmatic papillae of *Cynara cardunculus* L." Planta **203**(2): 204-212.

Rashotte, A. M., S. R. Brady, R. C. Reed, S. J. Ante and G. K. Muday (2000). "Basipetal auxin transport is required for gravitropism in roots of *Arabidopsis*." Plant Physiology **122**: 481-490.

Rasmussen, O., C. A. Baggerud, H. C. Larssen, K. Evjen and T.-H. Iversen (1994). "The effect of 8 days of microgravity on regeneration of intact plants from protoplasts." Physiologia Plantarum **92**: 404-411.

Rasmussen, O., D. A. Klymchuk, E. L. Kordyum, L. A. Danevich, E. B. Tarnavskaya, V. V. Lozovaya, M. G. Tairbekov, C. Baggemd and T.-H. Iversen (1992). "The effect of exposure to microgravity on the development and structural organization of plant protoplasts flown on Biokosmos 9." Physiologia Plantarum **84**(162-170).

Rathore, K. S., R. J. Cork and K. R. Robinson (1991). "A cytoplasmic gradient of Ca^{2+} is correlated with the growth of lily pollen tubes." Developmental Biology **148**: 612-619.

Raudaskoski, M., H. Åström and E. Laitiainen (2001). "Pollen tube cytoskeleton structure and function." Journal of Plant Growth Regulation **20**: 113-130.

Rautengarten, C., B. Usadel, L. Neumetzler, J. Hartmann, D. Büssis and T. Altmann (2008). "A subtilisin-like serine protease essential for mucilage release from *Arabidopsis* seed coats." The Plant Journal **54**(3): 466-480.

Raven, J. A. and D. Edwards (2001). "Roots: evolutionary origins and biogeochemical significance." Journal of Experimental Botany **52**(suppl 1): 381-401.

Raven, P. H., R. F. Evert and S. Eichorn (1986). "Biology of plants. Worth Publ." Inc, New York.

Rayle, D. L. and R. Cleland (1970). "Enhancement of wall loosening and elongation by acid solutions." Plant Physiology **46**(2): 250-253.

Redgwell, R. J. and S. C. Fry (1993). "Xyloglucan endotransglycosylase activity increases during kiwifruit (*Actinidia deliciosa*) ripening (implications for fruit softening)." Plant Physiology **103**(4): 1399-1406.

Reinhardt, M. O. (1892). "Das Wachstum der Pilzhyphen." Jahrbuch der Wissenschaften in Botanik **23**: 479-566.

Reiter, W.-D., C. Chapple and C. R. Somerville (1997). "Mutants of *Arabidopsis thaliana* with altered cell wall polysaccharide composition." The Plant Journal **12**(2): 335-345.

Reiter, W.-D., C. C. S. Chapple and C. R. Somerville (1993). "Altered growth and cell walls in a fucose-deficient mutant of *Arabidopsis*." Science **261**(5124): 1032-1035.

Reiter, W.-D. and G. F. Vanzin (2001). "Molecular genetics of nucleotide sugar interconversion pathways in plants." Plant Molecular Biology **47**(1): 95-113.

Ren, C. and A. R. Kermode (2000). "An increase in pectin methyl esterase activity accompanies dormancy breakage and germination of Yellow Cedar seeds." Plant Physiology **124**(1): 231-242.

Renard, C. M. G. C., R. M. Weightman and J. F. Thibault (1997). "The xylose-rich pectins from pea hulls." International Journal of Biological Macromolecules **21**(1–2): 155-162.

Richmond, T. A. and C. R. Somerville (2000). "The cellulose synthase superfamily." Plant Physiology **124**(2): 495-498.

Ridley, B. L., M. A. O'Neill and D. Mohnen (2001). "Pectins: structure, biosynthesis, and oligogalacturonide-related signaling." Phytochemistry **57**(6): 929-967.

Robert, L. S., S. Allard, J. L. Gerster, L. Cass and J. Simmonds (1993). "Isolation and characterization of a polygalacturonase gene highly expressed in *Brassica napus* pollen." Plant Molecular Biology **23**(6): 1273-1278.

Röckel, N., S. Wolf, B. Kost, T. Rausch and S. Greiner (2008). "Elaborate spatial patterning of cell-wall PME and PMEI at the pollen tube tip involves PMEI endocytosis, and reflects the distribution of esterified and de-esterified pectins." The Plant Journal **53**(1): 133-143.

Rojas, Enrique R., S. Hotton and J. Dumais (2011). "Chemically mediated mechanical expansion of the pollen tube cell wall." Biophysical journal **101**(8): 1844-1853.

Romagnoli, S., G. Cai and M. Cresti (2003). "*In vitro* assays demonstate that pollen tube organelles use kinesin-related motor proteins to move along microtubules." Plant Cell **15**: 251-269.

Romagnoli, S., G. Cai, C. Faleri, E. Yokota, T. Shimmen and M. Cresti (2007). "Microtubule- and actin filament-dependent motors are distributed on pollen tube mitochondria and contribute differently to their movement." Plant Cell Physiology **48**: 345-361.

Römling, U., Mark Gomelsky and Michael Y. Galperin (2005). "C-di-GMP: the dawning of a novel bacterial signalling system." Molecular Microbiology **57**(3): 629-639.

Rösner, H., T. Wassermann, W. Möller and W. Hanke (2006). "Effects of altered gravity on the actin and microtubule cytoskeleton of human SH-SY5Y neuroblastoma cells." Protoplasma **229**: 225-234.

Rosso, M. G., Y. Li, N. Strizhov, B. Reiss, K. Dekker and B. Weisshaar (2003). "An *Arabidopsis thaliana*; T-DNA mutagenized population (GABI-Kat) for flanking sequence tag-based reverse genetics." Plant Molecular Biology **53**(1): 247-259.

Roudier, F., A. G. Fernandez, M. Fujita, R. Himmelspach, G. H. H. Borner, G. Schindelman, S. Song, T. I. Baskin, P. Dupree, G. O. Wasteneys and P. N. Benfey (2005). "COBRA, an *Arabidopsis* extracellular glycosyl-phosphatidyl inositol-anchored protein, specifically controls highly anisotropic expansion through its involvement in cellulose microfibril orientation." The Plant Cell Online **17**(6): 1749-1763.

Round, A. N., N. M. Rigby, A. J. MacDougall and V. J. Morris (2010). "A new view of pectin structure revealed by acid hydrolysis and atomic force microscopy." Carbohydrate Research **345**(4): 487-497.

Roux, S. J., A. Chatterjee, S. Hillier and T. Cannon (2003). "Early development of fern gametophytes in microgravity." Advances in Space Research **31**(1): 215-220.

Rowland, O. and F. Domergue (2012). "Plant fatty acyl reductases: Enzymes generating fatty alcohols for protective layers with potential for industrial applications." Plant Science **193–194**(0): 28-38.

Russin, W. A. and C. L. Trivett (2001). Vacuum-microwave combination for processing plant tissues for electron microscopy. Microwave Techniques and Protocols**:** 25-35.

Sachan, N., D. Rogers, K.-Y. Yun, J. Littleton and D. Falcone (2010). "Reactive oxygen species regulate alkaloid metabolism in undifferentiated <i>N. tabacum</i> cells." Plant Cell Reports **29**(5): 437-448.

Sack, F. D. (1997). "Plastids and gravitropic sensing." Planta (Berl) **203**: S63-S68.

Salmi, M., A. ul Haque, T. Bushart, S. Stout, S. Roux and D. Porterfield (2011). "Changes in gravity rapidly alter the magnitude and direction of a cellular calcium current." Planta: 1-10.

Sampedro, J. and D. Cosgrove (2005). "The expansin superfamily." Genome Biology **6**(12): 242.

Sanderfoot, A. A. and N. V. Raikhel (1999). "The specificity of vesicle trafficking: coat proteins and SNAREs." Plant Cell **11**: 629-641.

Sassen, M. M. A. (1964). "Fine structure of Petunia pollen grain and pollen tube." Acta Bot Neerl **13**: 174-181.

Sato, F., S. Takeda, H. Matsushima and Y. Yamada (1999). "Cell growth and organ differentiation in cultured tobacco cells under spaceflight condition." Biological Sciences in Space **13**(1): 18-24.

Scavetta, R. D., S. R. Herron, A. T. Hotchkiss, N. Kita, N. T. Keen, J. A. E. Benen, H. C. M. Kester, J. Visser and F. Jurnak (1999). "Structure of a plant cell wall fragment complexed to pectate lyase C." Plant Cell **11**(6): 1081-1092.

Schlüpmann, H., A. Bacic and S. M. Read (1994). "Uridine diphosphate glucose metabolism and callose synthesis in cultured pollen tubes of *Nicotiana alata* Link et Otto." Plant Phsyiology **105**: 659-670.

Schnurer, J. and T. Rosswall (1982). "Fluorescein diacetate hydrolysis as a measure of total microbial activity in soil and litter." Applied and Environmental Microbiology **43**(6): 1256-1261.

Scholl, R. L., S. T. May and D. H. Ware (2000). "Seed and molecular resources for *Arabidopsis*." Plant Physiology **124**(4): 1477-1480.

Schols, H. A. and A. G. J. Voragen (1996). Complex pectins: Structure elucidation using enzymes. Progress in Biotechnology. J. Visser and A. G. J. Voragen, Elsevier. **Volume 14:** 3-19.

Schopfer, P. (1996). "Hydrogen peroxide-mediated cell-wall stiffening in vitro in maize coleoptiles." Planta **199**(1): 43-49.

Schopfer, P. (2001). "Hydroxyl radical-induced cell-wall loosening in vitro and in vivo: implications for the control of elongation growth." The Plant Journal **28**(6): 679-688.

Schopfer, P. (2006). "Biomechanics of plant growth." American Journal of Botany **93**(10): 1415-1425.

Schwuchow, J., F. D. Sack and E. Hartmann (1990). "Microtubule distribution in gravitropic protonemata of the moss *Ceratodon* " Protoplasma **159**(1): 60-69.

Schwuchow, J. M., D. Kim and F. D. Sack (1995). "Caulonemal gravitropism and amyloplast sedimentation in the moss *Funaria*." Canadian Journal of Botany **73**: 1029-1035.

Sessa, G. and R. Fluhr (1995). "The expression of an abundant transmitting tract-specific endoglucanase (Sp41) is promoter-dependent and not essential for the reproductive physiology of tobacco." Plant Molecular Biology **29**(5): 969-982.

Shahali, Y., J.-P. Sutra, I. Haddad, J. Vinh, L. Guilloux, G. Peltre, H. Sénéchal and P. Poncet (2012). "Proteomics of cypress pollen allergens using double and triple one-dimensional electrophoresis." ELECTROPHORESIS **33**(3): 462-469.

Shedletzky, E., M. Shmuel, D. P. Delmer and D. T. A. Lamport (1990). "Adaptation and growth of tomato cells on the herbicide 2,6-dichlorobenzonitrile leads to production

of unique cell-walls virtually lacking a cellulose-xyloglucan network." Plant Physiology **94**: 980-987.

Shedletzky, E., M. Shmuel, T. Trainin, S. Kalman and D. P. Delmer (1992). "Cell wall structure in cells adapted to growth on the cellulose-synthesis inhibitor 2,6-dichlorobenzonitrile : A comparison between two dicotyledonous plants and a graminaceous monocot." Plant Physiology **100**: 120-130.

Shimmen, T., R. W. Ridge, I. Lambiris, J. Plazinski, E. Yokota and R. E. Williamson (2000). "Plant myosins." Protoplasma **214**: 1-10.

Shivanna, K. R. and B. M. Johri (1985). The angiosperm pollen. New Delhi, Wiley Eastern Limited.

Shreffler, W. G. (2011). "Microarrayed recombinant allergens for diagnostic testing." Journal of Allergy and Clinical Immunology **127**(4): 843-849.

Sieberer, B., H. Kieft, T. Franssen-Verheijen, A. Emons and J. Vos (2009). "Cell proliferation, cell shape, and microtubule and cellulose microfibril organization of tobacco BY-2 cells are not altered by exposure to near weightlessness in space." Planta **230**(6): 1129-1140.

Sievers, A., B. Buchen and D. Hodick (1996). "Gravity sensing in tip-growing cells." Trends in Plant Science **1**: 273-279.

Silva, N. F. and D. R. Goring (2001). "Mechanisms of self-incompatibility in flowering plants." Cellular and Molecular Life Sciences **58**: 1988-2007.

Sinclair, W. and A. J. Trewavas (1997). "Calcium in gravitropism: a re-examination." Planta (Berl) **203**: S85-S90.

Skagen, E. and T.-H. Iversen (1999). "Simulated weightlessness and hyper-g results in opposite effects on the regeneration of the cortical microtubule array in protoplasts from *Brassica napus* hypocotyls." Physiologia Plantarum **106**: 318-325.

Skagen, E. and T.-H. Iversen (2000). "Effect of simulated and real weightlessness on early regeneration stages of *Brassica napus* protoplasts." In Vitro Cellular & Developmental Biology-Plant **36**: 312-318.

Smirnova, A., N. Matveyeva, O. Polesskaya and I. Yermakov (2009). "Generation of reactive oxygen species during pollen grain germination." Russian Journal of Developmental Biology **40**(6): 345-353.

Smith, B. G. and P. J. Harris (1999). "The polysaccharide composition of Poales cell walls: Poaceae cell walls are not unique." Biochemical Systematics and Ecology **27**(1): 33-53.

Smith, L. G. and D. G. Oppenheimer (2005). "Spatial control of cell expansion by the plant cytoskeleton." Annual Review of Cell and Developmental Biology **21**(1): 271-295.

Smyth, D. R., J. L. Bowman and E. M. Meyerowitz (1990). "Early flower development in *Arabidopsis*." Plant Cell **2**(8): 755-767.

Soga, K., K. Harada, K. Wakabayashi, T. Hoson and S. Kamisaka (1999a). "Increased molecular mass of hemicellulosic polysaccharides is involved in growth inhibition of maize coleoptiles and mesocotyls under hypergravity conditions." Journal of Plant Research **112**: 273-278.

Soga, K., K. Wakabayashi, T. Hoson and S. Kamisaka (1999b). "Hypergravity increases the molecular size of xyloglucans by decreasing xyloglucan-degrading activity in azuki bean epicotyls." Plant Cell Physiology **40**: 581-585.

Soga, K., K. Wakabayashi, T. Hoson and S. Kamisaka (2001). "Gravitational force regulates elongation growth of *Arabidopsis* hypocotyls by modifying xyloglucan metabolism." Advances in Space Research **27**: 1011-1016.

Soga, K., K. Wakabayashi, S. Kamisaka and T. Hoson (2002). "Perception of gravity stimuli by mechanosensitive ion channels in plant seedlings." Plant Cell Physiology **43**: s182.

Soga, K., K. Wakabayashi, S. Kamisaka and T. Hoson (2005). "Mechanoreceptors rather than sedimentable amyloplasts perceive the gravity signal in hypergravity-induced inhibition of root growth in azuki bean." Functional Plant Biology **32**(2): 175-179.

Soga, K., K. Wakabayashi, S. Kamisaka and T. Hoson (2006). "Hypergravity induces reorientation of cortical microtubules and modifies growth anisotropy in azuki bean epicotyls." Planta **224**: 1485-1494.

Somerville, C. (2006). "Cellulose synthesis in higher plants." Annual Review of Cell and Developmental Biology **22**(1): 53-78.

Speranza, A., R. Crinelli, V. Scoccianti and A. Geitmann (2012). "Reactive oxygen species are involved in pollen tube initiation in kiwifruit." Plant Biology **14**(1): 64-76.

Staiger, C. J. and L. Blanchoin (2006). "Actin dynamics: old friends with new stories." Current Opinion in Plant Biology **9**: 554-562.

Starr, M. P. and F. Moran (1962). "Eliminative split of pectic substances by phytopathogenic soft-rot bacteria." Science **135**(3507): 920-921.

Staves, M. P. (1997). "Cytoplasmic streaming and gravity sensing in *Chara* internodal cells." Planta (Berl) **203**: S79-S84.

Steer, M. W. (1988). "Plasma membrane turnover in plant cells." Journal of Experimental Botany **39**: 987-996.

Steer, M. W. and J. M. Steer (1989). "Pollen tube tip growth." The New Phytologist **111**(3): 323-358.

Suen, D. F. and A. H. Huang (2007). "Maize pollen coat xylanase facilitates pollen tube penetration into silk during sexual reproduction." Journal of Biological Chemistry **282**: 625-636.

Sugimoto, K., R. E. Williamson and G. O. Wasteneys (2000). "New techniques enable comparative analysis of microtubule orientation, wall texture, and growth rate in intact roots of *Arabidopsis*." Plant Physiology **124**: 1493-1506.

Sun, Y., S. Veerabomma, H. A. Abdel-Mageed, M. Fokar, T. Asami, S. Yoshida and R. D. Allen (2005). "Brassinosteroid regulates fiber development on cultured cotton ovules." Plant and Cell Physiology **46**(8): 1384-1391.

Suslov, D. and J. P. Verbelen (2006). "Cellulose orientation determines mechanical anisotropy in onion epidermis cell walls." Journal of Experimental Botany **57**: 2183-2192.

Suzuki, K., L. Yang and F. Takaiwa (2012). "Transgenic rice accumulating modified cedar pollen allergen Cry j 2 derivatives." Journal of Bioscience and Bioengineering **113**(2): 249-251.

Swanson, R., A. F. Edlund and D. Preuss (2004). "Species specificity in pollen-pistil interactions." Annual review of genetics **38**: 793-818.

Szyjanowicz, P. M. J., I. McKinnon, N. G. Taylor, J. Gardiner, M. C. Jarvis and S. R. Turner (2004). "The irregular xylem 2 mutant is an allele of korrigan that affects the secondary cell wall of Arabidopsis thaliana." The Plant Journal **37**(5): 730-740.

Takayama, S. and A. Isogai (2003). "Molecular mechanism of self-recognition in Brassica self-incompatibility." Journal of Experimental Botany **54**(380): 149-156.

Takayama, S. and A. Isogai (2004). "Self-incompatibility in plants." Annual Review in Plant Biology **56**: 467-489.

Takayama, S., H. Shiba, M. Iwano, K. Asano, M. Hara, F.-S. Che, M. Watanabe, K. Hinata and A. Isogai (2000). "Isolation and characterization of pollen coat proteins of *Brassica campestris* that interact with *S* locus-related glycoprotein 1 involved in pollen–stigma adhesion." Proceedings of the National Academy of Sciences **97**(7): 3765-3770.

Takeda, S. and J. Paszkowski (2006). "DNA methylation and epigenetic inheritance during plant gametogenesis." Chromosoma **115**(1): 27-35.

Taniguchi, Y., A. Ono, M. Sawatani, M. Nanba, K. Kohno, M. Usui, M. Kurimoto and T. Matuhasi (1995). "*Cry j* I, a major allergen of Japanese cedar pollen, has pectate lyase enzyme activity." Allergy **50**(1): 90-93.

Taylor, L. P. and P. K. Hepler (1997). "Pollen germination and tube growth." **48**(1): 461-491.

Taylor, N. G. (2008). "Cellulose biosynthesis and deposition in higher plants." New Phytologist **178**(2): 239-252.

Taylor, N. G., R. M. Howells, A. K. Huttly, K. Vickers and S. R. Turner (2003). "Interactions among three distinct CesA proteins essential for cellulose synthesis." Proceedings of the National Academy of Sciences **100**(3): 1450-1455.

Tebbutt, S. J., H. J. Rogers and D. M. Lonsdale (1994). "Characterization of a tobacco gene encoding a pollen-specific polygalacturonase." Plant Molecular Biology **25**(2): 283-297.

The Arabidopsis Genome Initiative (2000). "Analysis of the genome sequence of the flowering plant *Arabidopsis thaliana*." Nature **408**(6814): 796-815.

Thompson, J. E. and S. C. Fry (1997). "Trimming and solubilization of xyloglucan after deposition in the walls of cultured rose cells." Journal of Experimental Botany **48**(2): 297-305.

Thompson, J. E. and S. C. Fry (2001). "Restructuring of wall-bound xyloglucan by transglycosylation in living plant cells." The Plant Journal **26**(1): 23-34.

Tian, G.-W., M.-H. Chen, A. Zaltsman and V. Citovsky (2006). "Pollen-specific pectin methylesterase involved in pollen tube growth." Developmental Biology **294**(1): 83-91.

Tian, G.-W., A. Mohanty, S. N. Chary, S. Li, B. Paap, G. Drakakaki, C. D. Kopec, J. Li, D. Ehrhardt, D. Jackson, S. Y. Rhee, N. V. Raikhel and V. Citovsky (2004). "High-Throughput Fluorescent Tagging of Full-Length Arabidopsis Gene Products in Planta." Plant Physiology **135**(1): 25-38.

Tindemans, S. H., N. Kern and B. M. Mulder (2006). "The diffusive vesicle supply center model for tip growth in fungal hyphae." Journal of Theoretical Biology **238**: 937-948.

Torki, M., P. Mandaron, R. Mache and D. Falconet (2000). "Characterization of a ubiquitous expressed gene family encoding polygalacturonase in Arabidopsis thaliana." Gene **242**(1-2): 427-436.

Tormo, J., R. Lamed, A. J. Chirino, E. Morag, E. A. Bayer, Y. Shoham and T. A. Steitz (1996). "Crystal structure of a bacterial family-III cellulose-binding domain: a general mechanism for attachment to cellulose." EMBO Journal **15**(21): 5739-5751.

Toyota, M., T. Furuichi, H. Tatsumi and M. Sokabe (2008). "Cytoplasmic calcium increases in response to changes in the gravity vector in hypocotyls and petioles of *Arabidopsis* seedlings." Plant Physiology **146**: 505-514.

Trick, M. and R. B. Flavell (1989). "A homozygous *S* genotype of *Brassica oleracea* expresses two *S*-like genes." Molecular and General Genetics MGG **218**(1): 112-117.

Trinci, A. P. J. and P. T. Saunders (1977). "Tip growth of fungal hyphae." Journal of General Microbiology **103**: 243-248.

Trotter, P. J., M. A. Orchard and J. H. Walker (1995). "Ca^{2+} concentration during binding determines the manner in which annexin V binds to membranes." Biochemical Journal **308**: 591-598.

Tsabary, G., Z. Shani, L. Roiz, I. Levy, J. Riov and O. Shoseyov (2003). "Abnormal `wrinkled' cell walls and retarded development of transgenic *Arabidopsis thaliana*t plants expressing endo-1,4-β-glucanase antisense." Plant Molecular Biology **51**(2): 213-224.

Tuinstra, M. R. and J. Wedel (2000). "Estimation of pollen viability in grain *Sorghum*." Crop Science **40**(4): 968-970.

Tupý, J. and L. Říhová (1984). "Changes and growth effect of pH in pollen tube culture." Journal of Plant Physiology **115**: 1-10.

Twell, D., S. K. Park and E. Lalanne (1998). "Asymmetric division and cell-fate determination in developing pollen." Trends in Plant Science **3**(8): 305-310.

Twell, D., J. Yamaguchi, R. A. Wing, J. Ushiba and S. McCormick (1991). "Promoter analysis of genes that are coordinately expressed during pollen development reveals pollen-specific enhancer sequences and shared regulatory elements." Genes & Development **5**(3): 496-507.

Valdivia, E., A. Stephenson, D. Durachko and D. Cosgrove (2009). "Class B β-expansins are needed for pollen separation and stigma penetration." Sexual Plant Reproduction **22**(3): 141-152.

Van Aelst, A. C. and J. L. Van Went (1992). "Ultrastructural immuno-localization of pectins and glycoproteins in *Arabidopsis thaliana* pollen grains." Protoplasma **168**(1): 14-19.

Van den Bosch, K. A., D. J. Bradley, J. P. Knox, S. Perotto, G. W. Butcher and N. J. Brewin (1989). "Common components of the infection thread matrix and the intercellular space identified by immunocytochemical analysis of pea nodules and uninfected roots." EMBO Journal **8**: 335-342.

van der Woude, W. J., D. J. Morré and C. E. Bracker (1971). "Isolation and characterization of secretory vesicles in germinated pollen of *Lilium longiflorum*." Journal of Cell Science **8**(2): 331-351.

van Loon, J. J. W. A. (2007). "Some history and use of the random positioning machine, RPM, in gravity related research." Advances in Space Research **39**(7): 1161-1165.

van Loon, J. J. W. A., J. Krause, H. Cunha, J. Goncalves, H. Almeida and P. Schiller (2008). The Large Diameter Centrifuge, LDC, for life and physical sciences and

technology. Proc. of the 'Life in Space for Life on Earth Symposium'. Angers, France, ESA SP-663**:** 22–27.

VandenBosch, K. A., D. J. Bradley, J. P. Knox, S. Perotto, G. W. Butcher and N. J. Brewin (1989). "Common components of the infection thread matrix and the intercellular space identified by immunocytochemical analysis of pea nodules and uninfected roots." EMBO Journal **8**: 335-342.

Vantard, M. and L. Blanchoin (2002). "Actin polymerization processes in plant cells." Curr Opin Plant Biol **5**(6): 502-506.

Vanzin, G. F., M. Madson, N. C. Carpita, N. V. Raikhel, K. Keegstra and W.-D. Reiter (2002). "The mur2 mutant of *Arabidopsis thaliana* lacks fucosylated xyloglucan because of a lesion in fucosyltransferase AtFUT1." Proceedings of the National Academy of Sciences **99**(5): 3340-3345.

Versteeg, C., F. M. Rombouts and W. Pilnik (1978). "Purification and some characteristics of two pectinesterase isoenzymes from orange." **11**: 267 274.

Vidal, S., T. Doco, P. Williams, P. Pellerin, W. S. York, M. A. O'Neill, J. Glushka, A. G. Darvill and P. Albersheim (2000). "Structural characterization of the pectic polysaccharide rhamnogalacturonan II: evidence for the backbone location of the aceric acid-containing oligoglycosyl side chain." Carbohydrate Research **326**(4): 277-294.

Vidali, L., S. T. McKenna and P. K. Hepler (2001). "Actin polymerization is essential for pollen tube growth." Molecular Biology of the Cell **12**(8): 2534-2545.

Vidali, L., E. Yokota, A. Y. Cheung, T. Shimmen and P. K. Hepler (1999). "The 135 kDa actin-bundling protein from *Lilium longiflorum* pollen is the plant homologue of villin." Protoplasma **V209**(3): 283-291.

Vieira, M., J. Pissarra, P. Veríssimo, P. Castanheira, Y. Costa, E. Pires and C. Faro (2001). "Molecular cloning and characterization of cDNA encoding cardosin B, an aspartic proteinase accumulating extracellularly in the transmitting tissue of *Cynara cardunculus* L." Plant Molecular Biology **45**(5): 529-539.

Vignon, M. R., L. Heux, M. E. Malainine and M. Mahrouz (2004). "Arabinan-cellulose composite in Opuntia ficus-indica prickly pear spines." Carbohydrate Research **339**(1): 123-131.

Vincken, J.-P., H. A. Schols, R. J. F. J. Oomen, M. C. McCann, P. Ulvskov, A. G. J. Voragen and R. G. F. Visser (2003). "If Homogalacturonan were a side chain of rhamnogalacturonan I. implications for cell wall architecture." Plant Physiology **132**(4): 1781-1789.

Volkmann, D. and F. Baluška (2006). "Gravity: one of the driving forces for evolution." Protoplasma **229**(2): 143-148.

Waldron, K. and C. Brett (1990). "Effects of extreme acceleration on the germination, growth and cell wall composition of pea epicotyls." Journal of Experimental Botany **41**: 71-77.

Wang, H., J. Li, R. M. Bostock and D. G. Gilchrist (1996a). "Apoptosis: a functional paradigm for programmed plant cell death induced by a host-selective phytotoxin and invoked during development." Plant Cell **8**: 375-391.

Wang, H., H.-m. Wu and A. Y. Cheung (1996b). "Pollination induces mRNA poly(A) tail-shortening and cell deterioration in flower transmitting tissue." The Plant Journal **9**(5): 715-727.

Wang, H., H. Q. Zheng, W. Sha, R. Zeng and Q. C. Xia (2006a). "A proteomic approach to analysing responses of *Arabidopsis thaliana* callus cells to clinostat rotation." Journal of Experimental Botany **57**(4): 827-835.

Wang, L., D. Hukin, J. Pritchard and C. Thomas (2006b). "Comparison of plant cell turgor pressure measurement by pressure probe and micromanipulation." Biotechnology Letters **28**: 1147–1150.

Wang, Q. L., L. D. Lu, X. Q. Wu, Y. Q. Li and J. X. Lin (2003). "Boron influences pollen germination and pollen tube growth in *Picea meyeri*." Tree Physiology **23**(5): 345-351.

Wang, R., Q.-Y. Jiao and D.-Q. Wei (2006c). "Mechanical response of single plant cells to cell poking: A numerical simulation model." Journal of Integrative Plant Biology **48**: 700-705.

Wang, W., L. Wang, C. Chen, G. Xiong, X.-Y. Tan, K.-Z. Yang, Z.-C. Wang, Y. Zhou, D. Ye and L.-Q. Chen (2011). "*Arabidopsis* CSLD1 and CSLD4 are required for cellulose deposition and normal growth of pollen tubes." Journal of Experimental Botany.

Wang, X., Y. Teng, Q. Wang, X. Li, X. Sheng, M. Zheng, J. Šamaj, F. Baluška and J. Lin (2006d). "Imaging of dynamic secretory vesicles in living pollen tubes of *Picea meyeri* using evanescent wave microscopy." Plant Physiology **141**: 1591-1603.

Wasteneys, G. O. and M. E. Galway (2003). "Remodeling the cytoskeleton for growth and form: An overview with some new views." Annual Review of Plant Biology **54**: 691-722.

Watahiki, M. K., A. J. Trewavas and R. M. Parton (2004). "Fluctuations in the pollen tube tip-focused calcium gradient are not reflected in nuclear calcium level: a comparative analysis using recombinant yellow cameleon calcium reporter." Sexual Plant Reproduction **17**: 125-130.

Wayne, R. and M. P. Staves (1996). "A down to earth model of gravisensing of Newton's Law of Gravitation from the apple's perspective." Physiologia Plantarum **98**: 917-921.

Wayne, R., M. P. Staves and A. C. Leopold (1992). "The contribution of the extracellular matrix to gravisensing in characean cells." Journal of Cell Science **101**: 611-623.

Wei, C., L. S. Lintilhac and P. M. Lintilhac (2006). "Loss of stability, pH, and the anisotropic extensibility of *Chara* cell walls." Planta **223**: 1058-1067.

Weise, S., O. A. Kuznetsov, K. H. Hasenstein and J. Z. Kiss (2000). "Curvature in *Arabidopsis* inflorescence stems is limited to the region of amyloplast displacement." Plant Cell Physiology **41**: 702-709.

Wellman, C. H. and J. Gray (2000). "The microfossil record of early land plants." Philosophical Transactions of the Royal Society of London. Series B: Biological Sciences **355**(1398): 717-732.

Western, T. L. (2006). "Changing spaces: the *Arabidopsis* mucilage secretory cells as a novel system to dissect cell wall production in differentiating cells." Canadian Journal of Botany **84**(4): 622-630.

Wheeler, R. M. (2010). "Plants for human life support in space: From Myers to Mars." Gravitational and Space Biology **23**: 25-34.

Wilhelm, J. and E. Frey (2003). "Elasticity of stiff polymers." Physical Review Letters **91**: 108103/108101-108104.

Willats, W. G. T., L. McCartney, W. Mackie and J. P. Knox (2001). "Pectin: cell biology and prospects for functional analysis." Plant Molecular Biology **47**: 9-27.

Williams, D. (2002). Isolation and integrated testing: an introduction to the Lunar-Mars Life Support Test Project. Isolation: NASA experiments in closed-environment living. H. Lane, R. Sauer and D. Feeback. San Diego, Univelt**:** 1-6.

Wilsen, K. L. and P. K. Hepler (2007). "Sperm delivery in flowering plants." Bioscience **57**: 835-844.

Wilsen, K. L., A. Lovy-Wheeler, B. Voigt, D. Menzel, J. G. Kunkel and P. K. Hepler (2006). "Imaging the actin cytoskeleton in growing pollen tubes." Sexual Plant Reproduction **19**: 51-62.

Wing, R., J. Yamaguchi, S. Larabell, V. Ursin and S. McCormick (1990). "Molecular and genetic characterization of two pollen-expressed genes that have sequence similarity to pectate lyases of the plant pathogen *Erwinia*." Plant Molecular Biology **14**(1): 17-28.

Winship, L. J., G. Obermeyer, A. Geitmann and P. K. Hepler (2010). "Under pressure, cell walls set the pace." Trends in Plant Science **15**(7): 363-369.

Wolf, L. (2008). Probiotic allergy relief, fighting crime with pollen. *Newscripts* In: Chemical and Engineering news. **86:** 33. 88

Wolf, S., K. Hématy and H. Höfte (2012). "Growth control and cell wall signaling in plants." Annual Review of Plant Biology **63**(1): 381-407.

Wolverton, C. and J. Z. Kiss (2009). "An update on plant space biology." Gravitational and Space Biology Bulletin **22**: 13-20.

Wolverton, C., J. Mullen, H. Ishikawa and M. Evans (2002). "Root gravitropism in response to a signal originating outside of the cap." Planta **215**: 153-157.

Wood, P. (2004). Pollen helps war crime forensics. BBC news.

Wood, P. and R. Fulcher (1983). "Dye interactions. A basis for specific detection and histochemistry of polysaccharides." Journal of Histochemistry and Cytochemistry **31**(6): 823-826.

Wu, H.-m. and A. Y. Cheung (2000). "Programmed cell death in plant reproduction." Plant Molecular Biology **44**(3): 267-281.

Wu, H.-m., O. Hazak, A. Y. Cheung and S. Yalovsky (2011). "RAC/ROP GTPases and auxin signaling." The Plant Cell **23**(4): 1208-1218.

Wu, S. S. H., D. F. Suen, H. C. Chang and A. H. C. Huang (2002). "Maize tapetum xylanase is synthesized as a precursor, processed and activated by a serine protease, and deposited on the pollen." Journal of Biological Chemistry **277**(50): 49055-49064.

Wu, Y., X. Qiu, S. Du and L. Erickson (1996). "PO149, a new member of pollen pectate lyase-like gene family from alfalfa." Plant Molecular Biology **32**(6): 1037-1042.

Yamamoto, R. and J. Z. Kiss (2002). "Disruption of the actin cytoskeleton results in the promotion of gravitropism in inflorescence stems and hypocotyls of *Arabidopsis*." Plant Physiology **28**: 669-681.

Yamamoto, Y., M. Nishimura, I. Hara-Nishimura and T. Noguchi (2003). "Behavior of vacuoles during microspore and pollen development in *Arabidopsis thaliana* " Plant and Cell Physiology **44**: 1192-1201.

Yang, C., D. Wei and F. Y. Zhuang (2008). "The force induced by organelles' weight in the microfilament is in the range of 0.1-1 pN." Acta Astronautica **63**(7-10): 923-928.

Yennawar, N. H., L.-C. Li, D. M. Dudzinski, A. Tabuchi and D. J. Cosgrove (2006). "Crystal structure and activities of EXPB1 (Zea m 1), a β-expansin and group-1 pollen allergen from maize." Proceedings of the National Academy of Sciences **103**(40): 14664-14671.

Yoder, M., N. Keen and F. Jurnak (1993). "New domain motif: the structure of pectate lyase C, a secreted plant virulence factor." Science **260**(5113): 1503-1507.

Yokota, E., S. Muto and T. Shimmen (2000). "Calcium-calmodulin suppresses the filamentous actin-binding activity of a 135-kilodalton actin-bundling protein isolated from lily pollen tubes." Plant Physiology **123**(2): 645-654.

Yokota, E. and T. Shimmen (1994). "Isolation and characterization of plant myosin from pollen tubes of lily." Protoplasma **177**(3-4): 153-162.

Yokota, E. and T. Shimmen (2006). The actin cytoskeleton in pollen tubes actin and actin binding proteins. The pollen tube: a cellular and molecular perspective, Plant Cell Monographs. R. Malhó. Berlin Heidelberg, Springer Verlag. **3:** 139-155.

Yokota, E., K. Takahara and T. Shimmen (1998). "Actin-bundling protein isolated from pollen tubes of lily - Biochemical and immunocytochemical characterization." Plant Physiology **116**(4): 1421-1429.

Yokoyama, R., J. K. C. Rose and K. Nishitani (2004). "A surprising diversity and abundance of xyloglucan endotransglucosylase/hydrolases in rice. Classification and expression analysis." Plant Physiology **134**(3): 1088-1099.

Yoshida-Shimokawa, T., S. Yoshida, K. Kakegawa and T. Ishii (2001). "Enzymic feruloylation of arabinoxylan-trisaccharide by feruloyl-CoA:arabinoxylan-trisaccharide-hydroxycinnamoyl transferase from *Oryza sativ*a." Planta **212**(3): 470-474.

Zablackis, E., J. Huang, B. Muller, A. G. Darvill and P. Albersheim (1995). "Characterization of the cell-wall polysaccharides of *Arabidopsis thaliana* leaves." Plant Physiology **107**(4): 1129-1138.

Zerzour, R., J. H. Kroeger and A. Geitmann (2009). "Polar growth in pollen tubes is associated with spatially confined dynamic changes in cell mechanical properties." Developmental Biology **334**: 437–446.

Zhao, Y. (2010). "Auxin biosynthesis and its role in plant development." Annual Review of Plant Biology **61**(1): 49-64.

Zimmermann, R. (2003). "Growing pains." Air & Space **Aug-Sep**: 31-35.

Zinkl, G. M. and D. Preuss (2000). "Dissecting *Arabidopsis* pollen-stigma interactions reveals novel mechanisms that confer mating specificity." Annals of Botany **85**(suppl_1): 15-21.

Zonia, L., S. Cordeira, J. Tupý and J. A. Feijó (2002). "Oscillatory chloride efflux at the pollen tube apex has a role in growth and cell volume regulation and is targeted by inositol 3,4,5,6-tetra*kis*phosphate." Plant Cell **14**: 2233-2249.

Zonia, L., S. Cordeiro and J. A. Feijó (2001). "Ion dynamics and hydrodynamics in the regulation of pollen tube growth." Sex Plant Reproduction **14**: 111- 116.

Zonia, L. and T. Munnik (2007). "Life under pressure: hydrostatic pressure in cell growth and function." Trends in Plant Science **12**: 90-97.

Zonia, L. and T. Munnik (2008). "Vesicle trafficking dynamics and visualization of zones of exocytosis and endocytosis in tobacco pollen tubes." J. Exp. Bot. **59**(4): 861-873.

Zonia, L. and T. Munnik (2009). "Uncovering hidden treasures in pollen tube growth mechanics." Trends in Plant Science **14**: 318-327.

Zonia, L. E., M. Müller and T. Munnik (2006). "Hydrodynamics and cell volume oscillations in the pollen tube apical region are integral components of the biomechanics of *Nicotiana tabacum* pollen tube growth." Cell Biochemistry and Biophysics **46**: 209-232.

Zykwinska, A. W., M.-C. J. Ralet, C. D. Garnier and J.-F. J. Thibault (2005). "Evidence for *in vitro* binding of pectin side chains to cellulose." Plant Physiology **139**(1): 397-407.

11 Curriculum vitæ

Youssef Chebli
Research assistant
Cellular and molecular biology - Microscopy

11.1 Languages

English, French, Arabic, Spanish

11.2 Expertise and skills

Molecular biology: PCR, RT-PCR, cloning, DNA and RNA purification, protein extraction and purification, Western blot, bacterial and plant transformation, fluorescent protein tagging...

Cell biology: eukaryotic cell culture, bacterial culture

Bioinformatics: primer designing, sequence alignment and analysis, protein sequence analysis for specific peptidic domains...

Electron microscopy: sample preparation (fixation, embedding, staining, ultra-sectioning...), transmission electron microscopy, scanning electron microscopy and environmental SEM, focussed ion beam.

Photonic microscopy: sample preparation (fixation, labelling, immuno-histochemistry...), epifluorescence microscopy, confocal microscopy (fixed cells and live imaging, FRAP...).

Communication: Writing scientific projects, communications, papers, review articles and grant proposals. Preparing and presenting scientific posters and PowerPoint presentations.

11.3 Informatic skills

Word, Excel, Power Point, Windows, EndNote, Image J, Bioinformatic tools

11.4 Education

2012 Université de Montréal, département des sciences biologiques, Institut de recherche en biologie végétale, Montreal, Qc, Canada.

Ph.D in biological sciences (Thesis defense planned for the end of October 2012)

2006 Université Saint-Joseph, faculté des sciences, département de sciences de la vie et de la terre, Mar Roukoz, Lebanon.
Research master 1 in structure and interaction of macromolecules and functional genomics (**European Credit Transfer** and Accumulation **System)**

2005 Université Saint-Joseph, faculté des sciences, département de sciences de la vie et de la terre, Mar Roukoz, Lebanon.
Bachelor in Life and Earth sciences.

Georgetown University certificate of English language proficiency test.
Level: **Advanced proficiency.**

2002 Collège Mont La Salle, Ain Saadé, Lebanon.
Lebanese Baccalauréat, major: Life and Earth sciences
French Baccalauréat, major: Life and Earth sciences

11.5 Lab experience

2007-2012 : Université de Montréal, département des sciences biologiques, Institut de recherche en biologie végétale, Montreal, Qc, Canada.

PhD research project under the supervision of Dr.Anja Geitmann on the subject: "Cell wall composition regulates cell shape and growth behaviour in pollen tubes"

During my PhD, I was interested in the molecular players controlling the cell wall composition and its mechanical properties. I combined cellular and molecular biology with high-resolution imaging to decipher how the pollen tube shapes its cylindrical geometry.
During my PhD I was able to:
Determine the mechanical and biological roles played by cellulose and pectins during pollen tube growth.
Determine the role of pectate lyases during pollen development and pollen tube growth
In collaboration with the European Space Agency, determine the role played by hyper-gravity and omnilateral gravity on the pollen tube intracellular dynamics and cell wall formation.

2005-2006 : Université Saint-Joseph, faculté des sciences, département de sciences de la vie et de la terre, Mar Roukoz, Lebanon.

Internship under the supervision of Dr. Mireille Kallassy Aouad on the subject: "Identification and characterization of genes encoding biopesticides produced by strains of *Bacillus thuringiensis* isolated in Lebanon"

During my internship I was responsible of isolating *Bacillus thuringiensis* strains expressing biopesdicides incoded by the *Cry1A* gene family. For each strain, I had to determine which *Cry1A* genes were expressed, amplify, clone them in *E.coli* and sequence them.
The aim of the project was to find strains able to replace chemical pesticides in fighting plant pathogens efficiently without harming the ecosystem and the plant (crops) development.

2004 - 2005 : Université Saint-Joseph, faculté des sciences, centre d'analyse et de recherche, faculté de pharmacie, département de toxicologie. Lebanon

Internship under the supervison of Dr. André Khoury on the subject: "Ochratoxin A in Lebanese grapes and wines, occurrence, origin and corrective techniques"

During this internship, I was assisting a PhD student (Dr. André Khoury) in his several experiments ranging from identifying and isolating ocharatoxin A producing fungi (*Aspergillus*), extracting ochratoxin A from grapes and wines by immuno-affinity columns and analyzing the extracts by ELISA and HPLC-FLD.

2002 - 2004: Université Saint-Joseph, Botanical garden of the faculté des sciences, Mar Roukoz, Lebanon.

Planting and maintenance of the botanical garden under the supervision of Dr. Bou Dagher Kharrat Magda.

2004: Laboratory of the Bhannès hospital center, Dahr el Souwan, Lebanon.

During my internship, I was trained on how to manipulate human biological samples for medical analysis. I was also trained to perform haematological, immunological, biochemical and microbiological analysis on several samples ranging from blood, urine, faeces to placenta and cerebrospinal fluid.

11.6 Working and teaching experience

Giving private lessons to students of different grades in biology, chemistry, mathematics and physics.

2008-2012 Reviewing scientific manuscripts (under the supervision of Dr. Anja Geitmann) for: Plant Cell, Plant physiology, Sexual Plant Reproduction, Plant Journal, Current Biology, Plant Biology and Protoplasma.

2011 Université de Montréal, département des sciences biologiques, Institut de recherche en biologie végétale, Montreal, Qc, Canada.
Lecture to Masters students on: *Focused Ion Beam* and *Analytical Electron Microscopy*

2010 Université Saint-Joseph, faculté des sciences, département de sciences de la vie et de la terre, Mar Roukoz, Lebanon.
Lecture to Masters students on: *Marking and tracking fluorescent proteins in vivo*.

Eureka Festival, Montreal, Qc, Canada
Université de Montréal booth: *What is pollen used for?*

2008-2011 Université de Montréal, faculté des arts et des sciences, département des sciences biologiques, Montreal, Qc, Canada
As part of the SEUR project (Sensibilisation aux Études, à l'Université et à la Recherche), Université de Montréal, training of fifth grade students during a session of plant anatomy practical course.

2008 Université de Montréal, département des sciences biologiques, Institut de recherche en biologie végétale, Montreal, Qc, Canada.
In charge of the workshop '*sample preparation and possessing*' as part of the IRBV microscopy summer course.

2007 Université de Montréal, département des sciences biologiques, Institut de recherche en biologie végétale, Montreal, Qc, Canada.
Teaching assistant of the practical courses of plant anatomy (BIO2372).
Professor: Dr. Anja Geitmann

2006 Université Saint-Joseph, faculté des sciences, département de sciences de la vie et de la terre, Mar Roukoz, Lebanon.
Teaching assistant of the practical courses of molecular biology (048MOLTL6).
Professor: Dr. Mireille Kallassy Awad

11.7 Conferences and presentations

2012 *XXII International Congress on* ***Sexual Plant Reproduction****,* Melbourne, Australia.
Oral presentation: **What makes a pollen tube a tube?**
Poster presentation: **Spatio-temporal distribution of pectate lyases in *Arabidopsis* pollen tubes**.

2011 *38th Annual Meeting of the Microscopical Society of Canada, MSC-SMC,* University of Ottawa, Ottawa, On, Canada.
Oral and poster presentations: **Correlation between spatial distribution of cell wall components and growth behavior in tip growing cells.**
Participation to the course: Super-resolution.

2010 *Plant Biology 2010* (joint meeting of the Canadian and American societies of plant physiology), Montreal, Qc, Canada.
Poster presentation : **Apical growth in pollen tubes: the mechanics behind it.**
Volunteer for the local organizing committee of the CSPP.
Chairman of the **Pollen Biology** minisymposium.
Participation to the course: Guidelines for preparing digital art workshop.

XVII Congress of the Federation of European Societies of Plant Biology (FESPB), Valencia, Spain.
Poster presentation: **Shaping a protuberance - the mechanics of cellular growth.**

2009 *60th International Astronautical Congress* Daejeon, Republic of Korea.
Oral presentation : **The pollen tube- an ideal model system to study non statocyte plant cell response to gravity.**

Université de Montréal, département des sciences biologiques, Institut de recherche en biologie végétale, Montreal, Qc, Canada.
Oral presentation **Life and after-life of a pollen tube** (Vie et 'après-vie' d'un tube pollinique).

Symposium of biology. Université de Montréal, département des sciences biologiques, Montreal, Qc, Canada.
Judge of the oral presentations in the molecular and cellular biology session.

2008 *Second Montreal Plant Meeting*, McGill University, Montreal, Qc, Canada.
Poster presentation: **Optimization of growth conditions for frozen stored *Arabidopsis thaliana* pollen.**

Frontiers of Sexual plant reproduction, Tuscon Az, USA.
Poster presentation : **Optimization of growth conditions for frozen stored *Arabidopsis thaliana* pollen.**

19th International Conference on Arabidopsis *Research*, Montreal, Qc.
Poster presentation: **Optimization of growth conditions for frozen stored *Arabidopsis thaliana* pollen.**

50th annual meeting of the Canadian society of plant physiologists (CSPP-SCPV) Ottawa, On, Canada.
Presentation of two posters:
1- **Optimization of growth conditions for frozen stored *Arabidopsis thaliana* pollen.**
2- **Microwave assisted processing of plant cells for optical and electron microscopy.**

35th Annual Meeting of the Microscopical Society of Canada, MSC-SMC, McGill University, Montreal, Qc, Canada.
Poster presentation : **Microwave assisted processing of plant cells for optical and electron microscopy.**
Participation to the theoretical and practical mini-course on **Image analysis.**

Symposium of biology. Université de Montréal, département des sciences biologiques, Montreal, Qc, Canada.
Judge of the oral presentations in the molecular and cellular biology session.

2007 *First Montreal Plant Meeting*, McGill University, Montreal, Qc,Canada.

Université de Montréal, département des sciences biologiques, Institut de recherche en biologie végétale, Montreal, Qc, Canada.
Oral presentation : **Quantitative parameters characterizing *Arabidopsis* pollen tube architecture**. (Paramètres quantitatifs déterminant l'architecture du tube pollinique d'*Arabidopsis thaliana*.)

Università degli Studi di **Siena** (University of Siena), Siena, Italy**.**
As part of the funding of the Human Frontier Science Program.
Annual meeting of the members of A. Geitmann (Université de Montréal), M. Cresti (Università degli Studi di Siena), J. Dumais (Harvard University) and L. Mahadevan (Harvard University) labs on the subject: Mechanical modeling of pollen tube growth
Oral presentation: **Quantitative parameters characterizing *Arabidopsis* pollen tube architecture**.

Symposium of biology. Université de Montréal, département des sciences biologiques, Montreal, Qc, Canada.
Oral presentation : ***Arabidopsis thaliana:* cell wall architecture of the pollen tube** (*Arabidopsis thaliana*: architecture pariétale du tube pollinique).

2004 Université Saint-Joseph, faculté des sciences, Mar Roukoz, Lebanon.
2003 Oral presentaion : **Phytotherapy, between myth and reality** (La phytothérapie entre mythe et réalité).

11.8 Publications

Chebli Y, Kaneda M, Zerzour R, Geitmann A (2012). "The cell wall of the Arabidopsis thaliana pollen tube - spatial distribution, recycling and network formation of polysaccharides." Plant Physiology 160:1-16

Chebli Y and Geitmann A (2011) "Single cell experimental models in gravity research on plants" Frontiers in Plant Science 2:56. doi: 10.3389/fpls.2011.00056.

Fayant P, Girlanda O, **Chebli Y**, Villemure I, Geitmann A (2010). "Finite element model of self similar tip growth in pollen tubes" Plant Cell 22: 2579–2593.

Aouar L, **Chebli Y**, Geitmann A (2010) "Morphogenesis of complex plant cell shapes – the mechanical role of crystalline cellulose in growing pollen tubes." Sexual Plant Reproduction 23: 15-27.

Bou Daher F, **Chebli Y**, Geitmann A (2009) "Optimization of conditions for germination of cold-stored *Arabidopsis thaliana* pollen". Plant Cell Reports 28: 347-457.

Chebli Y, BouDaher F, Sanyal M, Aouar L and Geitmann A (2008). "Microwave assisted processing of plant cells for optical and electron microscopy." Bulletin of the Microscopical Society of Canada 36(3): 15-19.

Chebli Y, Geitmann A (2007) "Mechanical principles governing pollen tube growth." Functional Plant Science and Biotechnology 1: 232-245.

In preparation or submitted

Chebli Y, Pujol L, Shojaeifard A, Brouwer I, van Loon J, Geitmann A. "Role of hypergravity on pollen tube cell wall formation". In revision – PlosOne.

Chebli Y, Geitmann A. "Spatio-temporal expression of pectate lyases in Arabidopsis male gametophyte'.

11.9 Scholarships and awards

2012 International Plant Biomechanics Meeting, Clermont-Ferrand, France
Award for the poster entitled :'*Perception of gravity stress in non-statocyte plant cells'*.

Université de Montréal
Merit scholarship of the Département des sciences biologiques.
Value : 2000$

XXII International Congress on Sexual Plant Reproduction, Melbourne, Australia.
Award for the best student oral presentation
Value : 250$ and the medal of the International Association of Sexual Plant Reproduction Research.

2011 Microscopical Society of Canada (MSC-SMC), Ottawa, Canada.
Gérard T. Simon award for the best student presentation in biological sciences.
Value : 500$ and the covering of the expenses related to the conference.

2010 Marie Victorin doctoral scholarship
First recipient of the Marie-Victorin doctoral scholarship awarded by the Institut de Recherche en Biologie Végétale.
Value : 3 000$

2008 FQRNT
Doctoral scholarship from the Fond Québécois de la Recherche sur la Nature et les Technologies.
Value: 20 000$ per year for 3 years.
Declined because of scholarship accumulation.

NSERC / Ann Oaks doctoral scholarship
First recipient of the Ann Oaks doctoral scholarship awarded by the Canadian Society of Plant Physiologists (CSPP-SCPV).
Value: 21 000$ per year for 3 years.

2007 Université de Montréal
Scholarship for direct transfer from Masters to PhD.
Value : 7 000$ per year on 2 years.

Travel scholarship

2012 **Direction des Relation Internationale** (Université de Montréal) scholarship (value 2500$), **Jacques-Rousseau** scholarship (value of 500$), scholarship from the International Association of Sexual Plant Reproduction Research (value of 500$) to participate to participate to the *XXII International Congress on Sexual Plant Reproduction,* Melbourne, Australia.

2011 **Jacques-Rousseau** scholarship (value of 600$) to participate to the *38th Annual Meeting of the Microscopical society of Canada,* Ottawa, On, Canada.

2010 **Carl Zeiss** scholarship (value 800$) to participate to the *Plant Biology 2010* (joint CSPP-ASPB congress), Montreal, Qc, Canada.
Direction des Relation Internationale (Université de Montréal) scholarship (value 2000$) to participate to the *XVII Congress of the Federation of European Societies of Plant Biology*, Valencia Spain.

2009 **Canadian Space Agency** scholarship (value 2630$) to participate to the *60th International Astronautical Congress* Daejeon, Republic of Korea.

2008 **Jacques-Rousseau** scholarship (value 850$) and scholarship from the **University of Arizona** (value 500$) to participate to the *Frontiers of Sexual plant reproduction* Tuscon, Az, US.
Carl Zeiss scholarship (value 300$) to participate to the *19th International Conference on Arabidopsis Research 2008*, Montreal, Qc, Canada.
Georges H. Duff scholarship (value 180$) to participate to the *50th annual meeting of the Canadian society of plant physiologists,* Ottawa, On, Canada.
Jacques-Rousseau scholarship (value 150$) to participate to the *35th Annual Meeting of the Microscopical Society of Canada,* Montreal, Qc, Canada.

2007 **Carl Zeiss scholarship** (value 500$) to participate to the annual meeting of the teams benefiting from funds from the Human Frontier Science Program, Siena, Italy.

11.10 Activities and Hobbies

Theatre:
Completed workshops: Interpretation1 (The character) and Interpretation2 (The play). Centre des activités culturelles. Université de Montréal.

First aid: Completed the first level of first aid courses with the Red Cross
Translation French-English-French

Reading, swimming, philately, history, traveling, Sudoku, chess, crossword

11.11 References

Dr. Anja Geitmann

Professeur titulaire / Full professor
Institut de recherche en biologie végétale, département de sciences biologiques, Université de Montréal. Montréal, Qc, Canada
Phone +1 514 343 2117
Fax +1 514 343 2288

Dr. David Morse

Professeur titulaire / Full professor
Institut de recherche en biologie végétale, département de sciences biologiques, Université de Montréal. Montréal, Qc, Canada
Phone : +1 514 343 2133
Fax : +1 514 343 2288

Dr. Mireille Kallassy Aouad

Professeur agrégé / Associate professor
Département de sciences de la vie et de la terre, faculté des sciences, Université Saint-Joseph, Mar Roukoz, Lebanon
Phone : +961 142 1300 and 1421 367
Fax : +961 453 2657

Dr. Magda Bou Dagher Kharrat

Professeur agrégé / Associate professor
Département de sciences de la vie et de la terre, faculté des sciences, Université Saint-Joseph, Mar Roukoz, Lebanon
Phone : +961 142 1300 and 1421 367
Fax : +961 453 2657